National Library of Canada
Bibliothèque nationale du Canada

Canadian Theses Service
Service des thèses canadiennes

Ottawa, Canada
K1A 0N4

NOTICE

The quality of this microform is heavily dependent upon the quality of the original thesis submitted for microfilming. Every effort has been made to ensure the highest quality of reproduction possible.

If pages are missing, contact the university which granted the degree.

Some pages may have indistinct print especially if the original pages were typed with a poor typewriter ribbon or if the university sent us an inferior photocopy.

Previously copyrighted materials (journal articles, published tests, etc.) are not filmed.

Reproduction in full or in part of this microform is governed by the Canadian Copyright Act, R.S.C. 1970, c. C-30.

AVIS

La qualité de cette microforme dépend grandement de la qualité de la thèse soumise au microfilmage. Nous avons tout fait pour assurer une qualité supérieure de reproduction.

S'il manque des pages, veuillez communiquer avec l'université qui a conféré le grade.

La qualité d'impression de certaines pages peut laisser à désirer, surtout si les pages originales ont été dactylographiées à l'aide d'un ruban usé ou si l'université nous a fait parvenir une photocopie de qualité inférieure.

Les documents qui font déjà l'objet d'un droit d'auteur (articles de revue, tests publiés, etc.) ne sont pas microfilmés.

La reproduction, même partielle, de cette microforme est soumise à la Loi canadienne sur le droit d'auteur, SRC 1970, c. C-30.

NL-339 (r. 88/04)

Canada

THE UNIVERSITY OF ALBERTA

Mineralogy of the 334 Pod, 11A Zone, Dawn Lake, Saskatchewan

by

Evan Clarendon Radhay Persaud

A THESIS

SUBMITTED TO THE FACULTY OF GRADUATE STUDIES AND RESEARCH

IN PARTIAL FULFILMENT OF THE REQUIREMENTS FOR THE DEGREE

OF Master of Science

Geology

EDMONTON, ALBERTA

Fall 1987

Permission has been granted to the National Library of Canada to microfilm this thesis and to lend or sell copies of the film.

The author (copyright owner) has reserved other publication rights, and neither the thesis nor extensive extracts from it may be printed or otherwise reproduced without his/her written permission.

L'autorisation a été accordée à la Bibliothèque nationale du Canada de microfilmer cette thèse et de prêter ou de vendre des exemplaires du film.

L'auteur (titulaire du droit d'auteur) se réserve les autres droits de publication; ni la thèse ni de longs extraits de celle-ci ne doivent être imprimés ou autrement reproduits sans son autorisation écrite.

ISBN 0-315-41017-5

THE UNIVERSITY OF ALBERTA

RELEASE FORM

NAME OF AUTHOR Evan Clarendon Radhay Persaud

TITLE OF THESIS Mineralogy of the 334 Pod, 11A Zone, Dawn Lake, Saskatchewan

DEGREE FOR WHICH THESIS WAS PRESENTED Master of Science

YEAR THIS DEGREE GRANTED Fall 1987

Permission is hereby granted to THE UNIVERSITY OF ALBERTA LIBRARY to reproduce single copies of this thesis and to lend or sell such copies for private, scholarly or scientific research purposes only.

The author reserves other publication rights, and neither the thesis nor extensive extracts from it may be printed or otherwise reproduced without the author's written permission.

(SIGNED) Evan C R Persaud

PERMANENT ADDRESS:

520 L MICHENER PARK, EDMONTON,
ALBERTA T6H4M5, CANADA

DATED 19th October 1987

THE UNIVERSITY OF ALBERTA

FACULTY OF GRADUATE STUDIES AND RESEARCH

The undersigned certify that they have read, and recommend to the Faculty of Graduate Studies and Research, for acceptance, a thesis entitled Mineralogy of the 334 Pod, 11A Zone, Dawn Lake, Saskatchewan submitted by Evan Clarendon Radhay Persaud in partial fulfilment of the requirements for the degree of Master of Science.

.....

Supervisor

R. St. J. Lambert

.....

.....

.....

Date.....

Dedications

To my parents and Aunt Sosie

Abstract

The 334 Pod of U-Ni mineralisation is a cylindro-spherical body located below unconformity-associated uranium ore in the 11A Zone at Dawn Lake, northern Saskatchewan. The 334 Pod occurs mainly in chloritised quartzo-feldspathic metasediments located beneath graphitic metapelites. An assemblage of U-Ni-Co-Fe-Pb-Zn-Cu-V-Mn-Au-Ag-Bi-Te-Sb-As-S was observed in the 334 Pod.

Three stages of mineralisation have been observed. The first stage coincides with diabase dyke activity at 1350 Ma and is characterised by arsenides, sulpharsenides and pitchblende. The second stage is associated with a second pulse of diabase dyke activity at 1100-1000 Ma and is characterised by pitchblende and sulphides. The third mineralisation stage (< 350 Ma) is associated with post-Carboniferous uplift and is characterised by pitchblende with high silica contents. Gangue minerals are illite-chlorite (first and second stages), hematite (second stage) and calcite (third stage). Three varieties of pitchblende were observed.

Chemical ages of pitchblende mineralisation are 1339 Ma (pitchblende I), 1149 Ma (pitchblende II) and 27-271 Ma (pitchblende III).

Acknowledgements

The author is indebted to Dr. R.D. Morton for suggesting the area of research, and for the invaluable assistance and supervision during the course of this work.

Thanks are due to the Saskatchewan Mining and Development Corporation and to Asamera for their kind assistance in this project. In particular, the guidance and help extended by Dr. P.J. Clarke and Dr. H. Ibrahim during the collection phase of this study are gratefully acknowledged.

Dr. D.G.W. Smith is thanked for permitting the extensive use of his N.S.E.R.C - funded electron microprobe facilities. Thanks also go to Mr. S. Launspach who helped with the electron microprobe analyses and data reduction.

The author also wishes to thank Dr. and Mrs. A. Nedd, and Dr. A. Changkakoti who offered valuable help and encouragement during the course of this study.

Last, but not least, my sincere gratitude to my wife Rita, without whose constant love, consistent encouragement and tremendous input this thesis would never have been completed.

Table of Contents

Chapter		Page
I.	HISTORY OF EXPLORATION AND PREVIOUS WORK	1
	A. General	1
	B. Dawn Lake Property	5
	C. Previous Work	8
	D. Historical Background and Aims of Thesis	8
II.	REGIONAL GEOLOGY	12
	A. Introduction	12
	B. General Geology	12
	C. Cree Lake Zone	14
	C.1 General	14
	C.2 Geology	15
	C.3 Lithology	15
	C.4 Structure	16
	C.5 Metamorphism	17
	D. Wollaston Domain	17
	D.1 General	17
	D.2 Geology	17
	D.3 Structure	19
	D.4 Metamorphism	20
	E. Mudjatik Domain	20
	E.1 General	20
	E.2 Geology	21
	E.3 Structure	22
	E.4 Metamorphism	23
	F. The Wollaston-Mudjatik Junction	23
	G. Athabasca Group	24

H. Diabase Dykes In The Athabasca Basin 27
I. The Age Of The Athabasca Group 29
J. Uranium Mineralisation In The Crèe Lake Zone 31
III. LOCAL GEOLOGY OF DAWN LAKE 33
A. Regional Setting of the Dawn Lake Deposits 33
B. Lithologies 33
C. Regolith (Palaeo-weathering profile) 39
D. Athabasca Group 42
E. Structure 42
E.1 General 42
E.2 Structure-11A Zone 43
IV. MINERALOGY OF THE 334 POD 45
A. Introduction 45
B. Mineralogy of 334 Pod - General 45
C. Mineralogy of the 334 Pod - Methods 49
D. Oxides 50
D.1 Pitchblende 50
D.2 Pitchblende I 51
D.3 Pitchblende II 55
D.4 Pitchblende III 55
D.5 Pitchblende-Discussion 55
E. Arsenides 74
E.1 Rammelsbergite [$NiAs_2$] 75
E.2 Safflorite [$CoAs_2$] 75
E.3 Nickeline [NiAs] 77
F. Sulpharsenides 86
F.1 Gersdorffite [NiAsS] 86

F.2 Gersdorffite (normal variety) 91
F.3 Arsenian Gersdorffite 106
F.4 Bismuthian Gersdorffite 108
F.5 Cobaltite [CoAsS] 108
G. Sulphides 109
G.1 Marcasite [FeS_2] 109
G.2 Pyrite [FeS_2] 111
G.3 Bravoite [$(Fe,Ni)S_2$] 111
G.4 Violarite [$FeNi_2S_4$] 112
G.5 Millerite [NiS] 114
G.6 Chalcopyrite [$CuFeS_2$] 117
G.7 Sphalerite [ZnS] 120
G.8 Galena [PbS] 121
G.9 Copper Sulphide 121
H. Tellurides 122
I. Gold 129
J. Gangue minerals 129
J.1 General 129
J.2 Illite-chlorite alteration 129
J.3 Hematite gangue 130
J.4 Carbonate gangue 130
K. Paragenesis 130
V. CHEMICAL AGES 135
A. Introduction 135
B. Chemical Ages - Pitchblende I 136
C. Chemical ages - pitchblende II 136
D. Chemical ages - pitchblende III 139

E. Discussion 141

F. Conclusion 142

VI. DISCUSSION 146

A. Introduction 146

B. Source of Ore-Related Elements 147

B.1 General 147

B.2 The source of metals: Hudsonian-related syngenetic and synmetamorphic protores 148

C. Origin of Fluids 151

C.1 Fluid Inclusion Studies 151

C.2 Groundwater Geochemistry 153

C.3 Origin of fluids — speculation 155

D. Release of Uranium 156

E. Transportation and deposition of uranium 157

E.1 Transportation of uranium 157

E.2 Deposition of uranium 157

E.2.1 Reduction 158

E.2.2 Adsorption-Reduction 159

E.2.3 Boiling 161

E.2.4 Electro-precipitation 161

F. Transportation of arsenic 163

F.1 Deposition of arsenides and sulpharsenides 163

G. Depositional model 165

VII. BIBLIOGRAPHY 168

VIII. APPENDIX I 182

A. Abstract 183

B. Introduction 183

C. Geological Setting 185

D. Host Lithologies 185
E. The graphitic quartz-chlorite-feldspar gneiss (metasiltstone?) 187
F. The graphite-cordierite-biotite-feldspar gneiss (metapelite) 187
G. The anatectic-pegmatoids 188
H. Structure 188
I. Mineralization 189
J. Chemical Analytical Methods 189
K. Bismuthian Gersdorffite 190
L. The colour, reflectance and hardness of Bi-gersdorffites 198
M. Conclusions 202
N. Acknowledgements 202
O. References 203
IX. APPENDIX II 206
A. Introduction 207
B. The Calculation of Apparent Ages of Uranium minerals from chemical analyses 208
C. Computing Method 211
D. Users Guide to the Programs 212
X. APPENDIX III 222
A. Electron microprobe methods 223
XI. APPENDIX IV 225
A. NISOMI 226

List of Tables

Table — Page

1. Non-metalliferous minerals observed in thin sections from DDH 334 37

2. Metalliferous minerals observed in polished sections from the 334 Pod (DDH 334) 47

3. Ionic radii of selected ions in 8-fold co-ordination 52

4. Quantitative colour and reflectance data for pitchblendes 53

5. Chemical compositions of first generation pitchblendes (pitchblende I) from the 334 Pod, 11A Zone, Dawn Lake, Saskatchewan 66

6. Chemical compositions of second generation pitchblendes (pitchblende II) from the 334 Pod, 11A Zone, Dawn Lake, Saskatchewan 68

7. Chemical compositions of third generation pitchblendes (pitchblende III) from the 334 Pod, 11A Zone, Dawn Lake, Saskatchewan 71

8. Summary of chemical data for pitchblendes I, II and III from the 334 Pod, 11A Zone, Dawn Lake, Saskatchewan 75

9. Chemical compositions (in wt.%) and atomic compositions of rammelsbergites from the 334 Pod, 11A Zone, Dawn Lake, Saskatchewan 76

10. Chemical compositions (in wt.%) and atomic compositions of nickelines from the 334 Pod, 11A Zone, Dawn Lake, Saskatchewan 84

11. Chemical compositions (in wt.%) and atomic compositions of gersdorffites (334-145.4) paragenetically earlier than pitchblende I from the 334 Pod, 11A Zone, Dawn Lake, Saskatchewan 93

12. Chemical compositions (in wt.%) and atomic compositions of gersdorffites (334-143.8) paragenetically later than pitchblende I from the 334 Pod, 11A Zone, Dawn Lake, Saskatchewan 96

13. Chemical compositions (in wt.%) and atomic compositions of gersdorffites (334-143.2: paragenetically later than pitchblende I but not associated with bismuthian gersdorffite) from the 334 Pod, 11A Zone, Dawn Lake, Saskatchewan 98

14. Chemical compositions (in wt.%) and atomic compositions of gersdorffites (334-143.2: paragenetically later than pitchblende I and associated with bismuthian gersdorffite) from the 334 Pod, 11A Zone, Dawn Lake, Saskatchewan 100

15. Chemical compositions (in wt.%) and atomic compositions of gersdorffites (334-147.0: paragenetically later than pitchblende I and associated with bismuthian gersdorffite) from the 334 Pod, 11A Zone, Dawn Lake, Saskatchewan 103

16. Chemical compositions (in wt.%) and atomic compositions of arsenian gersdorffites from the 334 Pod, 11A Zone, Dawn Lake, Saskatchewan 107

17. Chemical compositions (in wt.%) and atomic compositions of nickelian cobaltites from the 334 Pod, 11A Zone, Dawn Lake, Saskatchewan 110

18. Chemical compositions (in wt.%) and atomic compositions of sulphides from the 334 Pod, 11A Zone, Dawn Lake, Saskatchewan 113

19. Comparison of non-uraniferous minerals from various unconformity-associated uranium deposits within the Athabasca Basin-Cree Lake Zone region 134

20. Chemical ages of first generation pitchblendes (pitchblende I) from the 334 Pod, 11A Zone, Dawn Lake, Saskatchewan 137

21. Chemical ages of second generation pitchblendes (pitchblende II) from the 334 Pod, 11A Zone, Dawn Lake, Saskatchewan 138

22. Chemical ages of third generation pitchblendes (pitchblende III) from the 334 Pod, 11A Zone, Dawn Lake, Saskatchewan 140

23. Summary of ages (in Ma) for first, second and third generation pitchblendes, potassic alteration associated with first-stage mineralisation, and diabase dyke activity associated with Athabasca Basin-Cree Lake Zone uranium deposits 143

24. Average chemical composition of groundwaters in contact with mineralisation at Dawn Lake, Saskatchewan (calculated from data of Cramer, 1986) 154

List of Figures

Figure — Page

1. Schematic geological map of Northern Saskatchewan showing major crustal subdivisions and locations of uranium deposits 3

2. Location map of the Dawn Lake uranium deposits 9

3. Geology of the Athabasca Basin 25

4. Palaeo-currents of the Athabasca Group rocks in the eastern Cree Lake Zone, northern Saskatchewan 28

5. Generalized sub-Athabasca Group basement geology and mineralisation in the Dawn Lake area 34

6. Lithologic section of DDH 334, 11A Zone, Dawn Lake, Saskatchewan 35

7. Mineralogical and colour zonation in the palaeo-weathering (regolith) profile of metasemipelite from the McClean Lake area 41

8. Structural and electrical controls on mineralisation in the Dawn Lake area 44

9. Generalized longitudinal section through, and plan of 11A Zone mineralisation, Dawn Lake, Saskatchewan 46

10. Reflectivity and colour data for first and second generation pitchblendes from the 334 Pod, 11A Zone, Dawn Lake, Saskatchewan 54

11. As:S ratios of gersdorffites (334-145.4) paragenetically earlier than pitchblende I 94

12. As:S ratios of gersdorffites (334-143.8) paragenetically later than pitchblende I 97

13. As:S ratios of gersdorffites (334-143.2) paragenetically later than pitchblende I (but not associated with bismuthian gersdorffite) 99

14. As:S ratios of gersdorffites (334-143.2) paragenetically later than pitchblende I (and associated with bismuthian gersdorffite) 101

15. As:S ratios of gersdorffites (334-147.0) paragenetically later than pitchblende I (and associated with bismuthian gersdorffite) 104

16. Paragenesis of 334 Pod mineralisation, 11A Zone, Dawn Lake, Saskatchewan 132

17. Histogram of chemical ages of first, second and third generation pitchblendes from the 334 Pod, 11A Zone, Dawn Lake, Saskatchewan 144

List of Plates

Plate — Page

1. Asamera's Dawn Lake camp, June 1982 8

2. 334 Pod mineralised core samples (DDH 334) 13

3. Assemblage: nickeline-gersdorffite-pitchblende I-gersdorffite-galena 59

4. Assemblage: gersdorffite-pitchblende I-gersdorffite-bismuthian gersdorffite 59

5. Gersdorffite filling syneresis cracks in massive pitchblende I 61

6. Assemblage: gersdorffite-pitchblende II-pitchblende III-galena 61

7. Assemblage: pitchblende I-gersdorffite-pitchblende II-galena 63

8. Assemblage: pitchblende I-gersdorffite-bismuthian gersdorffite-gersdorffite-pitchblende III 63

9. Assemblage: rammelsbergite-pitchblende I-gersdorffite 65

10. Assemblage: rammelsbergite-nickeline-pitchblende I-gersdorffite 65

11. Assemblage: rammelsbergite-gersdorffite-pitchblende I-gersdorffite 67

12. Brecciated colloform (botryoidal) pitchblende I partially healed by gersdorffite .. 67

13. Assemblage: safflorite-rammelsbergite-nickeline-gersdorffite-cobaltite 81

14. Assemblage: cobaltite-bismuthian gersdorffite-cobaltite-gersdorffite 83

15. Zoned gersdorffite with cores showing different stages of corrosion 88

16. Gersdorffite core partially replaced by pyrite 88

17. Gersdorffite exhibiting zonal and core replacement by pyrite 90

18. Gersdorffite exhibiting core replacement by pyrite and bravoite 90

19. Remobilised nickel: violarite grains 116

20. Remobilised nickel: gersdorffite cores replaced by millerite 116

21. Remobilised nickel: millerite tree-like body coating gersdorffite associated with bismuthian gersdorffite 119

22. Remobilised nickel: millerite laths 119

23. Gold and associated bismuth telluride enclosed by pitchblende I..... 124

I. HISTORY OF EXPLORATION AND PREVIOUS WORK

A. General

Development of unconformity-associated uranium deposits at Key Lake, Cluff Lake and Rabbit Lake in northern Saskatchewan has, in part, enabled Canada to recently become the world's major producer of uranium (Fig. 1). Production at Key Lake, the world's largest uranium-producing mine, presently accounts for 12 per cent of the free world's uranium. The Cigar Lake deposit, discovered in 1981, is claimed to be the largest high-grade uranium deposit ever discovered, and to have the potential to exceed the production of Key Lake. It is therefore not surprising that a large volume of literature has accumulated on deposits of this type, (which also occur in the Pine Creek Geosyncline, Northern Territory, Australia), since the discovery of Rabbit Lake by Gulf Minerals in October, 1968.

Geological mapping in the Athabasca Basin area was first carried out in 1892 by J.B. Tyrell, who charted the route from Lake Athabasca to Prince Albert via Wollaston Lake and the Foster Lakes (Tyrell and Dowling, 1896). Tyrell reported extensive areas of granites and gneiss overlain by sandstones, which he classified as the Athabasca Formation. Tyrell and Dowling (1896) observed sandstone outcrops on islands in Lake Athabasca and along the north and south shores of the lake. More detailed studies of the north shore were performed by Camsell (1915) and Alcock (1915, 1917), and of the south shore by Alcock (1916, 1920, 1936). Tyrell made the first mention of mineralisation in the area when he reported on the presence of Iron Formation at Fish Hook Bay on Lake Athabasca (Tyrell and Dowling, 1896).

Pitchblende was initially discovered in two small veins near Fish Hook Bay in July 1935, during a search for base- and precious-metals (Alcock, 1936). In 1944, the military significance of uranium led to a re-evaluation of all areas in Canada where uranium minerals had been previously reported (Beck, 1977). Exploration of the north shore of Lake Athabasca in the Beaverlodge area resulted in the discoveries of the

Figure 1. Schematic geological map of northern Saskatchewan (modified from Lewry and Sibbald, 1979; Hoeve and Quirt, 1987) showing major crustal subdivisions and locations of uranium deposits.
(1) Key Lake; (2) Cluff Lake; (3) Rabbit Lake; (4) Collins Bay; (5) Dawn Lake; (6) Midwest Lake; (7) Cigar Lake; (8) West Bear; (9) Eagle Point; (10) McClean Lake; (11) Nicholson; (12) Raven and Horseshoe; (13) Fond-du-lac; (14) Maurice Bay; (15) Johnson Island; (16) Stewart Island

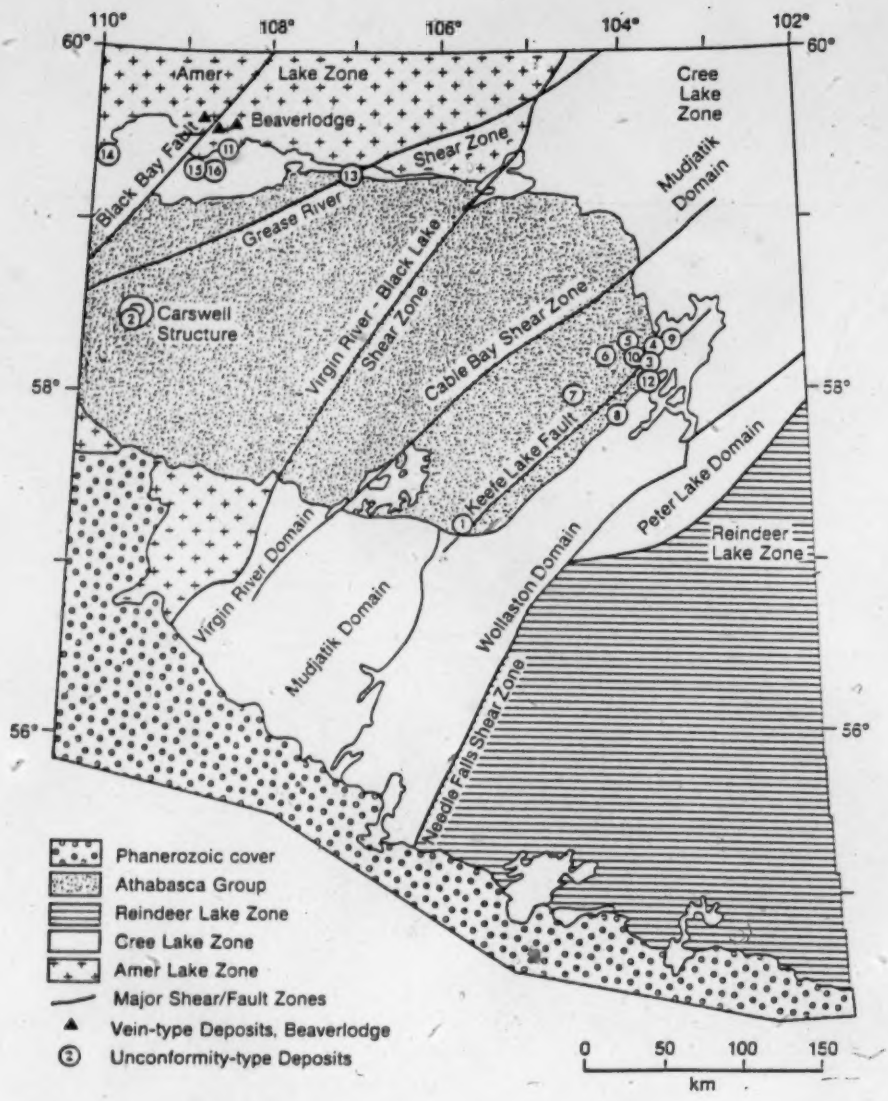
110°
108°
106°
104°
102°
60°
58°
56°
Amer
Lake Zone
Beaverlodge
Cree
Lake
Zone
Black Bay Fault
Shear Zone
Mudjatik
Domain
Grease River
Carswell
Structure
Virgin River - Black Lake
Shear Zone
Cable Bay Shear Zone
Keefe Lake Fault
Peter Lake Domain
Reindeer
Lake Zone
Virgin River Domain
Mudjatik Domain
Wollaston Domain
Needle Falls Shear Zone
Phanerozoic cover
Athabasca Group
Reindeer Lake Zone
Cree Lake Zone
Amer Lake Zone
Major Shear/Fault Zones
Vein-type Deposits, Beaverlodge
Unconformity-type Deposits
0
50
100
150
km

Ace-Fay-Verna (1946) and Gunnar (1952) deposits, as well as many smaller ones. Exploration oriented towards vein-deposits of the Beaverlodge-type, then spread rapidly to other parts of northern Saskatchewan in the 1950's. Although several pitchblende deposits were found at various localities, all, except for the small Nisto deposit at Black Lake were considered to be either too small or too low grade for profitable exploration (Beck, 1977).

For many years the Athabasca Basin was ignored as an area for exploration, for only one uranium occurrence had been reported (Kermeen, 1955) and exploration was discouraged by thick fluvio-glacial overburden (Lang, 1952; Beck, 1977). In 1965, geologists from the French Atomic Energy Commission (CEA) began working in northern Saskatchewan to evaluate the possibility of initiating a uranium exploration program (Tona *et al.*, 1985). Systematic exploration of the Basin began with airborne radiometric surveys over the Fond du Lac area in 1966 and over the Carswell Structure and the Cree Lake area in 1967 (Tona *et al.*, 1985). During this time models of sandstone-type mineralisation (Finch, 1967) and of the supergene concept (Moreau *et al.*, 1966) became exploration guidelines.

The first discovery in the Athabasca Basin, after only five months of exploration, was that of the Rabbit Lake deposit in October 1968, by Gulf Minerals Ltd. working around the eastern edge of the Basin. In 1969, Amok Ltd., operating for the CEA-Amok-Pechiney syndicate, discovered the Cluff "D" orebody at Cluff Lake in the Carswell Structure (Tona *et al.*, 1985). An intensive exploration programme subsequently resulted in the discoveries of the following orebodies at Cluff Lake: "N" (1970), "Claude" (1972), "OP" (1973) and "Dominique-Peter" (1974). The presence of mineralised boulders in glacial sediments played a significant role in these discoveries (Saracoglu *et al.*, 1983).

The discovery of the Rabbit Lake deposit in 1968 caused a staking rush which resulted in hundreds of exploration permits blanketing the Athabasca Basin and the Wollaston domain. Apart from the discoveries by Gulf Minerals Ltd. of "Raven"

(1972) and "Horseshoe" (1974), which occur wholly within rocks of the Wollaston domain not possessing a sandstone cover, nothing of importance was apparently found in the eastern part of the Athabasca Basin and most of the ground was dropped (Beck, 1977). In 1974, uranium was discovered in meta-arkoses of the Wollaston Domain of Duddridge Lake, resulting in a number of exploration projects in the Wollaston domain (Beck, 1977; Haughton, 1977). The discovery of uranium-nickel mineralised boulders in glacial overburden at Zimmer Lake led to the discovery of the Key Lake deposits (Watkinson *et al.*, 1975; Saracoglu *et al.*, 1983). The discovery of the Gaertner (1975) and Deilmann (1976) ore bodies at Key Lake by Uranerz-Inexco Oil-SMDC led to a period of selective staking, as it was then realized that the Rabbit Lake, Cluff Lake and Key Lake deposits were actually related to the unconformity between the clastic sediments of the Athabasca Basin and the metamorphosed basement rocks (Beck, 1977). It was realized also that the Key Lake deposits were underlain by graphitic metapelites of the crystalline basement (Sibbald, 1983).

As the Collins Bay A Zone, discovered in 1976 by Gulf Minerals Ltd., occupied a similar geological position to the Key Lake deposits, graphitic basement rocks, recognizable as electromagnetic conductors, were identified as a possible factor controlling uranium mineralization (Sibbald, 1983). Application of this exploration concept or, as it became subsequently known, the 'Key Lake model' resulted in the identification of the Collins Bay A Zone as a significant deposit and the discoveries of the Collins Bay B Zone (1977), Midwest Lake (1978), Dawn Lake (1978, 1980), McClean Lake (1979, 1980), Eagle Point (1980), Cigar Lake (1981) and JEB (1982) deposits.

B. Dawn Lake Property

The Dawn Lake unconformity-associated uranium deposits comprising four mineralised zones (11, 11A, 11B and 14 Zones) are 20 km northwest of the Rabbit Lake, 9 km northeast of the Midwest Lake, and 8.5 km northwest of the McClean

Lake deposits. The 14 Zone is about 2 km northeast of Dawn Lake. Dawn Lake can be reached by float-equipped aircraft from Wollaston Lake village, 50 km to the east, and from La Ronge, 352 km to the south. Air flights (Norcanair) from Saskatoon to Wollaston Lake village are scheduled twice a week. A winter road connects the Dawn Lake property to the all-weather gravel La Ronge-Rabbit Lake Saskatchewan Highway 102-105.

The majority partner in the ownership of the Dawn Lake property is the Saskatchewan Mining Development Corporation (50.75%) which is also the present field operator.

The Keefe Lake-Henday Lake joint-venture, covering the projects of Dawn Lake, McArthur River and Waterbury Lake, was formed in 1976 to cover the permits acquired by Dr. H.B. Lyall for Kelvin Energy (Fouques *et al.*, 1986). Asamera Inc., a Calgary-based oil and gas firm became the operator of the joint-venture while the Saskatchewan Mining Development Corporation (SMDC) acquired 50 per cent interest in the project by virtue of the Saskatchewan provincial government's Crown Equity Participation Program (Fouques *et al.*, 1986). In 1979 the Keefe Lake-Henday Lake joint-venture was divided into three zones, with Asamera Inc. remaining as operator of the Dawn Lake project (Plate 1).

Exploration began with an airborne radiometric and magnetic survey and a seismic survey (Tremblay, 1982). In 1977, geochemical sampling of lake-, bog- and stream-sediments, in addition to prospecting and surficial geology studies, were followed by airborne electromagnetic and magnetic surveys. Selected anomalous areas were tested by ground electromagnetic surveys (Turam EM) in 1978 (Clarke and Fogwill, 1981, 1985).

The "11" and "14" Zones were discovered at Dawn Lake in 1978 by holes testing Turam conductors (Clarke and Fogwill, 1981, 1985). Drilling along the geophysical extension of the "11" Zone resulted in the discoveries of the "11A" and "11B" Zones in 1979 and 1980 (Clarke and Fogwill, 1981, 1985). A location map of

Plate 1. Asamera's DAWN Lake camp, June 1982

the Dawn Lake uranium deposits is given in Fig. 2.

C. Previous Work

The only descriptive papers published to date on the geology of the Dawn Lake deposits are by Clarke and Fogwill (1981, 1985, 1986), and by Harper (1982). However, the data in all of these papers are virtually identical. The first paper by Clarke and Fogwill (1981) titled 'Geology of the Asamera Dawn Lake Uranium Deposits, Athabasca Basin, Northern Saskatchewan' was published in the CIM Geology Division Uranium Field Excursion Guide Book. Its more detailed companion paper titled 'Geology of the Dawn Lake uranium deposits, northern Saskatchewan' in CIM Special Volume 32 (Geology of Uranium Deposits : Proceedings of the CIM-SEG Uranium Symposium, September 1981, Saskatoon; T.I.I. Sibbald and W. Petruk, eds.) was not published until 1985. This latter paper was republished without changes in 1986 in CIM Special Volume 33 (Uranium Deposits of Canada; E.L. Evans, ed.). In addition a precis of the work of Clarke and Fogwill was done by Harper (1982): Groundwater geochemical data from Dawn Lake were presented by Cramer (1986).

D. Historical Background and Aims of Thesis

On May 18, 1982 a research proposal consisting of three research topics:

(i) mineralogy of metalliferous intersections at Dawn Lake;
(ii) petrographic and geochemical studies of wall rocks; and
(iii) geochronology of the ores in wall rocks

was submitted by Dr. R.D. Morton and E.C.R. Persaud to Asamera Inc., Saskatoon. Asamera's reply to the proposal was favourable and their order of priority for the three research topics was as listed above (letter of May 27, 1982). Asamera suggested that the research topics be divided among at least two graduate students.

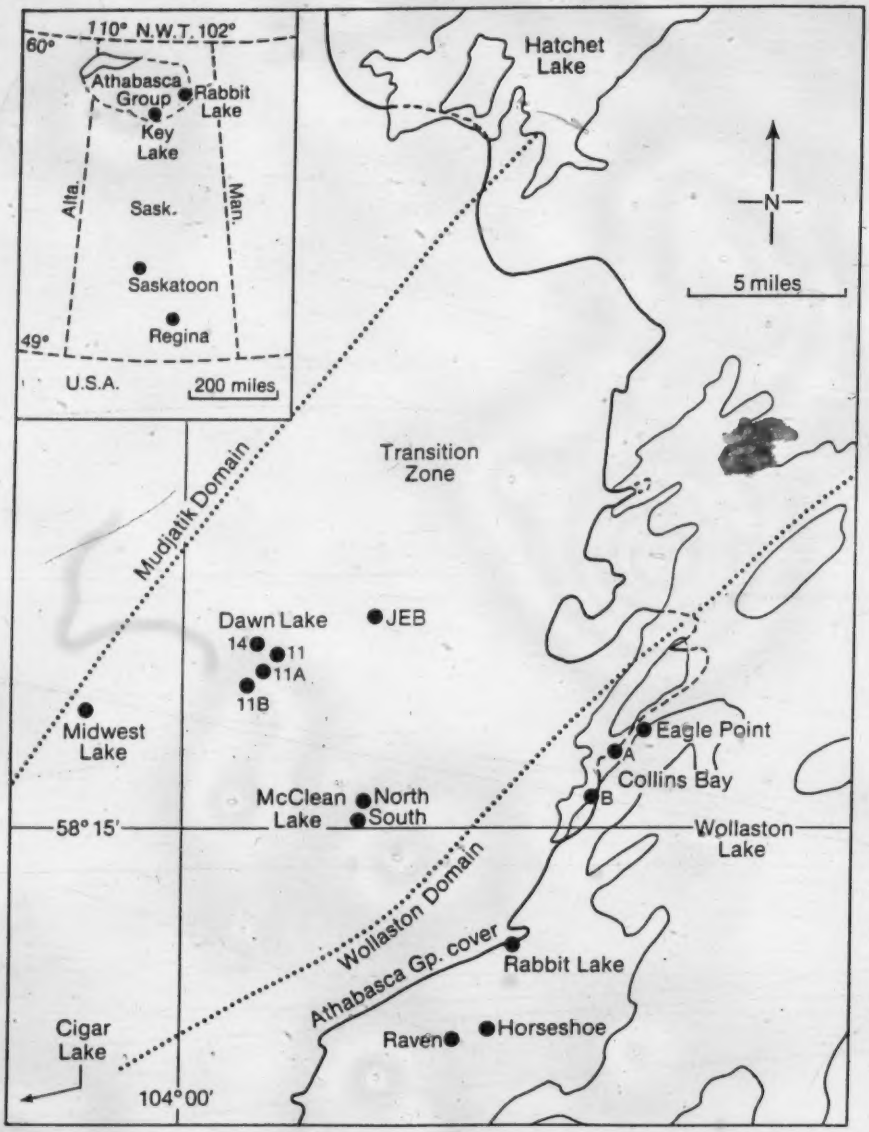

Figure 2. Location map of the Dawn Lake uranium deposits

According to Asamera, 'Topic 1: Mineralogy of the Metalliferous Intersections' was most necessary to their understanding of the deposits and their processability. It was proposed to perform a thorough mineralogical study of metalliferous intersections encountered during drilling. However, in early June 1982, Asamera decided on a specific study of the 334 Pod basement mineralization which was discovered in 1981 (Plate 2). Core collection from Asamera's racks at Dawn Lake occurred in June 1982. However, in late 1982, Asamera Inc. resigned as operator of the Dawn Lake property and SMDC assumed the role of operator before funding arrangements could be finalized. Funding for this project came in the form of an NSERC grant to Dr. R.D. Morton in late 1984. The majority of the research work in this thesis took place between November 1984 and September 1987.

This thesis is primarily intended as a study of the 334 Pod uranium-nickel mineralization occurring in metamorphosed basement rocks of the Aphebian Wollaston Group within the 11A Zone, Dawn Lake, northern Saskatchewan. A study of the chemical ages of different generations of pitchblende mineralization was also carried out.

Plate 2. 334 Pod mineralised samples

II. REGIONAL GEOLOGY

A. Introduction

The following detailed review of previous publications pertaining to the lithostructural character of the Dawn Lake area and its environs is presented herein with the objective of examining the possible roles of the Athabasca Group of basement suites in the genesis of uraniferous hydrothermal fluids during either regional metamorphism or thermal events associated with the intrusion of an ubiquitous diabase suite.

B. General Geology

The early Proterozoic (Aphebian) Manikewan mobile belt of the Churchill tectonic province occupies over 600000 km^2 of the northern parts of the provinces of Saskatchewan and Manitoba and extends into the Northwest Territories (Stauffer, 1984). It forms part of the larger Trans-Hudson orogenic belt that extends for over 5000 km through Greenland, the Canadian Churchill Province and the north-central United States (Green *et al.*, 1985).

Where the belt is exposed it is bounded to the north and northwest by the Archean Churchill (Western) craton, and to the south and southwest by the Archean Superior craton. Where the belt is buried under Phanerozoic sediments, it is bounded to the southwest by the Archean Wyoming craton and to the east by the Superior craton (Green *et al.*, 1985). In the exposed belt the general structural grain trends NNE in the southwest, curving to trend E-W in the northeast.

The Manikewan mobile belt has been divided into three tectonic zones and each zone has been subdivided into a number of lithotectonic belts or domains (units) which have been studied extensively in recent times (Sibbald *et al.*, 1977; McRitchie, 1977; Lewry and Sibbald, 1977, 1980; Bailes and McRitchie, 1978; Lewry *et al.*, 1978, 1981, 1985; Weber and Scoates, 1978; Peredery, 1979; Bailes, 1980; Ray and Wanless,

1980; Lewry, 1981; Baragar and Scoates, 1981; Stauffer, 1984; Fumerton *et al.*, 1984; Drury, 1985; Green *et al.*, 1985; Hegner and Hulbert, 1987; Chauvel *et al.*, 1987; Van Schmus *et al.*, 1987). The Manikewan mobile belt includes the margins of the Superior craton (Churchill-Superior Boundary Zone) and the Churchill craton (Cree Lake zone) which have been remobilised by the Hudsonian orogeny, as well as the intervening Reindeer Lake Zone (a region of disparate terranes, mainly Proterozoic in age) (Stauffer, 1984). The Cree Lake Zone includes the Virgin River, Mudjatik, Wollaston, Seal River and Nejanilini domains. The Reindeer Lake Zone contains the vestiges of two volcanic island arcs (the La Ronge-Lynn Lake belt and the Flin Flon Snow Lake belt), a massive batholithic complex (the Rottenstone-Chipewyan domain) and the remains of two ocean-type basins (the Reindeer-South Indian Lakes belt and the Kisseynew belt). Within the largely Proterozoic terrane exist three regions of unknown origin (the Peter Lake complex, the Glennie Lake domain and the Hanson Lake block) that possess anomalous ages, lithological, structural and/or metamorphic relationships with adjacent domains (Lewry, 1981; Lewry *et al.*, 1981, 1985; Stauffer, 1984).

Except for the youngest intrusive rocks and the relatively undeformed and unmetamorphosed Fox River belt of the Churchill-Superior Boundary Zone, all rock units within the belt are characterised by intense polyphase deformation and regional metamorphism varying from lower greenschist to hornblende granulite facies (Lewry and Sibbald, 1977, 1980; Bailes and McRitchie, 1978; Fraser *et al.*, 1978; Lewry *et al.*, 1981; Stauffer, 1984). In contrast, rocks away from the margin of, and towards the interior of, the Churchill (Western) craton underwent variable but relatively weak thermotectonic overprinting during the Hudsonian orogeny (Lewry *et al.*, 1978). The Superior craton, where exposed, was largely unaffected by Proterozoic events except along its northwestern margin (the Churchill-Superior Boundary Zone) (Weber and Scoates, 1978; Baragar and Scoates, 1981; Green *et al.*, 1985).

The middle Proterozoic (Helikian) Athabasca Group, comprised mainly of fluvial sandstones, overlies the central-northwestern part of the exposed Manikewan

mobile belt and part of the Churchill craton (Amer Lake Zone) (Fig. 1). It is a remnant of a formerly extensive clastic sheet and was possibly derived mainly from the eroding Manikewan mobile belt to the southeast (Ramaekers and Dunn, 1977; Ramaekers, 1981).

The structural evolution of the Manikewan mobile belt has been ascribed to the Hudsonian orogeny, a sequence of events that occurred over a period of 80 Ma beginning at about 1910 Ma (Van Schmus *et al.*, 1987). There are now sufficient reliable geochronologic data to place reasonable limits on the timing of the main tectonic events. Comprehensive summaries of these data are given in Green *et al.* (1985) and Van Schmus *et al.* (1987). Models of Proterozoic plate tectonics involving the opening and closing of ocean basins have been advanced recently for the evolution of the Manikewan mobile belt (Lewry, 1981; Stauffer *et al.*, 1984; Green *et al.*, 1985). They are based upon the recognition of lithotectonic belts or domains and structural features that are equivalent to the main components of a Wilson Cycle of present day plate tectonics.

C. Cree Lake Zone

C.1 General

The Cree Lake zone is a mobile sector within the Manikewan mobile belt (Stauffer, 1984). It forms the southwestern margin of the Churchill (Western) craton and was affected by the Hudsonian orogeny. In northern Saskatchewan, it is subdivided into the Wollaston, Mudjatik and Virgin River domains (Lewry and Sibbald, 1977; Lewry *et al.*, 1978) (Fig. 1). There is some geological evidence for including the Peter Lake complex as part of the Cree Lake zone (Lewry *et al.*, 1981). The Needle Falls and Parker Lake shear zones partially define its eastern boundary, whilst its western boundary is defined in part by the Virgin River shear zone and the Black Lake fault zone.

C.2 Geology

The Cree Lake zone displays a broad bilateral symmetry in metamorphic and structural styles. Its constituent domains exhibit metamorphic continuity and appear to have no major structural or lithologic discontinuities (Lewry and Sibbald, 1977, 1980; Lewry *et al.*, 1978). The zone contains highly deformed, complexly folded, and metamorphosed Aphebian sedimentary and volcanic rocks lying on remobilised Archean granitoid rocks (Lewry *et al.*, 1978; Lewry and Sibbald, 1980). Although most of the granitoids appear to be remobilised Archean basement, some appear to have originated by *in-situ* migmatisation and anatexis of the overlying Aphebian supracrustals (Lewry and Sibbald, 1977, 1980; Lewry *et al.*, 1978). Discrete allochthonous Hudsonian plutons are generally lacking in the Cree Lake zone (Lewry *et al.*, 1978; Lewry and Sibbald, 1980).

In the Virgin River and Wollaston domains, supracrustal rocks occur in narrow, linear, generally continuous zones. Narrow, non-linear, discontinuous zones of supracrustals characterise the Mudjatik domain. In the Virgin River and Mudjatik domains, there is a greater proportion of granitoid rocks to supracrustals, whereas in the Wollaston domain, granitoids and supracrustals occur in roughly equal proportions (Lewry and Sibbald, 1977, 1980).

C.3 Lithology

Near its southeastern boundary in the eastern Wollaston domain, early Aphebian supracrustals, consisting of immature, coarse clastic rocks intercalated with mafic volcanic rocks have been interpreted as continental rift (aulacogen fill) deposits (Lewry and Sibbald, 1980). These were probably deposited in the early stages of the opening of the Manikewan Sea in early Aphebian time (Stauffer, 1984). Later Aphebian supracrustals, which lie unconformably upon the aulacogen deposits and unconformably upon Archean basement over the rest of the Cree Lake zone, probably represent continental shelf-miogeoclinal deposits (Lewry and Sibbald, 1980). These supracrustals

are dominantly semipelitic gneisses in the Virgin River domain, higher grade psammitic to pelitic gneisses and mafic granulites in the Mudjatik domain and quartzites, pelitic gneisses (which are commonly graphitic), psammitic gneisses and calc-silicates in the Wollaston domain (Lewry and Sibbald, 1977, 1980).

Granitoid gneisses occur throughout the Cree Lake zone and are locally charnockitic in the Mudjatik domain (Lewry and Sibbald, 1977, 1980; Lewry *et al.*, 1978). Reconstituted supracrustals are locally preserved in zones of agmatitic, schlieric and nebulitic migmatites (Lewry and Sibbald, 1980). In the Wollaston domain, granitoids within the supracrustals may have resulted from anatexis of the supracrustals (Lewry, 1977; Lewry and Sibbald, 1980). Conversely, rocks of granitic composition and granite pegmatoids within the basement and supracrustals may represent anatectic fractions released during the development of mantled gneiss domes in the Wollaston domain (Lewry and Sibbald, 1980).

C.4 Structure

Three deformational events are evident in the Virgin River and Mudjatik domains and two in the Wollaston domain (Lewry and Sibbald, 1980). The first event involving vertical and lateral flow with the development of recumbent migmatite lobes is common to all domains; granitic gneiss domes being developed in the Wollaston domain. The second event, involving coeval crossfolding, is not seen in the Wollaston domain. It was either not developed or was obliterated by the latest tectonic event. The third event, involving compressional tectonics, resulted in the refolding of the migmatite lobes and crossfolds and the flattening of granitic gneiss domes, leaving a dome and basin interference pattern. Outcrop patterns that result from this polyphase folding are linear in the Virgin River and Wollaston domains and vary from irregular to arcuate to concentric in the Mudjatik domain (Lewry and Sibbald, 1977, 1980).

C.5 Metamorphism

The core of the Cree Lake zone, comprising all of the Mudjatik domain and much of the Virgin River and Wollaston domains, is characterised by low to medium pressure, upper amphibolite-granulite facies assemblages (Lewry and Sibbald, 1977, 1980; Lewry *et al.*, 1978). While there is a gradual decrease in metamorphic grade outwards across the core from its centre, there is rapid convergence of more steeply dipping isograd surfaces and a transition to lower grade zones of the low to medium pressure, middle to lower amphibolite facies adjacent to the margins, which are, in part, major shear zones with a long history of repeated movement (Lewry and Sibbald, 1977, 1980; Lewry *et al.*, 1978). These phenomena within the Cree Lake zone are thought to be indicative of a thermal dome straddling its core (Lewry and Sibbald, 1980).

It has been suggested that only one broad, thermal peak or plateau of extended duration, accompanied or punctuated by deformational episodes, was achieved; and that the early, imposed metamorphic conditions persisted beyond the close of the last significant deformational episode (Lewry et al., 1978; Lewry and Sibbald, 1980).

D. Wollaston Domain

D.1 General

The Wollaston domain is a subdivision of the Cree Lake zone (Lewry and Sibbald, 1977) (Fig. 1). It is bounded on the west by the Mudjatik domain and to the east by the Needle Falls shear zone. It is essentially coincident with the Wollaston Lake belt (Money, 1968; Money *et al.*, 1970).

D.2 Geology

The Wollaston domain is a NE-SW trending, linear belt of supracrustals and granitoid rocks intermixed in approximately equal proportions (Lewry and Sibbald, 1977). The supracrustals form narrow, generally continuous zones between granitoid

domes.

The Wollaston Group supracrustals (Ray, 1977) exhibit a consistent stratigraphy, although spatially restricted, continental rift-type (aulacogenic ?) assemblages are present at the base of the succession (Lewry and Sibbald, 1980; Sibbald, 1983). The continental rift-type assemblages occur locally in the eastern part of the Wollaston domain (e.g. Compulsion River belt) and consist of immature, highly feldspathic, meta-arkoses; polymictic conglomerates and intercalated mafic to intermediate volcanics (Lewry and Sibbald, 1980). Throughout most of the domain, however, the granitoid basement is directly overlain by a dominantly meta-pelitic unit which is graphitic, although a few metres of basal quartzite or meta-arkose can locally intervene between the basement and the graphitic meta-pelites (Gilboy, 1975; Ray, 1977; Potter, 1977; Lewry, 1977).

Overlying the lower meta-pelitic unit is a succession of calcareous and non-calcareous meta-arkoses, interlayered with subordinate calc-silicate bearing rocks and minor pelitic-semipelitic metasediments. This middle meta-arkosic unit is overlain by an upper mixed metasedimentary unit characterised by associated thick quartzites and amphibolites (Sibbald, 1977). It is composed of a well-layered, basal, meta-arkose —— calc-silicate rock —— carbonate sequence which is overlain by quartzites, amphibolites, sillimanite meta-arkoses, pelitic gneisses and calcareous meta-arkosic to semipelitic metasediments. This upper mixed metasedimentary unit, the uppermost supracrustal sequence yet discovered in the Wollaston domain, correlates broadly with the Hidden Bay assemblage (Wallis, 1971).

Granitoids within the Wollaston domain mostly represent remobilised Archean basement, which occurs as foliated, generally homogenous granite-granodiorite bodies present within the cores of periclinal inliers (Lewry and Sibbald, 1980; Sibbald, 1983). The Johnson River granite, a domed basement inlier, has been dated by the U-Pb zircon method at 2494±38 Ma (Ray and Wanless, 1980).

Younger, weakly-foliated to unfoliated granitoids and granite pegmatites within the basement and supracrustals were probably generated as anatectic fractions released during formation of granitoid domes. Unfoliated granitoids in the supracrustals could also have been generated by *in-situ* anatexis of the supracrustals themselves (Lewry, 1977; Lewry and Sibbald, 1980; Sibbald, 1983).

Syn-tectonic to post-tectonic Hudsonian intrusives in the area consist of weakly-foliated to unfoliated, concordant and discordant, microgranite to granite pegmatite sheets, lenses and pods in most supracrustal rocks; weakly-foliated, slightly porphyritic, biotite adamellite forming subconcordant sheets and irregular bodies a few tens of metres thick in the vicinity of Rabbit Lake; and rare, unfoliated, discordant, biotite lamprophyre dykes a few metres wide, one occurring south of First Link Lake and two north of Raven Lake (Lewry and Sibbald, 1980; Sibbald, 1983). A Rb-Sr isochron from the Middle Lake granite, a younger intrusive granite, yields an age of 1765±30 Ma corresponding to metamorphic setting after the main Hudsonian event (Bell and Macdonald, 1982).

D.3 Structure

Two main deformational events have been recognised in the Wollaston domain (Wallis, 1971; Ray, 1977, 1980; Sibbald, 1977, 1979; Lewry, 1977; Lewry *et al.*, 1981; Gilboy, 1982), namely:

(i) An older event causing a penetrative foliation parallel to the basement-cover contact, and thus in general to compositional layering, was developed in the basement and overlying supracrustals during an earlier event. Coeval crossfolding is generally not observed.

(ii) A later deformative event in which the early foliation was refolded by tight, upright-to-steeply inclined, doubly-plunging, minor and major folds with NE trending axial surfaces.

These folds give the domain its linear character (Lewry and Sibbald, 1980; Sibbald, 1983). Granitoid domes occupy major, doubly-plunging, antiformal cores. One or more later sets of folds of minor importance have also been recognised (Wallis, 1971; Scott, 1973; Sibbald, 1977).

In the northeastern part of the Wollaston domain, a prominent set of northerly trending faults marking the northerly extension of the Tabbernor fault system crosscuts the domain (Sibbald, 1983).

D.4 Metamorphism

Low- to medium-pressure upper amphibolite to granulite facies assemblages characterize most of the Wollaston domain (Lewry et al., 1978). A rapid decrease in metamorphic grade to middle to lower amphibolite facies occurs in most areas adjacent to the Needle Falls shear zone, with the disappearance of hypersthene, sillimanite and cordierite, and the appearance of prograde muscovite, staurolite and andalusite in metapelitic rocks. In some areas, higher-grade assemblages occur adjacent to the Needle Falls shear zone (Lewry *et al.*, 1978). In the Wollaston domain, metamorphic mineral growth occurred during the first and after the second deformation events. Retrograde metamorphism accompanied the later fold movements (Lewry *et al.*, 1978).

E. Mudjatik Domain

E.1 General

The Mudjatik domain is a subdivision of the Cree Lake zone (Lewry and Sibbald, 1977) (Fig. 1). It is bounded to the west by the Virgin River domain and to the east by the Wollaston domain.

E.2 Geology

The Mudjatik domain consists mainly of granitoid gneisses. Supracrustal rocks are arranged in thin, discontinuous zones with non-linear outcrop patterns ranging from arcuate to closed loop (Lewry and Sibbald, 1977, 1980; Lewry *et al.*, 1978; Sibbald, 1983).

Granitoid gneisses within the Mudjatik domain for the most part are interpreted as remobilised Archean basement. A Rb-Sr isochron of 2613±93 Ma has been obtained from granitoid gneisses flanking the Midwest deposit to the west (Worden *et al.*, 1985). Some granitoid gneisses were apparently derived from migmatisation and anatexis of the supracrustals, relicts of which are locally preserved in zones of agmatitic, schlieric and nebulitic migmatites (Lewry and Sibbald, 1980; Sibbald, 1983).

Granitoid gneisses form a complexly mixed group of rocks of broadly granitic composition, i.e., quartz (10 - 40 per cent), plagioclase and/or K-feldspar, and one or more of the following mafic constituents: biotite, hornblende, hypersthene, garnet, cordierite and iron oxides (Lewry and Sibbald, 1977).

Texturally, the granitoid gneisses are of variable character ranging from homogenous or massive to inhomogenous or layered. All intermediates between these two end members apparently exist and admixture appears to occur on all scales (Lewry and Sibbald, 1977, 1980; Sibbald, 1983). Layering is dependent upon biotite content and leucosomal segregation. Massive varieties apparently have invaded and replaced layered varieties during remobilisation.

Along the flank of the eastern margin of the Athabasca Basin, in the vicinity of Collins Bay, exposed granitoid gneisses of the Mudjatik domain are commonly pink to grey, medium-grained and contain quartz (10-40 per cent), plagioclase, K-feldspar and biotite (0-10 per cent) (Sibbald, 1983). Along the flank of the northeastern margin of the Athabasca Lake and in the vicinity of Hatchet Lake, exposed rocks of the Mudjatik domain consist chiefly of granitoid gneisses with several elongate, narrow belts of pelitic to semipelitic metasedimentary gneiss (Ray, 1978). The granitoid gneisses

are well-layered quartzo-feldspathic migmatitic gneisses containing thin layers of amphibolite and biotite schist; pink, massive to well-foliated granitic rocks with amphibolite xenoliths formed when the original layering was destroyed by increasing remobilisation; and massive to well foliated, medium- to coarse-grained, dark, hypersthene-bearing charnockitic granitoids (Ray, 1978; Sibbald, 1983).

Supracrustal rocks of the Mudjatik domain are considered to be Aphebian in age and equivalent to the Aphebian Wollaston Group of the Wollaston domain (Lewry and Sibbald, 1980). They include pelitic to psammitic gneisses, mafic granulites (amphibolites, pyribolites and pyriclasites) and subordinate quartzites, calc-silicate rocks, marbles, ultramafic rocks and oxide-silicate-sulphide facies banded iron formation in the region southwest of the Cree Basin (Ramaekers, 1981), a sub-basin of the Athabasca Basin; and pelitic to semipelitic gneisses, calc-silicate rocks, marbles, amphibolites and quartzites in the area to the northeast of the Cree basin (Lewry and Sibbald, 1980; Sibbald, 1983).

E.3 Structure

Three major deformational events are recognised in the Mudjatik domain (Lewry and Sibbald, 1977, 1980; Sibbald, 1983). The first event gave rise to a flat-lying, penetrative foliation and coeval isoclinal folding, on both a minor and major scale, and was responsible for migmatite nappe formation and the occurrence of supracrustal zones at different structural levels within the granitoid gneisses. The second and third major events produced suborthogonally oriented, upright fold sets on WNW and NE axial surfaces, respectively, deforming the early foliation into a dome and basin interference pattern. In some areas, a fourth generation of minor folds with gently dipping axial surfaces is developed sporadically.

Two generations of faults are recognised (Sibbald, 1983). An earlier set of thrust faults are on average NE-trending. Later reactivation of these faults resulted in them cutting the Athabasca Group (Clarke and Fogwill, 1981, 1985). A later set of

faults with left-lateral-strike slip forms part of the north-trending Tabbernor fault system.

E.4 Metamorphism

Metamorphic mineral assemblages of the Mudjatik domain indicate low- to medium-pressure upper amphibolite to granulite facies conditions (Lewry and Sibbald, 1977, 1980; Lewry *et al.*, 1978). Granitoid gneisses are locally charnockitic and hypersthene is common in mafic granulites (Lewry and Sibbald, 1977; Ray, 1978; Gilboy, 1978). Pelitic and semipelitic metasediments commonly contain cordierite and accessory hercynite, and generally have undergone advanced migmatisation (Gilboy, 1982).

High-grade metamorphism appears to have accompanied the three major deformational events and retrograde effects are generally only locally or weakly developed (Lewry and Sibbald, 1977, 1980; Lewry *et al.*, 1978).

F. The Wollaston-Mudjatik Junction

Rocks of the Wollaston and Mudjatik domains are exposed in areas northeast, east and southwest of the Cree sub-basin of the Athabasca basin. In these areas, the junction between the domains is fairly well defined (Lewry and Sibbald, 1977, 1980; Ray, 1978; Sibbald, 1983). Where these domains are overlain by Athabasca Group sediments, their junction is not well defined (Clarke and Fogwill, 1981; Sibbald, 1983).

The Wollaston and Mudjatik domains are distinguished mainly on the basis of their lithostructural characteristics and contrasting structural styles. Additional criteria are differences in character of the granitoid rocks and the supracrustals (Ray, 1978; Lewry and Sibbald, 1980).

Lewry and Sibbald (1980) proposed a generalised thermotectonic model for the evolution of the Cree Lake zone. If this model is valid, then the junction separates a region of migmatite nappe lobes (Mudjatik) from one characterised by mantled gneiss

doming (Wollaston). The junction will be marked by a discordance along which allochthonous Mudjatik domain elements are brought into contact with autochthonous elements of the Wollaston domain.

Clarke and Fogwill (1981), however, have proposed the existence of a Mudjatik-Wollaston transition zone in the region west of Wollaston Lake. This transition zone would be located between the Hatchet Lake - Waterbury Lake lineament to the west and the Collins Bay - Lampin Lake junction to the east (Clarke and Fogwill, 1981; Sibbald, 1983). Several major uranium deposits (Cigar Lake, Midwest Lake, Dawn Lake, McClean Lake, JEB) would be located above and within this transition zone.

G. Athabasca Group

The Athabasca Group rocks today occupy an elliptical basin measuring over 400 km east to west and over 200 km north to south in northern Saskatchewan and Alberta. The Athabasca Basin has been subdivided, on the basis of seismic studies, into three NE-trending sub-basins: the Jackfish, Mirror and Cree Basins (Hobson and MacAulay, 1969, Ramaekers, 1981). The existence of these sub-basins has been confirmed by stratigraphic analysis (Ramaekers, 1979, 1980, 1981). These sub-basins coalesced at an early stage when they were infilled by sediments of the Middle Proterozoic (Helikian) Athabasca Group, a molasse wedge shed from the eroding Manikewan mobile belt (Ramaekers, 1981). Chemical and petrographic studies in addition to stratigraphic and sedimentologic analysis suggest that the sediments of the Athabasca Group were immature at the time of deposition and are first-cycle deposits derived from a quartz-rich metamorphic source (Ramaekers, 1981).

The Paleohelikian Athabasca Group consists of unmetamorphosed, quartz-rich clastics and dolomites, and has been intruded by diabase dykes (Ramaekers, 1981). It comprises the Manitou Falls, Fair Point, Lazenby, Wolverine Point, Locker Lake, Otherside, Tuma Lake, Douglas and Carswell Formations (Ramaekers, 1981) (Fig. 3).

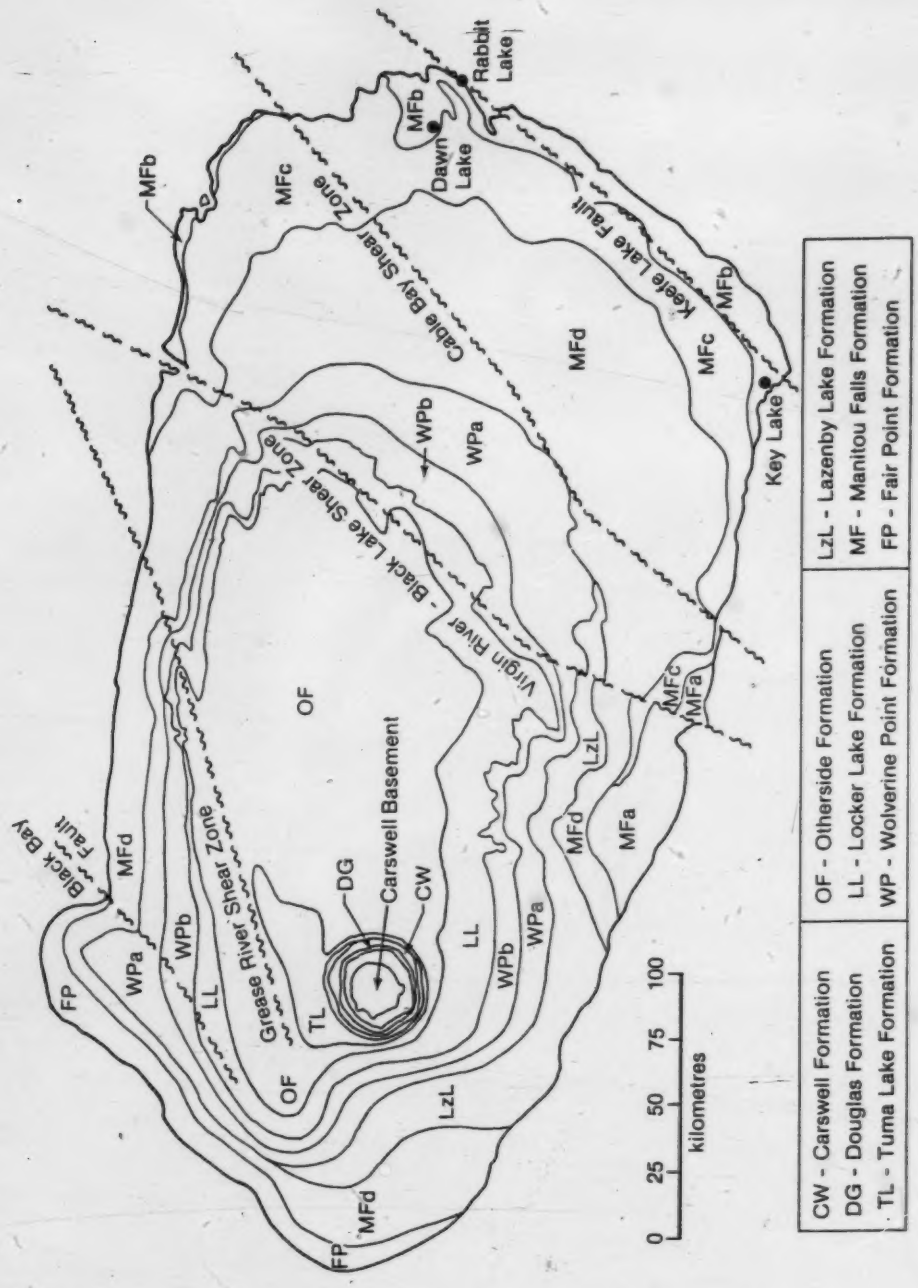

Figure 3. Geology of the Athabasca Basin (modified from Ramaekers, 1980; Hoeve and Quirt, 1987)

Ramaekers (1980, 1981) characterised the bulk of the Athabasca Group as nearshore marine, commonly with a tidal influence, largely on the basis of hummocky cross-bedding and herringbone cross-bedding; the Manitou Falls Formation is the sole exception, where low paleocurrent variance at the outcrop level and abundant clay intraclasts in some horizons are taken to indicate interbedded fluvial units. In the Cree Basin, all formations above the lowest member of the Wolverine Point Formation (Wolverine Point A) which occurs in the western part of this sub-basin, have been eroded (Ramaekers, 1981).

In the eastern part of the Cree Basin, the Manitou Falls members B, C and D form an eastward-thickening wedge of fluviatile sandstones and conglomerates that comprise the regressive phase of the Athabasca Group (Ramaekers, 1981, 1983) (Fig. 3). The Manitou Falls B, the lowermost member of this sequence, consists of eastward-coarsening interbedded sandstones and clast-supported conglomerates which may attain a thickness of up to 300 metres (Ramaekers, 1981). Ramaekers (1983) showed this member to have the highest mean permeability compared to other sandstone members and formations. The rocks of this unit are interpreted as conglomeratic braided stream deposits (Ramaekers, 1981, 1983). Palaeocurrent directions define a number of radiating alluvial fans. These fans or bajadas can be divided into two major regional sedimentary tongues or deposystems, one derived from the northeast (Moosonees), the other (Ahenakew) from the eastern side of the basin (Ramaekers, 1977, 1981, 1983).

In the Dawn Lake area, the sandstones and conglomerates of the Athabasca Group have been assigned to the B member of the Manitou Falls Formation (Ramaekers, 1981). Drill core data allow these rocks to be divided into three units, namely: (1) an upper unit of medium- to coarse-grained sandstone, 30 to 70 metres in thickness; (2) a middle unit of polymictic conglomerate, 5-10 metres thick; and (3) a lower unit of medium- to coarse-grained sandstone and discontinuous basal conglomerate, about 30 metres in thickness. The basal conglomerate occupies depressions in the pre-Athabasca Group topography. Palaeocurrent vectors show that these

sediments were derived from the south-east, and generalised flowlines cross the strike of the underlying basement at a high angle (Ramaekers, 1981, 1983) (Fig. 4). From palaeocurrent data and sedimentological analyses it has been suggested that the conglomerates of the Wollaston Lake area represent the northern sector of a large alluvial fan (Ramaekers, 1981, 1983).

H. Diabase Dykes In The Athabasca Basin

The Athabasca Group has been intruded by an extensive series of diabase dykes which have penetrated highest into the sediments of the Mirror Basin (Ramaekers, 1981). Dyke outcrops are uncommon. Diabase dykes are reflected as prominent linear magnetic anomalies (Ramaekers and Hartling, 1979, Hoeve *et al.*, 1980). They reoccupied Hudsonian N-S faults and formed or occupied extensive northwesterly fracture zones or faults (Ramaekers and Hartling, 1979). The dykes generally dip steeply NE or SW but some individual bodies displaying a great variation in strike and dip may be sill-like structures (Ramaekers and Hartling, 1979). They are generally columnar, jointed and range from a few to a hundred metres in width.

The dykes are composed mainly of labradorite, augite and magnetite with minor olivine, orthoclase, quartz, biotite, hornblende and chlorite (Ramaekers and Hartling, 1979). Some dykes intersected by drillholes are serpentinised. They show evidence of rapid cooling and of baking of the adjacent sandstone. Pitchblende mineralisation occurs in some dyke rocks, along fractures and is accompanied by chloritic host-rock alteration. Thermally altered sandstone near the dykes may also be mineralised (Hoeve *et al.*, 1980).

Age limits for dyke emplacement suggested by K-Ar methods are 777±25 Ma (Armstrong and Ramaekers, 1984) and 1230 Ma (Burwash *et al.*, 1962). Rb-Sr dates , however suggest a narrower interval with ages ranging from 1080±100 Ma (Ray, 1980) and 1100±100 Ma (Armstrong and Ramaekers, 1984) to 1310±70 Ma (Armstrong and Ramaekers, 1984).

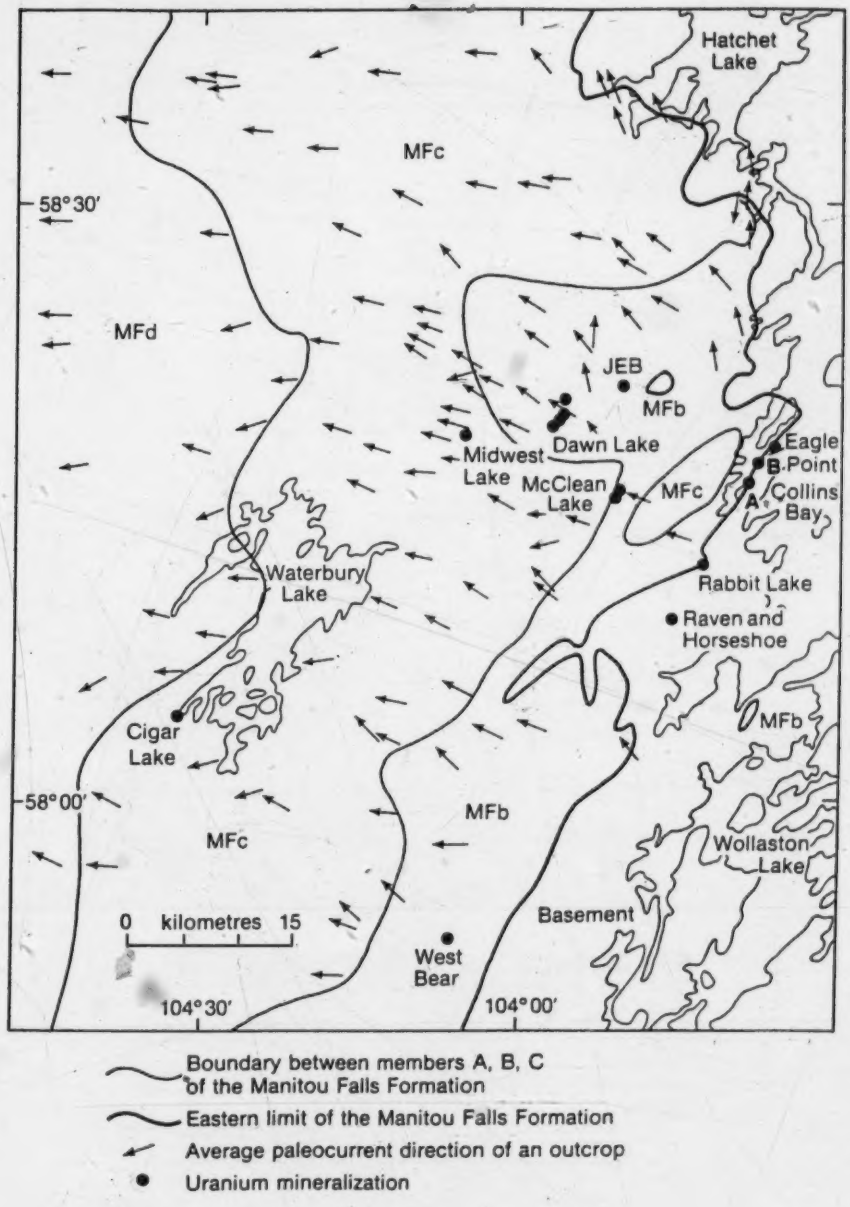

Figure 4. Palaeo-currents of the Athabasca Group rocks in the eastern Cree Lake Zone, northern Saskatchewan (modified from Ramaekers, 1983)

I. The Age Of The Athabasca Group

The age of the Athabasca Group is a subject of continuing controversy (Ramaekers, 1981; Cumming *et al.*, 1987). A minimum age of 1513±24 Ma (Rb-Sr: whole rock) for the onset of sedimentation in the Athabasca Basin was obtained on the tuffaceous unit of the Wolverine Point B member (Bell and Blenkinsop, 1980; Ramaekers, 1980, 1981). Bray *et al.* (1987) reported ages of 1484±55 Ma (K-Ar: illite) and 1459±4 Ma (Ar-Ar: illite) for the underlying Manitou Falls Formation near the McClean Lake uranium deposit.

Cumming *et al.* (1987), however, obtained two distinct U-Pb ages in the range 1650-1700 Ma for authigenic fluorapatite from the Wolverine Point B member, and goyazite [$SrAl_3(PO_4)(OH)_5$] from the underlying Fair Point Formation. The Wolverine Point Formation, the earlier of the two marine intercalations in the Athabasca Group, is located approximately 1000m above the basin floor (Ramaekers, 1981; Wilson, 1985). Thus it would appear that by 1650 Ma, approximately 1000m of sediments were already laid down in the Athabasca Basin.

Hoffman (1984, 1987a, 1987b) argued that major cratonisation of North America and northern Europe occurred between 1950-1800 Ma ago, with the assembly of several Archean cratonic elements and intervening 1900-1850 Ma old convergent plate-margin assemblages into a major early Proterozoic continental craton.

Van Schmus *et al.* (1987) have presented geochronological evidence (U-Pb: zircon) to show that the main period of magmatism associated with the Reindeer Lake Zone of the Trans-Hudson Orogeny spanned a relatively short interval (1910-1830 Ma). Formation of marginal volcanic arcs was well advanced by 1880-1870 Ma ago and was followed by major plutonism and accretion of the Reindeer Lake Zone complex to the reworked continental margin (Cree Lake Zone) by about 1860-1850 Ma ago. By 1830 Ma, major thermotectonism had waned or ceased. Sm-Nd geochronological studies yielded similar ages for Hudsonian volcanism and plutonism (Chauvel *et al.*, 1987; Hegner and Hulbert, 1987). A high-grade metamorphic, mineral-forming event occurred

at about 1775 Ma (Van Schmus *et al.*, 1987); this age is identical to that obtained for first generation pitchblendes of Beaverlodge-type mineralization (1780 Ma: Koeppel, 1968). Most Rb-Sr whole rock ages (1700-1750 Ma) reported from the Reindeer Lake Zone are distinctly younger than the U-Pb zircon ages and may represent resetting during a later period of tectonic activity, or isotopic closure with decrease in temperature subsequent to the metamorphic event at 1775 Ma (Van Schmus *et al.* (1987).

Ramaekers (1981) suggested that the Martin Lake Basin as well as the sub-basins within the Athabasca Basin were formed as a series of pull-apart structures related to transcurrent faulting. Ramaekers (1981) has also suggested that the sediments of the Athabasca Group, like those of the Martin Formation, were immature at the time of deposition and were first-cycle deposits derived from a quartz-rich metamorphic source. If that was the case, then Athabasca Group and Martin Formation sediments represent molasse wedges shed off the Trans-Hudson Orogen (Ramaekers, 1981). If the Wolverine Point Formation volcanics were related to Hudsonian volcanism, then it would appear that the initial phase of Athabasca Group sedimentation would have to be bracketed by the end of Reindeer Lake Zone volcanism at 1875 Ma (Van Schmus *et al.*, 1987), and the phosphate cementation age of 1700 Ma (Cumming *et al.*, 1987).

The idea that Athabasca Basin sedimentation commenced before 1700 Ma is supported by geochronological data from the possible coeval Martin Formation and the Thelon Formation. The Martin Formation has been dated at 1730±100 Ma by a combination of K-Ar ages (Fraser *et al.*, 1970) and palaeomagnetic data (Evans and Bingham, 1973). Three distinct similar U-Pb ages (1720±6 Ma, 1685 ±4 Ma, and 1647 Ma were obtained for authigenic phosphates (fluorapatite and goyazite) from the Thelon Formation (G. Cumming, pers. comm.). Authigenic phosphate cementation in the Thelon Formation at 1720±6 Ma followed Pitz Formation volcanism at about 1760 Ma (Rb-Sr: whole rock; G. Cumming, pers. comm.). Considering that the age of the

Pitz Formation volcanics resembles the younger Rb-Sr ages (1700-1750 Ma) of Reindeer Lake Zone magmatic events, an older age for the Pitz Formation volcanics would not be unreasonable.

J. Uranium Mineralisation In The Cree Lake Zone

Uranium deposits in the Cree Lake Zone are termed "unconformity-associated deposits". Morton (1977) has argued that the term is semantically unfortunate as it places too much emphasis upon the role of the sub-Athabasca Group unconformity alone in the genesis of these deposits. Major deposits in this sector are the Cigar Lake, Collins Bay, Dawn Lake, Eagle Point, Horseshoe, JEB, Key Lake, McClean Lake, Midwest Lake, Raven and West Bear deposits (Figs. 1, 2). Minor occurrences are at Close Lake, Natona Bay and Sand Lake.

Uranium mineralisation can occur in the unmetamorphosed Athabasca Group sediments above and at the unconformity, in regolith at and below the unconformity and in altered, metamorphosed basement rocks of the Wollaston Group below the regolith. The deposits may be associated with or be without significant graphite. Graphite associated with a deposit is capable of producing a clear EM response (Saracoglu *et al.*, 1983). Deposits associated with significant graphite are Cigar Lake, Collins Bay, Dawn Lake, Eagle Point, JEB, Key Lake, McClean Lake, Midwest Lake and West Bear. The Rabbit Lake, Raven and Horseshoe deposits are not associated with significant graphite. In these cases graphite may have been destroyed during mineralisation (Fogwill, 1985).

In basement suites of the Wollaston domain and the transitional Mudjatik-Wollaston junction, stratabound uranium mineralisation occurs in graphitic metapelites, calc-silicates and in pegmatoids. Ores occur in a lower meta-pelitic unit (Collins Bay, Eagle Point, McClean Lake, Key Lake, Midwest Lake), a middle meta-arkosic unit (Rabbit Lake, JEB, Raven, Horseshoe) and in an upper mixed metasedimentary unit (Dawn Lake). At Rabbit Lake, Eagle Point and Dawn Lake (11B

Zone), Raven and Horseshoe, the ore lies entirely in basement rocks. The bulk of the mineralisation at Key Lake and Dawn Lake is hosted by basement rocks (Dahlkamp, 1978; Clarke and Fogwill, 1985). The Collins Bay A Zone is hosted entirely by regolith, above which most of the Athabasca Group has been removed (Heine, 1981).

The deposits in direct contact with the Sub-Athabasca Group unconformity are Cigar Lake, Collins Bay (B Zone), Dawn Lake (11 and 11A Zones), JEB, Key Lake, McClean Lake, Midwest Lake and West Bear. At Cigar Lake, Dawn Lake (11 Zone), JEB, McClean Lake, Midwest Lake and West Bear, the bulk of the ore reserves is in direct contact with the unconformity. Most of the ore at Collins Bay (B zone) lies within Athabasca Group sediments just above the unconformity (Heine, 1981).

Rarely does mineralisation occur in Athabasca Group sediments high above the unconformity (e.g., Dawn Lake 14 Zone: Clarke and Fogwill, 1981, 1985; Cigar Lake-perched mineralization: Fouques *et al.*, 1986).

III. LOCAL GEOLOGY OF DAWN LAKE

A. Regional Setting of the Dawn Lake Deposits

Geophysical and drill data have been used to interpret the basement geology of the Dawn Lake deposits, which occur below 100 metres of Athabasca Group clastic sediments, and glacial overburden (Clarke and Fogwill, 1981, 1985) (Fig. 5). A regional magnetic survey of the NEA/IAEA study area (Kornik, 1980) places the Dawn Lake deposits in a broad area of low magnetics far from any higher magnetic basement 'domes', which probably are Archean magnetite-bearing gneisses of granitic origin (Clarke and Fogwill, 1981, 1985). The Dawn Lake deposits are apparently higher in the Aphebian stratigraphy than the Midwest Lake, McClean Lake and Collins Bay deposits which lie close to the edges of the Archean gneissic domes.

McNutt (1980) recognized three stratigraphic sequences within the Wollaston Group in this area through variations in magnetic character and the relative abundance of EM conductors. These, in ascending order are a lower metapelitic sequence, a middle or intermediate meta-arkosic sequence and an upper mixed metasedimentary sequence, all deposited above the more magnetic Archean granitoid gneisses. The Dawn Lake deposits occur in the upper mixed metasedimentary sequence (Clarke and Fogwill, 1981, 1985) (Fig. 5).

B. Lithologies

At Dawn Lake, approximately 100 metres of Helikian (Middle Proterozoic). Athabasca Group sandstones and conglomerates overlie Aphebian (Lower Proterozoic), Wollaston Group calcareous, pelitic and psammitic metasediments cut by anatectic pegmatoids (Clarke and Fogwill, 1985). In the 11A Zone, above the 334 Pod, 86 metres of Athabasca Group rocks (unmetamorphosed sandstones and conglomerates) overlie Aphebian sediments and pegmatoid rocks. The local metamorphic suite contains the following rock units (Fig. 6):

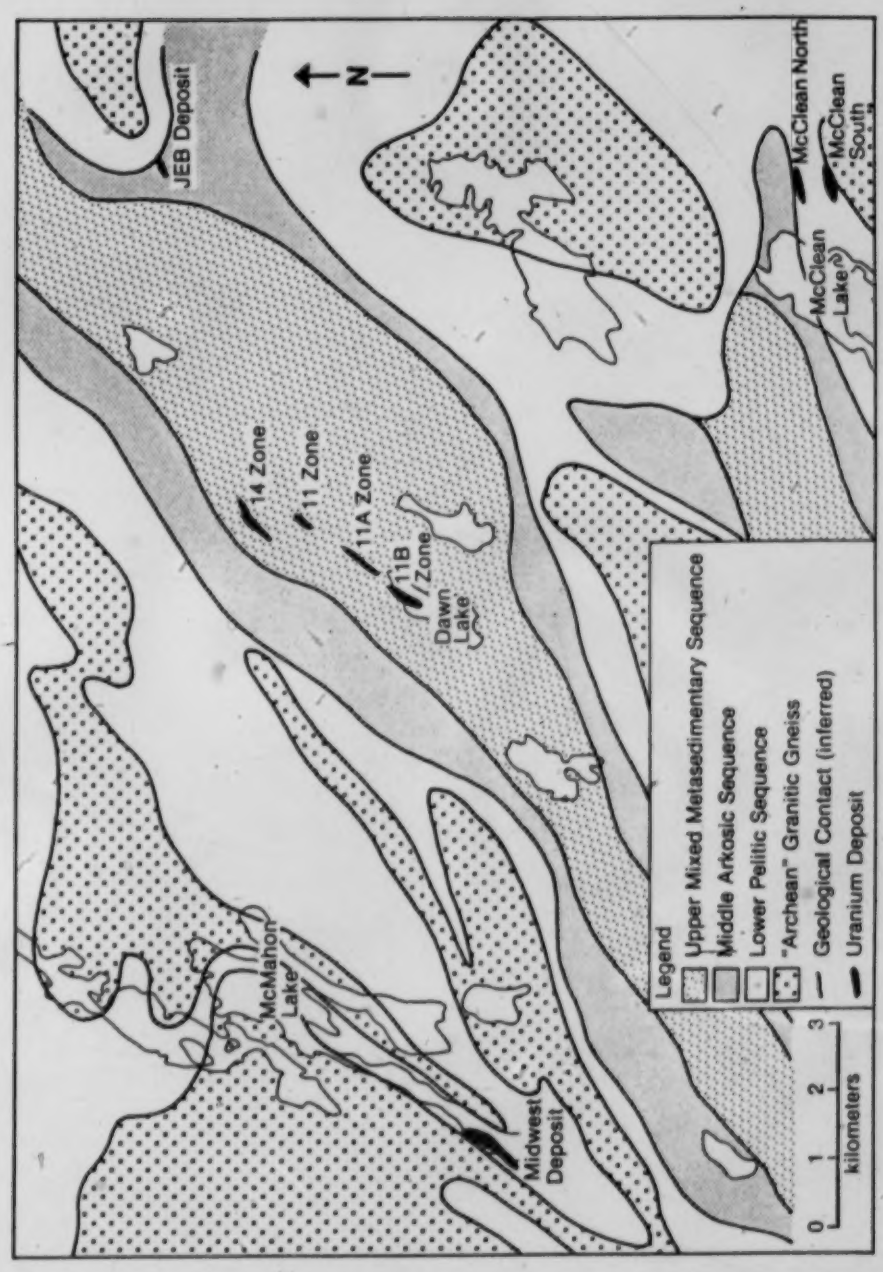

Figure 5. Generalised sub-Athabasca Group basement geology and mineralisation in the Dawn Lake area (modified after Clarke and Fogwill, 1985, 1986)

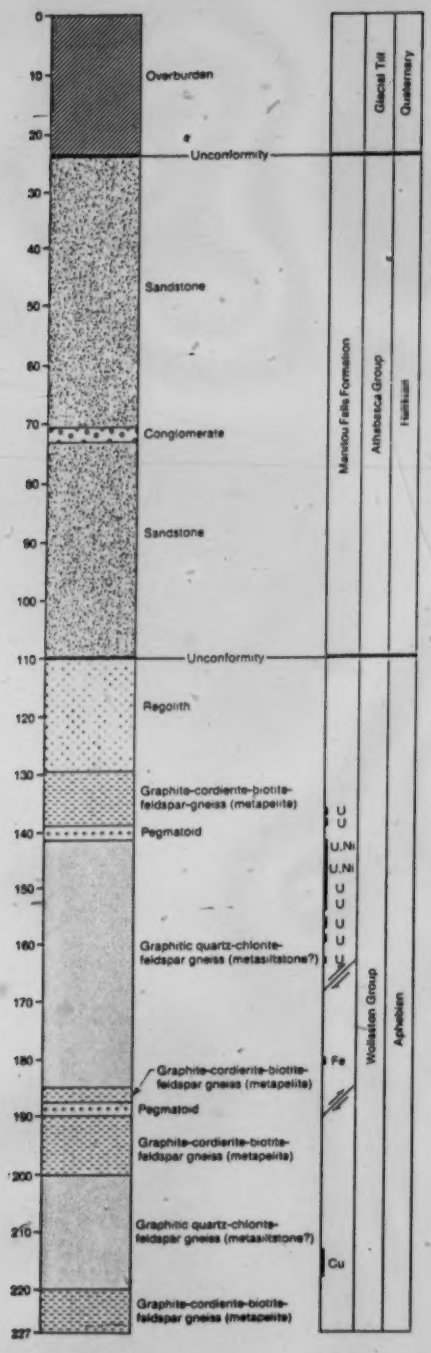

Figure 6. Lithologic section of DDH 334, 11A Zone, Dawn Lake, Saskatchewan

(i) graphite-cordierite-biotite-feldspar gneiss (metapelite)

(ii) graphitic quartz-chlorite-feldspar gneiss (metasiltstone?)

(iii) anatectic pegmatoids.

Below the Athabasca Group-Wollaston Group unconformity, a palaeo-weathering profile or 'regolith' has developed on the Wollaston Group metamorphic rocks. A list of minerals observed during the examination of thin sections from DDH 334 is given in Table 1.

(i) The graphite-cordierite-biotite-feldspar gneiss (metapelite)

The graphite-cordierite-biotite-feldspar gneiss hosts little of the uranium-nickel mineralization in 334 Pod. This rock type is dark grey in hand specimen, fine- to medium-grained and well-foliated. The major minerals in this unit are quartz (25-30%), feldspar (30-40%), biotite (15-20%), cordierite (5-10%) and graphite (5-10%). This rock type is termed metapelite by Clarke and Fogwill (1985). It corresponds to the McClean Lake metasemipelite of Macdonald (1980, 1985).

Quartz in this rock type has two modes of occurrence. The first consists of small rounded to sub-rounded grains less than 0.5 mm, poikilitically enclosed in cordierite and plagioclase and later quartz. Quartz inclusions are also observed in tourmaline (var. dravite). The second and major occurrence of quartz is present as polycrystalline aggregates of strained, interlocking, anhedral crystals exhibiting undulose extinction.

Plagioclase is rarely fresh and is almost always saussuritized. Even in the samples from the deepest part of drill holes, plagioclase is almost totally destroyed. Plagioclase normally exhibits a poikiloblastic texture, enclosing quartz grains and flakes of biotite and graphite.

Biotite occurs as strongly pleochroic grains (light-brown to dark reddish-brown), possessing a preferred orientation parallel to the compositional

Table 1: Non-metalliferous minerals observed in thin sections from DDH 334.

	Depth(m)	Qtz	Plg	Kfs	Crd	Btt	Chl	Tml	Epd	Ill	Pin	Grp	Car
1)	106.3	x	-	-	-	-	-	x	-	x	-	-	-
2)	107.4	x	-	-	-	-	-	-	-	x	-	-	-
3)	115.7	x	a	-	-	a	x	x	-	x	-	-	-
4)	119.0	x	a	-	-	a	x	x	-	x	-	-	-
5)	120.2	x	a	-	-	a	x	x	-	x	-	-	-
6)	125.1	x	a	-	-	a	x	x	-	x	-	-	-
7)	126.5	x	a	-	a	a	x	x	-	x	x	-	-
8)	130.3	x	a	-	-	a	x	x	-	x	-	x	-
9)	132.2	x	a	-	a	a	x	x	-	x	x	x	-
10)	134.6	x	a	-	-	a	x	-	-	x	-	x	-
11)	141.0	x	?	?	-	-	-	x	-	x	-	-	x
12)	142.5	x	?	?	-	-	-	x	-	x	-	x	x
13)	154.3	x	a	?	-	-	x	-	-	x	-	x	x
14)	163.2	x	a	?	-	-	x	-	-	x	-	x	-
15)	165.0	x	a	?	-	-	x	-	-	x	-	x	-
16)	171.0	x	a	?	-	-	x	-	-	x	-	x	-
17)	181.0	x	a	x	-	-	x	-	x	x	-	x	-
18)	188.0	x	a	a	-	-	-	x	-	x	-	-	-
19)	190.2	x	?	-	x	x	?	x	-	?	x	x	-
20)	195.0	x	?	-	x	x	?	-	-	?	x	x	-
21)	195.5	x	?	-	a	x	?	-	-	?	x	x	-
22)	195.8	x	?	-	x	x	?	x	-	?	x	x	-
23)	199.0	x	?	-	x	x	?	-	-	?	x	x	-
24)	204.8	x	x	-	x	-	-	x	-	x	x	x	-
25)	209.5	x	x	x	-	-	-	x	-	x	-	x	-
26)	212.5	x	x	x	-	-	-	x	-	x	-	x	-
27)	213.6	x	x	x	-	-	-	-	-	x	-	x	-
28)	217.0	x	x	x	?	-	-	-	-	x	?	x	-
29)	222.0	x	x	-	x	x	?	x	-	x	x	x	-

Qtz: quartz; Plg: plagioclase; Kfs: K-feldspar; Crd: cordierite; Btt: biotite;

Chl: chlorite; Tml: tourmaline; Epd: epidote; Ill: illite; Pin: pinite;

Grp: graphite; Car: carbonate; x: present; a: altered; ?: uncertain

layering of the rock. Biotite is poikilitically enclosed by cordierite and plagioclase, and appears to be intimately associated with graphite. Pleochroic haloes in biotite were not observed.

Graphite occurs as elongated flakes of up to 1 mm in length that are oriented parallel to the foliation. Graphite is poikilitically enclosed by cordierite and plagioclase and appears to be intimately associated with biotite.

Accessory minerals in this rock type are rutile, magnetite, apatite and tourmaline (var. dravite). Two varieties of tourmaline (dravite) are observed. The first is an earlier porphyroblastic bronze-coloured, anhedral to subhedral dravite with occasional quartz inclusions, whilst the second is characterised by radiating acicular aggregates of white tourmaline. Radiating acicular aggregates of tourmaline develop under non-stress conditions, e.g., post-tectonically in regionally metamorphosed rocks (Spry, 1969).

(ii) The graphitic quartz-chlorite-feldspar gneiss (metasiltstone?)

The graphitic quartz-chlorite-feldspar gneiss unit hosts the bulk of the uranium-nickel mineralization in the 334 Pod. It also hosts chalcopyrite mineralization 50 metres below the 334 Pod. This rock is typically fine- to medium-grained, banded and well-foliated. It is composed mainly of quartz (20-30%), feldspars (microcline, plagioclase: 30-40%) and chlorite (15-20%). Graphite occurs in amounts of up to 10% modal, but generally is less than 5% modal. Tourmaline (var. dravite) usually occurs in amounts of 1-2% modal, but locally may be the predominant mineral phase in veinlets. Accessory minerals are rutile, anatase, apatite and epidote (var. pistacite).

Quartz occurs as polycrystalline aggregates of strained, interlocking, anhedral crystals exhibiting undulose extinction. Plagioclase is generally totally saussuritised. Microcline is less altered than plagioclase and exhibits simple twinning. Chlorite varies from pale-green to colourless varieties. Graphite occurs as elongated flakes parallel to the foliation. Tourmaline occurs in two forms: (a) as large, anhedral to

subhedral, bronze-coloured dravite grains either in veinlets or scattered randomly, and (b) as small radial, acicular aggregates of white dravite. The white dravite appears to have occurred later than the bronze dravite.

In the vicinity of mineralization, the feldspars and graphite are totally destroyed leaving an assemblage of quartz-chlorite-illite. Hematite and calcite were added later during different phases of mineralization.

(iii) The anatectic pegmatoids

Two types of anatectic pegmatoids of Hudsonian age have been recognized in drill core. The first are thin, segregation pegmatoids, usually a few centimetres thick, occurring in metapelitic rocks (Clarke and Fogwill, 1985). The second variety which may be intrusive is generally several metres thick, massive and coarse-grained (Fig. 6). This second variety hosts some of the uranium mineralization. Both pegmatoid types characteristically exhibit relatively conformable contacts with the enclosing metasedimentary rocks and have essentially the same composition (Clarke and Fogwill, 1985). They are composed of feldspars (plagioclase, K-feldspar), quartz and tourmaline (vars. schorl and dravite). The black tourmaline (schorl) grains are up to 4 cm in length, occurring commonly in quartz-rich areas and sometimes containing inclusions of quartz.

In the regolith, the pegmatoid retained their original textures, although quartz was the only remaining primary mineral.

The tourmaline-bearing pegmatoid rocks were believed to have originated by anatexis of boron-rich host sediments, characteristic of evaporite-bearing sequences (Harper, 1982).

C. Regolith (Palaeo-weathering profile)

Macdonald (1980, 1985) argued that chemical weathering of the Aphebian and Archean crystalline basement in a warm, moist climate produced a regionally-developed weathering profile similar to present day lateritic profiles. Macdonald (1980) presented

data to show:

(i) the formation of a bleached zone in the uppermost part of the profile due to alteration from reducing diagenetic solutions operating at the Athabasca Group-Wollaston-Group unconformity;

(ii) recrystallisation of illite from all zones in the profile;

(iii) transformation of Mg-smectite in the green zone to Mg-dioctahedral chlorite; and

(iv) the possible transformation of goethite in the red zone to hematite.

The regolith above the 334 Pod has developed principally on the graphite-cordierite-biotite-feldspar gneiss lithology (termed metapelite by Clarke and Fogwill, 1985) and is about 20 metres thick. It comprises an upper bleached zone, a red (hematitic) zone, a transitional red-green zone and a basal green (chloritic) zone that grades into 'fresh' metapelite. This regolithic colour zonation is characteristic of regolithic alteration of metasemipelitic rocks in the absence of superimposed mineralization effects in the McClean Lake area (Macdonald, 1980) (Fig. 7).

In the bleached zone, all the primary minerals except quartz have been replaced mainly by kaolinite and illite (sericite). In the red zone, kaolinite is absent, biotite is completely replaced by illite (sericite) and hematite; illite is much greater than chlorite, and quartz is the only surviving primary mineral. In the red/green transitional zone, chlorite increases at the expense of illite (sericite), biotite exhibits pale-green pleochroism; minor graphite is present, and rutile, magnetite, pyrite, marcasite and radial, white tourmaline are accessory minerals. The green zone is composed primarily of chlorite and illite (sericite), possesses biotite exhibiting pale-green to pale-brown pleochroism; has minor graphite and accessory magnetite and rutile.

In the regolith, hematite is the principal, non-radioactive oxide, rutile occurring in minor amounts and magnetite in trace amounts. Pyrite is the principal sulphide, occurring in trace amounts as does marcasite.

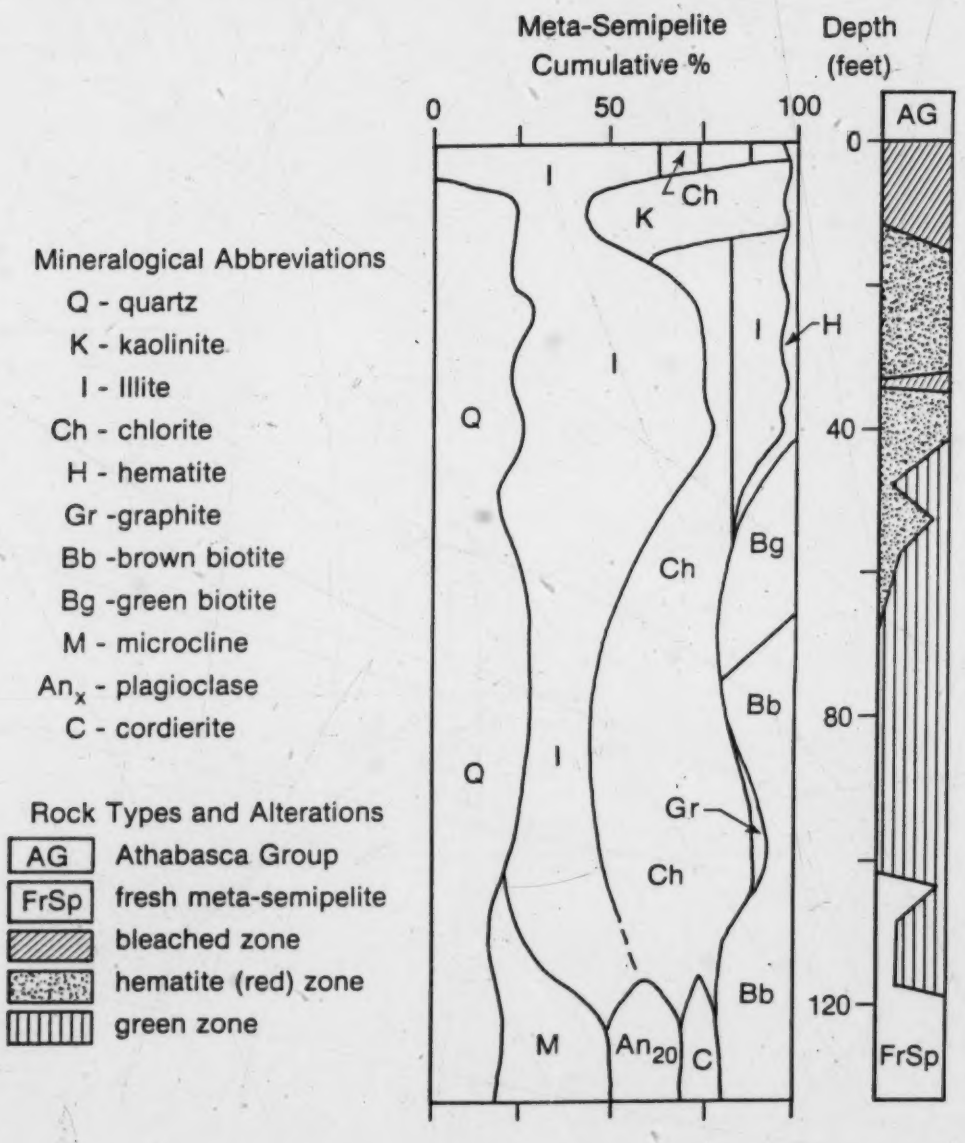

Figure 7. Mineralogical and colour zonation in the palaeo-weathering (regolith) profile of meta-semipelite from the McClean Lake area (modified after Macdonald, 1980, 1985)

Accompanying the alteration of feldspars, cordierite and biotite to clays and chlorite, is a flattening of the dip of the foliation from fresh basement rocks (75-80°) to 0-10° at the unconformity. Flat shearing was observed at and near the base of the regolith indicating relative movement between the Athabasca Group and the more competent Wollaston Group basement rocks (Clarke and Fogwill, 1985).

D. Athabasca Group

In the vicinity of the 334 Pod, the Athabasca Group rocks consist of medium- to coarse-grained, cream to purple, cross-bedded sandstone and pebbly sandstone. A 2.5 to 3.0 m grey conglomeratic horizon occurs about 40 m above the Athabasca Group-Wollaston Group unconformity and provides an excellent marker for determining fault movements.

E. Structure

E.1 General

The Wollaston Group basement suite was folded during the Hudsonian orogeny and underwent upper amphibolite facies regional metamorphism (Lewry and Sibbald, 1977, 1980; Lewry et al., 1978). The major fold-axes trend NE-SW, with later cross-folds trending ENE-WSW (Lewry et al., 1978; Lewry and Sibbald, 1980).

In the Dawn Lake area a major fault direction NE-SW paralleled the strike of the basement stratigraphy (Clarke and Fogwill, 1985). Other fault directions are ENE-WSW (often with thrust components), N-S (related to the Tabbernor fault system) and NW-SE (associated with diabase dykes) (McNutt, 1982; Clarke and Fogwill, 1985). All these faults cut the cover of the Athabasca Group rocks. It is believed that the NE-SW and ENE-WSW trending faults represent reactivated pre-Athabasca Group faults, whilst those trending NS and NW-SE postdate the Athabasca Group cover (McNutt, 1982; Clarke and Fogwill, 1985).

Fault zones appeared to contain deeper clay alteration, and the majority of the basement mineralization in the 11A and 11B Zones was associated with such alteration zones of greater thickness than normal regolithic alteration (Clarke and Fogwill, 1985).

E.2 Structure-11A Zone

In the 11A Zone, the basement metamorphic rocks strike N40° and dip steeply northwest. This observation was based on electromagnetic and magnetic surveys, and on drillhole data (Clarke and Fogwill, 1985). Compositional layering and the major foliation direction were essentially parallel in these rocks (Clarke and Fogwill, 1985). In thin sections of basement rocks occurring below the 334 Pod mineralization, two foliation directions were observed to occur at approximately 25° to each other. One direction appeared to be the regional Wollaston domain trend of N45°E and the second was interpreted to be at N70°E (a trend observed in the Wollaston and Mudjatik domains).

Drillhole data along the '11' graphitic conductor indicated the presence of (i) a major fault zone with limited displacement trending at N40°E and dipping steeply to the west (i.e., parallel to compositional layering and foliation) and (ii) minor cross-faults trending at N70°E (Clarke and Fogwill, 1985) (Fig. 8). The 334 Pod of uranium-nickel mineralization occurs at the intersection of the major fault zone trending N40°E and a minor cross-fault trending N70°E (Fig. 8). Faults shown on Fig. 6 were based on brecciation and shearing observed in drillholes and projected along zones of deeper clay alteration extending downwards into the basement.

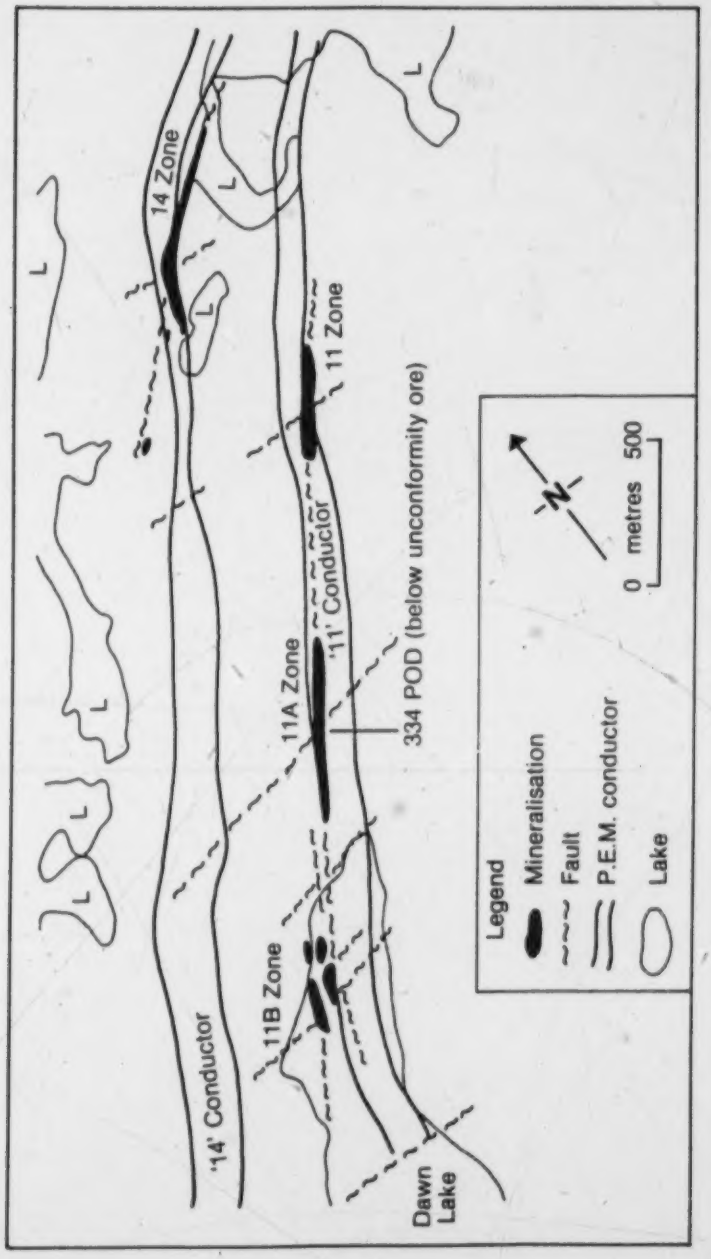

Figure 8. Structural and electrical controls on mineralisation in the Dawn Lake area (modified from Clarke and Fogwill, 1981, 1985, 1986)

IV. MINERALOGY OF THE 334 POD

A. Introduction

As outlined to date, the 334 Pod is a cylindro-spherical body with significant uranium-nickel mineralization (Fig. 9). Vertical zonation of mineralization within the pod has been observed with a pitchblende-arsenide-sulpharsenide assemblage prevailing in the upper part of the pod, whilst a pitchblende-sulphide assemblage dominates in the lower part of the pod.

Virtually all of the mineralized drill hole intersections of the 334 Pod occur below altered to 'fresh' graphitic metapelitic rocks (Fig. 6). However, only a small portion is hosted by the graphitic metapelites (Fig. 6). The bulk of the mineralization is hosted by the graphitic quartz-chlorite-feldspar gneiss. In and around the 334 Pod, the host rocks are intensely chloritised, and exhibit a dark-green colouration. Some mineralization occurs in anatectic pegmatoid rocks. Hematite alteration occurs in the lower part of the pod. Calcite was observed immediately above the uppermost area of mineralization, and also in the lower part of the pod cutting earlier chlorite and hematite alteration.

B. Mineralogy of 334 Pod - General

A summary of metalliferous and gangue minerals occurring in the 334 Pod is given in Table 2. Metalliferous minerals identified include pitchblende (3 varieties), arsenides (rammelsbergite, safflorite and nickeline), sulpharsenides (gersdorffite-several varieties; cobaltite), sulphides (galena, sphalerite, chalcopyrite, pyrite, bravoite, violarite, millerite and an unidentified Cu-S mineral), bismuth tellurides and native gold. Gangue minerals include chlorite, illite, hematite and calcite.

The upper part of the 334 Pod is characterised by the pitchblende-arsenide-sulpharsenide assemblage and chlorite-illite gangue. The lower part of the pod is characterised by a pitchblende-sulphide assemblage and a gangue

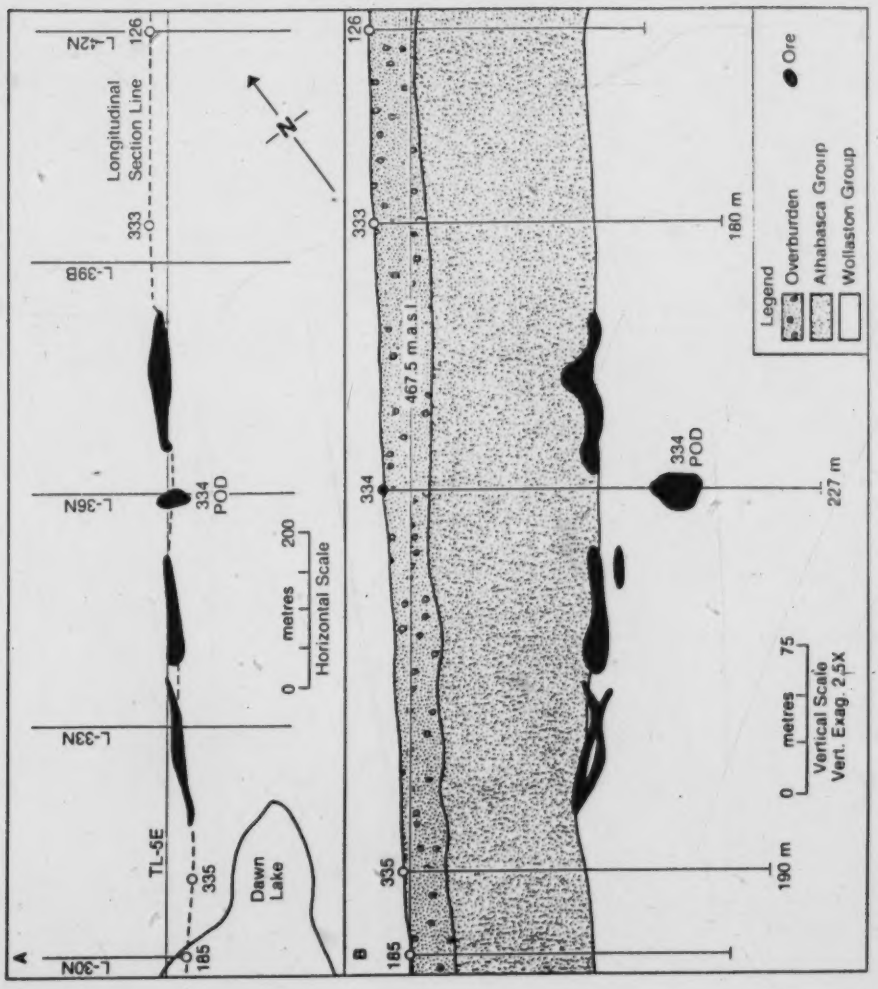

Figure 9.
A. Plan of the 11A Zone, Dawn Lake, Saskatchewan
B. Generalized longitudinal section through the 11A Zone, Dawn Lake, Saskatchewan. (Modified from Clarke and Fogwill, 1985, 1986)

Table 2: Metalliferous minerals observed in polished sections from the 334 Pod (DDH 334).

	Depth(m)	PI	PII	PIII	Rm	Sf	Nc	Gd	Cg	Bg	Ag	Cb	Mi	Vi	Br	Py	Cp	Cs	Gn	Sp	Bt	Au
1)	142.4	M	-	a	a	-	-	M	-	a	-	-	-	-	-	-	a	-	a	a	-	-
2)	143.2	M	-	a	-	-	-	M	-	a	a	-	-	-	-	-	-	-	a	-	a	-
3)	143.4	M	-	a	a	-	m	M	-	-	-	-	-	-	-	a	a	-	-	-	-	-
4)	143.7	M	-	a	a	-	M	m	-	-	-	-	-	a	a	a	a	-	a	-	-	-
5)	143.8	M	-	a	a	-	-	M	-	-	-	-	-	a	a	a	a	-	a	a	-	-
6)	144.0	M	a	a	a	-	M	M	-	a	-	-	-	a	a	a	a	-	-	-	-	-
7)	144.1	M	-	a	a	-	-	M	-	a	-	-	-	-	-	a	a	-	-	-	-	-
8)	145.3	M	-	a	a	-	M	M	-	-	-	-	-	-	-	a	a	-	-	-	-	-
9)	145.4	M	-	a	a	-	M	M	a	-	-	-	-	a	-	-	a	-	-	-	-	-
10)	145.6	M	-	a	a	-	M	M	-	-	-	-	-	-	-	-	a	-	-	-	-	-
11)	145.8	M	-	a	a	-	M	M	-	-	-	-	-	-	-	-	a	-	-	-	-	-
12)	146.4	m	M	a	-	-	-	a	-	-	-	-	-	-	-	a	a	a	a	a	-	-
13)	146.6	M	-	a	a	-	M	M	-	-	-	-	-	-	-	-	-	-	a	-	-	-
14)	146.8	M	-	a	a	-	-	M	-	-	-	-	-	-	-	-	a	-	-	-	-	-
15)	147.0	M	a	a	a	-	M	M	-	a	-	a	a	-	-	-	-	-	-	-	-	-
16)	148.3	M	-	a	a	-	-	M	-	-	-	-	-	-	-	a	a	-	-	-	-	-
17)	148.6	M	a	a	a	-	M	M	-	-	-	-	a	a	a	-	a	-	a	-	-	-
18)	148.7	M	a	a	a	a	M	M	-	-	-	-	a	a	a	a	-	-	-	-	-	-
19)	148.8	-	M	a	-	-	-	a	-	-	-	-	-	-	-	a	a	-	-	-	-	-
20)	149.0	-	M	a	-	-	-	a	-	-	-	-	-	-	-	a	a	-	a	a	-	-
21)	149.1	-	M	a	-	-	-	a	-	-	-	-	-	a	a	a	-	-	a	-	-	-
22)	150.3	-	M	a	-	-	-	-	-	-	-	-	-	-	-	a	-	a	a	-	-	-
23)	150.4	-	M	a	-	-	-	-	-	-	-	-	-	-	-	a	a	a	a	a	-	-
24)	150.5	-	M	a	-	-	-	-	-	-	-	a	-	-	-	a	-	a	a	a	a	a
25)	150.6	-	M	a	-	-	-	-	-	-	-	a	-	-	-	-	-	a	-	-	-	-
26)	151.1	-	M	a	-	-	-	-	-	-	-	-	-	-	-	a	a	a	a	-	-	-
27)	152.4	-	M	a	-	-	-	-	-	-	-	-	-	-	-	a	a	-	m	-	-	-
28)	152.8	-	M	a	-	-	-	-	-	-	-	-	-	-	-	a	m	a	a	a	-	-
29)	153.0	-	M	a	-	-	-	-	-	-	-	-	-	-	-	a	m	-	a	a	-	-
30)	154.0	-	M	a	-	-	-	-	-	-	-	-	-	-	-	a	m	-	a	-	-	-

Table 2 (Contd.): Metalliferous minerals observed in polished sections from the 334 Pod (DDH 334).

M: major mineral; m: minor mineral; a: accessory mineral;

PI: pitchblende I; PII: pitchblende II; PIII: pitchblende III; Rm: rammelsbergite;

Sf: safflorite; Nc: nickeline; Gd: gersdorffite; Cg: cobaltian gersdorffite;

Bg: bismuthian gersdorffite; Ag: arsenian gersdorffite; Cb: cobaltite; Mi: millerite;

Vi: violarite; Br: bravoite; Py: pyrite; Cp: chalcopyrite; Cs: copper sulphide;

Gn: galena; Sp: sphalerite; Bt: bismuth telluride; Au: gold

assemblage of chlorite-illite-hematite-calcite.

Pitchblende is the most abundant mineral in the 334 Pod. The most abundant non-uraniferous minerals are gersdorffite and nickeline. Amongst the opaque minerals, bismuthian gersdorffite and violarite have not been reported from other unconformity-associated uranium deposits within the Athabasca Basin. In fact, bismuthian gersdorffite had not been identified previously.

C. Mineralogy of the 334 Pod - Methods

Between March 1985 and September 1987, the electron microprobe facilities of the Department of Geology, University of Alberta were used to perform quantitative and qualitative analyses on ore and gangue minerals from the 334 Pod basement mineralization.

Quantitative analysis of ore minerals involved:

(i) the accumulation of wavelength-dispersive and energy-dispersive data, and
(ii) the treatment of these data using the FORTRAN IV computer program EDATA2 (Smith *et al.*, 1981) to generate chemical compositions and atomic ratios of metalliferous minerals (Appendix 3).

Metalliferous minerals characterised quantitatively included pitchblende (3 varieties), arsenides (rammelsbergite, nickeline), sulpharsenides (gersdorffite- several varieties; cobaltite) and sulphides (galena, chalcopyrite, bravoite, violarite and millerite). Gangue minerals were only studied qualitatively.

Qualitative analyses of metalliferous minerals were performed primarily to verify zonal sequences previously observed during routine microscopic investigation. Qualitative analyses were also carried out to investigate reflectance variations observed during NISOMI investigations of ore minerals. Qualitative analyses of metalliferous minerals involved the acquiring of (a) secondary electron, and (2) back-scattered electron images.

The NISOMI-84 (Nottingham Integrated System for Opaque Mineral Identification) computer-controlled automated reflectance-measuring system provided reflectance and colour data for ore minerals (Appendix 4). The use of this system was very important in characterising the different pitchblende generations.

Prior to use of the aforementioned methods, however, was the employment of routine microscopic methods involving polished thin sections and polished mounts. All polished thin sections and polished mounts used were made by Mr. Peter Black of the Dept. of Geology, Univ. of Alberta.

D. Oxides

The main oxides observed in the 334 Pod are pitchblende and hematite. Accessory rutile has also been observed. Three types of pitchblende are present:

1. pitchblende I (an early, lustrous variety displaying colloform, botryoidal and reniform habits);
2. pitchblende II (an intermediate, slightly less reflective variety displaying colloform, botryoidal, ringlike and euhedral habits);
3. pitchblende III (a late, dull, amorphous variety replacing rims and inhabiting shrinkage cracks of earlier pitchblendes).

D.1 Pitchblende

Uranium oxides at Dawn Lake are termed pitchblendes and not differentiated into uraninites and pitchblendes, because X-ray crystallographic studies were not carried out.

Uraninite is isostructural with fluorite, CaF_2, and consists of uranium in 8-fold cubic coordination (Frondel, 1958; Smith, 1984). Oxidation of UO_2 occurs by an oxygen interstitial mechanism and thus the formula for uraninite should be UO_{2+x} (Gronvold, 1955). The cell size varies linearly with composition, with $a_o(A) = 5.470 - 0.1080X$, where X is the deviation from stoichiometry of the oxygen (Smith, 1984).

The limiting value for X is 0.25 (Smith, 1984). Above the composition $UO_{2.25}$, the cubic structure yields to a related tetragonal form (Willis, 1978). Table 3 gives the ionic radii of ions in 8-fold coordination that can substitute for U^{4+} and U^{6+} in the uraninite and pitchblende structures (Henderson, 1982).

Pitchblende is the major oxide mineral present in the 334 Pod. Megascopically, it may vary from massive to porous. The most porous ore occurs mainly in the lower 5m of the 334 Pod, although porous ore does occur in places higher up cutting the massive arsenide-sulpharsenide ore.

Three types of pitchblendes have been identified on the basis of their textures, reflectivity, chemical composition, and paragenetic position. These types are:

(i) pitchblende I (first generation pitchblende)

(ii) pitchblende II (second generation pitchblende)

(iii) pitchblende III (third generation pitchblende)

Published analyses of thorium-free pitchblendes from other unconformity-deposits within the Athabasca Basin-Cree Lake Zone area are available only for the Rabbit Lake (Rimsaite, 1977) and Midwest Lake (Wray *et al.*, 1985) deposits. Rabbit Lake pitchblendes were shown to contain minor amounts of calcium, iron, titanium, silicon and aluminium. Midwest Lake pitchblendes were shown to contain minor amounts of calcium, titanium, vanadium, manganese, iron, nickel, arsenic, silicon and aluminium .The Midwest Lake pitchblendes were examined using the electron microprobe facilities at the Dept. of Geology of the Univ. of Alberta by Dr. D.G.W. Smith and S. Launspach, and reported in Wray *et al.* (1985).

D.2 Pitchblende I

Pitchblende I occurs as dark, lustrous, botryoidal, colloform, reniform and radial bodies (Plates 3-12). Reflectivity and colour data for pitchblende I samples are presented in Table 4 and Figure 10. Chemical composition data for 12 pitchblende I samples are presented in Table 5.

Table 3: Ionic radii of selected ions in 8-fold co-ordination[1]

U^{4+}	Pb^{4+}	Ca^{2+}	U^{6+}	Zn^{2+}	Fe^{2+}	Fe^{3+}	Mn^{2+}	Ti^{4+}
1.00	0.94	1.12	0.86	0.90	0.92	0.78	0.96	0.74

[1]: Data are unavailable for nickel and vanadium in 8-fold co-ordination

Table 4: Quantitative colour and reflectance data for pitchblendes.

Pitchblende/ standard variety:		1		2		3
Data class		Mean	Range	Mean	Range	--
Dominant wavelength(dλ)		--	461.6-470.6	--	457.2-466.3	--
Saturation Purity(Pe%)		--	2.5-3.0	--	2.8-3.4	--
Luminance(Y)		15.9	15.7-16.3	15.5	15.1-15.9	--
Trichromatic coefficients	x	0.305	0.305-0.306	0.305	0.304-0.316	--
	y	0.309	0.308-0.309	0.308	0.307-0.308	--
$R_{(air\ @\ 470\ nm)}\%$		16.6	16.4-16.9	16.2	15.9-16.6	21.8
$R_{(air\ @\ 546\ nm)}\%$		15.9	15.7-16.2	15.4	15.0-15.8	21.0
$R_{(air\ @\ 589\ nm)}\%$		15.8	15.4-16.1	15.4	15.0-15.7	20.8
$R_{(air\ @\ 650\ nm)}\%$		15.8	15.7-16.3	15.4	15.1-15.7	20.5

1. Pitchblende I, 334 Pod, 11A Zone, Dawn Lake, Saskatchewan
2. Pitchblende II, 334 Pod, 11A Zone, Dawn Lake, Saskatchewan
3. SiC (Carl Zeiss Standard #474281-080)

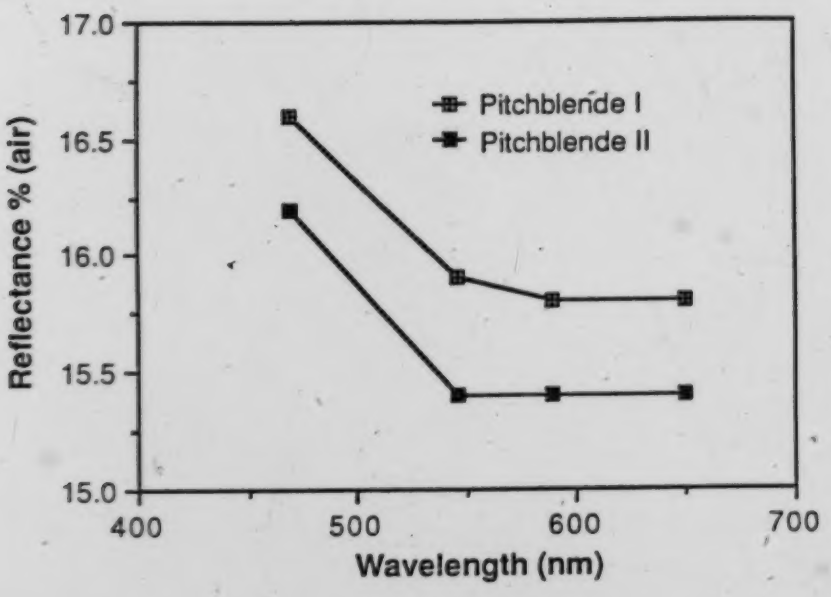

Figure 10. Reflectivity and colour data for first and second generation pitchblendes from the 334 Pod, 11A Zone, Dawn Lake, Saskatchewan

Pitchblende I possesses the highest reflectivity of all the pitchblende types and contains variable but minor amounts of calcium, titanium, vanadium, manganese, iron, nickel and zinc.

D.3 Pitchblende II

Pitchblende II occurs as lighter coloured, colloform , botryoidal, radial, ring-like and euhedral bodies, that are less lustrous than pitchblende I (Plates 6, 7). Reflectivity and colour data for pitchblende II samples are presented in Table 4 and Figure 10. Chemical compositions of 18 pitchblende II samples are presented in Table 6.

Pitchblende II chemical compositions are similar to those of pitchblende I, the major differences being the lower lead and higher calcium contents in pitchblende II samples (Tables 6, 8).

D.4 Pitchblende III

Pitchblende III occurs as dark, generally amorphous, rim coatings on, and shrinkage crack/fracture fillings in paragenetically earlier pitchblendes (I and II) (Plates 7-12). Chemical compositions of 13 pitchblende III samples are presented in Table 7.

Pitchblende III samples generally contain much less lead than pitchblendes I and II (Table 8). Pitchblende III also contains more vanadium and less iron and nickel than pitchblendes I and II (Table 8).

Two distinct types of pitchblende III have been distinguished chemically (Table 7, 8). Pitchblende III replacing pitchblende I (Analyses 1-6, Table 7) contains less calcium and silicon, but on the average more lead than pitchblende III replacing pitchblende II (analyses 7-13, Table 7).

D.5 Pitchblende-Discussion

In the 334 Pod, pitchblende I (U/Pb: 4.34-5.09) contained less calcium than paragenetically later than pitchblende II (U/Pb: 5.12-7.58). This pattern is repeated at

Plate 3. Assemblage: nickeline-gersdorffite-pitchblende I-gersdorffite-galena.
Secondary electron image
The following features are shown on this plate:

(i) nickeline (N) is replaced by gersdorffite (G) along rims and fractures
(ii) gersdorffite-altered rims of nickeline are coated by colloform pitchblende I (P1)
(iii) syneresis cracks in pitchblende I are filled by a later generation of gersdorffite which also formed an outer coating on pitchblende I
(iv) some cavities in nickeline are filled with galena (g)
(v) corroded quartz grains (Q) are enclosed in the phyllosilicate matrix

Plate 4. Assemblage: gersdorffite-pitchblende I-gersdorffite -bismuthian gersdorffite
Back scattered electron image
The following features are shown on this plate:

(i) brecciated gersdorffite (G) grains are enclosed by botryoidal pitchblende I (P1)
(ii) brecciated pitchblende I (to the right) has been healed by later gersdorffite fillings
(iii) bismuthian gersdorffite (bg) inclusions are present in gersdorffite

Q
400μm

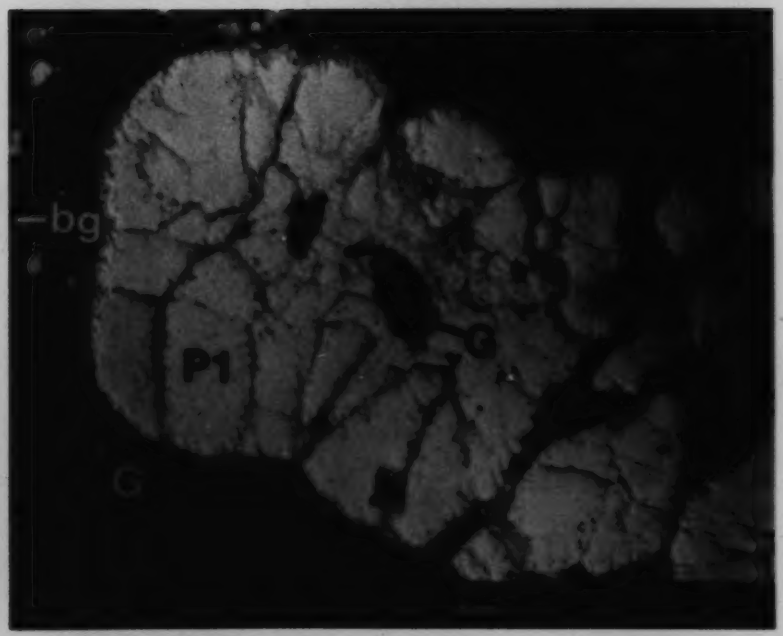
bg
P1
G

Plate 5. This reflected light image shows gersdorffite (G) filling some syneresis cracks in massive pitchblende I (P1).
Reflected light: 100X

Plate 6. Assemblage: gersdorffite-pitchblende II-pitchblende III -galena
The following features are shown on this plate:

(i) gersdorffite (G) is coated by pitchblende II (P2)
(ii) pitchblende II is altered to pitchblende III (P3) along rims of fractures
(iii) ubiquitous very fine-grained galena (g) is associated with pitchblende III.

Reflected light: 100X

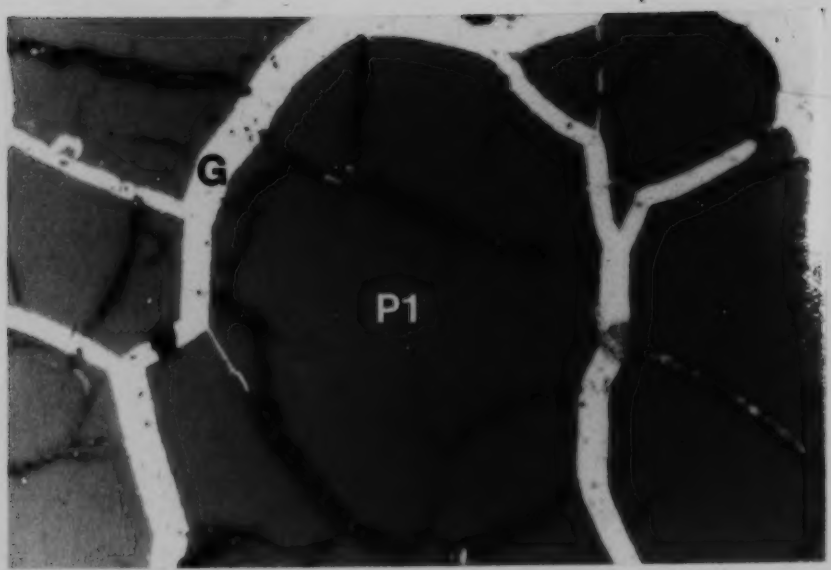
G
P1

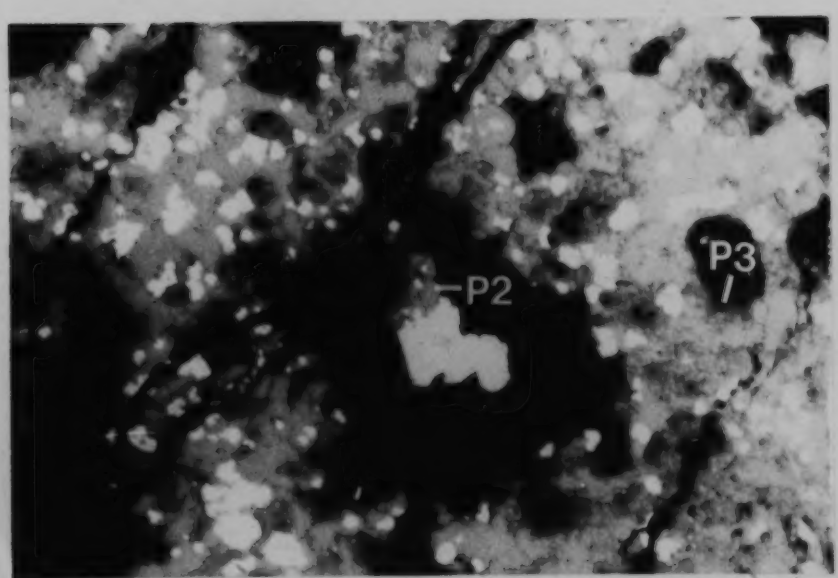
P2
P3

Plate 7. Assemblage: pitchblende I-gersdorffite-pitchblende III -galena
Back scattered electron image
The following features are shown on this plate:

(i) radial pitchblende I (P1) is replaced by pitchblende III (P3)
(ii) radial pitchblende I is coated by gersdorffite (G)
(iii) gersdorffite rims are replaced by pitchblende III and galena (g)
(iv) fractures in gersdorffite are replaced by pitchblende III

Plate 8. Assemblage: pitchblende I-gersdorffite-bismuthian gersdorffite -gersdorffite-pitchblende III
Back scattered electron image
The following features are shown on this plate:

(i) radial pitchblende I (P1) is coated by gersdorffite (G) containing bismuthian gersdorffite (bg) bands
(ii) some syneresis cracks and fractures in pitchblende I are invaded by gersdorffite
(iii) pitchblende I is altered to pitchblende III (P3) along rims, fractures and syneresis cracks
(iv) gersdorffite is coated by pitchblende III
(v) bismuthian gersdorffite is selectively replaced by pitchblende III

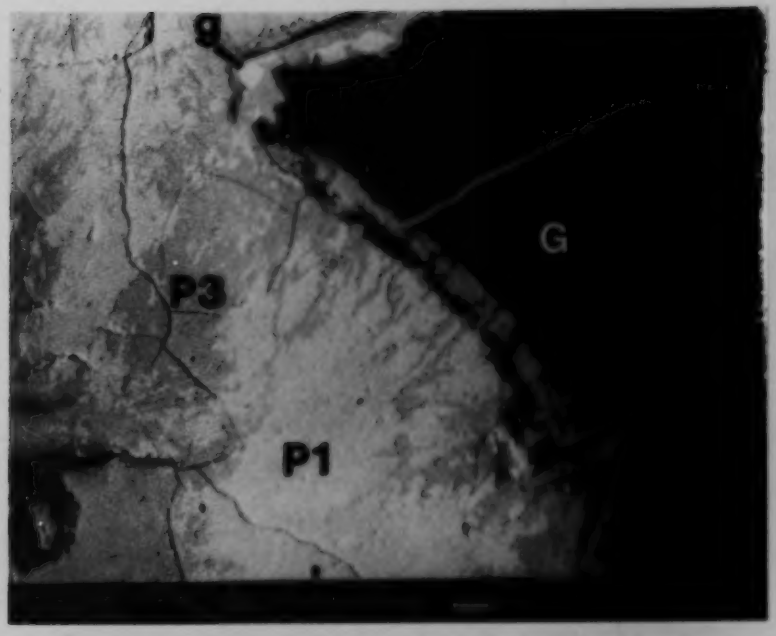
g
G
P3
P1

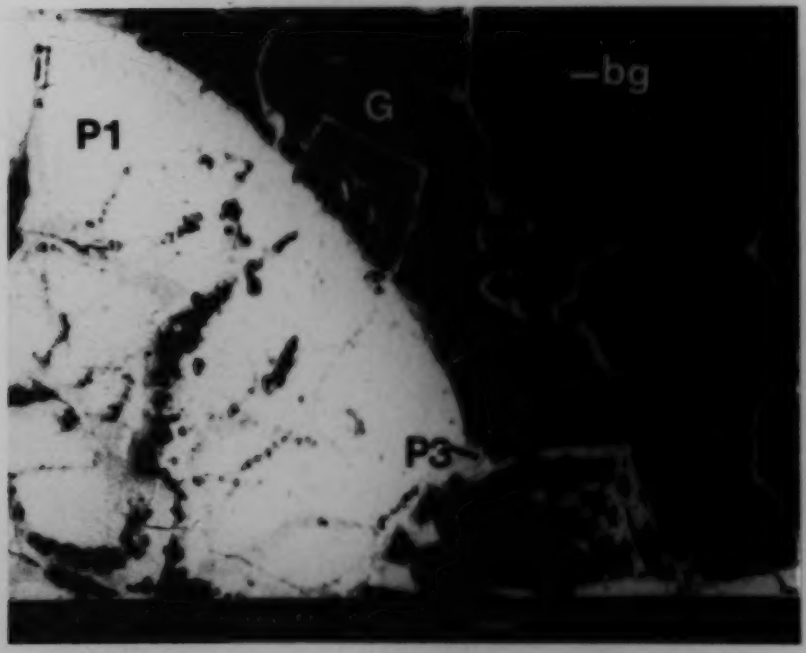
P1
G
bg
P3

Plate 9. Assemblage: rammelsbergite-pitchblende I-gersdorffite
The following features are shown on this plate:

(i) rammelsbergite(R) exhibits a skeletal replacement texture in gersdorffite (G)
(ii) gersdorffite has filled fractures and cracks in pitchblende I (P1)

Reflected light: 100X

Plate 10. Assemblage: rammelsbergite-nickeline-pitchblende I -gersdorffite
The following features are shown on this plate:

(i) gersdorffite has replaced rammelsbergite (R) and nickeline (N)
(ii) pitchblende I (P1) appears to be enclosed by gersdorffite (G)

Reflected light: 100X

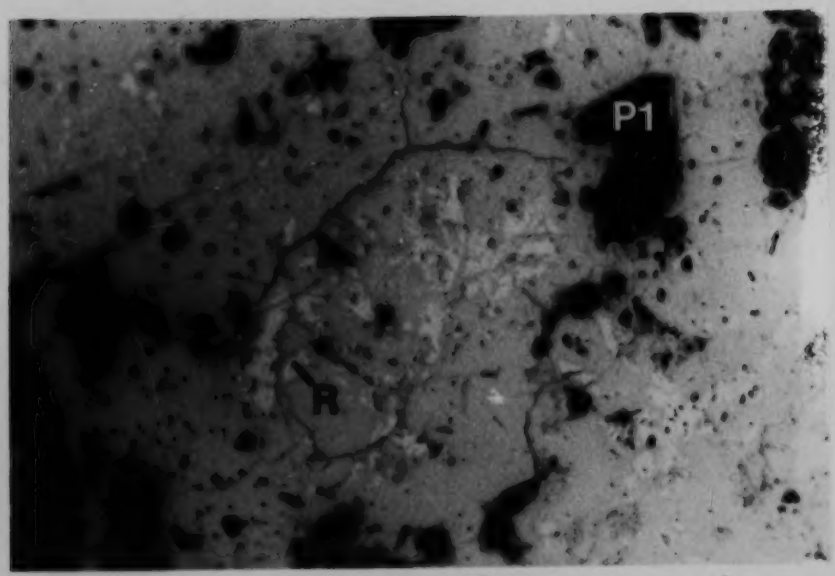
P1
R

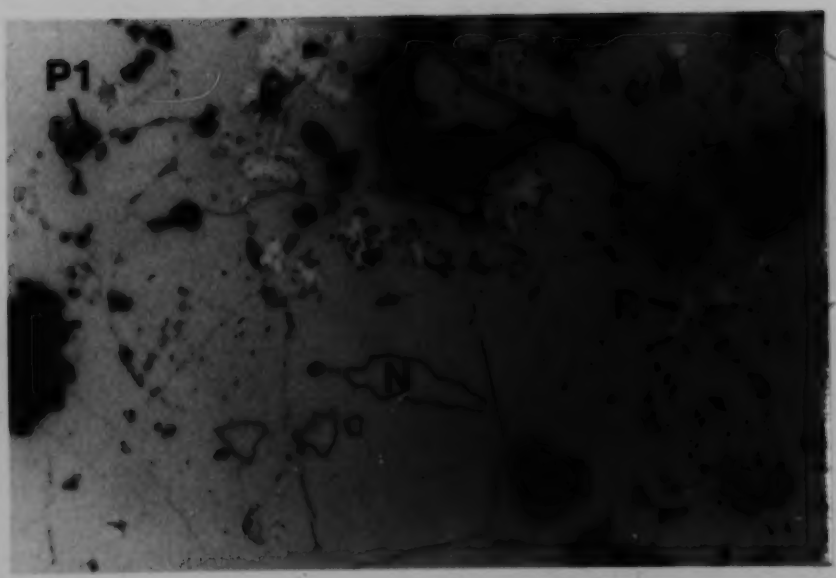
P1

Plate 11. Assemblage: rammelsbergite-gersdorffite-pitchblende I -gersdorffite
The following features are shown on this plate:

(i) rammelsbergite (R) is replaced by gersdorffite (G)
(ii) the phyllosilicate matrix has been partially replaced by a mesh-like network of gersdorffite strands
(iii) gersdorffite is replaced by colloform pitchblende I (Pl)
(iv) some syneresis cracks in pitchblende I are partially filled by later gersdorffites

Reflected light: 100X

Plate 12. Brecciated colloform (botryoidal) pitchblende I (Pl) partially healed by gersdorffite (G)
Reflected light: 100X

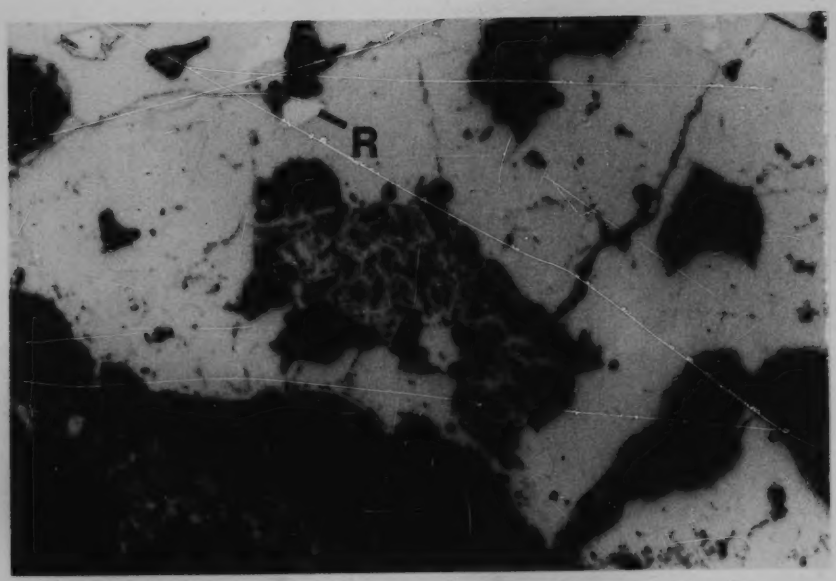
R

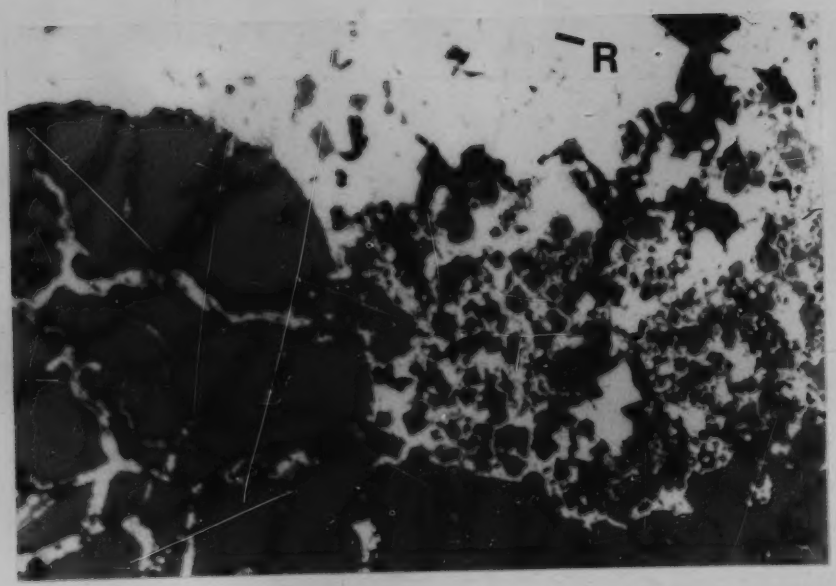
R

Table 5 : Chemical compositions of first generation pitchblendes (pitchblende I) from the 334 Pod, 11A Zone, Dawn Lake, Saskatchewan.

No.	1	2	3	4	5	6
SAMPLE	334-142.4	334-142.4	334-143.2	334-143.2	334-145.3	334-145.3
U (wt.%)	69.27	69.87	68.27	70.24	68.70	69.20
Th (wt.%)	ND	ND	ND	ND	ND	ND
Pb (wt.%)	15.79	14.70	15.58	13.79	15.82	15.00
Zn (wt.%)	0.49	0.44	0.41	0.63	0.49	0.52
Ni (wt.%)	0.38	0.44	0.27	0.30	0.41	0.47
Fe (wt.%)	0.35	0.43	0.26	0.34	0.26	0.37
Mn (wt.%)	0.16	0.14	ND	0.15	0.07	0.11
V (wt.%)	0.11	0.10	0.28	0.28	0.07	ND
Ti (wt.%)	ND	ND	0.07	0.07	ND	ND
Ca (wt.%)	1.18	1.49	1.34	1.18	1.09	1.15
Total	87.73	87.61	86.48	86.98	86.94	86.82
UO_2 (wt.%)	78.59	79.26	77.45	79.69	77.94	78.51
ThO_2 (wt.%)	ND	ND	ND	ND	ND	ND
PbO (wt.%)	17.01	15.84	16.78	14.85	17.04	16.16
ZnO (wt.%)	0.61	0.55	0.51	0.78	0.61	0.65
NiO (wt.%)	0.48	0.56	0.35	0.38	0.52	0.60
FeO (wt.%)	0.45	0.55	0.34	0.44	0.33	0.47
MnO (wt.%)	0.20	0.18	ND	0.19	0.09	0.14
V_2O_5 (wt.%)	0.19	0.18	0.50	0.50	0.12	ND
TiO_2 (wt.%)	ND	ND	0.12	0.12	ND	ND
CaO (wt.%)	1.66	2.08	1.88	1.65	1.53	1.61
Total	99.19	99.20	97.93	98.60	98.18	98.14
U/Pb	4.39	4.75	4.38	5.09	4.34	4.61
U/Ca	58.70	46.89	50.94	59.53	63.03	60.17
Chemical Age (Ma)	1400	1307	1402	1230	1413	1341

Table 5 (Contd.): Chemical compositions of first generation pitchblendes (pitchblende I) from the 334 Pod, 11A Zone, Dawn Lake, Saskatchewan.

No.	7	8	9	10	11	12
SAMPLE	334-145.3	334-145.3	334-145.3	334-145.3	334-146.4	334-146.4
U (wt.%)	69.27	70.06	69.43	69.57	68.43	67.57
Th (wt.%)	ND	ND	ND	ND	ND	ND
Pb (wt.%)	14.65	14.68	14.53	13.93	15.82	15.24
Zn (wt.%)	0.50	0.44	0.70	0.68	0.85	0.68
Ni (wt.%)	0.69	0.46	0.54	0.62	0.36	0.24
Fe (wt.%)	0.32	0.33	0.38	0.41	0.44	0.41
Mn (wt.%)	0.17	0.18	0.20	0.14	0.22	0.13
V (wt.%)	ND	0.07	0.14	0.11	0.08	0.19
Ti (wt.%)	ND	ND	ND	ND	ND	ND
Ca (wt.%)	1.14	1.10	1.29	1.30	1.12	1.50
Total	86.74	87.32	87.21	86.76	87.32	85.96
UO_2 (wt.%)	78.58	79.47	78.77	78.92	77.63	76.65
ThO_2 (wt.%)	ND	ND	ND	ND	ND	ND
PbO (wt.%)	15.78	15.82	15.65	15.00	17.04	16.42
ZnO (wt.%)	0.62	0.55	0.88	0.84	1.06	0.85
NiO (wt.%)	0.88	0.59	0.69	0.78	0.46	0.31
FeO (wt.%)	0.41	0.43	0.49	0.52	0.56	0.53
MnO (wt.%)	0.22	0.23	0.26	0.18	0.29	0.17
V_2O_5 (wt.%)	ND	0.13	0.26	0.20	0.15	0.34
TiO_2 (wt.%)	ND	ND	ND	ND	ND	ND
CaO (wt.%)	1.60	1.54	1.80	1.82	1.56	2.10
Total	98.09	98.76	98.80	98.26	98.75	97.37
U/Pb	4.73	4.77	4.78	4.99	4.33	4.43
U/Ca	60.76	63.70	53.82	53.52	61.10	45.05
Chemical Age (Ma)	1313	1302	1301	1252	1417	1388

Table 6 : Chemical compositions of second generation pitchblendes (pitchblende II) from the 334 Pod, 11A Zone, Dawn Lake, Saskatchewan.

No.	1	2	3	4	5	6
SAMPLE	334-144.0	334-144.0	334-146.4	334-146.4	334-146.4	334-146.4
U (wt.%)	68.86	69.50	69.40	69.69	69.68	70.99
Th (wt.%)	ND	ND	ND	ND	ND	ND
Pb (wt.%)	13.11	12.40	12.87	12.80	12.43	9.36
Zn (wt.%)	0.37	0.37	0.54	0.68	0.84	0.61
Ni (wt.%)	0.43	0.38	0.20	0.32	0.21	0.25
Fe (wt.%)	0.49	0.35	0.42	0.50	0.42	0.62
Mn (wt.%)	0.14	0.16	0.19	0.17	0.16	0.20
V (wt.%)	0.09	0.06	0.11	0.16	0.15	0.13
Ti (wt.%)	ND	ND	ND	ND	ND	ND
Ca (wt.%)	1.56	1.43	1.73	1.70	1.46	2.04
Total	85.05	84.41	85.46	85.02	85.35	84.20
UO_2 (wt.%)	78.12	78.84	78.73	79.06	79.05	80.53
ThO_2 (wt.%)	ND	ND	ND	ND	ND	ND
PbO (wt.%)	14.13	13.36	13.87	13.79	13.39	10.08
ZnO (wt.%)	0.46	0.46	0.67	0.85	1.04	0.76
NiO (wt.%)	0.55	0.48	0.25	0.40	0.27	0.32
FeO (wt.%)	0.62	0.45	0.54	0.64	0.54	0.79
MnO (wt.%)	0.19	0.21	0.24	0.22	0.20	0.26
V_2O_5 (wt.%)	0.16	0.10	0.20	0.28	0.27	0.23
TiO_2 (wt.%)	ND	ND	ND	ND	ND	ND
CaO (wt.%)	2.18	2.00	2.43	2.38	2.04	2.85
Total	96.41	96.00	96.93	97.62	96.79	95.82
U/Pb	5.25	5.60	5.39	5.44	5.61	7.58
U/Ca	44.14	48.60	40.12	40.99	47.73	34.80
Chemical Age (Ma)	1198	1131	1170	1160	1131	861

Table 6 (Contd.): Chemical compositions of second generation pitchblendes (pitchblende II) from the 334 Pod, 11A Zone, Dawn Lake, Saskatchewan.

No.	7	8	9	10	11	12
SAMPLE	334-147.0	334-147.0	334-149.0	334-149.0	334-149.0	334-149.0
U (wt.%)	68.55	69.87	69.05	69.55	69.49	70.05
Th (wt.%)	ND	ND	ND	ND	ND	ND
Pb (wt.%)	13.23	12.61	13.49	13.29	12.94	12.92
Zn (wt.%)	0.51	0.36	0.67	0.67	0.82	0.77
Ni (wt.%)	0.42	0.28	0.39	0.41	0.52	0.51
Fe (wt.%)	0.51	0.40	0.50	0.41	0.57	0.57
Mn (wt.%)	0.09	0.09	0.19	0.18	0.29	0.29
V (wt.%)	0.16	0.08	0.08	0.15	0.19	0.16
Ti (wt.%)	ND	ND	ND	ND	ND	ND
Ca (wt.%)	1.33	1.33	1.38	1.36	1.41	1.35
Total	84.80	85.02	85.75	86.02	86.23	86.62
UO_2 (wt.%)	77.76	79.26	78.34	78.89	78.83	79.47
ThO_2 (wt.%)	ND	ND	ND	ND	ND	ND
PbO (wt.%)	14.25	13.59	14.53	14.31	13.94	13.92
ZnO (wt.%)	0.63	0.44	0.83	0.84	1.02	0.96
NiO (wt.%)	0.53	0.36	0.50	0.53	0.67	0.65
FeO (wt.%)	0.66	0.52	0.64	0.53	0.73	0.73
MnO (wt.%)	0.12	0.12	0.25	0 23	0.38	0.37
V_2O_5 (wt.%)	0.29	0.15	0.14	0.27	0.34	0.29
TiO_2 (wt.%)	ND	ND	ND	ND	ND	ND
CaO (wt.%)	1.86	1.86	1.93	1.90	1.98	1.89
Total	96.10	96.30	97.16	97.50	97.89	98.28
U/Pb	5.18	5.54	5.12	5.23	5.37	5.42
U/Ca	51.54	52.53	50.04	51.14	49.28	51.89
Chemical Age (Ma)	1212	1143	1225	1202	1175	1165

Table 6 (Contd.): Chemical compositions of second generation pitchblendes (pitchblende II) from the 334 Pod, 11A Zone, Dawn Lake, Saskatchewan.

No.	13	14	15	16	17	18
SAMPLE	334-149.0	334-150.5	334-150.5	334-152.8	334-152.8	334-152.8
U (wt.%)	70.08	69.53	70.44	68.87	70.01	69.74
Th (wt.%)	ND	ND	ND	ND	ND	ND
Pb (wt.%)	11.41	13.30	11.58	12.59	12.46	11.29
Zn (wt.%)	0.77	0.55	0.75	0.65	0.47	0.51
Ni (wt.%)	0.57	0.43	0.39	0.29	0.18	0.22
Fe (wt.%)	0.66	0.40	0.53	0.34	0.37	0.51
Mn (wt.%)	0.45	0.08	0.20	0.20	ND	0.10
V (wt.%)	0.20	0.14	0.19	0.10	ND	ND
Ti (wt.%)	0.06	ND	ND	ND	ND	0.11
Ca (wt.%)	1.50	1.43	1.70	1.64	1.35	1.65
Total	85.70	85.86	85.78	84.68	84.84	84.13
UO_2 (wt.%)	79.50	78.88	79.91	78.13	79.42	79.12
ThO_2 (wt.%)	ND	ND	ND	ND	ND	ND
PbO (wt.%)	12.29	14.33	12.47	13.56	13.42	12.16
ZnO (wt.%)	0.96	0.69	0.93	0.81	0.58	0.64
NiO (wt.%)	0.73	0.55	0.50	0.36	0.23	0.27
FeO (wt.%)	0.84	0.52	0.68	0.44	0.47	0.65
MnO (wt.%)	0.58	0.11	0.25	0.26	ND	0.13
V_2O_5 (wt.%)	0.35	0.25	0.34	0.19	ND	ND
TiO_2 (wt.%)	0.10	ND	ND	ND	ND	0.18
CaO (wt.%)	2.09	2.00	2.38	2.29	1.88	2.30
Total	97.74	97.33	97.47	96.04	96.00	95.45
U/Pb	6.14	5.23	6.08	5.47	5.62	6.18
U/Ca	46.72	48.62	41.44	41.99	51.86	42.27
Chemical Age (Ma)	1042	1203	1051	1156	1128	1037

Table 7 : Chemical compositions of third generation pitchblendes (pitchblende III) from the 334 Pod, 11A Zone, Dawn Lake, Saskatchewan.

No.	1	2	3	4	5	6
SAMPLE	334-142.4	334-142.4	334-146.4	334-146.4	334-146.4	334-146.4
U (wt.%)	72.98	72.49	67.00	68.69	68.55	72.04
Th (wt.%)	ND	ND	ND	ND	ND	ND
Pb (wt.%)	1.95	1.70	7.24	2.14	1.76	1.15
Zn (wt.%)	0.49	0.32	0.26	0.69	0.62	0.58
Ni (wt.%)	0.27	0.31	0.30	0.21	0.20	0.36
Fe (wt.%)	0.21	0.29	0.16	0.22	0.12	0.16
Mn (wt.%)	0.46	0.50	ND	ND	ND	0.11
V (wt.%)	0.38	0.41	0.44	0.52	0.58	0.53
Ti (wt.%)	ND	ND	ND	1.31	1.38	ND
Ca (wt.%)	1.71	2.03	1.39	0.97	1.00	2.20
Si (wt.%)	1.88	1.90	1.32	2.01	1.98	1.37
Total	80.33	79.95	78.11	76.76	76.19	78.50
UO_2 (wt.%)	82.79	82.24	76.01	77.91	77.77	81.72
ThO_2 (wt.%)	ND	ND	ND	ND	ND	ND
PbO (wt.%)	2.10	1.83	7.80	2.30	1.90	1.24
ZnO (wt.%)	0.60	0.40	0.32	0.86	0.78	0.72
NiO (wt.%)	0.34	0.39	0.38	0.26	0.25	0.46
FeO (wt.%)	0.27	0.38	0.21	0.29	0.16	0.21
MnO (wt.%)	0.60	0.64	ND	ND	ND	0.14
V_2O_5 (wt.%)	0.68	0.72	0.78	0.93	1.03	0.95
TiO_2 (wt.%)	ND	ND	ND	2.18	2.30	ND
CaO (wt.%)	2.39	2.84	1.95	1.35	1.40	3.08
SiO_2 (wt.%)	4.02	4.06	2.83	4.30	4.23	2.94
Total	93.79	93.50	90.28	90.38	89.82	91.46
U/Pb	37.42	42.64	9.25	32.10	38.95	62.64
U/Ca	42.68	35.71	48.20	70.81	68.55	32.74
U/Si	38.82	38.15	50.76	34.17	34.62	52.58
Chemical Age (Ma)	187	165	717	218	180	113

Table 7 (Contd.): Chemical compositions of third generation pitchblendes (pitchblende III) from the 334 Pod, 11A Zone, Dawn Lake, Saskatchewan.

No.	7	8	9	10	11	12	13
SAMPLE	334-152.8	334-152.8	334-152.8	334-152.8	334-152.8	334-154.0	334-154.0
U (wt.%)	66.88	65.16	63.88	69.08	63.88	69.52	71.45
Th (wt.%)	ND	ND	ND	ND	ND	ND	ND
Pb (wt.%)	2.61	0.55	0.47	0.39	0.24	0.85	0.87
Zn (wt.%)	0.44	0.36	0.27	0.50	0.30	0.49	0.25
Ni (wt.%)	0.11	0.14	0.12	0.28	0.15	0.12	0.12
Fe (wt.%)	0.07	ND	0.16	0.36	0.08	0.20	0.26
Mn (wt.%)	0.19	0.25	0.23	0.66	0.24	0.14	0.26
V (wt.%)	0.32	0.48	0.54	0.54	0.52	0.33	0.26
Ti (wt.%)	0.14	0.17	ND	ND	0.07	ND	0.06
Ca (wt.%)	4.06	4.30	4.17	4.29	3.90	4.01	4.15
Si (wt.%)	3.30	4.10	4.82	2.43	4.26	3.28	2.28
Total	78.12	75.51	74.66	78.53	73.64	78.94	79.96
UO_2 (wt.%)	75.87	73.91	72.47	78.36	72.47	78.87	81.05
ThO_2 (wt.%)	ND	ND	ND	ND	ND	ND	ND
PbO (wt.%)	2.81	0.59	0.51	0.42	0.26	0.91	0.94
ZnO (wt.%)	0.54	0.45	0.34	0.62	0.37	0.61	0.31
NiO (wt.%)	0.14	0.18	0.15	0.36	0.20	0.16	0.15
FeO (wt.%)	0.10	ND	0.21	0.47	0.11	0.26	0.34
MnO (wt.%)	0.24	0.32	0.30	0.85	0.31	0.18	0.33
V_2O_5 (wt.%)	0.57	0.85	0.96	0.97	0.92	0.59	0.47
TiO_2 (wt.%)	0.23	0.28	ND	ND	0.12	ND	0.10
CaO (wt.%)	5.67	6.01	5.83	6.00	5.45	5.61	5.80
SiO_2 (wt.%)	7.06	8.77	10.32	5.19	9.11	7.01	4.87
Total	93.23	91.36	91.09	93.24	89.32	94.20	94.36
U/Pb	25.62	118.5	135.9	177.1	266.2	81.79	82.13
U/Ca	16.47	15.15	15.32	16.10	16.38	17.34	17.22
U/Si	20.27	15.89	13.25	28.43	15.00	21.20	31.34
Chemical Age (Ma)	271	60	52	40	27	87	86

Table 8: Summary of chemical data for pitchblendes I, II and III from the 334 Pod, 11A Zone, Dawn Lake, Saskatchewan.

	PI	PII	PIII(a)	PIII(b)
U(wt.%)	67.57-70.24	68.55-70.99	67.00-72.98	63.88-71.45
Pb(wt.%)	13.79-15.82	9.36-13.49	1.15- 2.14	0.24- 2.61
Zn(wt.%)	0.41- 0.85	0.36- 0.84	0.32- 0.69	0.25- 0.50
Ni(wt.%)	0.24- 0.69	0.20- 0.57	0.20- 0.36	0.11- 0.28
Fe(wt.%)	0.26- 0.43	0.34- 0.66	0.16- 0.29	0.00- 0.36
Mn(wt.%)	0.00- 0.20	0.00- 0.45	0.00- 0.50	0.14- 0.66
V(wt.%)	0.00- 0.28	0.00- 0.20	0.38- 0.58	0.26- 0.54
Ti(wt.%)	0.00- 0.07	0.00- 0.11	0.00- 1.38	0.00- 0.17
Ca(wt.%)	1.09- 1.50	1.33- 2.04	0.97- 2.20	3.90- 4.30
Si(wt.%)	-- ND --	-- ND --	1.32- 2.01	2.43- 4.82
U/Pb	4.34- 5.09	5.12- 7.58	9.25-62.64	25.62-266.2
U/Ca	45.05-63.70	34.80-52.53	32.74-70.81	15.15-17.34
U/Si	---------	---------	34.17-52.58	13.25-28.43

Midwest Lake where early colloform pitchblende (U/Pb: 5.1) contained less calcium than presumably later radial pitchblende (pitchblende II?) (U/Pb: 5.7) (Wray *et al.*, 1985).

Unlike the early and intermediate pitchblendes at Midwest Lake, early (pitchblende I) and intermediate (pitchblende II) 334 Pod pitchblendes were virtually free of silica and titania. This may be explained by the Midwest Lake pitchblendes being at the unconformity while the 334 Pod pitchblendes are in the basement. Unconformity mineralization is associated with the dissolution of quartz and the destruction of resistate minerals at the base of the Athabasca Group (Hoeve and Quirt, 1987).

Third generation pitchblendes (pitchblende III) in the 334 Pod generally possessed U/Pb weight ratios of less than 10, and contain higher calcium, silicon and vanadium concentrations than pitchblendes of earlier generations. This pattern was repeated at Midwest Lake where later pitchblendes (U/Pb>10) possessed higher concentrations of calcium, silicon and vanadium than earlier pitchblendes.

Pitchblende III in the 334 Pod always possessed a silica component indicating either that it was partially converted to coffinite or that it was intimately mixed with domains of coffinite. Pure coffinite was not observed, although some pitchblende III analyses indicated a high coffinite component (Table 7).

A pattern noticed was that the oxide total decreased from pitchblende I to pitchblende III (Tables 5, 6, 7, 8). This may be due to (1) deviation from stoichiometric UO_2 (i.e., UO_{2+x} instead of UO_2); (2) hydration of pitchblendes; and (3) porosity of pitchblende III (-coffinite?) phases.

E. Arsenides

Arsenide minerals recognized in the 334 Pod are rammelsbergite, safflorite and nickeline. Rammelsbergite appears to be the oldest metalliferous mineral deposited in the 334 Pod. Deposition of rammelsbergite is followed by that of nickeline. Whereas

rammelsbergite is a minor mineral in the 334 Pod, nickeline is second only in abundance to gersdorffite, amongst the non-uraniferous metalliferous minerals.

E.1 Rammelsbergite [$NiAs_2$]

Rammelsbergite appears to be the earliest metalliferous mineral phase in the 334 Pod at Dawn Lake. It occurs as small, anhedral inclusions in nickeline and gersdorffite. Replacement textures of rammelsbergite by nickeline and gersdorffite indicate that rammelsbergite grains were much larger than at present. Rammelsbergite has been observed over a 6.3m depth interval in the upper part of the pod.

Electron microprobe analyses were obtained for rammelsbergites (a) enclosed by nickeline (analyses 3, 6, 7, 9 and 10; Table 9) and (b) enclosed by gersdorffite (analyses 2, 4, 5 and 8; Table 9). Rammelsbergites enclosed by gersdorffites exhibit higher iron and sulphur concentrations than those enclosed by nickeline. Metal to non-metal ratios vary between 1.02:1.98 and 1.00:2.00, indicating almost perfect stoichiometry. Iron occurs in amounts of up to 0.09 wt.%; cobalt, up to 0.29 wt.%; and sulphur, up to 0.58 wt.%. Antimony was observed in one sample.

Yund (1962) suggested that the maximum sulphur content of natural rammelsbergites was approximately 1 wt.%. It is evident that the 334 Pod rammelsbergites have not exceeded this limit.

Rammelsbergite has also been recognized in the Key Lake (Dahlkamp, 1978; von Pechmann, 1985), McClean Lake (Wallis *et al.*, 1983, 1985, 1986), Midwest Lake (Wray *et al.*, 1985), Collins Bay A (Ruzicka, 1986) and Cigar Lake (Fouques *et al.*, 1986; Ruzicka and LeCheminant, 1987) deposits. It has not been observed in the Carswell Structure deposits of the Amer Lake Zone (Ruhlmann, 1985).

E.2 Safflorite [$CoAs_2$]

Safflorite was observed to occur as small anhedral grains in the massive arsenide-sulpharsenide ore. Safflorite along with rammelsbergite probably were the oldest

Table 9: Chemical composition (in wt.% and atomic compositions of rammelsbergites from the 334 Pod, 11 A Zone, Dawn Lake, Saskatchewan.

	Location	Fe	Co	Ni	As	Sb	S	Total
(1)		----	----	28.15	71.85	----	----	100.00
(2)	334-144.0	0.09	0.22	28.00	71.49	ND	0.21	100.01
(3)	334-144.0	ND	0.12	28.19	71.68	ND	0.01	100.00
(4)	334-144.1	0.08	0.22	28.48	70.76	0.17	0.45	100.16
(5)	334-145.3	0.09	0.10	28.25	70.97	ND	0.58	99.99
(6)	334-145.3	ND	0.11	28.16	70.96	ND	0.10	99.33
(7)	334-145.3	ND	0.29	27.98	71.66	ND	0.07	100.00
(8)	334-145.4	0.06	0.19	28.13	70.92	ND	0.11	99.41
(9)	334-145.4	ND	0.13	28.25	70.80	ND	0.12	99.30
(10)	334-145.4	ND	0.27	27.97	70.90	ND	0.13	99.27
(11)	Midwest L	ND	ND	27.60	72.00	ND	ND	99.60
	Atomic composition on the basis of Fe+Co+Ni+As+Sb+S = 3.0							
(1)		----	----	1.00	2.00	----	---	
(2)	334-144.0	0.00	0.01	0.99	1.99	----	0.01	
(3)	334-144.0	----	0.00	1.00	2.00	----	0.00	
(4)	334-144.1	0.00	0.01	1.00	1.95	0.00	0.03	
(5)	334-145.3	0.00	0.00	1.00	1.96	----	0.04	
(6)	334-145.3	----	0.00	1.01	1.98	----	0.01	
(7)	334-145.3	----	0.01	0.99	2.00	----	0.00	
(8)	334-145.4	0.00	0.01	1.00	1.98	----	0.01	
(9)	334-145.4	----	0.00	1.01	1.98	----	0.01	
(10)	334-145.4	----	0.01	1.00	1.98	----	0.01	
(11)	Midwest L	----	----	0.99	2.01	----	----	

1: rammelsbergite (ideal composition)
2 — 10: rammelsbergites, 11A Zone, Dawn Lake, Saskatchewan (this study)
11: rammelsbergite, Midwest Lake, Saskatchewan (Wray et al., 1985)

ore minerals in the 334 Pod. It frequently possessed a spongy appearance and was replaced by nickeline, cobaltite and gersdorffite (Plate 13).

Safflorite has also been observed at the nearby McClean Lake (Wallis *et al.*, 1983, 1985, 1986) and Midwest Lake (Wray et al., 1985) deposits.

E.3 Nickeline [NiAs]

Amongst the non-uraniferous metallic minerals, nickeline is second only to gersdorffite in abundance. Nickeline occurs as replacements of rammelsbergites, as massive, anhedral grains, with or without earlier rammelsbergite inclusions, and as small, anhedral inclusions in later gersdorffite. Nickeline is observed to be replaced by gersdorffite and pyrite. Pitchblende I is observed as crack and fracture fillings in nickeline. Galena also occurs as cavity fillings in nickeline .

Electron microprobe analyses were done (a) in core regions and (b) near boundaries with gersdorffite. Operating conditions, standards, counting times and data collection methods used were the same as for rammelsbergites.

Iron was found to occur in amounts of up to 0.10 wt.%; cobalt, up to 0.20 wt.%; antimony, up to 0.12 wt.%; and sulphur, up to 0.32 wt.%. Metal to non-metal ratios exhibited a limited range from 0.99 to 1.01 indicating that the 334 Pod nickelines possess nearly perfect stoichiometric compositions (Table 10).

Nickelines with sulphur concentrations above 0.06 wt.% occurred generally next to gersdorffites. Core regions generally contained less than 0.06 wt.% sulphur. Nickelines with higher cobalt concentrations (>0.05 wt.%) appeared to occur in the upper part of the 334 Pod.

In the Athabasca Basin, nickeline has been observed at the Rabbit Lake (Rimsaite, 1977), Key Lake (Dahlkamp, 1978; von Pechmann, 1985), McClean Lake (Wallis *et al.*, 1983, 1985, 1986), Midwest Lake (Wray *et al.*, 1985), West Bear (Ruzicka, 1986), Collins Bay A and B (Ruzicka, 1986) and Cigar Lake (Fouques *et al.*, 1986) deposits; and at the Zimmer Lake (Watkinson *et al.*, 1975) and Natona Bay

Plate 13. Assemblage: safflorite-rammelsbergite-nickeline -gersdorffite-cobaltite

13a. Back scattered electron image

(i) Early safflorite (s) and rammelsbergite (r) are replaced by nickeline (n)
(ii) Safflorite, rammelsbergite, and nickeline are replaced by cobaltite (c) and gersdorffite (g)

13b. Co X-ray

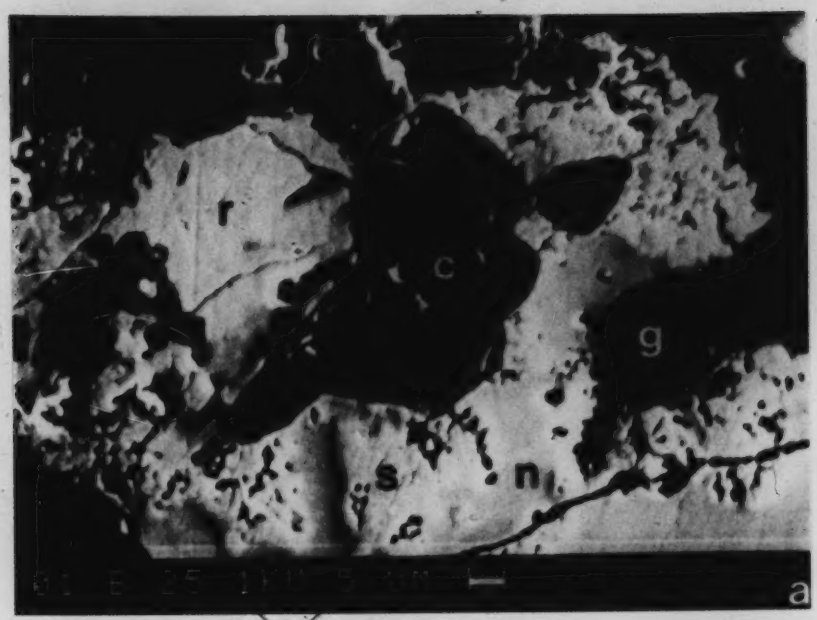
r
c
g
s
n
a

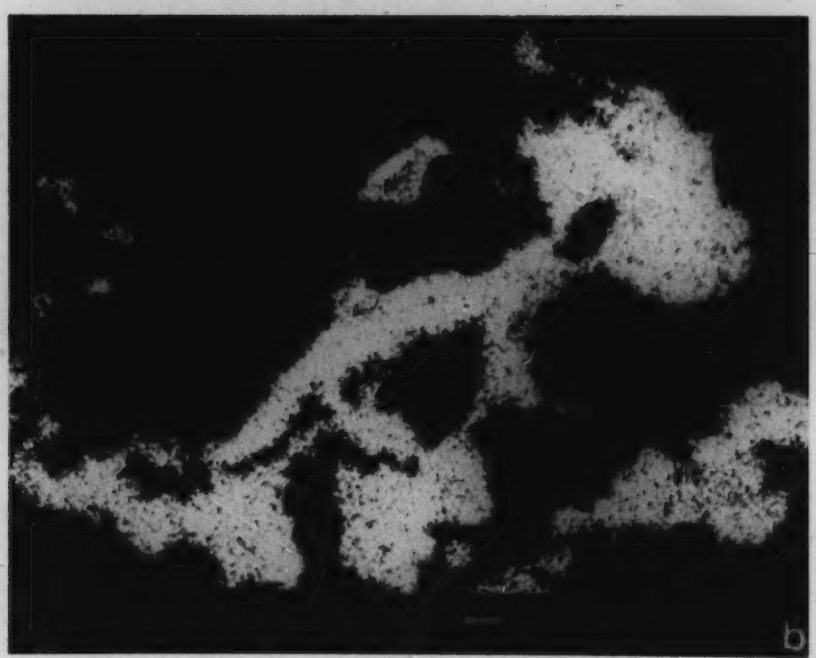
b

13c. S X-ray

13d. Ni X-ray

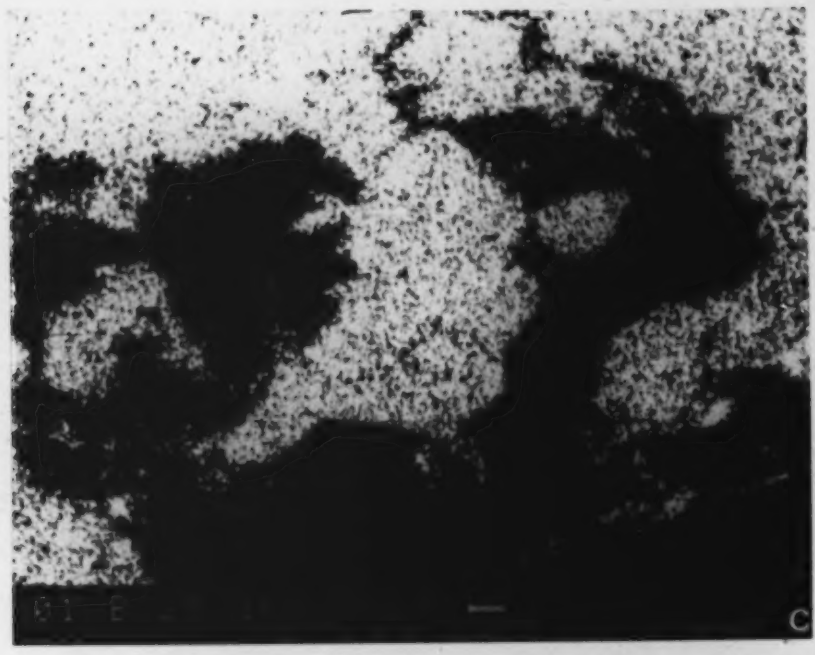
c

d

13e. As X-ray

Plate 14. Assemblage: cobaltite-bismuthian gersdorffite-cobaltite-gersdorffite
Back scattered electron image

(i) Cobaltite (C) cores are coated by bismuthian gersdorffite (bg) which, in turn, is coated by later cobaltite
(ii) Late gersdorffite (G) forms an outer rim on the earlier cobaltite-bismuthian gersdorffite-cobaltite

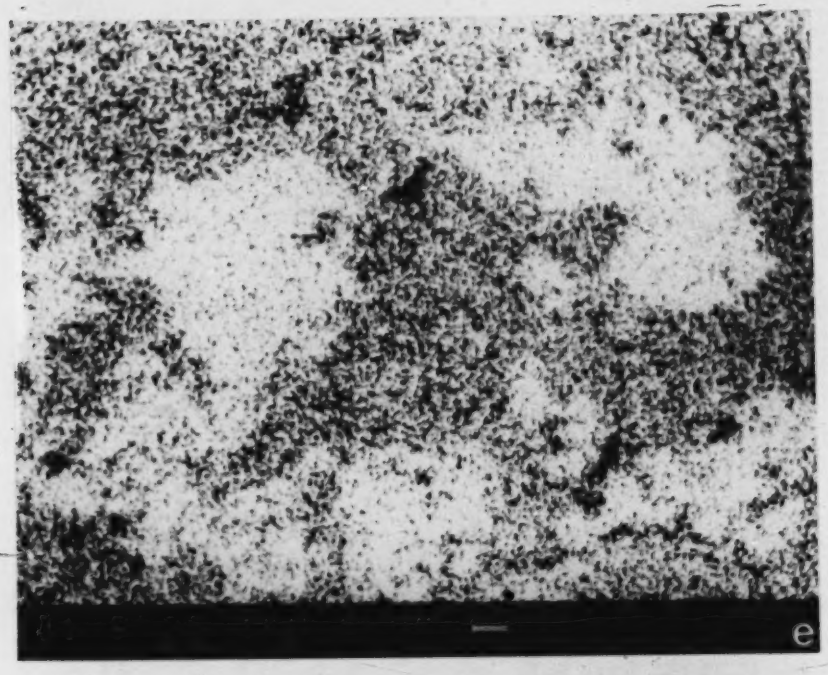
e

Table 10: Chemical compositions (in wt.%) and atomic compositions of nickelines from the 334 Pod, 11A Zone, Dawn Lake, Saskatchewan

	Location	Fe	Co	Ni	As	Sb	S	Total
(1)		----	----	43.93	56.07	----	----	100.00
(2)	334-144.0	ND	0.20	43.43	56.11	ND	0.09	99.83
(3)	334-145.4	ND	0.12	43.00	56.31	ND	0.04	99.47
(4)	334-145.4	ND	0.10	43.03	55.87	ND	0.04	99.04
(5)	334-145.4	ND	0.09	43.55	56.01	ND	0.04	99.68
(6)	334-144.0	0.06	0.08	43.53	56.23	0.10	0.01	100.01
(7)	334-145.4	ND	0.08	43.30	56.17	ND	0.03	99.58
(8)	334-145.4	ND	0.05	43.58	56.01	ND	0.03	99.67
(9)	334-148.6	ND	0.04	44.13	55.60	ND	0.07	99.84
(10)	334-148.6	0.08	0.04	44.35	55.76	ND	0.21	100.44
(11)	334-148.6	ND	0.03	44.29	55.59	0.06	0.01	99.98
(12)	334-148.6	ND	0.03	44.09	55.50	ND	0.04	99.66
(13)	334-148.6	0.06	0.02	44.22	55.80	0.06	0.32	100.48
(14)	334-148.6	0.10	0.02	44.13	55.66	ND	0.24	100.15
(15)	334-148.6	0.03	0.02	44.37	55.59	ND	0.10	100.11
(16)	334-148.6	0.09	0.02	44.28	55.51	0.11	0.08	100.09
(17)	334-148.6	0.09	0.02	44.06	55.66	ND	0.07	99.91
(18)	334-148.6	0.06	0.02	43.84	55.75	ND	0.11	99.78
(19)	334-148.6	0.03	0.02	44.12	55.48	0.10	0.01	99.76
(20)	334-148.6	ND	0.01	44.35	55.88	ND	0.07	100.32
(21)	334-148.6	ND	0.01	44.30	55.67	ND	0.02	100.00
(22)	334-148.6	ND	0.01	44.07	55.71	ND	0.06	99.85
(23)	334-148.6	ND	0.01	44.21	55.45	0.12	0.01	99.80
(24)	334-148.6	ND	0.01	44.27	55.48	ND	0.01	99.77
(25)	334-148.6	ND	ND	43.99	55.58	ND	ND	99.57
(26)	334-148.6	ND	ND	44.02	55.48	0.10	0.01	99.76
(27)	334-144.0	0.08	ND	44.14	55.72	ND	0.07	100.01

Table 10 (Contd.): Chemical compositions (in wt.%) and atomic compositions of nickelines from the 334 Pod, 11A Zone, Dawn Lake, Saskatchewan.

	Atomic composition on the basis of Fe+Co+Ni+As+Sb+S = 2.0						
(1)		----	----	1.00	1.00	----	----
(2)	334-144.0	----	0.01	0.99	1.00	----	0.00
(3)	334-145.4	----	0.00	0.99	1.01	----	0.00
(4)	334-145.4	----	0.00	0.99	1.01	----	0.00
(5)	334-145.4	----	0.00	1.00	1.00	----	0.00
(6)	334-144.0	0.00	0.00	0.99	1.01	0.00	0.00
(7)	334-145.4	----	0.00	0.99	1.00	----	0.00
(8)	334-145.4	----	0.00	1.00	1.00	----	0.00
(9)	334-148.6	----	0.00	1.00	0.99	----	0.00
(10)	334-148.6	----	0.00	1.00	0.99	----	0.01
(11)	334-148.6	0.00	0.00	1.01	0.99	0.00	0.00
(12)	334-148.6	----	0.00	1.01	0.99	----	0.00
(13)	334-148.6	0.00	0.00	1.00	0.99	0.00	0.01
(14)	334-148.6	0.00	0.00	1.00	0.99	----	0.01
(15)	334-148.6	0.00	0.00	1.01	0.99	----	0.00
(16)	334-148.6	0.00	0.00	1.01	0.99	0.00	0.00
(17)	334-148.6	0.00	0.00	1.00	0.99	0.00	0.00
(18)	334-148.6	0.00	0.00	1.00	1.00	ND	0.00
(19)	334-148.6	0.00	0.00	1.01	0.99	0.00	0.00
(20)	334-148.6	----	0.00	1.01	0.99	----	0.00
(21)	334-148.6	----	0.00	1.01	0.99	----	0.00
(22)	334-148.6	----	0.00	1.00	0.99	----	0.00
(23)	334-148.6	----	0.00	1.01	0.99	0.00	0.00
(24)	334-148.6	ND	0.00	1.01	0.99	----	0.00
(25)	334-148.6	----	----	1.01	0.99	----	----
(26)	334-148.6	----	----	1.01	0.99	0.00	0.00
(27)	334-144.0	0.00	----	1.01	0.99	----	0.00

(1): nickeline (ideal composition)
(2) — (11): nickelines (this study)

(Ruzicka and LeCheminant, 1986) occurrences. In the Carswell Structure deposits in the Amer Lake Zone, nickeline has been observed as an accessory mineral (Ruhlmann, 1985).

F. Sulpharsenides

Sulpharsenide minerals identified in the 334 Pod at Dawn Lake are gersdorffite and cobaltite. Gersdorffite is the most abundant non-uraniferous mineral in the 334 Pod. Its abundance is slightly greater than that of nickeline. Gersdorffite occurs in four varieties: (a) normal, (b) cobaltian, (c) arsenian and (d) bismuthian. Cobaltian gersdorffite occurs locally but is rare. One grain of arsenian gersdorffite was observed. Bismuthian gersdorffite has not been previously described in the mineralogical literature.

F.1 Gersdorffite [NiAsS]

Gersdorffite is the most abundant nickel mineral in the 334 Pod at Dawn Lake.

It occurs as rims and replacements of rammelsbergite and nickeline, as dendrites coated by pitchblende I, as later coatings on and shrinkage crack fillings in pitchblende I, as euhedral grains grading into massive interlocking anhedra and as coats on cobaltite. Euhedral grains and massive interlocking anhedra may or may not contain bismuthian gersdorffite bands. Gersdorffite is replaced by millerite, bravoite and pyrite (Plates 15-18). Replacement occurs from the core outwards towards the rim. This texture can be easily misinterpreted as gersdorffite replacing millerite, bravoite and pyrite. At Key Lake, bravoite inclusions in gersdorffite were used to support the argument that deposition of bravoite preceded that of gersdorffite (von Pechmann, 1985). However, the bravoite inclusion textures in gersdorffite at Key Lake closely resemble those at Dawn Lake and probably represent later replacements of gersdorffite. Violarite, probably, also is a replacement of gersdorffite. Arsenian and bismuthian gersdorffite are treated separately.

Plate 15. Zoned gersdorffite (G) with cores showing different stages of corrosion
Back scattered electron image

Plate 16. Gersdorffite (G) core partially replaced by pyrite (PY)
Back scattered electron image

G

G
P
G

Plate 17. Gersdorffite (G) exhibiting zonal and core replacement by pyrite (PY)
Back scattered electron image

Plate 18. Gersdorffite (G) exhibiting core replacement by pyrite (PY) and bravoite (BR)
Back scattered electron image

PY
G

PY
G
BR

In the Cree Lake Zone, gersdorffites have been observed at the Key Lake (Dahlkamp, 1978; von Pechmann, 1985), McClean Lake (Wallis *et al.*, 1983, 1985, 1986), Midwest Lake (Wray *et al.*, 1985), Collins Bay B (Ruzicka, 1986) and Cigar Lake (Fouques *et al.*, 1986; Ruzicka and LeCheminant, 1987) deposits, as well as at the Zimmer Lake (Watkinson *et al.*, 1975) and Natona Bay (Ruzicka and LeCheminant, 1986) occurrences. Gersdorffite has been observed as an accessory mineral in the Carswell Structure unconformity-associated uranium deposits of the Amer Lake Zone (Ruhlmann, 1985).

F.2 Gersdorffite (normal variety)

Normal gersdorffite is present in the upper 7m of the 334 Pod at Dawn Lake (Table 2). It occurs before and after the deposition of pitchblende I. Gersdorffite occurring before the deposition of pitchblende I consists of (a) early (inclusions, crack fillings) and (b) late (massive) replacements of nickeline and rammelsbergite, and (c) dendrites. Massive interlocking gersdorffite anhedra coat pitchblende I. These massive gersdorffite anhedra grade into subhedral to euhedral grains. Later subhedral to euhedral grains may or may not contain bismuthian gersdorffite bands. Grains containing bismuthian gersdorffite bands are considered to have formed later than grains not containing bismuthian gersdorffite.

In order to characterise the various normal gersdorffites, electron microprobe analyses have been done on:

(A) Gersdorffite preceding pitchblende I

(i) early replacements of nickeline (334-145.4)

(ii) late replacements of nickeline (334-145.4)

(B) Gersdorffite succeeding pitchblende I

(i) massive anhedra coating pitchblende I (334-143.8)

(ii) euhedral grains not containing bismuthian gersdorffite (334-143.2)

(iii) euhedral grains containing bismuthian gersdorffite (334-143.2)

(iv) euhedral grains containing bismuthian gersdorffite (334-147.0)

Method

Operating conditions were an accelerating voltage of 15kV and a probing current of 3.3nA. Counting times were 240s for both standards and samples. The following standards were used: arsenopyrite (S,Fe,As), pure cobalt (Co), pararammelsbergite (Ni) and pure antimony (Sb). Wavelength dispersive (S,Fe,Co,As) and energy dispersive (Ni,Sb) data were collected simultaneously and reduction of these data was carried out using the computer program EDATA2 (Smith *et al.*, 1981). The detection limits for the operating conditions used were determined to be 0.01 wt.% for S,Fe,Co and As, and 0.02 wt.% for Ni and Sb.

Results

(A) Gersdorffite preceding pitchblende I

In polished mount 334-145.4 gersdorffite was observed to be replacing nickeline along cracks. A later, more massive gersdorffite continued to replace nickeline. Pitchblende I was observed to occur in cracks cutting the later gersdorffite. Electron microprobe analyses of the early and later replacements are given in Table 11. The early gersdorffites possessed As:S ratios of 1.02-1.04 (Fig. 11) and high nickel concentrations. An exception was noted in one area where cobaltian gersdorffite was present.

The later gersdorffites possessed lower As:S ratios (0.98-1.00) (Fig. 11), lower nickel contents and higher cobalt contents than the earlier gersdorffites.

(B) Gersdorffite preceding pitchblende I

(i) Massive anhedra coating pitchblende I

A massive anhedral grain coating pitchblende I was chosen at random for electron microprobe analyses from a mass of interlocking gersdorffite anhedra not containing bismuthian gersdorffite (polished mount 334-143.8).

Table 11: Chemical compositions (in wt.%) and atomic compositions of gersdorffites (334-145.4) paragenetically earlier than pitchblende I from the 334 Pod, 11A Zone, Dawn Lake , Saskatchewan.

	Location	Fe	Co	Ni	As	Sb	S	Total
(1)	334-145.4	0.02	0.78	34.79	45.48	NA	19.02	100.09
(2)	334-145.4	0.05	1.09	34.40	45.75	NA	18.79	100.08
(3)	334-145.4	0.01	0.34	35.67	45.49	NA	18.77	100.29
(4)	334-145.4	0.16	9.60	24.53	46.04	NA	18.99	99.32
(5)	334-145.4	0.09	3.27	32.20	45.59	NA	19.47	100.62
(6)	334-145.4	0.02	3.02	32.93	44.64	NA	19.30	100.01
(7)	334-145.4	0.02	2.77	33.04	44.81	NA	19.37	100.01
	Atomic composition on the basis of Fe+Co+Ni+As+Sb+S = 3.0							
(1)	334-145.4	0.00	0.02	0.98	1.01	----	0.99	
(2)	334-145.4	0.00	0.03	0.98	1.01	----	0.98	
(3)	334-145.4	0.00	0.01	1.01	1.01	----	0.97	
(4)	334-145.4	0.01	0.27	0.70	1.03	----	0.99	
(5)	334-145.4	0.00	0.09	0.91	1.00	----	1.00	
(6)	334-145.4	0.00	0.08	0.93	0.99	----	1.00	
(7)	334-145.4	0.00	0.08	0.93	0.99	----	1.01	

1 — 3: gersdorffites (early)
4: cobaltian gersdorffite (early)
5 — 7: gersdorffites (late)

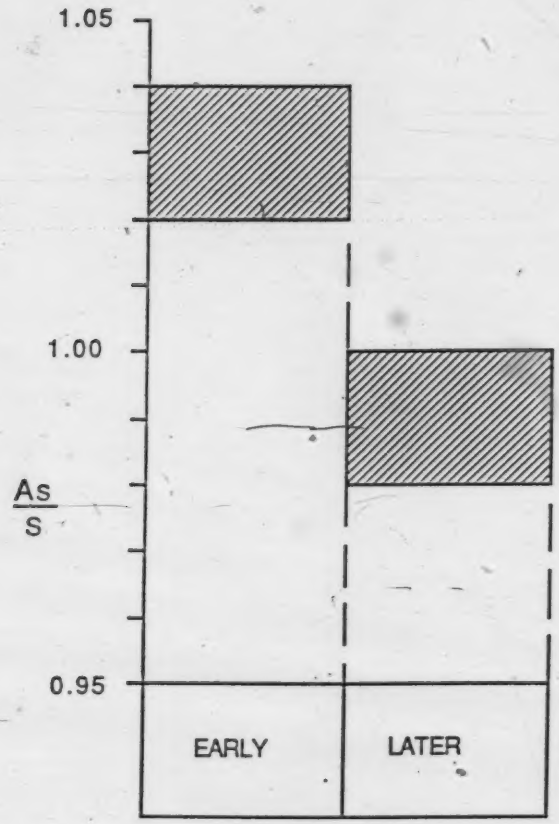

Figure 11. As:S ratios of gersdorffites (334-145.4) paragenetically earlier than pitchblende I

Analyses of core regions (zone 1) yielded As:S ratios of 0.94-0.96 (Fig. 12), whilst analyses of outer regions (zone 2) yielded As:S ratios of 0.98-1.00 (Fig. 12). Nickel increased slightly, whilst cobalt may have decreased slightly towards the outer regions (Table 12).

(ii) Euhedral grains not containing bismuthian gersdorffite (334-143.2)

An euhedral grain without bismuthian gersdorffite bands from polished mount 334-143.2 was examined. Paragenetically, this grain occurred before the deposition of bismuthian gersdorffite, and after the deposition of pitchblende 1. Zone 1 is the core region, zones 2 and 3 are intermediate areas, and zone 4 is the rim area. Analyses of gersdorffites As:S ratios were 1.02 for zone 1, 1.05-1.06 for zone 2, 1.08 for zone 3, and 1.11 for zone 4 (Table 13). Thus, it is evident that the As:S ratio (Fig. 13) increases progressively from core regions to rim areas. As the As:S ratio increases, there is a corresponding decrease in nickel content. Cobalt concentrations vary erratically whilst iron concentrations are generally low.

(iii) Euhedral grains containing bismuthian gersdorffite (334-143.2)

A subhedral or semi-euhedral grain of gersdorffite containing bismuthian gersdorffite bands was selected at random from a group of such grains which were isolated from each other in the phyllosilicate matrix. Paragenetically, these grains probably are representative of the very late stages of gersdorffite deposition. Zone 1 represents normal gersdorffite in the core region, zone 2 represents normal gersdorffite between zone 1 and the bismuthian gersdorffite zone (zone 3), while zone 4 represents normal gersdorffite in the rim region outside of zone 3. As:S ratios were 1.01-1.02 for zone 1, 1.02-1.03 for zone 2, and 1.13-1.15 for zone 4 (Table 14; Fig. 14). Zone 3 bismuthian gersdorffites from this grain were not analyzed. However, bismuthian gersdorffites generally possess As+Bi:S ratios similar to those for zone 4 gersdorffites (Appendix 1). Nickel concentrations increased from zone 1 to zone

Table 12: Chemical compositions (in wt.%) and atomic compositions of gersdorffites (334-143.8) paragenetically later than pitchblende I from the 334 Pod, 11A Zone, Dawn Lake, Saskatchewan

	Location	Fe	Co	Ni	As	Sb	S	Total
(1)	334-143.8	ND	1.17	34.04	43.55	NA	19.74	98.50
(2)	334-143.8	ND	1.66	33.99	43.70	NA	19.58	98.93
(3)	334-143.8	ND	1.23	33.99	44.20	NA	19.53	98.95
(4)	334-143.8	0.06	0.92	34.34	44.99	NA	19.61	99.92
(5)	334-143.8	ND	1.33	34.12	45.13	NA	19.48	100.06
	Atomic composition on the basis of Fe+Co+Ni+As+Sb+S = 3.0							
(1)	334-143.8	----	0.03	0.97	0.97	----	1.03	
(2)	334-143.8	----	0.05	0.96	0.97	----	1.02	
(3)	334-143.8	----	0.03	0.97	0.98	----	1.02	
(4)	334-143.8	0.00	0.03	0.97	0.99	----	1.01	
(5)	334-143.8	----	0.04	0.96	1.00	----	1.00	

1 — 3: zone 1
4 — 5: zone 2

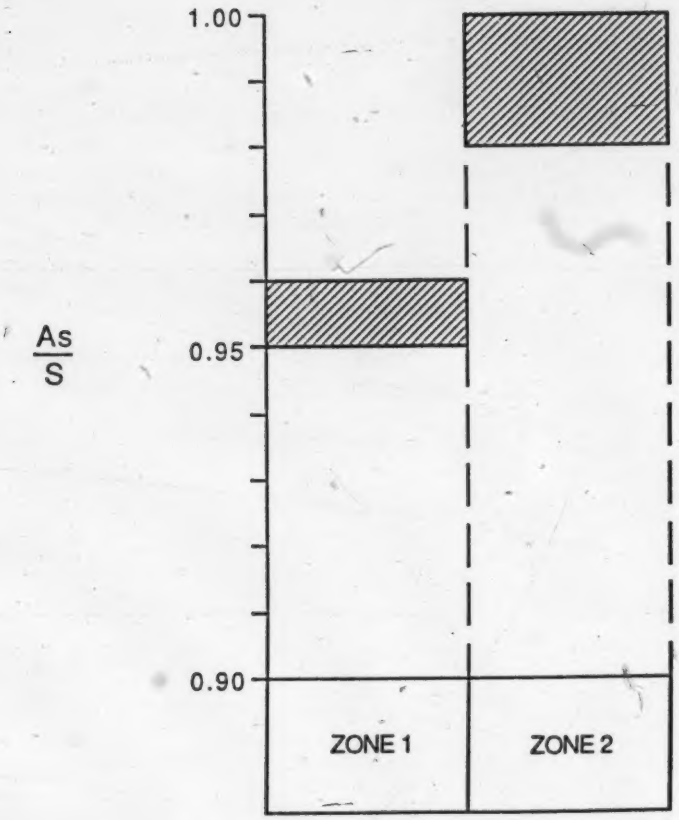

Figure 12. As:S ratios of gersdorffites (334-143.8) paragenetically later than pitchblende I

Table 13: Chemical compositions (in wt.%) and atomic compositions of gersdorffites (334-143.2: paragenetically later than pitchblende I but not associated with bismuthian gersdorffite) from the 334 Pod, 11A Zone, Dawn Lake, Saskatchewan.

	Location	Fe	Co	Ni	As	Sb	S	Total
(1)	334-143.2	0.02	1.08	32.69	45.49	0.41	18.97	98.65
(2)	334-143.2	0.04	0.78	33.14	47.16	0.42	19.18	100.72
(3)	334-143.2	0.02	0.98	32.70	46.68	0.37	19.03	99.77
(4)	334-143.2	0.03	0.78	33.01	47.00	0.40	19.10	100.61
(5)	334-143.2	0.02	0.98	32.48	47.30	0.40	18.84	100.02
(6)	334-143.2	0.05	1.60	31.74	47.92	0.46	18.89	100.66
(7)	334-143.2	0.05	1.04	31.86	48.04	0.43	18.60	100.02
(8)	334-143.2	0.02	0.97	31.89	48.28	0.40	18.44	100.00
	Atomic composition on the basis of Fe+Co+Ni+As+Sb+S = 3.0							
(1)	334-143.2	0.00	0.03	0.94	1.02	0.01	1.00	
(2)	334-143.2	0.00	0.02	0.93	1.04	0.01	0.99	
(3)	334-143.2	0.00	0.03	0.93	1.04	0.01	0.99	
(4)	334-143.2	0.00	0.02	0.93	1.05	0.01	0.99	
(5)	334-143.2	0.00	0.03	0.92	1.06	0.01	0.98	
(6)	334-143.2	0.00	0.05	0.90	1.06	0.01	0.98	
(7)	334-143.2	0.00	0.03	0.91	1.08	0.01	0.97	
(8)	334-143.2	0.00	0.03	0.91	1.08	0.01	0.97	

1: zone 1
2 — 4: zone 2
5 — 6: zone 3
7 — 8: zone 4

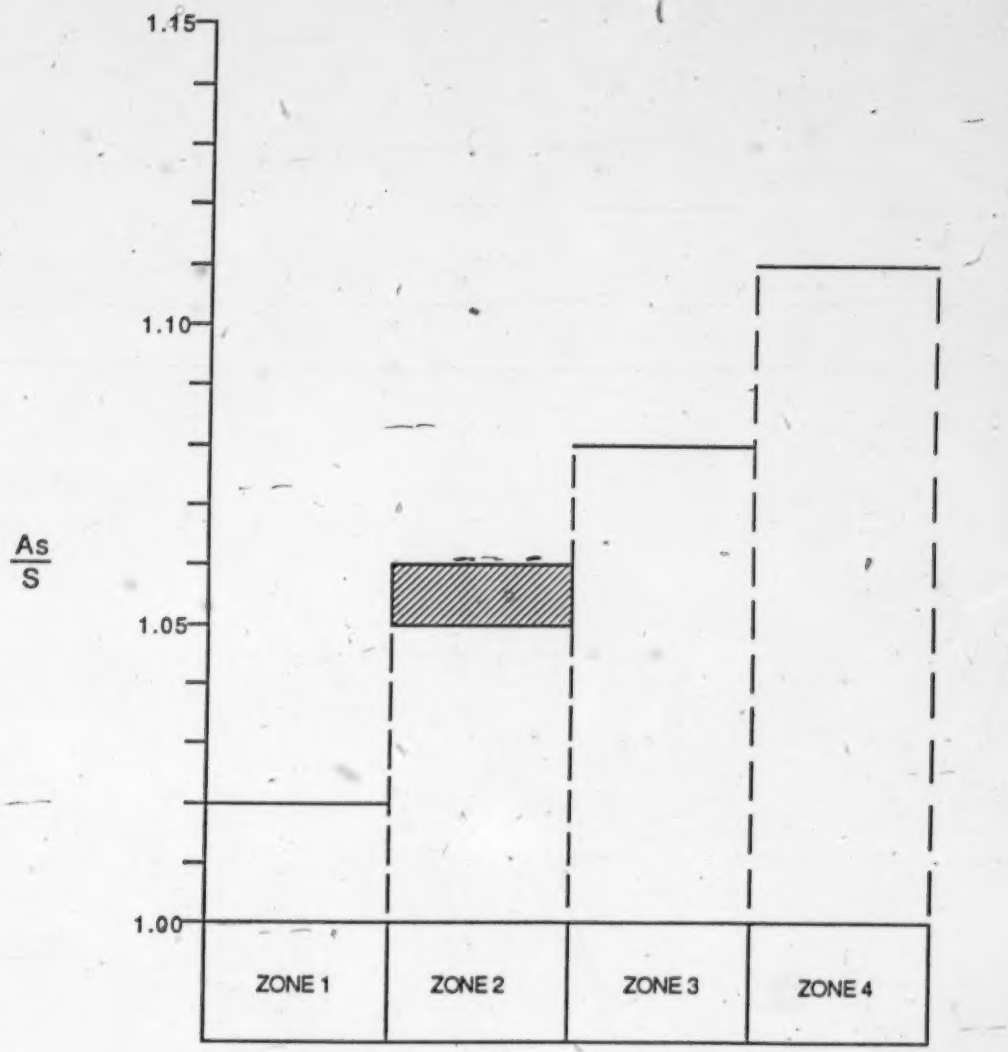

Figure 13. As:S ratios of gersdorffites (334-143.2) paragenetically later than pitchblende I
(but not associated with bismuthian gersdorffite)

Table 14: Chemical compositions (in wt.%) and atomic compositions of gersdorffites (334-143.2: paragenetically later than pitchblende I and associated with bismuthian gersdorffite) from the 334 Pod, 11A Zone, Dawn Lake Saskatchewan.

	Location	Fe	Co	Ni	As	Sb	S	Total
(1)	334-143.2	0.21	3.75	29.75	46.10	0.45	19.34	99.60
(2)	334-143.2	0.09	4.29	30.23	45.33	0.33	19.25	99.52
(3)	334-143.2	0.11	2.81	32.03	45.42	0.30	18.95	99.62
(4)	334-143.2	0.09	2.95	32.03	46.13	0.32	19.06	100.57
(5)	334-143.2	0.11	1.86	31.71	47.56	0.29	17.71	99.23
(6)	334-143.2	0.11	1.95	31.24	47.35	0.31	17.77	98.71
(7)	334-143.2	0.10	2.18	31.45	48.07	0.32	17.89	100.01
(8)	334-143.2	0.10	2.20	31.37	46.91	0.25	17.77	98.60
(9)	334-143.2	0.10	2.31	31.06	47.53	0.31	17.78	99.09
	Atomic composition on the basis of Fe+Co+Ni+As+Sb+S = 3.0							
(1)	334-143.2	0.00	0.11	0.85	1.03	0.00	1.01	
(2)	334-143.2	0.00	0.12	0.86	1.01	0.00	1.00	
(3)	334-143.2	0.00	0.08	0.92	1.01	0.00	0.99	
(4)	334-143.2	0.00	0.08	0.91	1.02	0.00	0.99	
(5)	334-143.2	0.00	0.05	0.92	1.08	0.00	0.94	
(6)	334-143.2	0.00	0.06	0.91	1.08	0.00	0.95	
(7)	334-143.2	0.00	0.06	0.91	1.08	0.00	0.94	
(8)	334-143.2	0.00	0.06	0.91	1.07	0.00	0.95	
(9)	334-143.2	0.00	0.07	0.90	1.08	0.00	0.94	

1 — 2: zone 1
3 — 4: zone 2
5 — 9: zone 4

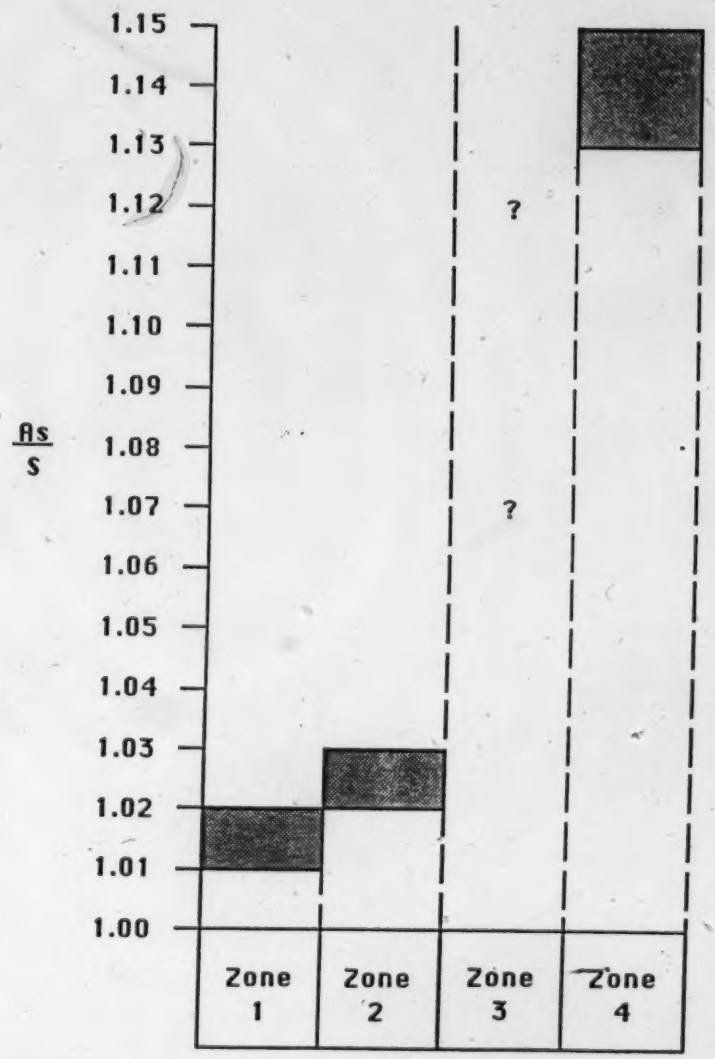

Figure 14. As:S ratios of gersdorffites (334-143.2) paragenetically later than pitchblende I
(and associated with bismuthian gersdorffite)

2, whilst in zones 2 and 4 they were essentially the same. Cobalt decreased from zone 1 to zone 2; zone 4 concentrations were lower than those of zone 2. Similar iron concentrations were observed in zones 1, 2 and 4.

(iv) Euhedral grains containing bismuthian gersdorffite (334-147.0)

A subhedral grain of gersdorffite containing bismuthian gersdorffite bands was chosen at random from several similar grains from polished mount 334-147.0. Paragenetically, this grain was formed after the deposition of pitchblende I, and before the deposition of pitchblende II. The analysis of this grain was done in order to provide a comparison with results obtained for a similar grain from higher up in the ore zone (see (iii) immediately above). The difference between this grain and the grain from polished mount 334-143.2 was that this grain contained two distinct generations of bismuthian gersdorffite.

The zonal sequence from core (zone 1) to rim (zone 7) was as follows:

Zone 1 : normal gersdorffite
Zone 2 : normal gersdorffite
Zone 3 : bismuthian gersdorffite
Zone 4 : normal gersdorffite
Zone 5 : bismuthian gersdorffite
Zone 6 : normal gersdorffite
Zone 7 : normal gersdorffite

Zone 2 and zone 6 are boundary zones.

Zone 1 gersdorffites were characterised by Ni:(Ni+Co+Fe) atomic ratio of 0.98, cobalt concentrations between 0.53 and 0.61 wt.%, low iron concentrations (0.02-0.04 wt.%), and As:S atomic ratios of 0.99 and 1.01 (Table 15; Fig. 15). Zone 2 gersdorffites were characterised by Ni:(Ni+Co+Fe) atomic ratios of 0.95-0.96, As:S atomic ratios of 1.04-1.06

Table 15: Chemical compositions (in wt.%) and atomic compositions of gersdorffites (334-147.0: paragenetically later than pitchblende I and associated with bismuthian gersdorffite) from the 334 Pod, 11A Zone, Dawn Lake, Saskatchewan.

	Location	Fe	Co	Ni	As	Sb	S	Total
(1)	334-147.0	0.02	0.61	35.25	44.78	0.22	19.47	100.35
(2)	334-147.0	0.03	0.55	35.09	44.97	0.33	19.40	100.37
(3)	334-147.0	0.04	0.53	35.07	45.33	0.31	19.26	100.54
(4)	334-147.0	0.07	1.84	32.65	45.11	0.27	18.62	98.56
(5)	334-147.0	0.09	1.41	33.53	46.01	0.20	18.57	99.83
(6)	334-147.0	0.13	2.79	32.29	45.58	0.31	18.54	99.64
(7)	334-147.0	0.16	0.64	35.00	45.09	0.26	19.05	100.20
(8)	334-147.0	0.27	0.15	35.46	43.73	0.33	19.84	99.78
(9)	334-147.0	0.38	0.13	35.16	44.63	0.34	19.47	100.11
(10)	334-147.0	0.43	0.14	35.18	44.41	0.21	19.69	100.06
(11)	334-147.0	0.44	0.20	35.08	43.71	0.34	19.82	99.59
(12)	334-147.0	0.49	0.22	35.35	45.03	0.29	19.62	101.00
(13)	334-147.0	0.96	0.26	34.84	44.62	0.25	19.70	100.63
(14)	334-147.0	0.97	0.22	34.76	44.56	0.30	19.49	100.30
	Atomic composition on the basis of Fe+Co+Ni+As+Sb+S = 3.0							
(1)	334-147.0	0.00	0.02	0.99	0.99	0.00	1.00	
(2)	334-147.0	0.00	0.02	0.99	0.99	0.00	1.00	
(3)	334-147.0	0.00	0.02	0.99	1.00	0.00	0.99	
(4)	334-147.0	0.00	0.05	0.94	1.02	0.00	0.98	
(5)	334-147.0	0.00	0.04	0.96	1.03	0.00	0.97	
(6)	334-147.0	0.00	0.08	0.92	1.02	0.00	0.97	
(7)	334-147.0	0.00	0.02	0.99	1.00	0.00	0.99	
(8)	334-147.0	0.01	0.00	1.00	0.96	0.00	1.02	
(9)	334-147.0	0.01	0.00	0.99	0.99	0.00	1.01	
(10)	334-147.0	0.01	0.00	0.99	0.98	0.00	1.01	
(11)	334-147.0	0.01	0.01	0.99	0.97	0.00	1.02	
(12)	334-147.0	0.01	0.01	0.99	0.99	0.00	1.01	
(13)	334-147.0	0.03	0.01	0.97	0.98	0.00	1.01	
(14)	334-147.0	0.03	0.01	0.98	0.98	0.00	1.00	

1 — 3: zone 1
4 — 5: zone 2
6: zone 4
7: zone 6
8 — 14: zone 7

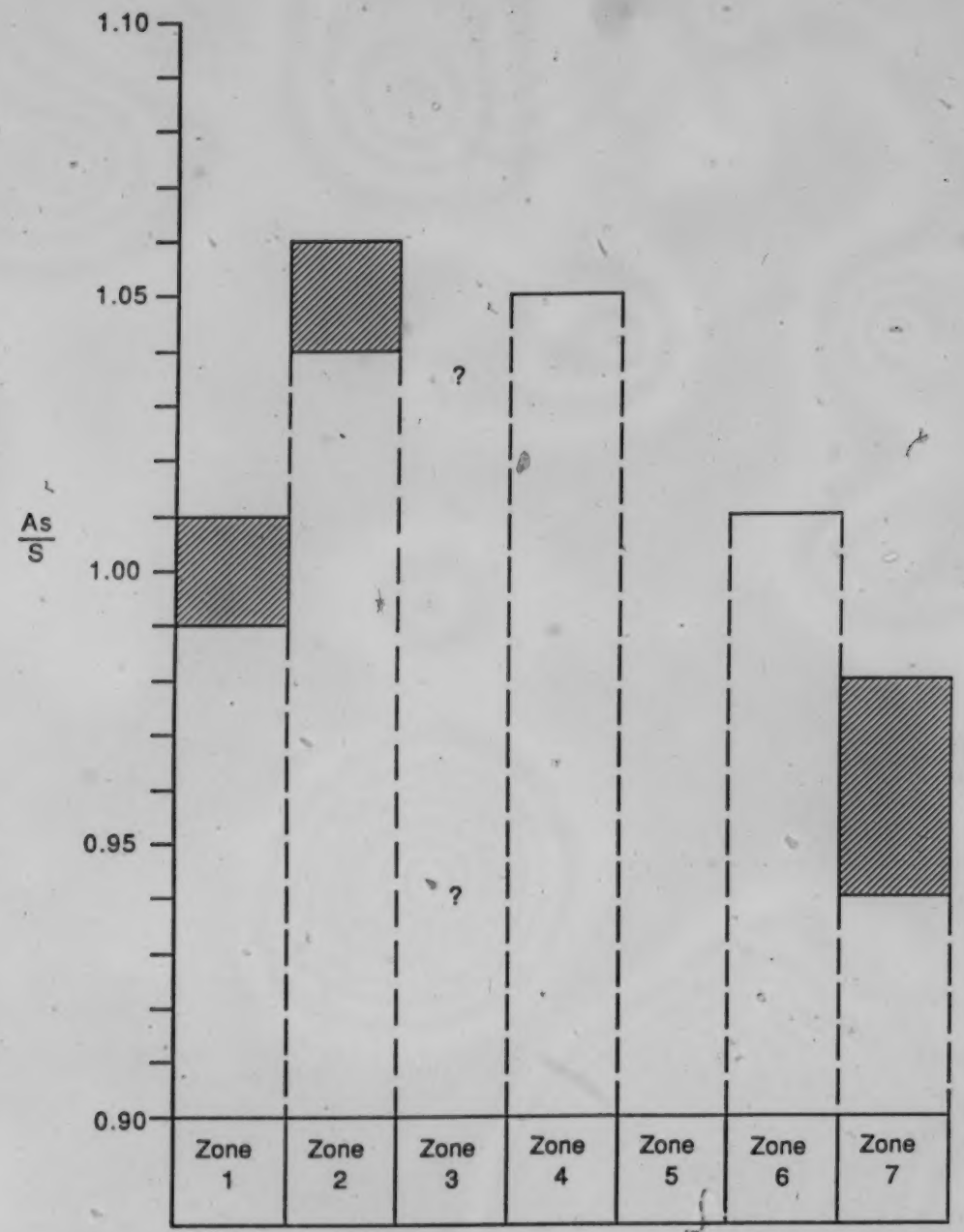

Figure 15. As:S ratios of gersdorffites (334-147.0) paragenetically later than pitchblende I
(and associated with bismuthian gersdorffite)

and exhibited approximately three-fold increases in the concentrations of cobalt and iron relative to zone 1 gersdorffites. Zone 4 gersdorffites possessed the highest cobalt concentration (2.79 wt.%) and the lowest Ni:(Ni+Co+Fe) atomic ratio (0.92) observed amongst the five normal gersdorffite zones. The As:S atomic ratio (1.05) was similar to that for zone 2 gersdorffites. The Ni:(Ni+Co+Fe) atomic ratio (0.98) and As:S atomic ratio (1.01) of zone 6 gersdorffites were similar to those of zone 1 gersdorffites. Relative to zone 4 gersdorffites, zone 6 gersdorffites exhibited lower cobalt but similar iron concentrations. Zone 7 gersdorffites were characterised by Ni:(Ni+Co+Fe) atomic ratios of 0.93-0.99 and As:S atomic ratios of 0.94-0.98. Zone 7 gersdorffites possessed the highest iron (0.27-0.97 wt.%) and lowest cobalt (0.13-0.26 wt.%) concentrations of the five normal gersdorffite zones.

Conclusions

Gersdorffite precipitation occurred in two stages, i.e., (a) before the deposition of pitchblende I and (b) after the deposition of pitchblende I.

(a) Gersdorffite preceding the deposition of pitchblende I

Early gersdorffite replacing nickeline, in general, had higher As:S ratios (1.02-1.04), higher nickel and lower cobalt concentrations than later gersdorffite (As:S=0.98-1.00).

(b) Gersdorffite succeeding pitchblende I

Nucleation of gersdorffite appears to occur at As:S ratios of about 0.94-0.96. Growth of gersdorffite in the early stages appears to be characterised by increasing As:S ratios of up to 1.11. In areas of bismuthian gersdorffite deposition, high As:S ratios appear to be common. Support for this comes from high (As+Bi):S ratios in bismuthian gersdorffite regions (Appendix 1). Late gersdorffites

exhibit decreasing As:S ratios (0.94-0.98) which are almost identical to those of the earliest gersdorffites succeeding pitchblende I.

F.3 Arsenian Gersdorffite

One small, anhedral grain of arsenian gersdorffite occurring in the phyllosilicate matrix was identified in the polished mount 334-143.2. However, it was not identified during routine microscopic investigations, but during qualitative energy dispersive analysis of gersdorffite grains. Its dimensions were about 40 μm x 30 μm and its edges showed signs of corrosion.

Ten points on the surface of the grain were chosen at random for electron microprobe analysis. Operating conditions, counting times, standards and data collection techniques were the same as for normal gersdorffites.

Microprobe analyses indicated that a core region of higher As:S ratios (3.48-3.60) was present, and that As:S ratios gradually decreased towards the rim areas (2.83-2.85) (Table 16).

The average composition of the core region (analyses 1-4; Table 16) was :

$$(Ni_{1.01}\ Fe_{0.01}\ Co_{0.00})\ (As_{1.54}\ Sb_{0.00}\ S_{0.44})$$

The average composition of the intermediate region (analysis 5-8; Table 16) was:

$$(Ni_{1.01}\ Fe_{0.01}\ Co_{0.00})\ (As_{1.51}\ Sb_{0.00}\ S_{0.47})$$

The average composition of the outer (rim) region (analysis 9-10; Table 16) was:

$$(Ni_{1.00}\ Fe_{0.01}\ Co_{0.00})\ (As_{1.47}\ Sb_{0.00}\ S_{0.52})$$

Yund (1962) stated that arsenic and sulphur can substitute for each other in the gersdorffite structure between compositional limits of $NiAs_{1.77}S_{0.23}$ to $NiAs_{0.77}S_{1.23}$. Antimony can substitute for both sulphur and arsenic (Yund, 1962).

The compositions obtained for this arsenian gersdorffite were found to lie within the compositional limits given by Yund (1962). Iron and cobalt concentrations were essentially the same throughout the grain, whilst antimony concentrations varied erratically.

Table 16: Chemical compositions (in wt.%) and atomic compositions of arsenian gersdorffite from the 334 Pod, 11A Zone, Dawn Lake, Saskatchewan.

	Location	Fe	Co	Ni	As	Sb	S	Total
(1)		----	----	35.40	45.20	----	19.40	100.00
(2)	334-143.2	0.26	0.09	30.99	61.25	0.21	7.21	100.01
(3)	334-143.2	0.32	0.08	31.36	60.93	ND	7.20	99.88
(4)	334-143.2	0.27	0.10	31.21	61.59	0.10	7.46	100.73
(5)	334-143.2	0.26	0.09	31.72	60.55	0.14	7.40	100.16
(6)	334-143.2	0.28	0.11	31.58	61.03	0.07	7.89	100.96
(7)	334-143.2	0.27	0.09	31.04	60.53	0.12	7.95	100.00
(8)	334-143.2	0.31	0.12	31.24	59.37	0.07	7.88	98.98
(9)	334-143.2	0.41	0.10	31.16	59.77	0.08	8.00	99.53
(10)	334-143.2	0.32	0.11	31.43	59.62	0.14	8.89	100.50
(11)	334-143.2	0.27	0.09	31.72	59.68	0.11	9.00	100.85
	Atomic composition on the basis of Fe+Co+Ni+As+Sb+S = 3.0							
(1)		----	----	1.00	1.00	----	1.00	
(2)	334-143.2	0.01	0.00	1.00	1.55	0.00	0.43	
(3)	334-143.2	0.01	0.00	1.02	1.54	----	0.43	
(4)	334-143.2	0.01	0.00	1.01	1.54	0.00	0.44	
(5)	334-143.2	0.01	0.00	1.02	1.53	0.00	0.44	
(6)	334-143.2	0.01	0.00	1.01	1.52	0.00	0.46	
(7)	334-143.2	0.01	0.00	1.00	1.52	0.00	0.47	
(8)	334-143.2	0.01	0.00	1.01	1.51	0.00	0.47	
(9)	334-143.2	0.01	0.00	1.01	1.51	0.00	0.47	
(10)	334-143.2	0.01	0.00	0.99	1.48	0.00	0.52	
(11)	334-143.2	0.01	0.00	1.00	1.47	0.00	0.52	

1: gersdorffite (ideal composition)
2 — 11: arsenian gersdorffites (this study)

Arsenian gersdorffite has not been described from any other Athabasca Basin unconformity-associated uranium deposit. However, it has been recognised in ores from Cobalt, Ontario (Petruk *et al.*, 1971) and the Camsell River sector, Great Bear Lake, N.W.T. (Changkakoti, 1985; Changkakoti and Morton, 1986).

The arsenian gersdorffite probably formed during changes in the As:S ratio of the ore fluid. Its paragenetic position is uncertain, but it probably formed during the nickeline-gersdorffite transition. If this is so, then this arsenian gersdorffite probably represents the earliest generation of gersdorffite in the 334 Pod.

F.4 Bismuthian Gersdorffite

This mineral which hitherto has not been described in the geological literature is the subject of a paper by the author accepted for publication in Neues Jahrbuch fur Mineralogie Monatshefte. A pre-print of this paper is given in Appendix I.

F.5 Cobaltite [CoAsS]

Cobaltite has a stoichiometric composition of CoAsS. Significant amounts of nickel and iron may proxy for cobalt, and sulphur and arsenic may substitute for each other (Bayliss, 1969; Rosner,1970; Petruk *et al.*, 1971; Misra and Fleet, 1975; Changkakoti and Morton, 1986).

Two generations of cobaltite have been observed in the 334 Pod at Dawn Lake. The first occurs as small, anhedral bodies replacing safflorite, and appears to be associated with gersdorffite replacing rammelsbergite and nickeline (Plate 13).

In the second instance cobaltite occurs generally as zoned, idiomorphic crystals set in a clay-chlorite matrix. Individual grains range from 5 to 20 μm (Plate 14) across. Sections across grains exhibit regular and irregular, pentagonal and hexagonal outlines. These crystals probably belong to the isometric diploidal or pyritohedral class.

The zonation (paragenetic) sequence from core to rim is: nickelian cobaltite(core) —— bismuthian gersdorffite —— nickelian cobaltite (rim) —— gangue

—— nickelian cobaltite (outer zone) —— gangue —— gersdorffite —— gangue.

The concentrations of cobalt and nickel in nickelian cobaltites respectively increased and decreased from early to late phases, whilst that of iron remained essentially constant (Table 17). There appeared to be a minor substitution of sulphur for arsenic in the early and intermediate phases.

Cobaltite has also been observed at the McClean Lake (Wallis *et al.*, 1983, 1985, 1986) and Cigar Lake (Fouques et al., 1986; Bruneton, 1986).

G. Sulphides

Sulphide minerals in the 334 Pod at Dawn Lake are common but not abundant. The sulphide minerals so far identified in the 334 Pod are pyrite, bravoite, violarite, millerite, chalcopyrite, sphalerite, galena and a copper sulphide which may be blaubleibender covellite. Galena is the most abundant of these accessory sulphide minerals. While these minerals are not of economic significance, they are all of mineralogical interest, and several of them (bravoite, violarite, millerite and blaubleibender covellite (?)) may be of genetic significance.

G.1 Marcasite [FeS_2]

Marcasite has been observed in unmineralised regolith above the 334 Pod. The pre-ore and ore-stage FeS_2 is pyrite, whilst regolithic FeS_2 is pyrite and marcasite. Marcasite occurs as small, twinned, anhedral grains in the phyllosilicate matrix. The traces of the twin composition planes of these grains are straight.

In addition to Dawn Lake, marcasite has been observed at the Cigar Lake (Ruzicka and LeCheminant, 1987) and Eagle Point deposits (Ruzicka and LeCheminant, 1987). Ruzicka and LeCheminant (1987) reported that marcasite is associated with uranium mineralisation both at Cigar Lake and Eagle Point.

Marcasite, whilst not of economic significance at Dawn Lake, is of mineralogical and genetic significance (Murowchick and Barnes, 1986). According to

Table 17: Chemical compositions (in wt.%) and atomic compositions of nickelian cobaltites from the 334 Pod, 11A Zone, Dawn Lake, Saskatchewan.

	Fe	Co	Ni	As	Sb	S	Total
1)	----	35.50	----	45.20	----	19.30	100.00
2)	1.35	18.29	15.15	44.20	0.42	19.66	99.07
3)	1.36	19.06	14.58	44.72	0.54	19.35	99.61
4)	1.30	19.73	14.32	45.21	0.45	19.52	100.53
5)	ND	21.20	12.42	46.84	1.25	17.83	99.54
6)	1.04	19.61	12.17	50.51	0.40	15.80	99.53
7)	ND	18.20	16.50	47.00	ND	17.50	99.20
8)	2.00	18.00	14.00	52.00	ND	15.50	101.50
9)	3.20	16.50	14.20	48.30	ND	17.50	99.70
	Atomic composition on the basis of Fe+Co+Ni+As+Sb+S = 3.0						
1)	----	1.00	----	1.00	----	1.00	
2)	0.04	0.52	0.43	0.98	0.01	1.02	
3)	0.04	0.54	0.41	0.99	0.01	1.01	
4)	0.04	0.55	0.40	1.00	0.01	1.00	
5)	----	0.61	0.36	1.06	0.02	0.95	
6)	0.03	0.58	0.36	1.17	0.01	0.85	
7)	----	0.53	0.48	1.07	----	0.93	
8)	0.06	0.52	0.41	1.18	----	0.83	
9)	0.10	0.48	0.41	1.09	----	0.92	

1) cobaltite (ideal composition)
2) nickelian cobaltite (core) (this study)
3) nickelian cobaltite (rim) (this study)
4) nickelian cobaltite (outer zone) (this study)
5) nickelian cobaltite, Great Bear Lake, N.W.T. (Changkakoti and Morton, 1986)
6) nickelian cobaltite, Great Bear Lake, N.W.T. (Changkakoti and Morton, 1986)
7) nickelian cobaltite, Cobalt, Ontario (Petruk et al., 1971)
8) nickelian cobaltite, Cobalt, Ontario (Petruk et al., 1971)
9) nickelian cobaltite, Cobalt, Ontario (Misra and Fleet, 1975)

Murowchick and Barnes (1986) the preservation of marcasite on a multimillion-year scale indicates that post-depositional temperatures did not exceed about 160°C.

G.2 Pyrite [FeS_2]

Pyrite was observed in unmineralized regolith above the 334 Pod, within the 334 Pod (Table 1), and in quartz veins in the graphitic quartz-chlorite-feldspar gneiss below the 334 Pod. Within the 334 Pod, pyrite occurs as core relacements of gersdorffite, as small anhedral grains in the phyllosilicate matrix, in anhedral, composite grains (pyrite-galena, pyrite-sphalerite) in the phyllosilicate matrix, as cavity fillings in pitchblende II, and as cores to later galena and an unidentified Cu-S mineral in both the phyllosilicate matrix and later calcite veins. In one instance, a pyrite core was observed to be separated from a bravoite horseshoe-like body by a thin, intermediate zone of phyllosilicate material.

Pyrite has been observed in the Rabbit Lake (Rimsaite, 1977), Key Lake (Dahlkamp, 1978; Voultsidis *et al.*, 1982; von Pechmann, 1985), McClean Lake (Wallis *et al.*, 1983, 1985, 1986), Midwest Lake (Wray *et al.*, 1985), Collins Bay B (Ruzicka, 1986), West Bear (Ruzicka, 1986) and Cigar Lake (Fouques *et al.*, 1986; Bruneton, 1986) deposits as well as at the Zimmer Lake (Watkinson *et al.*, 1975) and Natona Bay (Ruzicka and LeCheminant, 1986) occurrences.

Pyrite was also observed in the Carswell Structure deposits of the Amer Lake Zone (Ruhlmann, 1985).

G.3 Bravoite [$(Fe,Ni)S_2$]

The cubic disulphide series pyrite (FeS_2) — cattierite (CoS_2) — vaesite (NiS_2) exhibits solid-solutions between all three end-members (Vaughan, 1969; Vaughan and Craig, 1985). Vaughan (1969) defined an endmember of this cubic disulphide series as having one of either Fe, Co or Ni comprising a minimum of 80% of all cations, leaving all other intermediate compositions as bravoites.

Bravoite was observed to occur intermittently throughout the arsenide-sulpharsenide zone (Table 18). It occurs as very small, unzoned, anhedral grains in the phyllosilicate matrix, as cavity fillings in nickeline and as replacements of gersdorffite (Plate 18). In polished sections it can be confused with violarite. Electron microprobe analyses of three grains of bravoite near the base of the arsenide-sulpharsenide zone indicated Fe ranging from 19.27 to 19.95 wt.%, Ni ranging between 26.11 and 27.11 wt.%, and S ranging from 52.36 to 53.16 wt.% (Table 18). These analyses also indicated substitutions of small amounts of cobalt (0.51-0.74 wt.%) for iron and nickel, and antimony (0.22 to 0.35 wt.%) for sulphur. The average chemical composition of these bravoites is given by:

$$(Fe_{0.43}Co_{0.01}Ni_{0.55})(S_{2.01}Sb_{0.00})$$

All three bravoites plot within the compositional field of natural bravoites reported by Vaughan and Craig (1985).

Most natural bravoites occur as zoned crystals (Short and Shannon, 1930; Springer *et al.*, 1964; Ramdohr, 1980) in which nickel and cobalt show sympathetic relationships, both antipathetic to iron (Vaughan, 1969). However, those of the 334 Pod at Dawn Lake are not zoned. Similar unzoned bravoites were observed at the Koongarra unconformity-associated uranium deposit, Northern Territory, Australia (Snelling, 1980). In the Athabasca Basin, bravoites have also been observed at the Zimmer Lake occurrence (Watkinson *et al.*, 1975), and the Key Lake (Dahlkamp, 1978; von Pechmann, 1985; de Carle, 1986), McClean Lake (Wallis *et al.*, 1983, 1985, 1986), Cigar Lake (Fouques *et al.*, 1986) and Eagle Point deposits (Ruzicka and LeCheminant, 1987).

G.4 Violarite [$FeNi_2S_4$]

Violarite is a member of the thiospinel or sulphospinel minerals group, M_3S_4 where M maybe Fe, Co, Ni, Cu, Cr, In and possibly Pt (Vaughan and Craig, 1985). Previous studies have shown that thiospinel series carrollite ($CuCo_2S_4$) — linnaeite

Table 18: Chemical compositions (in wt.%) and atomic compositions of sulphides from the 334 Pod, 11A Zone, Dawn Lake, Saskatchewan.

	Fe	Co	Ni	Cu	As	Sb	Bi	Pb	S	Total
1)	NA	NA	NA	NA	0.01	0.37	1.48	84.67	13.46	99.99
2)	29.18	0.49	0.55	33.64	0.43	ND	NA	NA	35.71	100.00
3)	0.22	ND	64.01	ND	ND	ND	NA	NA	35.76	99.99
4)	0.17	ND	64.10	ND	ND	ND	NA	NA	35.72	99.99
5)	0.07	ND	64.17	ND	ND	ND	NA	NA	35.76	100.00
6)	ND	ND	64.35	ND	ND	ND	NA	NA	35.65	100.00
7)	0.03	0.18	64.04	ND	ND	ND	NA	NA	35.76	100.01
8)	14.16	7.28	36.07	ND	0.55	ND	NA	NA	41.94	100.00
9)	19.45	0.74	27.11	ND	ND	0.35	NA	NA	52.36	100.01
10)	19.27	0.53	26.81	ND	ND	0.22	NA	NA	53.16	99.99
11)	19.95	0.51	26.11	ND	ND	0.27	NA	NA	53.16	100.00

Atomic composition of sulphides

1)	----	----	----	----	0.00	0.01	0.02	0.97	1.00
2)	0.95	0.02	0.02	0.97	0.00	----	----	----	2.04
3)	0.00	----	0.99	----	----	----	----	----	1.01
4)	0.00	----	0.99	----	----	----	----	----	1.01
5)	0.00	----	0.99	----	----	----	----	----	1.01
6)	----	----	0.99	----	----	----	----	----	1.01
7)	----	0.00	0.99	----	----	----	----	----	1.01
8)	0.77	0.36	0.87	----	0.02	----	----	----	3.98
9)	0.42	0.02	0.56	----	----	0.00	----	----	1.99
10)	0.43	0.01	0.55	----	----	0.00	----	----	2.00
11)	0.43	0.01	0.54	----	----	0.00	----	----	2.01

1: galena
2: chalcopyrite
3 — 7: millerite
8: violarite
9 — 11: bravoite

(Co_3S_4) — polydymite (Ni_3S_4) — greigite (Fe_3S_4) is characterised by extensive solid solution (Vaughan *et al.*, 1971; Vaughan and Craig, 1978; Craig *et al.*, 1979a, 1979b; Vaughan and Craig, 1985). Vaughan and Craig (1985) suggested that all iron-nickel thiospinels (Ni, Fe)$_3S_4$ with or without other minor cations should be termed violarites, except for the end members, polydymite (Ni_3S_4) and greigite (Fe_3S_4).

Violarite was observed to occur intermittently over a 6.8m depth interval in the 334 Pod (Table 2). It occurs as very small, anhedral grains in the phyllosilicate matrix (Plate 19). In polished sections it can be easily misidentified as unzoned bravoite. An electron microprobe analysis of one grain of violarite yielded the following chemical composition (Table 18):

$$(Fe_{0.77}Co_{0.36}Ni_{1.87})(S_{3.98}As_{0.02})$$

which may be rewritten as:

$$(Fe_{0.77}Co_{0.23})(Ni_{1.87}Co_{0.13})(S_{3.98}As_{0.02})$$

This cobaltian violarite falls within the composition field of natural violarites, which is plotted in terms of relative amounts of the Ni_3S_4 — Fe_3S_4 — Co_3S_4 endmembers since minor cobalt is frequently present in violarites (Vaughan and Craig, 1985).

The presence of violarite in other unconformity-associated uranium deposits in the Athabasca Basin has not been reported. This is probably due to the misidentification of violarite as bravoite.

G.5 Millerite [NiS]

Millerite, the low-temperature nickel monosulphide polymorph is generally pure but may contain only small amounts of iron and cobalt in solid solution (Vaughan and Craig, 1985).

Millerite was observed to occur over a 0.1m depth interval in the 334 Pod, near the base of the arsenide-sulpharsenide assemblage (Table 2). It occurs as needles or laths grown on gersdorffite grains, and as cores replaced and coated by gersdorffite

Plate 19. Remobilised nickel: violarite grains (V) in the phyllosilicate matrix
Secondary electron image

Plate 20. Remobilised nickel: gersdorffite (G) cores replaced by millerite (M)
Backscattered electron image

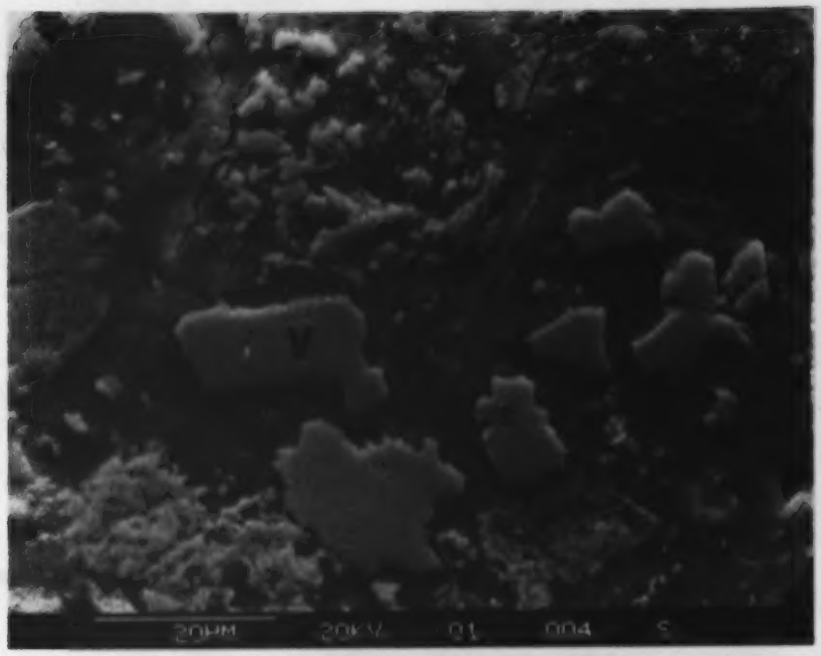
20μM
20kV
01
004
S

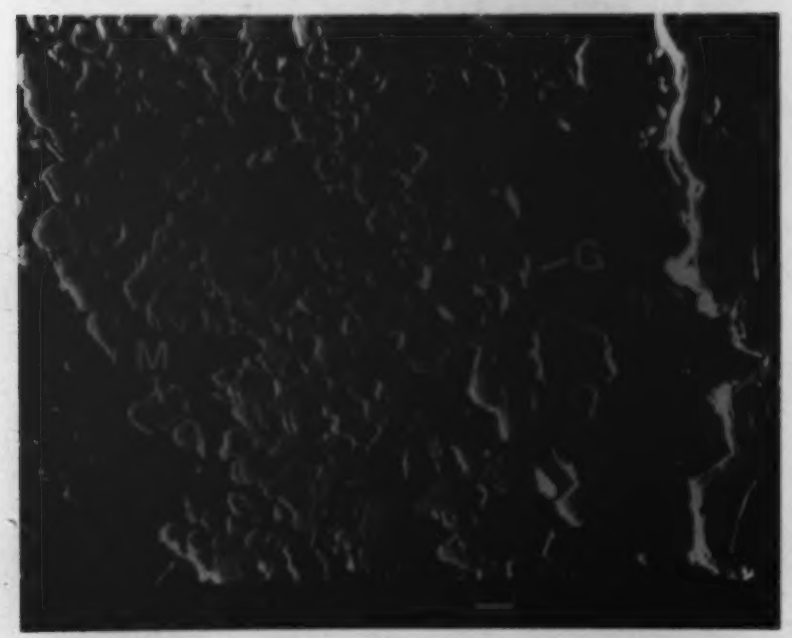

(Plates 20, 21, 22).

Electron microprobe analyses indicated that small amounts of iron and cobalt have substituted for nickel (Table 18). The maximum contents of iron and cobalt detected were 0.22 wt.% and 0.18 wt.%, respectively. The average chemical composition of millerite from the 334 Pod is given by:

$(Ni_{0.99}Fe_{0.00}Co_{0.00})S_{2.01}$

Millerite has also been reported from the Zimmer Lake occurrence (Watkinson *et al.*, 1975), and the Key Lake (Dahlkamp, 1978; von Pechmann, 1985), Midwest Lake (Wray *et al.*, 1985) and Collins Bay 'B' deposits (Ruzicka, 1986). However, microprobe analyses of millerite have been published only from Zimmer Lake (Watkinson *et al.*, 1975).

G.6 Chalcopyrite [$CuFeS_2$]

Chalcopyrite was observed to occur throughout the 334 Pod (Table 2). Within the arsenide-sulpharsenide zone, chalcopyrite occurs as (i) anhedral exsolution blebs in sphalerite, (ii) rims on gersdorffite and (iii) disseminated anhedral grains in the phyllosilicate matrix. Composite grains of chalcopyrite-galena-sphalerite and chalcopyrite-sphalerite set in the phyllosilicate gangue were also observed in this zone. Below the arsenide-sulpharsenide zone, chalcopyrite occurs as small disseminated anhedral grains in carbonate gangue. Chalcopyrite was observed to coat and replace sphalerite in the carbonate gangue. Throughout the 334 Pod, chalcopyrite was observed to be replaced by a blue-green unidentified copper sulphide mineral, which may be blaubleibender covellite.

Electron microprobe analyses of one chalcopyrite grain, from the upper part of the arsenide-sulpharsenide zone, indicated that minor amounts of nickel and cobalt proxied for copper and iron. A minor amount of arsenic was found to substitute for sulphur (Table 18).

Plate 21. Remobilised nickel: millerite (M) tree-like body coating gersdorffite (G) associated with bismuthian gersdorffite (bg)
Backscattered electron image

Plate 22. Remobilised nickel: millerite (M) laths
Backscattered electron image

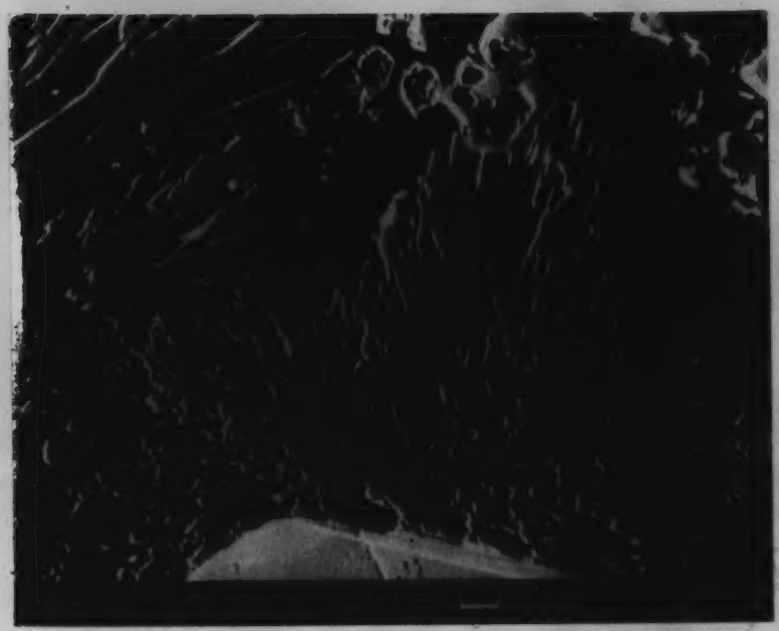

In addition to Dawn Lake, chalcopyrite has been recognised as an accessory mineral at the Rabbit Lake (Rimsaite, 1977), Key Lake (Dahlkamp, 1978; von Pechmann, 1985), McClean Lake (Wallis *et al.*, 1983, 1985, 1986), Cigar Lake (Fouques *et al.*, 1986), Collins Bay B (Ruzicka and LeCheminant, 1987) and Eagle Point deposits (Ruzicka and LeCheminant, 1987) and the Zimmer Lake (Watkinson *et al.*, 1975) and Natona Bay occurrences (Ruzicka and LeCheminant, 1986) in the eastern Cree Lake Zone. It has also been observed as an accessory mineral in the Carswell Structure unconformity-associated uranium deposits of the Amer Lake Zone (Ruhlmann, 1985).

G.7 Sphalerite [ZnS]

Sphalerite occurs intermittently throughout the 334 Pod (Table 2). It was observed in veinlets cross-cutting gersdorffite, as replacements of gersdorffite, as discontinuous rims on gersdorffite, and in small, anhedral, composite grains set in the phyllosilicate matrix. These grains may consist of coexisting sphalerite-galena pairs or coexisting sphalerite-galena-chalcopyrite triplets. In carbonate gangue below the arsenide-sulpharsenide zone, sphalerite occurs as overgrowths on pyrite cores, as intergrowths with pyrite, as intergrowths with chalcopyrite, as cores to chalcopyrite overgrowths, and as a constituent of small, anhedral composite sphalerite-galena and sphalerite-galena-chalcopyrite grains.

Sphalerite has also been reported from the Key Lake (Dahlkamp, 1978; von Pechmann, 1985), McClean Lake (Wallis *et al.*, 1983, 1985, 1986), Midwest Lake (Wray *et al.*, 1985) and Cigar Lake deposits (Fouques *et al.*, 1986), and the Zimmer Lake (Watkinson *et al.*, 1975) and Natona Bay occurrences (Ruzicka and LeCheminant, 198x) in the eastern Cree Lake Zone. Sphalerite has not been reported from the Carswell Structure deposits in the Amer Lake Zone (Ruhlmann, 1985).

G.8 Galena [PbS]

Galena is the most abundant sulphide mineral found in the 334 Pod. Ubiquitous idiomorphic galena grains are associated with sooty, lead-depleted pitchblende (pitchblende III) which rims and/or invades pitchblende I and pitchblende II. Galena also occurs in cavity fillings in nickeline and gersdorffite; as clusters of individual grains set in the phyllosilicate matrix; as replacement coats or rims on pyrite and chalcopyrite; as cores to pyrite and chalcopyrite replacement overgrowths; as euhedral grains in calcite gangue; and as a constituent of small, anhedral galena-sphalerite and galena-sphalerite-chalcopyrite composite grains.

An electron microprobe analysis of an idiomorphic grain indicated that minor bismuth and antimony proxied for lead, while minor arsenic substituted for sulphur.

Galena is present in all unconformity-associated uranium deposits.

G.9 Copper Sulphide

A blue copper sulphide mineral was observed mainly in the pitchblende II zone (Table 2). It coats and replaces chalcopyrite; replaces the core area of some chalcopyrite grains; occurs as individual rosettes in calcite gangue; forms coatings on pyrite and galena in calcite gangue; and, is coated by pyrite and galena. It was observed mainly as a replacement of chalcopyrite which was associated with calcite gangue. These observations suggest that it is of supergene origin.

In reflected light it appears to be blue in colour, whilst under crossed-nicols it exhibits marked anisotropy, the colours ranging from orange to copper brown. Its optical properties suggest that it may be blaubleibender covellite.

However, electron microprobe analyses of this mineral were inconclusive. Microprobe analyses consistently gave low totals (55-89 wt.%) suggesting that this mineral was very porous. EDA spectra indicated that manganese and iron were present in minor concentrations. This was supported by microprobe analyses. The chemical composition of this copper sulphide could not be determined due to the poor results

and because the atomic proportions of Cu:S varied considerably, between 1.20:1.00 (blaubleibender covellite) and 1.77:1.00 (anilite-digenite).

Copper sulphide minerals have been identified at several unconformity-associated deposits within the eastern Cree Lake Zone. Covellite was observed at the Rabbit Lake (Rimsaite, 1977), Key Lake (Voultsidis *et al.*, 1982; von Pechmann, 1985), Cigar Lake (Fouques *et al.*, 1986) and Eagle Point deposits (Ruzicka and Le Cheminant, 1987). At Key Lake, covellite occurs both in sandstone-hosted and basement-hosted ore (von Pechmann, 1986). Blaubleibender covellite occurs in the basement-hosted ore at Key Lake (Voultsidis *et al.*,1982; von Pechmann, 1986). At Key Lake, covellite and blaubleibender covellite were assumed to have been derived from chalcopyrite, although there was no direct evidence (von Pechmann, 1986). Digenite was identified at Cigar Lake (Fouques *et al.*, 1986) and Eagle Point (Ruzicka and Le Cheminant, 1987). Chalcocite occurs at the Rabbit Lake (Rimsaite, 1977), Cigar Lake (Fouques *et al.*, 1986) and the Raven and Horseshoe deposits (Ruzicka, 1986).

Ruhlmann (1985) reported that supergene oxidation processes produced a secondary digenite-covellite-chalcocite assemblage from precursor chalcopyrite at the Numac occurrence in the Carswell Structure of the Amer Lake Zone.

H. Tellurides

Bismuth telluride minerals were observed in polished mounts 334-143.2 and 334-150.5. Bismuth telluride in polished mount 334-143.2 was enclosed by pitchblende I. Bismuth telluride in polished mount 334-150.5 was associated with native gold and enclosed by pitchblende II (Plate 23).

Telluride minerals have been observed in the Carswell Structure deposits of the Amer Lake Zone (Ruhlmann, 1985).

Plate 23. Gold and associated bismuth telluride enclosed by pitchblende II

23a. Back scattered electron image

23b. Au X-ray

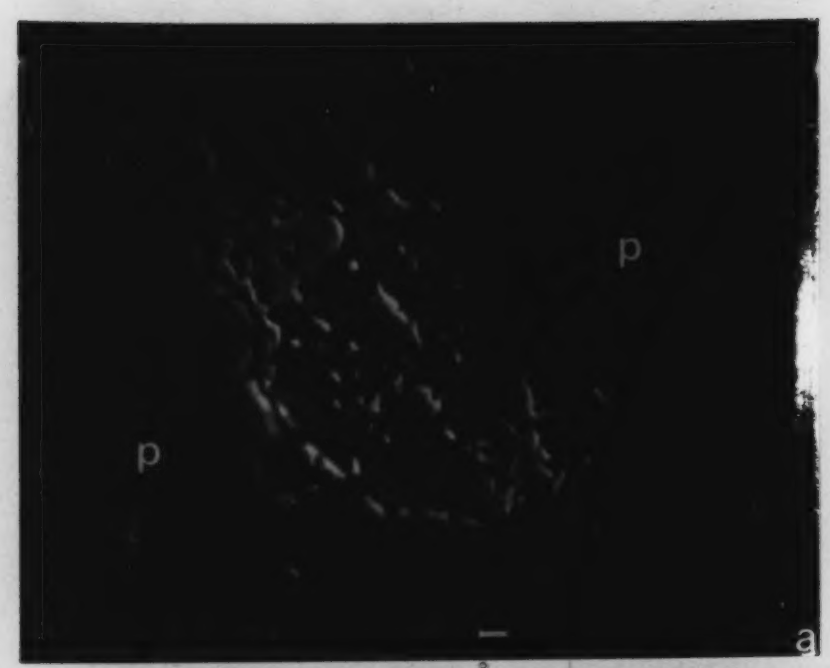
p
p
a

Au

23c. Bi X-ray

23d. Ag X-ray

Bi

Ag

23e. Te X-ray

Te

I. Gold

Native gold was observed to be associated with a bismuth telluride mineral enclosed in pitchblende II in polished mount 334-150.5 (Plate 23).

Wavelength dispersive analysis yielded the following data: gold (86.78 wt.%) and silver (12.25 wt.%). The atomic proportions of gold and silver were 1.59 and 0.41 respectively. The atomic ratio of gold to silver was approximately 4 to 1.

Gold has been reported from only one other unconformity-associated uranium deposit in the Athabasca Basin-Cree Lake Zone area, i.e., Collins Bay (Ruzicka, 1986). Gold has been observed in the Carswell Structure deposits of the Amer Lake Zone (Ruhlmann, 1985).

J. Gangue minerals

J.1 General

Gangue minerals observed in the 334 Pod were chlorite, illite, hematite and calcite. Alteration was studied qualitatively by routine microscopic investigations of thin- and polished thin-sections as well as by electron microprobe energy dispersive analysis.

J.2 Illite-chlorite alteration

In the 334 Pod at Dawn Lake, illite-chlorite alteration is common and is associated with the early arsenide-sulpharsenide assemblage preceding pitchblende I, and the later sulpharsenide-sulphide assemblage preceding pitchblende II.

Illite is a broad term used to describe a mixture of illite and kaolinite (Wallis *et al.*, 1986). Chlorite alteration consists of Fe-chlorite and Mg-chlorite, the latter being commonly misidentified as illite, because of its pale colour (Wallis *et al.*, 1986). Fe-chlorite is the most important constituent of the illite-chlorite assemblage because of its ability to reduce the hexavalent uranium ion.

J.3 Hematite gangue

In the 334 Pod, hematite occurs in association with pitchblende II. It is characterised by a vivid brick-red colour and replaces chlorite in the phyllosilicate matrix. It is cut and replaced by later sulphide-bearing carbonate veins.

A comprehensive account of the evolutionary sequence of hematite and illite in the Wollaston-McClean Lake area was given by Wallis *et al.* (1986). At least seven generations of hematite and five generations of illite were recognized.

In the 334 Pod at Dawn Lake only one generation of hematite was observed to occur although there were two main periods of pitchblende generation. At McClean Lake, as at Dawn Lake, this hematitic alteration was vivid red-brown in colour.

In unconformity-associated deposits where detailed paragenetic sequences are described, e.g., McClean Lake (Wallis *et al.*, 1983, 1985, 1986), Midwest Lake (Wray *et al.*, 1985) and Cigar Lake (Fouques *et al.*, 1986; Ruzicka and LeCheminant, 1987), hematite is always associated with pitchblende II. An association of pitchblende I-hematite has not been described in either of these deposits. In the 334 Pod, the pitchblende I-hematite association has not been observed.

J.4 Carbonate gangue

Calcite veins were observed immediately above the uppermost part of the 334 Pod mineralization and also in the lower 5 metres of the 334 Pod (Table 2). Calcite appeared to be associated with pitchblende III, galena and an unidentified Cu-S mineral. Calcite veins appear to enclose earlier formed sulphide minerals (pyrite, chalcopyrite, sphalerite and galena).

K. Paragenesis

Pitchblendes were examined by routine microscopic methods by NISOMI-84 (for reflectance and colour data) and by electron microprobe (chemical composition and atomic ratio data). Three types of pitchblendes were identified (I, II and III).

Pitchblende I was associated with gersdorffite precipitating before and after it. Gersdorffite occurring before pitchblende I was associated with cobaltite, and replaced nickeline, safflorite and rammelsbergite. Nickeline was observed to replace safflorite and rammelsbergite whilst safflorite and rammelsbergite appeared to coexist. Gangue minerals during this period were chlorite and illite. Thus the paragenetic sequence up to the deposition of pitchblende I was interpreted to be:

safflorite, rammelsbergite > nickeline > cobaltite, gersdorffite > pitchblende I.

Gersdorffite occurring after pitchblende I was associated with cobaltite and bismuthian gersdorffite. Gersdorffite was replaced by millerite, violarite, bravoite and pyrite. Gangue minerals during this period again appeared to be chlorite and illite. This period of mineralisation was followed by the precipitation of pitchblende II (which may have been remobilised pitchblende I) along with gold and bismuth tellurides. Hematitic alteration accompanied pitchblende II. The next period of mineralisation saw the formation of pyrite, chalcopyrite, galena and sphalerite, which were probably accompanied by chloritisation.

The next phase of mineralisation involved pitchblende III (with a variable coffinite component) formation which was accompanied by calcite. Galena appeared to accompany pitchblende III-calcite. Alteration of chalcopyrite to a Cu-S mineral (or minerals) appeared to occur during the pitchblende III-calcite phase.

This paragenetic sequence is consistent with the alternation of pulses of reducing and oxidizing fluids. The mineralisation sequence can be envisaged as occurring in three stages (Fig. 16):

Stage I: reducing (arsenides-sulpharsenides) —— oxidizing (pitchblende I) —— reducing (sulpharsenides)

Stage II: reducing (sulphides) —— oxidizing (pitchblende II-hematite) —— reducing (sulphides)

Stage III: oxidizing (pitchblende III-coffinite)

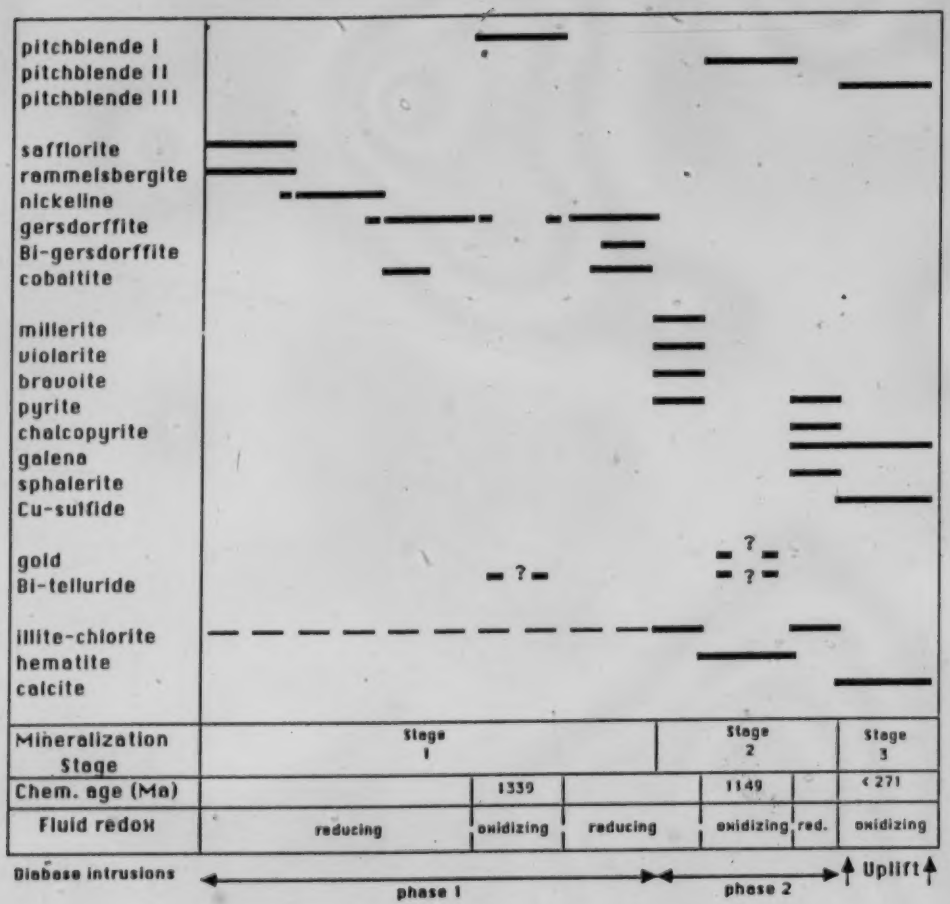

Figure 16. Paragenesis of 334 Pod mineralisation, 11A Zone, Dawn Lake, Saskatchewan

Stage I mineralisation representing the bulk of the mineralisation of the 334 Pod corresponds to an average chemical age of 1339 Ma. Stage II mineralisation corresponds to an average chemical age of 1149 Ma. Stage III mineralisation corresponds to chemical ages ranging from 27 to 271 Ma. Chemical ages of first, second and third generations are dealt with in the following chapter (Chapter V).

Stage I mineralisation of the 334 Pod corresponds to first stage mineralisation (U-Ni-Co-As-S±Bi; 1280-1350 Ma) observed in other unconformity-associated deposits in the Athabasca Basin-Cree Lake Zone area (e.g., Key Lake, McClean Lake, Midwest Lake, Cigar Lake and Collins Bay B).

Stage II mineralisation of the 334 Pod is similar to second stage mineralisation (U-Pb-Zn-Cu-Fe-S; 900-1100 Ma) observed in other unconformity-associated deposits in the Athabasca Basin-Cree Lake Zone area (e.g., Key Lake, McClean Lake, Midwest Lake, Cigar Lake and Collins Bay B).

Stage III mineralisation of the 334 Pod resembles the third stage mineralisation (U-Pb-Si; 0-350 Ma) observed in other unconformity-associated deposits in the Athabasca Basin-Cree Lake Zone area (e.g., Key Lake, McClean Lake, Midwest Lake, Cigar Lake and Collins Bay B).

A comparison of the non-uraniferous mineralisation of the Dawn Lake 334 Pod with those of the McClean Lake, Midwest Lake, Cigar Lake, Key Lake and Collins Bay B deposits is given in Table 19.

Table 19: Comparison of non-uraniferous minerals from various unconformity-associated uranium deposits within the Athabasca Basin-Cree Lake Zone region.

	334[1] Pod	Cigar[2] Lake	Midwest[3] Lake	McClean[4] Lake	Key[5] Lake	Collins[6] Bay B
Skutterudite	-	-	x	?	-	x
Safflorite	x	-	x	x	-	
Rammelsbergite	x	x	x	x	x	
Nickeline	x	x	x	x	x	x
Maucherite	-	-	-	-	x	
Cobaltite	x	x	x	x	-	
Gersdorffite	x	x	x	x	x	x
Bi-gersdorffite	x	-	-	-	-	
Marcasite	-	x	-	-	x	
Pyrite	x	x	x	x	x	x
Bravoite	x	x	x	x	x	
Violarite	x	?	-	-	-	
Millerite	x	-	x	-	x	x
Vaesite	-	-	-	-	x	
Galena	x	x	x	x	x	x
Sphalerite	x	x	x	x	x	
Chalcopyrite	x	x	x	x	x	x
Covellite	?	x	-	-	x	
Gold	x	-	-	-	-	-
Bi-telluride	x	-	-	-	-	-
Hauchecornite	-	-	-	-	x	-
Breithauptite	-	-	-	-	x	

1. This study
2. Bruneton, 1986
3. Wray et al., 1985; B. Cooper, pers. comm.
4. Wallis et al., 1983, 1985, 1986
5. Dahlkamp, 1978; Voultsidis et al., 1982; von Pechmann, 1985
6. Ruzicka, 1986

V. CHEMICAL AGES

A. Introduction

In the past, conventional U-Pb dating of uraninites and pitchblendes from unconformity-associated uranium deposits in the Athabasca Basin has suffered because of insufficient or inadequate characterisation of the uraniferous phases examined. Because of this, mixing of different generations of uraninites, pitchblendes, coffinites and other uraniferous phases may have occurred resulting in a multiplicity of ages for mineralization and remobilisation (Cumming and Rimsaite, 1979).

Adequate characterization of uraninites, pitchblendes and coffinites of different generations can be achieved by the determination of their chemical compositions (Baadsgaard et. al., 1984) and their chemical ages (Cameron-Schimann, 1978; Ruhlmann, 1985; Pagel and Ruhlmann, 1985). Examination of the linear chemical age formula of Cameron-Schimann (1978), however, found it to be inadequate for ages greater than about 300 Ma. It was necessary therefore, to develop a new method or methods of determining the chemical ages of pitchblendes and uraninites. The development of these new methods became part of this thesis research (Appendix 2).

The methods of determination of chemical ages of thorium-free uraninites or pitchblendes, which are characteristic of unconformity-associated uranium deposits, is a topic of a paper to be submitted to the Canadian Journal of Earth Sciences (Appendix 2). These methods involve the solving of quadratic, cubic and quartic equations in t, where t represents the chemical age of mineralization. The major assumptions are (1) that all lead in the uraninites or pitchblendes is of radiogenic origin and (2) that the uraninites or pitchblendes have been closed systems since deposition.

The chemical age data for pitchblendes from the 334 Pod, 11A Zone, Dawn Lake were obtained using these methods.

B. Chemical Ages - Pitchblende I

First generation pitchblendes (pitchblende I) are characterised by dark, lustrous, colloform, botryoidal, reniform and radial aggregates. Their occurrence in the 334 Pod is listed in Table 2.

Uranium and lead concentrations (in wt.%) of 12 pitchblende I samples from polished mounts 334-142.4, 334-143.2, 334-145.3 and 334-146.4 were obtained following electron microprobe wavelength dispersive analysis (Table 5).

Quadratic, cubic and quartic chemical ages of pitchblende I samples are given in Table 20. Also given in Table 20 is the corresponding linear chemical age for each sample as determined by the equation of Cameron-Schimann (1978).

Linear ages range from 1399 to 1648 Ma, quadratic ages from 1250 to 1448 Ma, cubic ages from 1234 to 1423 Ma and quartic ages from 1230 to 1417 Ma. Examination of the age sequence of any given pitchblende sample shows rapid convergence toward the quartic age. A pentic solution probably will reduce the quartic age by less than about 2 Ma at 1417 Ma.

C. Chemical ages - pitchblende II

Second generation pitchblendes (pitchblende II) from the 334 Pod are lighter coloured than pitchblende I and possess colloform, radial, ring-like and euhedral habits.

Uranium and lead concentrations (in wt.%) of 18 pitchblende II samples from polished mounts 334-144.0, 334-146.4, 334-147.0, 334-149.0, 334-150.5 and 334-152.8 are given in Table 6.

Quadratic, cubic and quartic ages of pitchblende II samples determined during this study are given in Table 21. The corresponding linear chemical age for each sample determined using the formula of Cameron-Schimann (1978) is also given in Table 21.

Linear ages range from 940 to 1392 Ma, quadratic ages range from 868 to 1245 Ma, cubic ages from 862 to 1228 Ma and quartic ages from 861 to 1225 Ma.

Table 20: Chemical ages of first generation pitchblendes (pitchblende I) from the 334 Pod, 11A Zone, Dawn Lake, Saskatchewan.

NO.	SAMPLE	Pb wt.%	U wt.%	Quadratic[1] Age (Ma)	Cubic[1] Age (Ma)	Quartic[1] Age (Ma)	Linear[1] Age (Ma)
(1)	334-142.4	15.79	69.27	1430	1406	1400	1625
(2)	334-142.4	14.70	69.87	1331	1311	1307	1499
(3)	334-143.2	15.58	68.27	1431	1407	1402	1626
(4)	334-143.2	13.79	70.24	1250	1234	1230	1399
(5)	334-145.3	15.82	68.70	1443	1418	1413	1641
(6)	334-145.3	15.00	69.20	1367	1346	1341	1545
(7)	334-145.3	14.65	69.27	1337	1317	1313	1507
(8)	334-145.3	14.68	70.06	1326	1306	1302	1493
(9)	334-145.3	14.53	69.43	1324	1305	1301	1491
(10)	334-145.3	13.93	69.57	1273	1255	1252	1427
(11)	334-146.4	15.82	68.43	1448	1423	1417	1648
(12)	334-146.4	15.24	67.57	1416	1393	1388	1607

[1]: Chemical ages, this study
[1]: Chemical age using linear equation of Cameron-Schimann (1978)

Table 21: Chemical ages of second generation pitchblendes (pitchblende II) from the 334 Pod, 11A Zone, Dawn Lake, Saskatchewan.

NO.	SAMPLE	Pb wt.%	U wt.%	Quadratic[1] Age (Ma)	Cubic[1] Age (Ma)	Quartic[1] Age (Ma)	Linear[1] Age (Ma)
(1)	334-144.0	13.11	68.86	1216	1201	1198	1357
(2)	334-144.0	12.40	69.50	1147	1133	1131	1272
(3)	334-146.4	12.87	69.40	1187	1173	1170	1322
(4)	334-146.4	12.80	69.69	1177	1163	1160	1309
(5)	334-146.4	12.43	69.68	1146	1133	1131	1271
(6)	334-146.4	9.36	70.99	868	862	861	940
(7)	334-147.0	13.23	68.55	1231	1215	1212	1375
(8)	334-147.0	12.61	69.87	1159	1145	1143	1286
(9)	334-149.0	13.49	69.05	1245	1228	1225	1392
(10)	334-149.0	13.29	69.55	1220	1205	1202	1362
(11)	334-149.0	12.94	69.49	1192	1177	1175	1327
(12)	334-149.0	12.92	70.05	1182	1167	1165	1314
(13)	334-149.0	11.41	70.08	1055	1044	1042	1160
(14)	334-150.5	13.30	69.53	1221	1206	1203	1363
(15)	334-150.5	11.58	70.44	1064	1053	1051	1172
(16)	334-152.8	12.59	68.87	1172	1158	1156	1303
(17)	334-152.8	12.46	70.01	1144	1131	1128	1268
(18)	334-152.8	11.29	69.74	1049	1039	1037	1154

[1]: Chemical ages, this study
[1]: Chemical age using linear equation of Cameron-Schimann (1978)

D. Chemical ages - pitchblende III

Third generation pitchblendes (pitchblende III) are characterised by dark, amorphous aggregates replacing pitchblende I and pitchblende II along rims, shrinkage cracks and fractures. Pitchblende III samples always possess a silica component and are always associated with euhedral (radiogenic?) galena crystals. Their occurrence in the 334 Pod is listed in Table 2.

Uranium and lead concentrations (in wt.%) of 6 pitchblende III samples replacing pitchblende I and 7 pitchblende III samples replacing pitchblende II are given in Table 7. Pitchblende III phases with higher coffinite components tend to replace pitchblende II, whilst pitchblende III phases with lower coffinite components tend to replace pitchblende I.

(a) pitchblende III replacing pitchblende I

Quadratic, cubic and quartic chemical ages of these pitchblende III samples are given in Table 22. Corresponding linear chemical ages for the samples calculated using the equation of Cameron-Schimann (1978) are also given in Table 22.

Linear ages range from 114 to 770 Ma, quadratic ages range from 113 to 721 Ma, whilst both cubic and quartic ages range from 113 to 717 Ma. Of the 6 samples studied, one has the anomalous quartic age of 717 Ma, while the rest range from 113 to 218 Ma. The oldest sample probably reflects a mixture of pitchblende I and pitchblende III.

(b) Pitchblende III replacing pitchblende II

Quadratic, cubic and quartic chemical ages of 7 pitchblende III samples replacing pitchblende II are given in Table 22. Corresponding linear ages for the samples as determined by the equation of Cameron-Schimann are also given in Table 22.

Linear chemical ages range from 87 to 278 Ma, whilst quadratic, cubic and quartic ages all range from 86 to 271 Ma.

Table 22: Chemical ages of third generation pitchblendes (pitchblende III) from the 334 Pod, 11A Zone, Dawn Lake, Saskatchewan.

NO.	SAMPLE	Pb wt.%	U wt.%	Quadratic[1] Age (Ma)	Cubic[1] Age (Ma)	Quartic[1] Age (Ma)	Linear[1] Age (Ma)
(1)	334-142.4	1.95	72.98	187	187	187	190
(2)	334-142.4	1.70	72.49	165	165	165	167
(3)	334-142.4	7.24	67.00	721	717	717	770
(4)	334-146.4	2.14	68.69	218	218	218	222
(5)	334-146.4	1.76	68.55	180	180	180	183
(6)	334-146.4	1.15	72.04	113	113	113	114
(7)	334-152.8	2.61	66.88	271	271	271	278
(8)	334-152.8	0.55	65.16	60	60	60	60
(9)	334-152.8	0.47	63.88	52	52	52	52
(10)	334-152.8	0.39	69.08	40	40	40	40
(11)	334-152.8	0.24	63.88	27	27	27	27
(12)	334-154.0	0.85	69.52	87	87	87	87
(13)	334-154.0	0.87	71.45	87	86	86	87

[1]: Chemical ages, this study
[2]: Chemical age using linear equation of Cameron-Schimann (1978)

E. Discussion

The mean quartic age of the pitchblende I samples is 1339 Ma. This age is similar to ages obtained for first generation pitchblendes from the Midwest Lake (1328±17 Ma: Baadsgaard et al., 1984; 1331±8 Ma: Worden et al., 1985), Cigar Lake (1300±? Ma: Ruzicka and LeCheminant, 1986), Key Lake (1350±4 Ma: Trocki et al., 1984; 1250±34 Ma: Hohndorf et. al., 1985), Rabbit Lake (1281±11 Ma: Cumming and Rimsaite, 1979) and Collins Bay (1281±80 Ma: Fryer and Taylor, 1984) deposits.

The mean quartic age of 1339 Ma is similar also to ages obtained for potassic alteration (illite, sericite) associated with first-stage mineralization at the nearby Midwest Lake (1337±11 Ma: Worden et. al., 1985) and McClean Lake (1321±44 Ma, 1319±3 Ma: Bray et. al., 1987) deposits.

The mean quartic age of pitchblende II samples is 1133 Ma. If the sample with the age of 861 Ma is excluded, the mean quartic age of the remaining 17 samples rises to 1149 Ma. Either of these ages is similar to ages obtained for second generation pitchblendes from the Midwest Lake (1110±28 Ma: Baadsgaard et. al., 1984; 1094±27 Ma: Worden et. al., 1985) and Rabbit Lake (1094±10 Ma: Cumming and Rimsaite, 1979) deposits. The mean quartic age of 1133 Ma (or 1149 Ma) is similar to the U-Pb age of about 1100 Ma obtained for second generation pitchblendes from Dawn Lake (G. Cumming, pers. comm.).

The mean quartic age of pitchblende II samples from Dawn Lake is similar also to the K-Ar age of 1084±27 Ma obtained from the nearby Midwest Lake dyke (Worden et. al., 1985).

The vast majority of the pitchblende III samples have quartic chemical ages ranging from 27 to 271 Ma. Pitchblende III replacing pitchblende I possesses a higher mean quartic age (175 Ma; analysis 3, Table 22 excluded) than that of pitchblende III replacing pitchblende II (89 Ma). Pitchblende III associated with pitchblende II always appears to be associated with more radiogenic (?) galena than pitchblende III

associated with pitchblende I.

Late remobilisation of earlier pitchblendes appears to have commenced during the Carboniferous and appears to have continued into the Cretaceous as reflected by third generation pitchblende/coffinite ages from the Midwest Lake (120-300 Ma: Baadsgaard et. al., 1984; 334±16 Ma: Worden et. al., 1985), Key Lake (300±6 Ma: Trocki et. al., 1984; 286±12 Ma: Hohndorf et. al., 1985), Rabbit Lake (194±32 Ma: Cumming and Rimsaite, 1979) and Collins Bay (334±0.2 Ma: Fryer and Taylor, 1984) deposits. The pitchblende III ages from Dawn Lake appear to belong to the post-Carboniferous period of remobilisation. Remobilisation appears to be related to uplift during this period (Hoeve and Quirt, 1987).

A summary of the ages mentioned in the discussion and the methods by which they were determined is listed in Table 23. A histogram of chemical ages of first, second and third generation pitchblendes from the 334 Pod is given in Fig. 17.

F. Conclusion

In the 334 Pod at Dawn Lake, the formation of first generation pitchblendes occurred at approximately 1339 Ma, second generation pitchblendes at 1149 Ma and third generation pitchblendes between 27 and 271 Ma. The close correspondence of chemical ages for first, second and third generation pitchblendes from the 334 Pod to the conventional U-Pb ages obtained for equivalent pitchblendes from other unconformity-associated uranium deposits within the Athabasca Basin (Cree Lake Zone) suggests that the chemical age dating methods can be used to provide a good approximation of the ages of mineralization.

It is suggested that prior to the conventional U-Pb dating of thorium-free pitchblendes, complete characterisation of thesee pitchblendes be done by the gathering of chemical composition and reflectivity data and the calculation of chemical ages. Chemical composition-reflectivity-chemical age characterisation of thorium-free pitchblendes should provide a powerful discriminatory tool for identifying different

Table 23 : Summary of ages (in Ma) for first, second and third generation pitchblendes, potassic alteration associated with first stage mineralisation, and diabase dyke activity associated with various deposits within the Cree Lake Zone, Saskatchewan

Deposit	Method	First Generation Pitchblende	Second Generation Pitchblende	Third Generation Pitchblende	Potassic[1] Alteration	Reference
Dawn Lake	Chemical Age	1339[2]	1149[2]	22-271		This study
	U-Pb	----	c.1100	?		G. Cumming pers. comm.
McClean Lake	Ar-Ar				1319± 3	Bray et al., 1987
	K-Ar				1321±44	Bray et al., 1987
Midwest Lake[3]	U-Pb	1328±17	1110±28	120-300		Baadsgaard et al., 1984
	U-Pb	1331± 8	1094±27	334±16		Worden et al., 1985
	Rb-Sr				1337±11	Worden et al., 1985
Cigar Lake	U-Pb	1300±?	----	?		Ruzicka and LeCheminant, 1986
Key Lake						
(Deilmann)	U-Pb	1350± 4	----	300±6		Trocki et al., 1984
(Gaertner)	U-Pb	1250±34	903±40	286±12		Hohndorf et al., 1985
Rabbit Lake	U-Pb	1281±11	1094±10	194±32		Cumming and Rimsaite, 1979
Collins Bay	Sm-Nd	1281±80	----	334±0.2		Fryer and Taylor, 1984
	K-Ar				1296±34	Tremblay, 1982

[1]: Potassic alteration associated with first stage mineralisation
[2]: Mean quartic chemical age (this study)
[3]: K-Ar age of 1084±54 Ma (Worden et al., 1985) for diabase dyke, Midwest Lake

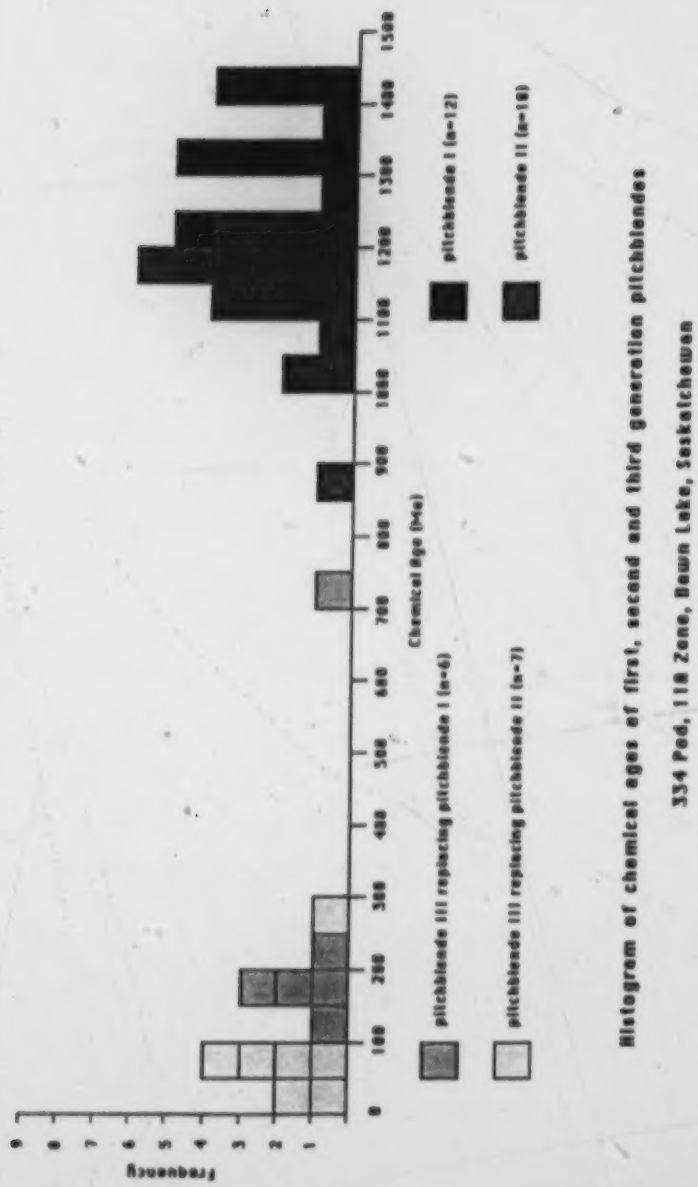
Histogram of chemical ages of first, second and third generation pitchblendes
334 Pod, 11A Zone, Dawn Lake, Saskatchewan
pitchblende I (n=12)
pitchblende II (n=18)
pitchblende III replacing pitchblende I (n=6)
pitchblende III replacing pitchblende II (n=7)
Chemical Age (Ma)
Frequency

Figure 17. Histogram of chemical ages of first, second and third generation pitchblendes from the 334 Pod, 11A Zone, Dawn Lake, Saskatchewan

generations of thorium-free pitchblendes that may occur in the same deposit.

Conventional U-Pb geochronological dating of the 334 Pod pitchblendes has been proposed as a topic for future research.

VI. DISCUSSION

A. Introduction

In addition to uranium, a broad suite of elements including Ni, Co, Fe, Cu, Pb, Zn, Mo, V, Mn, Ag, Au, Pt Group elements, Bi, Te, Se, Sb, As and S are present in unconformity-associated uranium deposits (Hoeve *et al.*, 1980). Mineralogical studies of the 334 Pod at Dawn Lake indicate the presence of Ni, Co, Fe, Cu, Pb, Zn, V, Mn, Ag, Au, Bi, Te, Sb, As and S in addition to uranium.

Continuing controversy ensues amongst geologists who have studied the Unconformity-Associated uranium deposits of the Athabasca Basin concerning:

(i) the source of the elements; and

(ii) the mechanism (or mechanisms) by which they were mobilised.

Proponents of the diagenetic-hydrothermal hypothesis argued for a *per descensum* origin of these deposits and were (and still are) of the opinion that the uranium and other elements were originally present in the clastic sediments of the Athabasca Group (Hoeve and Sibbald, 1978; Hoeve *et al.*, 1980; Hoeve and Quirt, 1984, 1987).

Alternatively, proponents of the *per descensum* supergene hypothesis have proposed that chemical weathering prior to the deposition of the Athabasca Group concentrated the ore-related elements just below the unconformity (Barbier, 1974; Knipping, 1974; Langford, 1974, 1978; Robertson and Lattanzi, 1974; Dahlkamp and Tan, 1977; Dahlkamp, 1978; Voultsidis *et al.*, 1982). However, the *per descensum* supergene origin for these deposits has rapidly lost favour because of:

(i) fluid inclusion studies of gangue minerals associated with uranium mineralisation which have indicated mineralisation temperatures approaching 200°C (Pagel *et al.*, 1980; Lawler and Crawford, 1982);

(ii) regolithic studies which indicated that no large scale depletions or enrichments of trace elements (Ni, V, Cu, Zn, Ag, Pb) associated with uranium mineralisation

occurred during pre-Athabasca Group weathering (Macdonald, 1980, 1985);

(iii) geochemical studies of fresh and altered metasediments away from mineralisation at Key Lake which indicated on the average no depletion of uranium or nickel (Voultsidis *et al.*, 1982).

Morton (1977) argued for a *per ascensum* origin whereby the uranium and other ore-forming elements were remobilised at depth by ascending hydrothermal fluids responding to diabase dyke activity. Deposition occurred below, at or above the unconformity depending upon where the necessary physico-chemical conditions for deposition were encountered. The *per ascensum* hydrothermal (hypogene) origin has been proposed for mineralisation at Key Lake although the source of the ore was not identified (Kirchner *et al.*, 1980; von Pechmann, 1985).

Strnad (1981) has proposed a metamorphogenic origin for the Key Lake mineralisation whereby the ore formed by lateral secretion.

B. Source of Ore-Related Elements

B.1 General

The source of the ore-related elements present in unconformity-associated ore deposits has been the subject of much controversy.

Proposed sources are (1) the Athabasca Group clastic sediments, (2) the metamorphic and crystalline basement and (3) Hudsonian-related syngenetic and synmetamorphic protores.

Resolution of this problem may come about by the use of Sm-Nd isotopic studies of the uranium mineralisation and the proposed sources. To date few Sm-Nd studies have been done (Fryer and Taylor, 1984; Maas *et al.*, 1986).

High initial $^{143}Nd/^{144}Nd$ values have been observed in uranium mineralisation from the Collins Bay deposit, Saskatchewan (Fryer and Taylor, 1984) and from unconformity-associated ores of the Alligator River Uranium Field, Northern Territory,

Australia (Maas *et al.*, 1986).

Fryer and Taylor (1984) concluded that much higher initial $^{143}Nd/^{144}Nd$ ratios should be expected than those observed (0.50988-0.51384) because the common uranium-bearing minerals contain elevated abundances of Sm (e.g. 700-1650 ppm in pitchblendes). Maas *et al.* (1986) found that the initial $^{143}Nd/^{144}Nd$ ratios of uranium mineralisation were consistently higher than those of their host and country rocks and on the basis of this observation concluded that wholesale leaching of Archean and most Proterozoic rocks could be excluded as a major mechanism for providing hydrothermal fluids with rare earth elements (REE) and uranium. Maas *et al.* (1986) claimed that the data are more consistent with derivation of ore-REE from sources having relatively primitive $^{143}Nd/^{144}Nd$ initial ratios and suggested that REE and uranium may have been derived from older uranium mineralisation.

However, the observation by Fryer and Taylor (1984) of lower initial $^{143}Nd/^{144}Nd$ ratios in uranium mineralisation may suggest that ascending hydrothermal solutions probably sampled both syngenetic/ synmetamorphic protores and country rocks.

In the past syngenetic and synmetamorphic protores have been neglected as a source of uranium whilst the Athabasca Group (<1-1.5 ppm U: Hoeve *et al.*, 1980; Wallis *et al.*, 1985, 1986; von Pechmann, 1985) and the Aphebian metasediments (4 ppm U: Ramaekers and Dunn, 1977; von Pechmann, 1985) have been favoured sources.

B.2 The source of metals: Hudsonian-related syngenetic and synmetamorphic protores

In this section the possibility that syngenetic and synmetamorphic protores were a source of metals for unconformity-associated mineralisation and 334 Pod-type mineralisation is discussed.

Hoeve *et al.* (1980) argued that unconformity-associated mineralisation, which generally is spatially related to the Athabasca Group-Wollaston Group unconformity

and is generally associated with graphitic metasediments of the Aphebian basement, seems to have been controlled by the presence of the unconformity rather than by factors related to Aphebian sedimentation or Hudsonan structural and metamorphic evolution, because no such mineralisation has been encountered outside the Athabasca Basin.

However, to deny any relationship of Aphebian sedimentation and Hudsonian structural and metamorphic evolution to the genesis of the unconformity-associated deposits because of their non-existence outside the Athabasca Basin should cause any reasonable geologist to ponder on the reason or reasons for their non-existence outside the Athabasca Basin. A reason that comes to mind immediately is that removal of the protective Athabasca Group cover would result in destruction of the unconformity-associated deposit. In fact part of the Key Lake deposit was destroyed by glacial activity. It was estimated that the Rabbit Lake deposit formed under at least 3 km of Athabasca Group sediments. The Rabbit Lake deposit when discovered, however, was devoid of Athabasca Group cover. Thus between 1300 Ma and the present, at least 3 km of sediment cover was removed from above an area that is now at the edge of the Athabasca Basin. How much farther did the Athabasca Group extend? How many unconformity-associated deposits have been destroyed?

Can syngenetic and synmetamorphic deposits have provided a source for the uranium found in the younger, high-grade, unconformity-associated deposits at the base of the Athabasca Group and in basement pods such as the 334 Pod at Dawn Lake?

Several publications described the occurrence of Hudsonian-related syngenetic/synmetamorphic uraniferous mineralisation in the Wollaston domain and in the eastern part of the adjacent Mudjatik domain. These occurrences are at:

(1) Blackstone Lake (Sibbald *et al.*, 1977)

(2) Burbidge Lake (Sibbald *et al.*, 1977)

(3) Cup Lake (Sibbald *et al.*, 1977)

(4) Duddridge Lake (Bretzlaff, 1976; Coombe, 1978)

(5) Yurchison Lake (Ray, 1980)

(6) Needle Lake (von Pechmann *et al.*, 1984); and

(7) Karpinka Lake (Williams-Jones and Sawiuk, 1985).

On the basis of their dominant host rock they have been distinguished as arkosic (Duddridge Lake, Karpinka Lake), calc-silicate (Burbidge Lake, Cup Lake, Needle Lake, Yurchison Lake) and pelite-pegmatoid (Blackstone Lake) types of deposits (Sibbald *et al.*, 1977; Lewry and Sibbald, 1979; Hoeve *et al.*, 1980).

The Duddridge Lake and Karpinka Lake deposits are suggested to be metamorphosed sandstone-type deposits. The Duddridge Lake mineralisation is characterised by an assemblage of U-Ni-Co-As-Se-Pb-Ag-Au-Mo-V whilst the Karpinka Lake mineralisation has the simpler assemblage of U-Ti-Fe and may have been detrital in origin. Calc-silicate types are characterised by U-Mo, and are interpreted as Aphebian syngenetic sedimentary concentrations recrystallised and remobilised during the Trans-Hudson Orogeny (Hoeve *et al.*, 1980).

The pelite-pegmatoid type of mineralisation is characterised by U-Mo-Pb-Cu-Zn and the host rocks are interpreted to be Aphebian black shales that underwent anatexis during the Hudsonian orogeny (Hoeve *et al.*, 1980). Uranium may have segregated with the pegmatoid material during high-grade metamorphism and anatexis (Hoeve *et al.*, 1980).

Uraniferous mineralisation from only two of these locations (Needle Lake and Karpinka Lake) have been dated by the U-Pb method. Uraninite from Needle Lake was dated at 1803±8 Ma (von Pechmann *et al.*, 1984). Karpinka Lake mineralisation (uraninite, braunerite) was dated at 1800±? Ma (analyst: H. Baadsgaard; Williams-Jones and Sawiuk, 1985).

Of these occurrences, the Karpinka Lake prospect has been the most extensively studied (Williams-Jones and Sawiuk, 1985). It is a stratabound uranium deposit hosted by Aphebian metasediments located just to the south of the Key Lake unconformity-associated uranium deposits (Fig. 1). Williams-Jones and Sawiuk (1985)

suggested that the demonstrable existence of Aphebian stratabound mineralisation and the observation that unconformity-associated deposits are controlled by faults parallel to the Aphebian gneissosity (as at Dawn Lake) lent support to previous suggestions (Morton and Beck, 1978) that the basement supplied the uranium (and other metals presumably) for the younger unconformity-associated deposits.

C. Origin of Fluids

C.1 Fluid Inclusion Studies

Spooner (1981) claimed that the origin of unconformity-associated uranium deposits in the Athabasca Basin "has been considerably clarified by fluid inclusion research". This statement was based on studies by Pagel (1975), Pagel and Jaffrezic (1977) and Pagel *et al.* (1979, 1980). However, Pagel *et al.* (1979) stated that "unfortunately, at present, no fluid inclusions have been found in gangue minerals ..... contemporaneous with pitchblende". Pagel *et al.* (1980) conducted fluid inclusion studies of euhedral quartz, dolomite, calcite, a pale green fine-grained chlorite after feldspar and a coarser-grained pale chlorite from the Rabbit Lake mine. According to Pagel *et al.* (1980) the positions of these minerals in the paragenetic sequence (Hoeve and Sibbald, 1978) was uncertain. The concerns expressed by Pagel and co-workers regarding the interpretation of their fluid inclusion data show Spooner's claim to be unreasonable and misleading.

Lawler and Crawford (1982) investigated fluid inclusions in quartz-bearing samples from the nearby Midwest Lake deposit. Lawler and Crawford (1982) concluded that:

(1) the dominant fluid in the alteration envelope around the orebody was low density CO_2;

(2) an oxidising saline aqueous fluid was present within the ore zone, both above and below the unconformity as indicated by the occurrence of aqueous inclusions with

hematite and halite daughter crystals;

(3) separate CO_2 and low salinity aqueous inclusions co-existed along healed fractures suggesting that the fluids were immiscible at the time of trapping: homogenisation temperatures of these coexisting inclusions suggested trapping conditions of 800-1000 bars and 200±25°C;

(4) inclusions in non-graphitic and graphitic gneisses outside the zone of intense alteration contained CH_4 and CO_2-CH_4 fluids; and

(5) aqueous fluids enriched in $CaCl_2$ occurred in some samples.

Lawler and Crawford (1982) suggested that (a) uranium ore deposition was associated with conditions which favoured an oxidising CO_2-rich fluid and (b) that major ore deposition may have resulted because of unmixing of CO_2 and aqueous brines. In the Midwest Lake area, assuming an average lithostatic pressure gradient of about 260 bars km^{-1}, 3 to 4 km of Athabasca Group sediments probably existed above the unconformity at the time of mineralisation.

Although fluid inclusion data are not available from Dawn Lake gangue minerals. the Midwest Lake data probably are good approximations of conditions during mineralisation at Dawn Lake.

Chemical analyses and microthermometric observatons of fluid inclusions in quartz and dolomite from the Rabbit Lake deposit have shown that these fluids were Na-Ca-Cl solutions with salinities about 30 wt.% NaCl equivalent (Pagel and Jaffrezic, 1977; Pagel *et al.*, 1979, 1980). Pagel and Jaffrezic (1977) showed that the Cl/Br weight ratio of these brines were very constant at a value of 55, a value much lower than seawater (≈300) and different from meteoric waters having dissolved halite (nx1000). Low Cl/Br weight ratios can be explained by (a) halite precipitation from the brine (Braitsch, 1971) or (b) release of Br by organic matter during its evolution (Wickman and Khattab, 1972). Pagel and Jaffrezic (1977) thus concluded that these low Cl/Br brines originated either in a marine evaporitic environment or by thermal degradation of marine organic matter, or both.

It is possible, thus, that these fluids could have acquired these chemical characteristics by reacting with Aphebian meta-evaporites and meta-pelites and with Archean granitic rocks of the basement. If this was the case then the mineralising fluids may have had a basement origin.

C.2 Groundwater Geochemistry

Cramer (1986) provided chemical composition data for groundwaters in contact with mineralisation at Dawn Lake (Table 24).

The unreactivity of the host rocks and the contained mineralisation of the Dawn Lake deposits towards the present day groundwaters (Cramer, 1986) is clearly shown by:

(1) near neutral pH values;

(2) low Eh values;

(3) low Cl^-, SO_4^{2-}, HCO_3^- and CO_3^{2-} concentrations;

(4) low concentrations of major cations Ca^{2+}, Mg^{2+}, Na^+ and K^+; and

(5) generally low concentrations of U, Ni, Co, V, Pb in groundwaters near the ore zones.

Frape and Fritz (1982) in a study of groundwater samples from a variety of locations in the crystalline rocks of the Canadian shield, found that their compositions changed with depth. Waters that occurred above approximately 650 metres were fresh or brackish, with total dissolved solids (TDS) less than 10000 mg ℓ^{-1}. Below 650 metres very saline waters, or brines occurred within major faults and shear zones. Frape *et al.* (1984) in a subsequent study classified Canadian Shield groundwaters as:

(i) fresh (TDS $< 10^3$ mg ℓ^{-1}; depth $<$ 200 m; T $<$ 10°C; pH: 6-7.5);

(ii) brackish (TDS: 10^3-10^4 mg ℓ^{-1}; depth: 200-600 m; T: 8-13°C; pH: 6.3-7.0);

(iii) saline (TDS: 10^4-10^5 mg ℓ^{-1}; depth: 600-1400 m; T: 13-23°C; pH: 6.0-8.2); and

(iv) brines (TDS $> 10^5$ mg ℓ^{-1}; depth $>$ 1200 m; T $>$ 18°C; pH: 5.0-7.0).

Table 24: Average chemical composition of groundwaters in contact with mineralisation at Dawn Lake, Saskatchewan (calculated from the data of Cramer, 1986)

	$\mu g\ \ell^{-1}$	$mg\ \ell^{-1}$
Na	3320	3.320
K	1474	1.474
Ca	369	0.369
Mg	221	0.221
Fe	1226	1.226
Ni	< 50	< 0.050
As	415	0.415
Pb	64	0.064
Co	< 100	0.100
V	< 10	0.010
U	3	0.003
F^-	128	0.128
Cl^-	876	0.876
P	< 250	< 0.250
NO_3^-	< 100	< 0.100
SO_4^{2-}	2444	2.444
HCO_3^-	29200	29.200
CO_3^{2-}	< 2000	< 2.000
----	-----	------
TDS	39250	39.250
pH	6.9	
T°(C)	---	
depth (m)	< 200	

The chemistry of fresh and brackish groundwaters is dominated by Na-Ca-HCO_3 whilst that of saline groundwaters and brines is dominated either by Ca-Na-Cl (mafic basement) or Na-Ca-Cl (granitic basement) (Frape *et al.*, 1984).

According to the classification of Frape *et al.* (1984), the present day groundwaters in contact with Dawn Lake mineralisation are fresh.

The unreactivity of the host rocks and/or their impermeability to groundwater in the vicinity of the Dawn Lake deposits, is probably a contributing factor to the continued existence of such large-tonnage, high-grade, reduced ore close to the surface.

C.3 Origin of fluids —— speculation

This scenario probably existed also during the period of tectonic quiescence between about 1000 Ma and 350 Ma. Since much unroofing of the Athabasca Group rocks has probably taken place since 350 Ma, deep reducing fluids were probably in contact with mineralisation during the 1000-350 Ma period. Prior to the initial stage of mineralisation, deep reducing fluids may also have been present in the Dawn Lake area. If Athabasca Basin sedimentation was well advanced by 1700 Ma then deep, probably hot, reduced fluids may have been present in the highly-faulted, metamorphosed basement rocks. Some of these faults may have extended down into the remobilised (domed) Archean crystalline (granitic) basement. These fluids would likely have been in contact with syngenetic and synmetamorphic protores in addition to the country rocks, and would have had at least 350 Ma to evolve into concentrated uranium-poor, but metal-rich brines.

Diabase dyke activity at about 1350-1250 Ma would have flushed these reduced metal-bearing fluids upwards. The rising thermal front may have also flushed reduced gaseous species (e.g. CH_4, H_2S) upwards.

Convective activity would have followed the initial upward pulse thus drawing reduced Athabasca Group formation waters down into the basement. As convective activity continued, oxidised Athabasca Group surficial waters would have gained access

to the basement. These oxidised fluids would have been responsible for uranium and rare earth element mobilisation. As diabase dyke activity waned and ceased, reduced fluids would have replaced oxidised ones.

This sequence of events would have been repeated with the second pulse of diabase dyke activity at 1100-1000 Ma.

Uplift and unroofing of the Athabasca Group rocks would have allowed oxidised, carbonate-bearing, surficial fluids to gain access to the basement.

D. Release of Uranium

Posey-Dowty *et al.* (1987) studied the dissolution rate of uraninite crystals and of uranium roll-front ore samples in bicarbonate solutions at 25°C, pH of 7.0 to 8.2, and variable oxygen pressure.

Posey-Dowty *et al.* (1987) concluded that:

(i) clay and other foreign materials appeared to have no major inhibitory effect on the dissolution kinetics of uraninite in bicarbonate solutions;

(ii) the single most important factor in uranium ore dissolution was the partial pressure of oxygen;

(iii) dry hexavalent uranium oxides leached almost instantaneously from ore in bicarbonate solutions;

(iv) bicarbonate concentration affected the total solubility of uranium oxides but not the dissolution rate;

(v) the rate law for dissolution of uraninite in highly undersaturated to saturated solutions was given by:

$$d[U]/dt = (kA/V)\ (p_{O_2})^{1/2}\ [(U_s - [U])/U_s]$$

where

A = surface area

V = volume of solvent

O_2 = partial pressure of oxygen

U_s = saturation concentration of U(VI) in solution

[U] = molal concentration of U(VI) in solution.

E. Transportation and deposition of uranium

E.1 Transportation of uranium

The calcium contents of pitchblendes (I, II and III) from the 334 Pod strongly suggest that the uranium present in the 334 Pod was transported as uranyl carbonate complexes, e.g. UO_2CO_3, $UO_2(CO_3)_2^{2-}$ and $UO_2(CO_3)_3^{4-}$.

McLennan and Taylor (1980) examined the relationship between rare earth elements (REE) and uranium mineralisation in the Cahill Formation of the Pine Creek Geosyncline, Northern Territory, Australia demonstrating a strong correlation between the heavy REE and U during transport and ore deposition stages in a low temperature hydrothermal system.

Fryer and Taylor (1984) observed the same relationship between the REE and U in pitchblendes from the Collins Bay unconformity-associated uranium deposit, Saskatchewan.

The strong depletion of the light REE in these ores indicated that uranium and the REE were transported in a hydrothermal fluid as soluble carbonate complexes (McLennan and Taylor, 1980; Fryer and Taylor, 1984).

Preliminary results of a study of REE associated with uranium mineralisation from the 11B Zone at Dawn Lake yield similar LREE-depleted and HREE-enriched patterns, with greatest enrichment in the Tb-Dy region (Persaud *et al.*, 1985, 1986).

E.2 Deposition of uranium

Several mechanisms for the deposition of uranium are discussed in this section. These are (1) reduction, (2) adsorption-reduction, (3) boiling and

(4) electro-precipitation.

E.2.1 Reduction

Oxidised uranium species are generally soluble and therefore mobile, whereas reduced uranium species are insoluble and generally immobile unless extremely acidic conditions prevail (Langmuir, 1978). Thus, the traditional genetic model explaining uranium deposition requires that the ore-forming solution encounters a reducing environment at the point of deposition.

Reduction of soluble hexavalent uranium species could have been carried out by reduced carbon (graphite, organic matter) and sulphur (sulphides) species as well as by ferrous iron in silicates, sulphides or oxides. Methane and hydrogen sulphide could have been produced by the reaction of upward-moving, metal-poor (early) and later metal-rich reduced fluids (flushed from deep reservoirs by diabase dyke activity) with syngenetic and synmetamorphic graphite and sulphides of the metamorphosed Aphebian basement. Trapping of these reduced species by aquicludes or aquitards at the unconformity or in the basement, would have been followed by uranium deposition when upward-moving, uranium-bearing oxidised fluids (that followed the reducing metal-rich fluids) came into contact with the reduced species.

However the concept of direct reduction of hexavalent uranium species as the only chemical control on ore deposition is inadequate to explain uraniferous mineralisation in the 334 Pod. The compositions of 334 Pod pitchblendes, obtained by electron microprobe WDA-EDA techniques, indicated that they were unlikely to be pure UO_2 but rather contain variable amounts of UO_3. Pitchblende II appears to be more oxidised than pitchblende I. This apparent deviation from the pure UO_2 composition indicated that variations in both pH and redox conditions were involved in their formation.

If uranium was transported as carbonate and hydroxyl complexes then some of the ways by which deposition of UO_2 could have taken place are:

(i) $2UO_2CO_3^0 + 2H_2O \rightarrow 2UO_3 + 2H_2CO_3 + O_2$

(ii) $2UO_2(CO_3)_2^{2-} + 2H_2O + 4H^+ \rightarrow 2UO_3 + O_2 + 4H_2CO_3$

(iii) $2UO_2(CO_3)_3^{4-} + 2H_2O + 8H^+ \rightarrow 2UO_3 + O_2 + 6H_2CO_3$

(iv) $2UO_2(OH)_2^0 \rightarrow 2UO_3 + 2H_2O + O_2$

E.2.2 Adsorption-Reduction

Adsorption is also a very efficient process of concentrating uranium on to finely divided species characterised by their large surface areas (Muto *et al.*, 1965; Giblin, 1980; Binns *et al.*, 1980; Giblin *et al.*, 1981).

Muto *et al.* (1965) speculated that discrete uraniferous phases developed from uranium initially adsorbed on substrates, such as clays or hydrous iron-(III) oxides, in response to changes to the chemistry of the sytems. Formation of discrete uranium minerals would have left the substrates free to adsorb further uranium (VI) ions. Thus, over a period of time, accumulations of uranium far in excess of what could be accomodated as adsorbed species would have developed in intimate association with adsorbate minerals.

Binns *et al.* (1980) described a chlorite-septechlorite-quartz (CSQ) intergrowth at the Jabiluka unconformity-associated uranium deposit, Australia, in which uranium levels of up to 1270 ppm (Gulson and Mizon, 1980) were observed. Binns *et al.* (1980) suggested that discrete concentrations of uraniniite formed by exsolution from uraniferous CSQ after the formation of CSQ, but provided no evidence to show whether uranium was adsorbed on to, or was present as a discrete U-rich phase in CSQ.

Giblin (1980) showed that the distribution coefficient (K_d) of uranium between a simulated groundwater (containing 100 μg U l^{-1}) and kaolinite, measured over the pH range 3.5 to 10 at 25°C, was found to reach a maximum of 35000 at pH 6.5. Giblin (1980) also carried out uranium addition in 10 sequential adsorption-reduction cycles until uranium levels of up to 1000 ppm were observed in kaolinite. At this stage the apparent distribution coefficient had risen to 85000,

more than double that achieved when uranium was adsorbed from 100 μg U l^{-1} solutions without the intermediate reduction steps. Kaolinite, mineralogically the most simple of the clay minerals, is the clay mineral having the smallest surface area and thus the least effective adsorption properties of all the phyllosilicates (Grim, 1968). Because kaolinite was used, the positive results for uranium adsorption on to it can be extrapolated to other more adsorptive phyllosilicates.

Ubiquitous clay minerals and chlorite are present in the vicinity of 334 Pod mineralisation. It is speculated here that pre-mineralisation phyllosilicates played a substantial role in uranium mineralisation of the 334 Pod.

Giblin (1980) proposed a mechanism that has been tested experimentally in part, to explain the development of uraniferous clays and chlorites. This mechanism involves adsorption of soluble oxidised U(VI) cations by negatively charged phyllosilicate particles followed by reduction of uranium, while attached to phyllosilicate mineral surfaces, to reduced uranium oxides which are held to or released from the negative phyllosilicate mineral surface on the basis of their surface charge. The surface charge on uranium oxide particles is determined by the oxide uranium-oxygen stoichiometry which is a function of the pH-Eh conditions prevailing in the system at the time of their formation.

The adsorption-reduction mechanism of Giblin (1980) can be used to explain the accumulation of large amounts of reduced uranium oxides if after their formation, separation of these discrete uranium phases from the phyllosilicate mineral surfaces occurred. Separation frees the phyllosilicate mineral surfaces for further adsorption of mobile uranium species. Non-separation excludes the phyllosilicates from further adsorption of mobile uranium.

Separation or non-separation of an uranium oxide phase is dependent upon the surface charge acquired by that phase upon formation (Giblin, 1980). The surface charge on uranium oxide particles is pH dependent; it is negative if greater than the pH at the point of zero surface charge (PZSC) and positive if lower.

The pH at PZSC is defined as the pH at which surface charge reversal occurs.

Thus if reduction occurs at a pH greater than the PZSC of an uranium oxide phase then the negatively charged phyllosilicate surface repels the uranium oxide, reversing the adsorption but with the difference that the uranium is now a solid species with the capacity for incorporation into crystalline aggregates (Giblin, 1980). In the U:O range from 1:2 to 1:2.8, the pH of the PZSC varies from 6 to 3 respectively at 25°C (Parks, 1965).

Unfortunately, the boundaries for pH-Eh stability fields for uranium species in general are unknown for the temperature range 100-200°C because of the lack of thermodynamic data. Attempts have been made to construct stability field diagrams for uranium species at high temperatures by using extrapolated thermodynamic data datermined at 25°C (Lemire and Tremaine, 1980; Romberger, 1984). However, it was decided not to use these data in this thesis because of the high degree of uncertainty regarding the stability field boundaries of the uranium species.

E.2.3 Boiling

Loss of CO_2, due to boiling, is a possible mechanism for UO_2 deposition (Poty *et al.*, 1974). Fluid inclusion studies of gangue minerals from the Rabbit Lake (Pagel and Jaffrezic, 1977; Pagel *et al.*, 1980) and Midwest Lake (Lawler and Crawford, 1982) deposits, however, show no evidence for boiling. If 3 km of Athabasca Group clastic sediments and a clay blanket were present above the upward-moving uranium-bearing oxidised fluids, boiling (or separation of the gaseous and liquid phases) probably would not have occurred.

E.2.4 Electro-precipitation

An electrochemical process has been proposed as a possible mechanism for uranium deposition (Robertson *et al.*, 1978; Tilsley, 1980).

Ions and charged complexes in natural and artificial solutions respond to applied electrical potential gradients by migrating at a rate which is a function of the voltage gradient and a constant characteristic of the ion or complex (Tilsley, 1980).

Self potentials are developed in the earth when volumes of differing Eh are connected electrically. Voltage differences across the axis of a conductive body such as a massive sulphide (or arsenide) body or a graphite schist (or gneiss) are frequently in the order of 500 to 700 mV and in some cases are in excess of 1000 mV (Kelly, 1957; Chisholm, 1957). Near the axis of a conductive structure, voltage gradients of 50 to 100 mV or more per metre are possible (Tilsley, 1980).

Uranium in solution as a positively charged complex (e.g. UO_2^{2+} or $UO_2(OH)^+$) would tend to migrate towards the low Eh surface of the conductor. Precipitation of UO_2 would occur if the upper stability Eh limit of the solid phase is crossed by the migrating complex. If during migration towards the conductor, the complex moves into a chemical environment with an Eh less than the upper stability limit of the solid phase, precipitation of the solid phase will occur.

Uranium in solution as a negatively charged complex (e.g. $UO_2(CO_3)_2^{2-}$ or $UO_2(CO_3)_3^{4-}$) would tend to migrate away from the low Eh surface of the conductor. If during migration away from the conductor, a chemical environment with an Eh less than the upper stability limit of a solid uranium oxide phase is encountered, precipitation of the solid phase will occur.

Since the uranium present in the 334 Pod was most probably transported as neutral and negative uranyl carbonate complexes, electro-precipitation of uranium was probably insignificant as a uranium deposition mechanism for 334 mineralisation.

However repulsion of negatively charged uranyl carbonate complexes by the graphitic conductor above the 334 Pod probably caused them to migrate into areas

where chemical reduction and adsorption-reduction uranium deposition mechanisms operated.

Ore constituents such as As and S which are transported as anions also would not collect at the negative electrode of the electrochemical cell (i.e., the graphitic conductor).

F. Transportation of arsenic

Arsenic probably was transported as thioarsenide complexes (AsS_2^-, $HAsS_2^0$; T: 100-250°C; pH: 4-6; -log a_{H_2S}: 1-3) and as arsenious acid ($H_3AsO_3^0$) at higher temperatures (>200°C), pH (>5) and oxygen fugacities (Heinrich and Eadington, 1986).

F.1 Deposition of arsenides and sulpharsenides

Possible diarsenide producing reactions are:

(i) $Ni^{2+} + 2AsS_2^- + 4H_2O \rightarrow NiAs_2 + 4H_2S + 2O_2$

(ii) $Ni^{2+} + 2AsS_2^- + 2H_2O + 4e^- \rightarrow NiAs_2 + 4HS^- + O_2$

(iii) $2Ni^{2+} + 4HAsS_2 + 6H_2O + 4e^- \longrightarrow 2NiAs_2 + 8H_2S + 3O_2$

(iv) $2Ni^{2+} + 4HAsS_2 + 2H_2O + 4e^- \longrightarrow 2NiAs_2 + 8HS^- + O_2$

(v) $2Ni^{2+} + 4HAsO_3 + 4e^- \longrightarrow 2NiAs_2 + 2H_2O + 5O_2$

Possible monoarsenide producing reactions are:

(i) $Ni^{2+} + AsS_2^- + 2H_2O + e^- \longrightarrow NiAs + 2H_2S + O_2$

(ii) $2Ni^{2+} + 2AsS_2^- + 2H_2O + 6e^- \longrightarrow 2NiAs + 4HS^- + O_2$

(iii) $4Ni^{2+} + 4HAsS_2 + 6H_2O + 8e^- \longrightarrow 4NiAs + 8H_2S + 3O_2$

(iv) $4Ni^{2+} + 4HAsS_2 + 2H_2O + 8e^- \longrightarrow 4NiAs + 8HS^- + O_2$

(v) $4Ni^{2+} + 4HAsO_3 + 8e^- \longrightarrow 4NiAs + 2H_2O + 5O_2$

Possible sulpharsenide producing reactions are:

(i) $2Ni^{2+} + 2AsS_2^- + 2H_2O + 2e^- \longrightarrow 2NiAsS + 2H_2S + O_2$

(ii) $4Ni^{2+} + 4AsS_2^- + 2H_2O + 8e^- \longrightarrow 4NiAsS + 4HS^- + O_2$

(iii) $4Ni^{2+} + 4HAsS_2 + 2H_2O + 8e^- \longrightarrow 4NiAsS + 4H_2S + O_2$

(iv) $Ni^{2+} + HAsS_2 + 3e^- \longrightarrow NiAsS + HS^-$

(v) $4Ni^{2+} + 4HAsO_3 + 4H_2S + 8e^- \longrightarrow 4NiAsS + 6H_2O + 3O_2$

The vast majority of these diarsenide-, monoarsenide-, and sulpharsenide-producing reactions require electrons in order to move to the right. A major electron producing reaction (or half cell) in geological environments is

$$Fe^{2+} \longrightarrow Fe^{3+} + e^-$$

In the Dawn Lake area as well as in other unconformity-associated deposits, this reaction is represented by the chlorite-hematite redox.

Arsenide and sulpharsenide deposition in the 334 Pod at Dawn Lake probably involved the chlorite/hematite redox reaction. However, arsenides and sulpharsenides in the 334 Pod at Dawn Lake are not observed to be associated with hematite. There are two possible reasons to account for this:

(i) hematite has been destroyed by later reducing solutions; or

(ii) the chlorite/hematite redox in the regolith provided the electrons which were then transmitted through the graphitic conductor below to the site of reaction below the conductor.

In 334 Pod mineralisation, diarsenides were observed to be replaced by monoarsenides and sulpharsenides whilst monoarsenides were replaced by sulpharsenides. Possible diarsenide-monoarsenide replacement reactions are:

(i) $NiAs_2 + 2H_2S + e^- \longrightarrow NiAs + AsS_2^- + 2H_2$

(ii) $NiAs_2 + 2HS^- \longrightarrow NiAs + AsS_2^- + H_2 + e^-$

(iii) $2NiAs_2 + 4H_2S \longrightarrow 2NiAs + 2HAsS_2 + H_2 + 4e^-$

(iv) $2NiAs_2 + 4HS^- \longrightarrow 2NiAs + 2HAsS_2 + H_2 + 4e^-$

(v) $4NiAs_2 + 6H_2O + 3O_2 \longrightarrow 4NiAs + 4H_3AsO_3$

Possible diarsenide-sulpharsenide replacement reactions are:

(i) $NiAs_2 + 3H_2S + e^- \longrightarrow NiAsS + AsS_2^- + 3H_2$

(ii) $2NiAs_2 + 6HS^- \longrightarrow 2NiAsS + 2AsS_2^- + 3H_2 + 4e^-$

(iii) $2NiAs_2 + 6H_2S \longrightarrow 2NiAsS + 2HAsS_2 + 5H_2$

(iv) $2NiAs_2 + 6HS^- \longrightarrow 2NiAsS + 2HAsS_2 + 2H_2 + 6e^-$

(v) $2NiAs_2 + 2H_2S + 3O_2 \longrightarrow 2NiAsS + 2HAsO_3 + H_2$

(vi) $2NiAs_2 + 2HS^- + 3O_2 \longrightarrow 2NiAsS + 2HAsO_3 + 2e^-$

Possible monoarsenide-sulpharsenide replacement reactions are:

(i) $NiAs + H_2S \longrightarrow NiAsS + H_2$

(ii) $2NiAs + 2HS^- \longrightarrow 2NiAsS + H_2 + 2e^-$

G. Depositional model

Data from the 334 Pod at Dawn Lake suggests a polygenetic history. The following sequence of events is envisioned:

(1) Syngenetic concentration ?-1900 Ma

Aphebian Wollaston Group sediments were deposited in a miogeoclinal environment. Uranium and other metallic ions were preferentially concentrated in black shales. These black shales were the precursors of the graphitic metapelites.

(2) Diagenetic enrichment ?-1900 Ma

Dewatering of the sedimentary pile as a result of progresive compaction and lithification caused redistribution and further concentration of uranium in pelitic horizons.

(3) Trans-Hudson Orogen 1900-1800 Ma

Thermal doming of the Archean granitic basement resulted in the mobilisation and expulsion of uranium and thorium along with H_2O, CO_2, F, Cl and other volatiles during partial melting. The passage of these fluids through adjacent pelites would augment, remobilise and further concentrate the uranium.

At Dawn Lake, anatectic pegmatoids are ubiquitous and appear to have formed by *in situ* melting of meta sedimentary rocks. Uranium and thorium would have been further concentrated in pegmatoid segregations.

The metamorphic, mineral-forming event at about 1800 Ma remobilised the uranium into the metasediments.

(4) Pre-Athabasca Group Peneplanation and Weathering 1800-1700 Ma

Isostatic reactivation of faults maintained them as principal passages for migrating solutions. Some metal redistribution and concentration may have occurred during retrograde metamorphism.

(5) Athabasca Group sedimentation 1700-1350 Ma

This was a period of relative tectonic quiescence. Diagenesis of the Athabasca Group may have resulted in limited remobilisation of metals. Metal-rich reduced brines evolved in the faulted basement rocks during this period.

(6) Hydrothermal mineralisation/diabase dyke activity 1350 Ma

Flushing of deep reduced fluids by diabase dyke activity resulted in deposition of arsenides and sulpharsenides of the 334 Pod. Reduced fluids gave way to oxidised fluids which precipitated pitchblende I. Late reduced fluids precipitated sulpharsenides. The majority of 334 Pod mineralisation was deposited during this stage.

(7) Hydrothermal mineraliation/diabase dyke activity 1100 Ma

Flushing of deep reduced fluids by diabase dyke activity resulted in remobilisation of earlier deposited arsenides and sulpharsenides. Oxidised fluids remobilised pitchblende I, precipitating pitchblende II. Late reduced fluids deposited trace to minor amounts of base metal sulphides.

(8) Uplift and unroofing of Athabasca Group rocks 350-0 Ma

Oxidised, carbonate-bearing, surficial fluids gained access to the 334 Pod mineralisation, remobilising earlier pitchblendes (I and II) to form pitchblende III - (coffinite). These fluids also caused supergene alteration of chalcopyrite, the

released sulphur reacting with radiogenic lead to form galena.

VII. BIBLIOGRAPHY

Alcock, F.J. (1915) Geology of the north shore of Lake Athabasca, Alberta and Saskatchewan. Geological Survey of Canada Summary Report 1914, 60-61.

Alcock, F.J. (1916) Lower Churchill River region, Manitoba. Geological Survey of Canada Summary Report 1915, 60-61.

Alcock, F.J. (1917) Black Bay and Beaverlodge Lake areas, Saskatchewan. Geological Survey of Canada Summary Report 1916, 152-156.

Alcock, F.J. (1920) The Athabasca Series. American Journal of Science,50, 25-32.

Alcock, F.J. (1936) Geology of the Lake Athabasca region, Saskatchewan. Geological Survey of Canada, Memoir 196 .

Armstrong, R.L. and Ramaekers, P. (1985) Sr isotopic study of Helikian sediment and diabase dikes in the Athabasca Basin, northern Saskatchewan. Canadian Journal of Earth Sciences, 22, 399-407.

Atkin, B.P. and Harvey, P.K. (1979) The use of quantitative colour values for opaque mineral identification. Canadian Mineralogist, 17, 639-647.

Atkin, B.P. and Harvey, P.K. (1982) NISOMI-82: An automated system for opaque-mineral identification in polished section; in: Hagni, R.D., ed., Process Mineralogy II: Applications in Metallurgy, Ceramics, and Geology. Symposium proceedings of the Process Mineralogy Committee of the Metallurgical Society of AIME, Dallas, Texas, February 1982.

Baadsgaard, H., Cumming, G.L. and Worden, J.M. (1984) U-Pb geochronology of minerals from the Midwest uranium deposit, northern Saskatchewan. Canadian Journal of Earth Sciences, 21, 642-648.

Bailes, A.H. (1980) Origin of Early Proterozoic volcaniclastic turbidites, south margin of the Kisseynew sedimentary gneiss belt, File Lake, Manitoba. Precambrian Research, 12, 197-225.

Bailes, A.H. and McRitchie, W.D. (1978) The transition from low to high grade metamorphism in the Kisseynew sedimentary gneiss belt, Manitoba. Geological Survey of Canada, Paper 78-10, 155-178.

Baragar, W.R.A. and Scoates, R.F.J. (1981) The Circum-Superior Belt: a Proterozoic plate margin? : in Kroner, A. ed., Precambrian plate tectonics. Elsevier, Amsterdam, 297-330.

Barbier, M.J. (1974) Continental weathering as a possible origin of vein type uranium deposits. Mineralium Deposita, 9, 271-288.

Bayliss, P. (1969) X-ray data, optical anisotropism, and thermal stability of cobaltite, gersdorffite, and ullmanite. Mineralogical Magazine, 37, 26-33.

Beck, L.S. (1977) Changing ideas on metallogenesis of Saskatchewan's uranium deposits. Canadian Mining Journal, 98, 49-51.

Bell, K. and Blenkinsop, J. (1980) Saskatchewan shield geochronology project; in: Summary of Investigations 1980. Saskatchewan Geological Survey Miscellaneous Report 80-4, 18.

Bell, K. and Macdonald, R. (1982) Geochronological calibration of the Precambrian Shield in Saskatchewan: in Summary of Investigations, 1982. Saskatchewan Geological Survey, Miscellaneous Report, 82-4, 17-22.

Binns, R.A., McAndrew, J. and Sun, S-S. (1980) Origin of uranium mineralisation at Jabiluka; in: Ferguson, J. and Goleby, A., eds., Uranium in the Pine Creek Geosyncline. IAEA, Vienna, 543-562.

Braitsch, O. (1971) Salt deposits: their origin and composition. Springer, Berlin.

Bray, C.J., Spooner, E.T.C., Hall, C.M., York, D., Bills, T.M. and Krueger, H.W. (1987) Laser probe $^{40}Ar/^{39}Ar$ and conventional K-Ar dating of illites associated with the McClean unconformity-related uranium deposits, northern Saskatchewan, Canada. Canadian Journal of Earth Sciences, 24, 10-23.

Bretzlaff, R.E. (1976) Genesis of uranium mineralisation at Duddridge Lake, Saskatchewan. Unpublished B.Sc thesis, Carleton University.

Bruneton, P. (1986) Geology of the Cigar Lake uranium deposit (Saskatchewan, Canada); in: Gilboy, C.F. and Vigrass, L.W., eds., Economic Minerals of Saskatchewan Geological Society Special Publication, 8, 99-119.

Burwash, R.A. (1969) Comparative Precambrian geochronology of the North American, European, and Siberian shields. Canadian Journal of Earth Sciences, 6, 357-365.

Burwash, R.A., Baadsgaard, H. and Morton, R.D. (1962) Precambrian K-Ar dates from the Western Canada Sedimentary Basin. Journal of Geophysical Research, 67, 1617-1623.

Cameron-Schimann, M. (1978) Electron microprobe study of uranium minerals and its application to some Canadian deposits. Unpublished Ph.D thesis, University of Alberta, 343 p.

Camsell, C. (1915) An explosion of the region between Athabasca and Great Slave lakes, Alberta and Saskatchewan. Geological Survey of Canada Summary Report 1914, 55-60.

Changkakoti, A. (1985) Mineralogic, fluid inclusion and isotopic investigations of the Great Bear Lake Silver Deposits, Northwest Territories. Unpublished Ph.D. thesis, University of Alberta, 220 p.

Changkakoti, A. and Morton, R.D. (1986) Electron microprobe analyses of native silver and associated arsenides from the Great Bear Lake silver deposits, Northwest Territories, Canada. Canadian Journal of Earth Sciences, 23, 1470-1479.

Chauvel, C., Arndt, N.T., Kielinzcuk, S. and Thom, A. (1987) Formation of Canadian 1.9 Ga old continental crust. I: Nd isotopic data. Canadian Journal of Earth Sciences, 24, 396-406.

Chisholm, E.O. (1957) Geophysical exploration of a lead-zinc deposit in Yukon Territory; in: Methods and Case Histories in Mining Geophysics. 6th Commonwealth Mining and Metallurgy Congress, 269-277.

Clarke, P.J. and Fogwill, W.D. (1981) Geology of the Asamera Dawn Lake uranium deposits, Athabasca Basin, northern Saskatchewan; in: CIM Geology Division Uranium Field Excursion Guidebook. Canadian Institute of Mining and Metallurgy, 19-36.

Clarke, P.J. and Fogwill, W.D. (1986) Geology of the Dawn Lake uranium deposits, northern Saskatchewan; in: Evans, E.L., ed., Uranium Deposits of Canada. Canadian Institute of Mining and Metallurgy, Special Volume 33,184-192.

Coombe, W. (1978) Wollaston base metals project, Duddridge Lake to Meyers Lake area; in: Summary of Investigations 1978. Saskatchewan Geological Survey Miscellaneous Report 78-10, 98-108.

Craig, J.R., Vaughan, D.J. and Higgins, J.B. (1979a) Phase relations in the Cu - Co - S system and mineral associations of the carrollite ($CuCo_2S_4$) —— linnaeite (Co_3S_4) series. Economic Geology, 74, 657-671.

Craig, J.R., Vaughan, D.J. and Higgins, J.B. (1979b) Phase equilibria in the copper-cobalt-sulphur system. Materials Research Bulletin, 14, 149-154.

Cramer, J.J. (1986) Sandstone-hosted uranium deposits in northern Saskatchewan as natural analogs to nuclear fuel waste disposal vaults. Chemical Geology, 55, 269-279.

Cumming, G.L. and Rimsaite, J.Y.H. (1979) Isotopic studies of lead-depleted pitchblende, secondary radioactive minerals, and sulphides from the Rabbit Lake uranium deposit, Saskatchewan. Canadian Journal of Earth Sciences, 16, 1702-1715.

Cumming, G.L., Krstic, D. and Wilson, J.A. (1987) Age of the Athabasca Group, northern Alberta [abstract]. Geological Association of Canada- Mineralogical Association of Canada Joint Annual Meeting, Saskatoon, 1987. Program with Abstracts, 35.

Dahlkamp, F.J. (1978) Geologic appraisal of the Key Lake U-Ni deposits, northern Saskatchewan. Economic Geology, 73, 1430-1449.

Dahlkamp, F.J. and Tan, B. (1977) Geology and Mineralogy of the Key Lake U-Ni Deposits, Northern Saskatchewan, Canada; in: Jones, M.J., ed., Geology, Mining and Extractive Processings of Uranium. IMM, London, 145-157.

de Carle, A.L. (1986) Geology of the Key Lake Deposits; in: Evans, E.L., ed., Uranium Deposits of Canada. The Canadian Institute of Mining and Metallurgy, Special Volume 33, 170-177.

Drury, M.J. (1985) Heat flow and heat generation in the Churchill Province of the Canadian shield and their palaeotectonic significance. Tectonophysics, 115, 25-44.

Evans, M.E. and Bingham, D.K. (1973) Palaeomagnetism of the Precambrian Martin Formation, Saskatchewan. Canadian Journal of Earth Sciences, 10, 1485-1493.

Finch, W.I. (1967) Geology of epigenetic uranium deposits in sandstone in the United States. United States Geological Survey Professional Paper 538, 121p.

Fogwill, W.D. (1985) Canadian and Saskatchewan uranium deposits: compilation, metallogeny, models, exploration; in: Sibbald, T.I.I. and Petruk, W., eds., Geology

of Uranium Deposits. Canadian Institute of Mining and Metallurgy, Special Volume 32, 3-19.

Fouques, J.P., Fowler, M., Knipping, H.D., and Schimann, K. (1986) The Cigar Lake uranium deposit: discovery and geological characteristics; in: Evans, E.L., ed., Uranium Deposits of Canada. The Canadian Institute of Mining and Metallurgy, Special Volume 33, 218-229.

Frape, S.K. and Fritz, P. (1982) The chemistry and isotopic composition of saline groundwaters from the Sudbury Basin, Ontario. Canadian Journal of Earth Sciences, 19, 645-661.

Frape, S.K., Fritz, P. and McNutt, R.H. (1984) Water-rock interaction and chemistry of groundwaters from the Canadian Shield. Geochemica et Cosmochemica Acta, 48, 1617-1627.

Fraser, J.A., Heywood, W.W. and Mazurski, M.A. (1978) Metamorphic map of the Canadian Shield. Geological Survey of Canada, Map 1475-A; Scale 1:3500000.

Fraser, J.A., Donaldson, J.A., Fahrig, W.F. and Tremblay, L.P. (1970) Helikian basins and geosynclines of the northwestern Canadian shield; in: Symposium on Basins and Geosynclines of the Canadian Shield. Geological Survey of Canada, Paper 70-40, 213-238.

Frondel, C. (1958) Systematic mineralogy of uranium and thorium. Bull. U.S. Geol. Surv. 1064, 400p.

Fryer, B.J. and Taylor, R.P. (1984) Sm-Nd direct dating of the Collins Bay hydrothermal uranium deposit, Saskatchewan. Geology, 12, 479-482.

Fumerton, S.L., Stauffer, M.R. and Lewry, J.F. (1984) The Wathaman batholith: largest known Precambrian pluton. Canadian Journal of Earth Sciences, 21, 1082-1097.

Giblin, A.M. (1980) The role of clay adsorption in genesis of uranium ores; in: Ferguson, J. and Goleby, A., eds., Uranium in the Pine Creek Geosyncline. IAEA, Vienna, 521-529.

Giblin, A.M., Batts, B.D. and Swaine, D.J. (1981) Laboratory simulation studies of uranium mobility in natural waters. Geochemica et Cosmochemica Acta, 45, 699-709.

Gilboy, C.F. (1975) The geology of the Foster Lake area; in: Summary of Investigations 1975. Saskatchewan Geological Survey, 29-34.

Gilboy, C.F. (1978) Reconnaissance geology, Stony Rapids area; in: Summary of Investigations 1978. Saskatchewan Geological Survey Miscellaneous Report 78-10, 35-42.

Gilboy, C.F. (1982) Sub-Athabasca basement geology project; in: Summary of Investigations 1982. Saskatchewan Geological Survey Miscellaneous Report 82-4, 12-15.

Green, A.G., Hajnal, Z. and Weber, W. (1985) An evolutionary model of the western Churchill Province and western margin of the Superior Province in Canada and the north-central United States. Tectonophysics, 116, 281-322.

Grim, R.E. (1968) Clay Mineralogy (2nd edition). McGraw-Hill, New York. 596 p.

Gronvold, F. (1955) High temperature X-ray of uranium oxides in the UO_2-U_3O_8 region. J. Inorg. Nucl. Chem., 1, 357-370.

Gulson, B.L. and Mizon, K.J. (1980) Lead isotope studies at Jabiluka; in: Ferguson, J.A. and Goleby, A., eds., Uranium in the Pine Creek Geosyncline. IAEA, Vienna, 439-455.

Harper, C.T. (1982) Uranium Metallogenetic Studies: Dawn Lake Property; in: Summary of Investigations 1982. Saskatchewan Geological survey Miscellaneous Report 82-4, 46-50.

Haughton, D.R. (1977) A multiple media geochemical survey of a boulder train associated with the Duddridge Lake uranium deposit, Saskatchewan; in: Dunn, C.E., ed., Uranium in Saskatchewan. Saskatchewan Geological Survey Special Publication, 3, 256-296.

Hegner, E. and Hulbert, H.L. (1987) Sm-Nd ages and origin of mafic-ultramafic intrusions from the Proterozoic Lynn Lake domain, Manitoba, Canadia (abstract). Geological Association of Canada - Mineralogical Association of Canada Joint Annual Meeting, Saskatoon, 1987. Program with abstracts, 54.

Heine, T. (1981) The Rabbit Lake deposit and the Collins Bay deposits; in: CIM Geology Division Uranium Field Excursion Guidebook, 87-102.

Heinrich, C.A. and Eadington, P.J. (1986) Thermodynamic predictions of the hydrothermal chemistry of arsenic, and their significance for the paragenetic sequence of some cassiterite-arsenopyrite-base metal sulfide deposits. Economic Geology, 81, 511-529.

Henderson, P. (1982) Inorganic Geochemistry. Pergamon Press, Oxford. 353 p.

Hobson, G.D. and MacAulay, H.A. (1969) A seismic reconnaissance survey of the Athabasca Formation, Alberta and Saskatchewan. Geological Survey of Canada. Paper 69-18, 23 p.

Hoeve, J. and Quirt,D. (1984) Uranium mineralisation and host rock alteration in relation to clay mineral diagenesis and evolution of the Middle Proterozoic Athabasca basin, Saskatchewan, Canada. Saskatchewan Research Council Publication R-855-2-B-84, 190 p.

Hoeve, J. and Quirt, D. (1987) A stationary redox front as a critical factor in the formation of high-grade, unconformity-type uranium ores in the Athabasca Basin, Saskatchewan, Canada. Bull. Mineral., 110, 157-171.

Hoeve, J. and Sibbald, T.I.I. (1977) Rabbit Lake uranium deposit; in: Dunn, C.E. ed., Uranium in Saskatchewan. Saskatchewan Geological Society Special Publication, 3, 331-354.

Hoeve, J. and Sibbald, T.I.I. (1978) On the genesis of Rabbit Lake and other unconformity-type uranium deposits in northern Saskatchewan, Canada. Economic Geology, 73, 1450-1473.

Hoeve, J., Sibbald, T.I.I., Ramaekers, P. and Lewry, J.F. (1980) Athabasca basin

unconformity-type uranium deposits: A special class of sandstone-type deposits ?; in: Ferguson, J. and Goleby, A., eds., Uranium in the Pine Creek Geosyncline. IAEA, Vienna, 575-594.

Hoffman, P.F. (1984) Assembly and growth of the North American in Proterozoic times [abstract]. 27th International Geological Congress, Moscow, USSR, Abstracts, Vol. IX, Part 1, 156-157.

Hoffman, P.F. (1987a) Birth of a craton [abstract]. Geological Association of Canada - Mineralogical Association of Canada Joint Annual Meeting, Saskatoon, 1987. Program with abstracts, 56.

Hoffman, P.F. (1987b) Is Great Slave Lake Shear Zone a continental transform fault? [abstract] Geological Association of Canada - Mineralogical Association of Canada Joint Annual Meeting, Saskatoon, 1987. Program with Abstracts, 56.

Hohndorf, A., Lenz, H., von Pechmann, E., Voultsidis, V. and Wendt, I. (1985) Radiometric age determinations on samples of Key Lake uranium deposits; in: Sibbald, T.I.I. and Petruk, W., eds., Geology of Uranium Deposits. Canadian Institute of Mining and Metallurgy Special Volume 32, 48-53.

Kelly, S.F. (1957) Spontaneous polarisation, or self-potential methods; in: Methods and Case Histories in Mining Geophysics. 6th Commonwealth Mining and Metallurgy Congress, 55-58.

Kermeen, J.S. (1955) A study of some uranium mineralisation in Athabasca sandstone near Stony Rapids, Northern Saskatchewan, Canada. Unpublished M.Sc thesis, University of Saskatchewan.

Kirchner, G., Lehnert-Thiel, K., Rich, J. and Strnad, J.G. (1980) The Key Lake U-Ni deposits: a model for Lower Proterozoic uranium deposition; in: Ferguson, J. and Goleby, A., eds., Uranium in the Pine Creek Geosyncline. IAEA, Vienna, 617-629.

Knipping, H.D. (1974) The concepts of supergene vs hypogene emplacement of uranium at Rabbit Lake, Saskatchewan, Canada; in: Formation of uranium ore deposits. IAEA, Vienna, 531-549.

Koeppel, V. (1968) Age and history of the uranium mineralisation of the Beaverlodge area, Saskatchewan. Geological Survey of Canada, Paper 67-31.

Kornik, L.J. (1980) The NEA-IAEA Test Area Magnetic Gradiometer Survey. Open File 713, 1:50,000. Geophysical Data Processing Section. Geological Survey of Canada. Department of Energy, Mines and Resources.

Lang, A.H. (1952) Uranium orebodies. How can more be found in Canada? Canadian Mining Journal, 73, June.

Langford, F.F. (1974) A supergene origin for vein-type uranium ores in light of the Western Australian calcrete-carnotite deposits. Economic Geology, 69, 516-526.

Langford, F.F. (1978) Origin of unconformity-type pitchblende deposits in the Athabasca Basin of Saskatchewan; in: Kimberley, M.M., ed., Short Course in Uranium Deposits: Their Mineralogy and Origin. Mineralogical Association of Canada, 485-499.

Langmuir, D. (1978) Uranium solution-mineral equilibria at low temperatures with application to sedimentary ore deposits. Geochemica et Cosmochemica Acta, 42, 547-569.

Lawler, J.P. and Crawford, M.L. (1982) Fluid inclusions in the Midwest Lake uranium deposit. Geological Society of America Abstracts with Programs 1982, 542 (09031).

Lemire, R.J. and Tremaine, P.R. (1980) Uranium and plutonium equilibria in aqueous solutions to 200°C. J. Chem. Eng. Data, 25, 361-370.

Lewry, J.F. (1977) Reconnaissance geology: Compulsion Bay area, Wollaston Lake; in: Summary of Investigations 1977. Saskatchewan Geological Survey, 30-36.

Lewry, J.F. (1981) Lower Proterozoic arc-microcontinent collisional tectonics in the western Churchill Province. Nature, 294(5836), 69-72.

Lewry, J.F. and Sibbald, T.I.I. (1977) Variations in lithology and tectonomorphic variations in the Precambrian basement of Northern Saskatchewan. Canadian Journal of Earth Sciences, 14, 1453-1467.

Lewry, J.F. and Sibbald, T.I.I (1979) A review of the pre-Athabasca basement geology in northern Saskatchewan; in: Parslow, G.R. ed., Uranium exploration techniques. Saskatchewan Geological Society Special Publication, 4, 19-58.

Lewry, J.F. and Sibbald, T.I.I (1980) Thermotectonic evolution of the Churchill Province in northern Saskatchewan, Tectonophysics, 68, 48-82.

Lewry, J.F., Sibbald, T.I.I. and Rees, C.J. (1978) Metamorphic patterns and their relation to tectonism and plutonism in the Churchill Province in northern Saskatchewan; in: Fraser, J.A. and Heywood, W.W., eds., Metamorphism in the Canadian Shield. Geological Survey of Canada, Paper 78-10, 139-154.

Lewry, J.F., Stauffer, M.R. and Fumerton, S.L. (1981) A Cordilleran-type batholitic belt in the Churchill Province in northern Saskatchewan. Precambrian Research, 14, 277-313.

Lewry, J.F., Sibbald, T.I.I. and Schledewitz, D.C.P. (1985) Reworking of Archean basement in the Western Churchill Province and its significance; in: Ayres, L.D., Thurston, P.C., Card, K.D. and Weber, W., eds., Archean Supracrustal Sequences. Geological Association of Canada Special Paper 28, 239-261.

Maas, R., McCulloch, M.T. and Campbell, I.H. (1986) Nd isotopic constraints on the original unconformity-type deposits. Australian National University Research School of Earth Sciences, Annual Report, 87.

Macdonald, C.C. (1980) Mineralogy and Geochemistry of a Precambrian Regolith in the Athabasca Basin. Unpublished M.Sc thesis. University of Saskatchewan.

Macdonald, C.C. (1985) Mineralogy and geochemistry of the sub-Athabasca regolith near Wollaston Lake; in: Sibbald, T.I.I. and Petruk, W., eds., Geology of Uranium Deposits. Canadian Institute of Mining and Metallurgy, Special Volume 32, 155-158.

McLennan, S.M. and Taylor, S.R. (1980) Rare earth elements in sedimentary rocks, granites and uranium deposits of the Pine Creek Geosyncline; in: Ferguson, J.A. and Goleby,A., eds., Uranium in the Pine Creek Geosyncline. IAEA, Vienna,

175-190.

McNutt, A. (1980) Interpretation of sub-Athabasca geology. Internal Report, Saskatchewan Mining Development Corporation.

McNutt, A. (1982) Report on geological investigations, 11B Zone, 284 Pod. Internal Report, Saskatchewan Mining Development Corporation.

McRitchie, W.D. (1977) Reindeer Lake-Southern Indian Lake: regional correlation. Manitoba Department of Energy and Mines, Report of Field Activities 1977, 13-18.

Misra, K.C. and Fleet, M.E. (1975) Textural and compositional variations in a Ni-Co-As assemblage. Canadian Mineralogist, 13, 8-14.

Money, P.L. (1968) The Wollaston Lake fold-belt system, Saskatchewan, Manitoba. Canadian Journal of Earth Sciences, 5, 1489-1504.

Money, P.L., Baer, A.J., Scott, B.P. and Wallis, R.H. (1970) The Wollaston Lake belt, Saskatchewan, Manitoba; in: Basins and geosynclines of the Canadian Shield. Geological Survey of Canada, Paper 70-40, 170-197.

Moreau, M., Poughon, A., Puibaraud, Y. and Sanselme, H. (1966) L'uranium et les granites. Chronique des mines et de la recherche miniere, No. 350, 47-51.

Morton, R.D. (1977) The Western and Northern Australian uranium deposits - exploration guides or exploration deterrents for Saskatchewan?; in: Dunn, C.E., ed., Uranium in Saskatchewan. Saskatchewan Geological Society Special Publication, 3, 211-254.

Morton, R.D. and Beck, L.S. (1978) The origins of the uranium deposits of the Athabasca region, Saskatchewan, Canada [abstract]. Economic Geology, 73, 1408.

Murowchick, J.B. and Barnes, H.L. (1986) Marcasite precipitation from hydrothermal solutions. Geochemica et Cosmochemica Acta, 50, 2615-2629.

Muto, T., Hirono, S. and Kurata, H. (1965) Some aspects of fixation of uranium from natural waters. Min. Geol., 15(74), 287-298.

Pagel, M. (1975) Determination des conditions physico-chemiques dc la silicification diagenetique des gres Athabasca (Canada) an moyen des inclusions fluides. C.R. Acad. Sc. Paris, Serie D, 280, 2301-2304.

Pagel, M. and Jaffrezic, H. (1977) Analyses chimiques des saumures des inclusions de quartz et de la dolomite du gisement d'uranium de Rabbit Lake (Canada). Aspect methodologique et importance genetique. C.R. Acad. Sci. Paris, Serie D, 284, 113-116.

Pagel, M. and Ruhlmann, F. (1985) Chemistry of uranium minerals in deposits and showings of the Carswell Structure (Saskatchewan, Canada); in: Laine, R., Alonso, D. and Svab, M., eds., The Carswell Structure Uranium Deposits, Saskatchewan. Geological Association of Canada Special Paper 29, 153-164.

Pagel, M., Poty, B. and Sheppard, S.M.F. (1979) Contribution to some Saskatchewan uranium deposits mainly from fluid inclusion and isotopic data. IUSPCG (extended abstracts), 155-158.

Pagel, M., Poty, B. and Sheppard, S.M.F. (1980) Contribution to some Saskatchewan uranium deposits mainly from fluid inclusion and isotopic data; in: Ferguson, J. and Goleby, A., eds., Uranium in the Pine Creek Geosyncline. IAEA, Vienna, 639-654.

Parks, G.A. (1965) The isoelectric points of solid oxides, solid hydroxides and aqueous hydrous complex systems. Chem. Rev., 65, 177-198.

Parslow, G.R., Brandstatter, F., Kurat, G. and Thomas, D.J. (1985) Chemical ages and mobility of U and Th in anatectites of the Cree Lake zone, Saskatchewan. Canadian Mineralogist, 23, 543-551.

Peredery, W.V. (1979) Relationship of ultramafic amphibolites to metavolcanic rocks and serpentinites in the Thompson belt, Manitoba. Canadian Mineralogist, 17,187-200.

Persaud, E.C.R., Morton, R.D. and Duke, M.J.M. (1985) REE associated with uranium mineralisation at Dawn Lake, northern Saskatchewan [abstract]. University of Alberta SLOWPOKE Facility Annual Report 1985, R7.

Persaud, E.C.R., Morton, R.D. and Duke, M.J.M. (1986) REE associated with uranium mineralisation at Dawn Lake, northern Saskatchewan [abstract]. University of Alberta SLOWPOKE Facility Annual Report 1986, R 19.

Petruk, W., Harris, D.C. and Stewart, J.M. (1971) Characteristics of the arsenides, sulpharsenides, and antimonides. Canadian Mineralogist, 11, 150-186.

Posey-Dowty, J., Axtmann, E., Crerar, D., Borcsik, M., Ronk, A. and Woods, W. (1987) Dissolution rate of uraninite and uranium roll-front ores. Economic Geology, 82, 184-194.

Potter, D. (1977) La Ronge-Wollaston belts base metals project: Sito Lake area; in: Summary of Investigations 1977. Saskatchewan Geological Survey, 105-110.

Poty, B., Leroy, J. and Cuney, M. (1974) Les inclusions fluides dans les minerais des gisements d'uranium intragranitiques du Limousin et du Fortz (Massif Central Francais); in: Formation of Uranium Ore Deposits. IAEA, Vienna, 569-582.

Ramaekers, p. (1977) Athabasca Formation, south-central edge (74G Area): I Reconnaissance geology; in: Summary of Investigations 1977. Saskatchewan Geological Survey, 157-163.

Ramaekers, P. (1979) Stratigraphy of the Athabasca basin; in: Summary of Investigations 1979. Saskatchewan Geological Survey Miscellaneous Report, 79-10, 154-160.

Ramaekers, P. (1980) Stratigraphy and tectonic history of the Athabasca Group (Helikian) of Northern Saskatchewan; in: Summary of Investigations 1980. Saskatchewan Geological Survey Miscellaneous Report, 80-4, 99-106.

Ramaekers, P. (1981) Hudsonian and Helikian basins of the Athabasca region, northern Saskatchewan; in: Campbell, F.H.A., ed., Proterozoic Basins of Canada. Geological Survey of Canada, Paper 81-10, 219-233.

Ramaekers,P. (1983) Geology of the Athabasca Group, NEA/IAEA Athabasca Test

Area; in: Cameron, E.M., ed., Uranium Exploration in Athabasca Basin, Saskatchewan, Canada. Geological Survey of Canada, Paper 82-11, 15-25

Ramaekers, P. and Dunn, C.E. (1977) Geology and geochemistry of the eastern margin of the Athabasca Basin; in: Dunn, C.E., ed., Uranium in Saskatchewan. Saskatchewan Geological Society Special Publication, 3, 297-322.

Ramaekers, P. and Hartling, A. (1979) Structural geology and intrusive events of the Athabasca Basins, and their bearing on uranium mineralisation; in: Parslow, G.R., ed., Uranium Exploration Techniques. Saskatchewan Geological Society Special Publication 4.

Ramdohr, P. (1980) The ore minerals and their intergrowths. Pergamon Press, Oxford.

Ray, G.E. (1977) Compilation geology. Foster Lake area (74A), including reconnaissance geological mapping of the Daly Lake (west) and part of the Middle Foster Lake area; in: Summary of Investigations 1977. Saskatchewan Geological Survey, 43-50.

Ray, G.E. (1978) Reconnaissance geology: Wollaston Lake (west) area (part of NTS area 64L); in: Summary of Investigations 1978. Saskatchewan Geological Survey Miscellaneous Report 78-10, 25-34.

Ray, G.E. (1980) Compilation bedrock geology: Geikie River area (NTS 74H); in: Summary of Investigations 1980. Saskatchewan Geological Survey Miscellaneous Report 80-4, 10-12.

Ray, G.E. and Wanless, R.D. (1980) The age and geological history of the Wollaston, Peter Lake and Rottenstone domains in northern Saskatchewan. Canadian Journal of Earth Sciences, 17, 333-347.

Rimsaite, J.Y.H. (1977) Mineral assemblages at the Rabbit Lake uranium deposit, Saskatchewan: A preliminary report. Report of Activities, Part B, Geological Survey of Canada, Paper 77-1B, 235-246.

Robertson, D.A. and Lattanzi, C.R. (1974) Uranium deposits of Canada, Geoscience Canada, 1, 8-19.

Robertson, D.S., Tilsley, J.E. and Hogg, G.M. (1978) The time-bound character of uranium deposits. Economic Geology, 73, 1409-1419.

Romberger, S.B. (1984) Transportation and deposition of uranium in hydrothermal systems at temperatures up to 300°C: geological implications; in: DeVivo, B., Ippolito, F., Capaldi, G. and Simpson, P.R., eds., Uranium geochemistry, mineralogy, geology, exploration and resources. IMM, London, 12-17.

Rosner, B. (1970) Mikrosonden-Untersuchungen an naturlichen Gersdorffiten. Neues Jahrbuch fur Mineralogie Monatschefte, 483-498.

Ruhlmann, F. (1985) Mineralogy and metallogeny of uraniferous occurrences in the Carswell Structure; in: Laine, R., Alonso, D., and Svab, M., eds., The Carswell Structure Uranium Deposits, Saskatchewan. Geological Association of Canada, Special Paper 29, 105-120.

Ruzicka, V. (1986) Uranium deposits in the Rabbit Lake-Collins Bay area, Saskatchewan; in: Evans, E.L., ed., Uranium Deposits of Canada. The Canadian

Institute of Mining and Metallurgy, Special Volume 33, 144-154.

Ruzicka, V. and Le Cheminant, G.M. (1984) Uranium deposit research, 1983; in: Current Research, Part A, Geological Survey of Canada, Paper 84-1A, 39-51.

Ruzicka, V. and Le Cheminant, G.M. (1985) Summary on uranium in Canada, 1984; in: Current Research, Part A, Geological Survey of Canada, Paper 85-1A, 15-22.

Ruzicka, V. and Le Cheminant, G.M. (1986) Developments in uranium geology in Canada, 1985; in: Current Research, Part A, Geological Survey of Canada , Paper 86-1A, 531-540.

Ruzicka, V. and Le Cheminant, G.M. (1987) Uranium investigations in Canada, 1986; in: Current Research, Part A, Geological Survey of Canada, Paper 87-1A, 249-262.

Saracoglu, N., Wallis, R.H., Brummer, J.J. and Golightly, J.P. (1983) Discovery of the McClean uranium deposits; in: Cameron, E.M., ed., Uranium Exploration in Athabasca Basin, Saskatchewan, Canada. Geological Survey of Canada, Paper 82-11, 51-70.

Scott, B.P. (1973) Progress report on the geology of the Wollaston Lake belt. Saskatchewan Geological Survey Special Publication, 1, 80 p.

Short, M.N. and Shannon, E.V. (1930) Violarite and other rare nickel sulphides. American Mineralogist, 15, 1-22.

Sibbald, T.I.I. (1977) Uranium metallogenetic studies: I Rabbit Lake, geology; in: Summary of Investigations 1977. Saskatchewan Geological Survey, 111-123.

Sibbald, T.I.I. (1979) NEA/IAEA test area: basement geology; in: Summary of Investigations 1979. Saskatchewan Geological Survey Miscellaneous Report 79-10, 77-85.

Sibbald, T.I.I. (1983) Geology of the crystalline basement, NEA/IAEA Athabasca Test Area; in: Cameron, E.M., ed., Uranium Exploration in Athabasca Basin, Saskatchewan, Canada. Geological Survey of Canada, Paper 82-11, 1-14.

Sibbald, T.I.I., Munday, R.J.C. and Lewry, J.F. (1977) The geological setting of uranium mineralisation in northern Saskatchewan; in: Dunn, C.E., ed., Uranium in Saskatchewan. Saskatchewan Geological Society Special Publication, 3, 51-98.

Smith, D.G.W., Gold, C.M., Tomlinson, D.A. and Wynne, D.A. (1981) EDATA2. A FORTRAN IV programme for processing energy and/or wavelength dispersive data from microbeam instruments to give quantitative compositional results. Datum Geoservices, Edmonton, Alberta.

Smith, D.K.,jr. (1984) Uranium mineralogy; in: DeVivo, B., Ippolito, F., Capaldi, G. and Simpson, P.R., eds., Uranium mineralogy, Geology, Exploration and Resources. Institution of Mining and Metallurgy, 201p.

Snelling, A.A. (1980) A geochemical study of the Koongarra uranium deposit, Northern Territory, Australia. Unpublished Ph.D thesis, University of Sydney. 286 p.

Spooner, E.T.C. (1981) Fluid inclusion studies of hydrothermal ore deposits; in: Hollister, L.S. and Crawford, M.L., eds., Short Course in Fluid Inclusions:

Applications to Petrology. Mineralogical Association of Canada, 209-240.

Springer, G., Schachner-Korn, D. and Long, J.V.P. (1964) Metastable solid solution relations in the system FeS_2 -CoS_2-NiS_2. Economic Geology, 59, 475-491.

Spry, A. (1969) Metamorphic Textures. Pergamon Press, Oxford. 350 p.

Stauffer, M.R. (1984) Manikewan: an early Proterozoic ocean in central Canada, its igneous history and orogenic closure. Precambrian Research, 25, 257-281.

Steiger, R.H. and Jager, E. (1977) Subcommission on geochronology convention on the use of decay constants in geo- and cosmochronology. Earth and Planetary Science Letters, 36, 359-362.

Strnad, J.G. (1981) The evolution of Lower Proterozoic epigenetic stratabound uranium deposits (a concept); in: Geoinstitut Beograd, ed., Proceedings - 26th International Geological Congress, Paris, 1980. Section 13, 99-166.

Tilsley, J.E. (1980) Continental weathering and development of palaeosurface-related uranium deposits: some genetic considerations; in: Ferguson, J. and Goleby, A., eds., Uranium in the Pine Creek Geosyncline. IAEA, Vienna, 721-732.

Tona, F., Alonso, D. and Svab, M. (1985) Geology and Mineralisation in the Carswell Structure - A General Approach; in: Laine, R., Alonso, D. and Svab, M., eds., The Carswell Structure Uranium Deposits, Saskatchewan. Geological Association of Canada Special Paper 29, 1-18.

Tremblay. (1982) Geology of the Uranium Deposits related to the sub-Athabasca unconformity, Saskatchewan. Geological Survey of Canada, Paper 81-20.

Trocki, L.K., Curtis, D.B., Gancarz, A.J. and Banar, J.C. (1984) Ages of major uranium mineralisation and lead loss in the Key Lake uranium deposit, northern Saskatchewan, Canada. Economic Geology, 79, 1378-1386.

Tyrrell, J.B. and Dowling, D.B. (1896) Report on the country between Athabasca lake and Churchill river, with notes on two routes travelled between the Churchill and Saskatchewan rivers. Geological Survey of Canada Annual Report Vol VIII Part D, 1895, 54D-66D.

Van Schmus, W.R., Bickford, M.E., Lewry, J.F. and Macdonald, R. (1987) U-Pb geochronology of the Trans-Hudson Orogen, northern Saskatchewan, Canada. Canadian Journal of Earth Sciences, 24, 407-424.

Vaughan, D.J. (1969) Zonal variation in bravoite. American Mineralogist, 54, 1075-1083.

Vaughan, D.J. and Craig, J.R. (1978) Mineral Chemistry of Metal Sulphides. Cambridge University Press, Cambridge.

Vaughan, D.J. and Craig, J.R. (1985) The crystal chemistry of iron-nickel thiospinels. American Mineralogist, 70, 1036-1043.

Vaughan, D.J., Burns, R.G. and Burns, V.M. (1971) Geochemistry and bonding of thiospinel minerals. Geochemica et Cosmochemica Acta, 35, 365-381.

von Pechmann, E. (1985) Mineralogy of the Key Lake U-Ni ore bodies, Saskatchewan, Canada: evidence for their formation by hypogene hydrothermal processes; in:

Sibbald, T.I.I., and Petruk, W., eds., Geology of Uranium Deposits. The Canadian Institute of Mining and Metallurgy, Special Volume 32, 27-37.

von Pechmann, E., Hohndorf, A. and Voultsidis, V. (1984) Synmetamorphic uranium mineralisation in the Needle Lake-Keefe Lake area, Wollaston Fold Belt, Saskatchewan, Canada; in: Wauschkuhn, A., Kluth, C. and Zimmerman, R.A., eds., Syngenesis and Epigenesis in the Formation of Mineral Deposits. Springer-Verlag, Berlin, 160-169.

Voultsidis, V., von Pechmann, E. and Clasen, D. (1982) Petrography, mineralogy and genesis of the U-Ni deposits, Key Lake, Sask., Canada; in: Amstutz, G.C., El Goresy, A., Frenzel, G., Kluth, C., Moh, G., Wauschkuhn, A., and Zimmermann, R.A., eds., Ore Genesis — The State of the Art. Springer-Verlag Berlin Heidelberg, 469-490.

Wallis, R.H. (1971) The geology of the Hidden Bay area, Saskatchewan. Saskatchewan Department of Mineral Resources, Report No. 137, 1-76.

Wallis, R.H., Saracoglu, N., Brummer, J.J. and Golightly, J.P. (1983) Geology of the McClean Uranium Deposits; in: Cameron, E.M., ed., Uranium Exploration in Athabasca Basin, Saskatchewan, Canada. Geological Survey of Canada, Paper 82-11, 71-110.

Wallis, R.H., Saracoglu, N., Brummer, J.J. and Golightly, J.P. (1983) The geology of the McClean uranium deposits, northern Saskatchewan; in: Sibbald, T.I.I. and Petruk, W., eds., Geology of Uranium Deposits. Canadian Institute of Mining and Metallurgy, Special Volume 32, 101-131.

Wallis, R.H., Saracoglu, N., Brummer, J.J. and Golightly, J.P. (1986) The geology of the McClean uranium deposits, northern Saskatchewan; in: Evans, E.L., ed., Uranium Deposits of Canada. The Canadian Institute of Mining and Metallurgy, Special Volume 33, 193-217.

Watkinson, D., Heslop, J.B. and Ewert, W.D. (1975) Nickel sulphide-arsenide assemblages associated with uranium mineralization, Zimmer Lake area, northern Saskatchewan. Canadian Mineralogist, 13, 198-204.

Weber, W. and Scoates, R.F.J. (1978) Archean and Proterozoic metamorphism in the northwestern Superior Province and along the Churchill-Superior boundary, Manitoba; in: Fraser, J.A. and Heywood, W.W., eds., Metamorphism in the Canadian Shield. Geological Survey of Canada, Paper 78-10, 5-16.

Wickman, F.E. and Khattab, K.M. (1972) Non destructive activation of fluid inclusions in fluorite. Economic Geology, 67, 236-239.

Williams-Jones, A.E. and Sawiuk, M.J. (1985) The Karpinka Lake uranium deposit, Saskatchewan: A possible metamorphosed Middle Precambrian sandstone-type uranium deposit. Economic Geology, 80, 1927-1941.

Willis, B.T.M. (1978) The defect structure of hyper-stoichiometric uranium oxide. Acta crystallogr. A34, 88-90.

Wilson, J.A. (1985) Geology of the basement beneath the Athabasca Basin in Alberta. Alberta Research Council Bulletin No. 55, 61 p.

Worden, J.M., Cumming, G.L. and Baadsgaard, H. (1985) Geochronology of host

rocks and mineralisation of the Midwest uranium deposits, northern Saskatchewan; in: Sibbald, T.I.I. and Petruk, W., eds., Geology of Uranium Deposits. Canadian Institute of Mining and Metallurgy, Special Volume 32, 67-72.

Wray, E.M., Ayres, D.E. and Ibrahim, H.J. (1985) Geology of the Midwest uranium deposit, northern Saskatchewan; in: Sibbald, T.I.I. and Petruk, W., eds., Geology of Uranium Deposits. Canadian Institute of Mining and Metallurgy, Special Volume 32, 54-66.

Yund, R.A. (1962) The system Ni-As-S: phase relations and mineralogical significance. American Journal of Science, 260, 761-782.

VIII. APPENDIX I

Bismuthian gersdorffites from the 334 Pod, 11A Zone, Dawn Lake, Saskatchewan, Canada.

by

E.C.R. Persaud, R.D. Morton and S. Launspach

Department of Geology

University of Alberta

Edmonton, Alberta

A. Abstract

Bismuthian gersdorffite, with an ideal composition of $Ni(As_{0.99}Bi_{0.10})S$, occurs in the 11A Zone of the Dawn Lake uranium-nickel deposit of northern Saskatchewan, Canada. Electron microprobe analyses of gersdorffites are presented, together with observations on colour, spectral-reflectance and hardness. Previous studies of the U-Ni deposits of the unconformity-associated type may have overlooked the presence of bismuthian gersdorffite, due to the fact that it is indistinguishable during routine reflected-light microscopy. This paper emphasizes the value of automated, quantitative spectral-reflectance data acquisition in the study of such minerals.

Keywords : Mineralogy, Uranium Deposit, Gersdorffite, Saskatchewan

B. Introduction

A number of unconformity-associated uraniferous deposits of polymetallic character are distributed within the eastern Cree Lake Zone of the Manikewan (Trans-Hudsonian) mobile belt of northern Saskatchewan, Canada (Fig. AI-1).

During a detailed investigation of the Dawn Lake deposit, gersdorffite with an unusual composition of $Ni(As_{0.90}Bi_{0.10})S$ was observed (as grain cores or as oscillatory growth-zones) within nickeliferous sub-zones, associated with uranium mineralization from the 334 Pod of the 11A Zone. Such bismuthian gersdorffites have hitherto not been recorded and thus it is our intent to augment the existing data on this sulpharsenide mineral and to point out that it might easily have been overlooked in other studies.

Unfortunately, the extremely small grain- and zone-sizes of the bismuthian gersdorffites did not permit the acquisition of X-ray diffraction data. Thus optical and chemical data alone are presented herein, together with an hypothesis on the genesis of this unusual (?) bismuthian sulpharsenide.

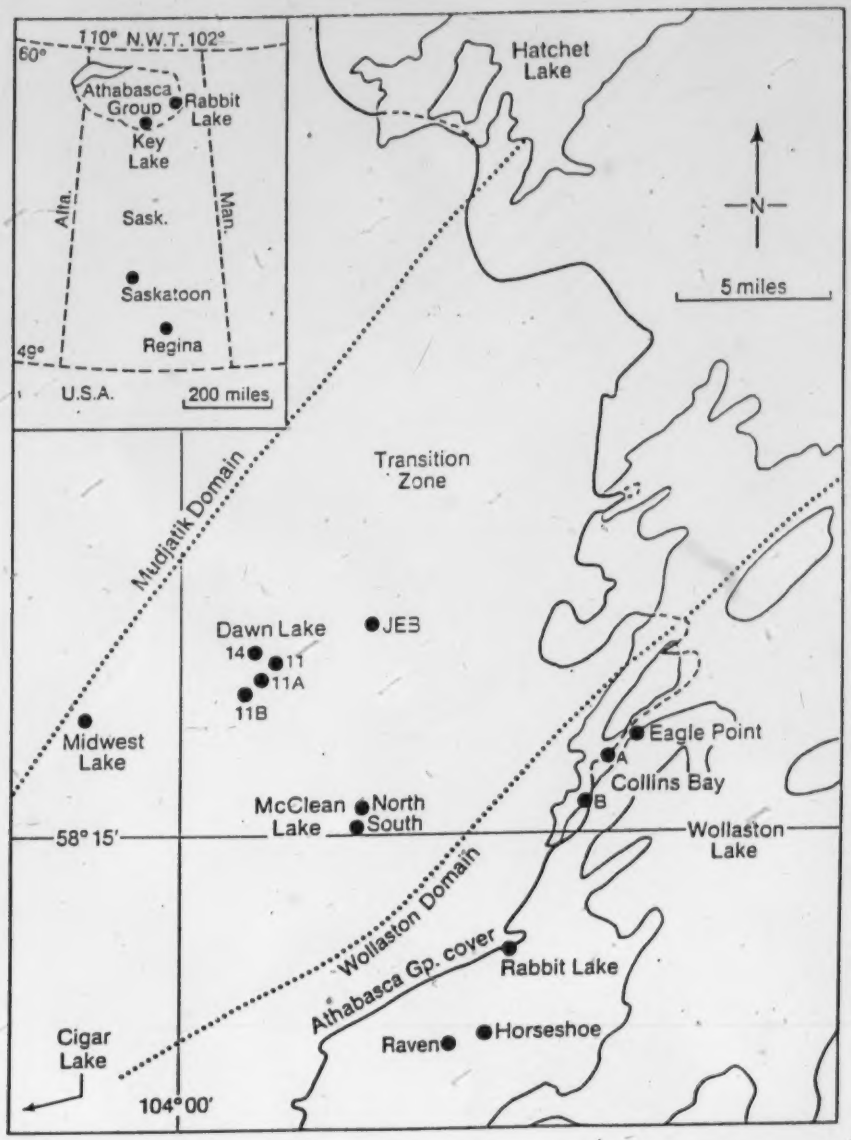

Figure AI-1. Location map of the Dawn Lake deposit.

C. Geological Setting

The Dawn Lake unconformity-associated deposits are situated within the Middle Proterozoic Athabasca Basin, some 340 kilometres north of La Ronge, Saskatchewan. The deposits lie to the east, northeast, northwest and southwest, respectively, of the Midwest Lake, Cigar Lake, McClean Lake and JEB deposits; see Figure AI-1.

Four zones of uraniferous mineralization, (namely, the 14, 11, 11A and 11B zones), have been discovered on the Dawn Lake property (Clarke and Fogwill, 1985). Uranium mineralization in the 14 Zone is restricted to Helikian Athabasca Group sediments, whilst the 11 Zone occurs mainly at the Athabasca Group/Basement (Wollaston Group) unconformity. The 11A Zone is also found at the unconformity plane and in pods within basement metasediments of the Wollaston Group, whilst the 11B Zone occurs entirely within basement metasediments. Sulpharsenide mineralization associated with the uranium mineralization in the 334 Pod, which occurs in the basement suite of the 11A Zone, is the topic of discussion for this paper.

D. Host Lithologies

At Dawn Lake, approximately 100 metres of Helikian (Middle Proterozoic), Athabasca Group sandstones and quartz-pebble conglomerates overlie Aphebian (Lower Proterozoic), Wollaston Group, calcareous, pelitic and psammitic metasediments, cut by anatectic pegmatoids (Clarke and Fogwill, 1985). Below the Athabasca Group-Wollaston Group unconformity, a paleo-weathering profile or regolith has developed on the Wollaston Group metamorphic suite. This regolith consists of fine-grained assemblages of quartz, clays, chlorite and hematite (Macdonald, 1985). Replacive silica is locally present.

In the 11A Zone, the local metamorphic suite conatins the following rock units (Fig. AI-2):

(i) graphitic quartz-chlorite-feldspar gneiss (metasiltstone?)

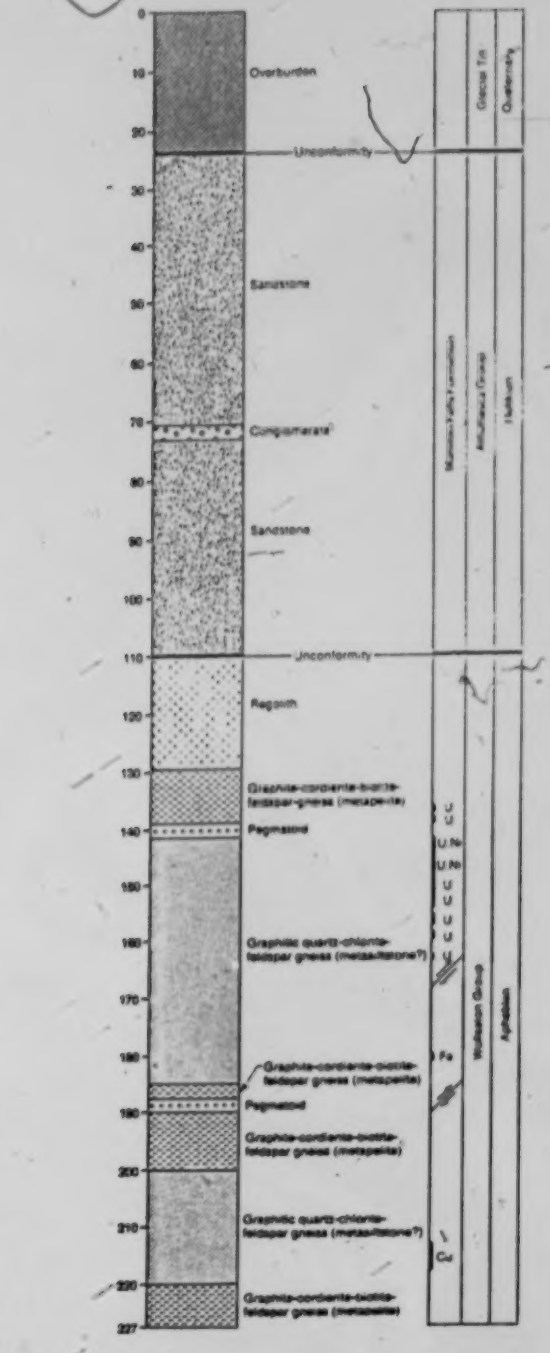

Figure AI-2. Stratigraphic section of Diamond Drill Hole #334 at Dawn Lake.

(ii) graphite-cordierite-biotite-feldspar gneiss (metapelite)

(iii) anatectic-pegmatoids.

E. The graphitic quartz-chlorite-feldspar gneiss (metasiltstone?)

The graphitic quartz-chlorite-feldspar gneiss unit hosts the bulk of the uranium- and nickel-mineralization in the 334 Pod. It also hosts chalcopyrite mineralization, 50 metres below the 334 Pod. This rock is typically fine- to medium-grained, banded and well-foliated. It is composed mainly of quartz, feldspars (microcline, plagioclase) and chlorite. Graphite occurs in amounts of up to 10% modal. Accessory minerals are tourmaline (vars., dravite and schorl), epidote (var. pistacite), anatase and rutile. In the vicinity of uranium-nickel mineralization, all the feldspars have been sericitized. Deeper in the section, K-feldspar is partially altered, whilst plagioclase is almost totally destroyed. In mineralized areas graphite is totally destroyed and carbonate veins are common.

F. The graphite-cordierite-biotite-feldspar gneiss (metapelite)

The graphite-cordierite-biotite-feldspar gneiss hosts little of the uranium-nickel mineralization. This rock-type is dark-grey in hand specimen, fine- to medium-grained and well-foliated. The major minerals in this metapelitic unit are quartz (25-30%), feldspar (30-40%), biotite (15-20%), cordierite (5-10%) and graphite (5-10%). Accessory minerals are tourmaline (var. dravite) and rutile.

The regolith has developed principally on this basement lithology. In the regolith, all primary minerals except quartz have been destroyed, whilst pyrite and marcasite have been formed. Immediately below the regolith and above the uranium-nickel mineralization, this metapelitic unit is intensely altered. Plagioclase is totally sericitized, the cordierite is highly pinitized and the biotite chloritized. Deeper in the section, away from mineralization, plagioclase is highly sericitized, the cordierite partially pinitized and the biotite relatively fresh.

G. The anatectic-pegmatoids

Two types of anatectic pegmatoids of Hudsonian age have been recognized in drill core. The first are thin, segregation pegmatoids, usually a few centimetres thick, occurring in metapelitic rocks (Clarke and Fogwill, 1985). The second variety which may be intrusive, is generally several metres thick and is coarser-grained (Fig. AI-2). This second variety hosts some of the uranium mineralization. Both pegmatoid types characteristically exhibit relatively conformable contacts with the enclosing metasedimentary rocks and have essentially the same composition. They are composed of feldspars (plagioclase, K-feldspar), quartz and tourmaline (var. schorl). In the regolith, the pegmatoid rocks retain their original textures, although quartz is the only remaining primary mineral.

H. Structure

The Wollaston Group basement suite was folded during the Hudsonian orogeny and underwent upper amphibolite facies regional metamorphism (Lewry and Sibbald, 1977, 1980; Lewry et al., 1978). The major fold axes trend NE-SW, with later cross-folds trending ENE-WSW (Lewry et al., 1978; Lewry and Sibbald, 1980).

In the Dawn Lake area a major fault direction NE-SW parallels the strike of the basement stratigraphy (Clarke and Fogwill, 1985). Other fault directions are ENE-WSW (often with thrust components), N-S (related to the Tabbernor fault system) and NW-SE (associated with diabase dykes), (McNutt, 1982; Clarke and Fogwill, 1985). All these faults cut the cover of Athabasca Group rocks. It is believed that the NE-SW and ENE-WSW trending faults reactivated pre-Athabasca Group faults, whilst those trending N-S and NW-SE post-date the Athabasca Group cover (McNutt, 1982; Clarke and Fogwill, 1985).

In the 11A Zone, the basement metamorphic rocks strike N40°E and dip steeply northwest. Compositional layering and foliation are essentially parallel in these rocks (Clarke and Fogwill, 1985). The 334 Pod of U-Ni mineralization occurs at the

intersection of a major fault trending N40°E and a minor cross-fault trending N70°E.

I. Mineralization

The 334 Pod of uranium-nickel mineralization occurs principally within sericitized or illitized quiartz-chlorite-feldspar rocks, below the base of the regolith. Mineralization appears in part to be fault-controlled (Fig. AI-2).

Arsenides (rammelsbergite, safflorite and nickeline along with sulpharsenides (gersdorffite, cobaltite) appear to constitute the earliest phases of the paragenesis. Pitchblende I and later sulpharsenides (gersdorffite, cobaltite and bismuthian gersdorffite) completed Stage I mineralisation.

Pitchblende II and minor sulphides (millerite, pyrite, bravoite, violarite, chalcopyrite, galena and sphalerite) comprise a second paragenetic stage. A final phase consisted of pitchblende III, galena and an unidentified copper sulphide mineral. In addition a Bi-Te mineral is intergrown with pitchblende I, whilst gold with traces of silver and a Bi-Te phase are present in pitchblende II. Illite-chlorite alteration accompanied Stage I and Stage II mineralisation. Hematite accompanied Stage II whilst calcite was coeval with Stage III of the paragenesis.

J. Chemical Analytical Methods

Samples were analyzed utilizing an ARL-SEMQ electron microprobe, equipped with an Ortec energy dispersive spectrometer. Operating conditions were an accelerating voltage of 15 kv and a probing current of 3.3 nA. Counting times were 240 s for both standards and samples.

Qualitative energy dispersive scans were used to examine areas of interest located by petrographic studies and to pinpoint areas for analyses. Analyses were then performed by wavelength dispersive techniques.

Bismuthian gersdorffite samples were analyzed for S, Fe, Co, Ni, As, Sb, Pb and Bi. Gersdorffite samples were analyzed for S, Fe, Co, Ni, As, Sb and Bi. The

analytical X-ray lines used were Ka (S, Fe, Co, Ni), La (As, Sb) and Ma (Pb, Bi). The following standards were used: arsenopyrite (S, Fe, As), pure cobalt (Co), pararammelsbergite (Ni), pure antimony (Sb), galena (Pb) and pure bismuth (Bi).

Reduction of wavelength-dispersion data was carried out using the EDATA2 computer program (Smith et al., 1981). The detection limits for the operating conditions used were determined to be 0.01 wt.% for S, Fe, Co, As and Pb;).02 wt.% for Ni and Sb; and 0.05 wt.% for Bi.

K. Bismuthian Gersdorffite

Gersdorffite has the stoichiometric composition of NiAsS. Significant amounts of cobalt and iron may substitute for nickel, and sulphur and arsenic may be mutually diadochic (Yund, 1962; Klemm, 1965; Rosner, 1970; Petruk et al., 1971; Paar and Chen, 1979; Bayliss, 1982; Changkakoti and Morton, 1986). Minor amounts of antimony may also substitute for arsenic (Yund, 1962; Paar and Chen, 1979; Bayliss, 1982; Changkakoti and Morton, 1986). The presence of bismuth in the gersdorffite structure, however, has hitherto not been reported. Gersdorffite from the 334 Pod at Dawn Lake (11A Zone) occurs as massive aggregates, as fillings within shrinkage-cracks cutting pitchblendes, as subhedral or brecciated grains and as discrete, idiomorphic crystals. Growth zones of Bi-rich gersdorffite were accidentally discovered during routine electron microprobe investigation of gersdorffites which appeared to be totally homogenous when viewed under a reflected-light microscope, using both normal and Nomarsky Phase Interference Contrast techniques. The zonal Bands, ranging from less than 1 to 10 mm in thickness, were revealed by marked contrast in images obtained during back-scattered electron (BSE) data acquisition (Fig. AI-3). This contrast is a function of the difference in the average atomic number (Z) between bismuthian gersdorffite (Z=33-36) and the neighbouring normal gersdorffite (Z=28-29). An individual growth zone was, in some cases, seen to be actually comprised of several bands of bismuthian gersdorffite. Bismuthian gersdorffite was seen to be selectively

Figure AI-3(a). Backscattered electron image showing zonational growth bands of Bi-gersdorffite (white) in normal gersdorffite (grey), Dawn Lake. 5μm scale shown.

Figure AI-3(b). Bi X-ray image showing Bi concentrated in the Bi-gersdorffite zonational growth-bands within normal gersdorffite from Dawn Lake.

Figure AI-3(c). X-ray image showing distribution of As in the gersdorffite from Dawn Lake. (Ni and S X-ray images show almost identical patterns).

Figure AI-3(d). Co X-ray image showing zonation of cobalt in gersdorffite from Dawn Lake. Cobalt increases from the centre of inner normal gersdorffite towards Bi-gersdorffite growth-bands and decreases outwards from Bi-gersdorffite growth-bands.

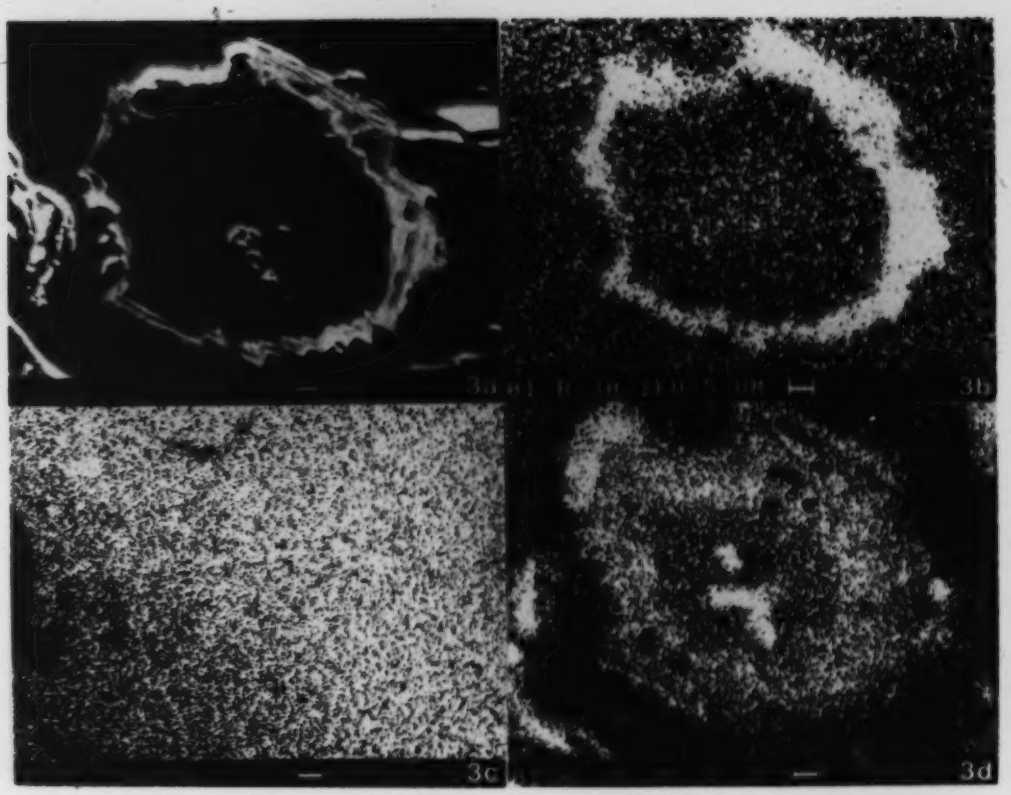
3b
3c
3d

replaced by pitchblende III (Fig. AI-4a).

The commonly observed generalized zonational sequence from core outwards was: gersdorffite (core) - bismuthian gersdorffite - gersdorffite (rim) - gangue - gersdorffite (outer zone) - gangue (fig. AI-3). The chemical zonation of the first three phases of this sequence is given in outer-zone gersdorffites contained no detectable bismuth (Table AI-1).

In a rare occurrence, the observed zonational sequence from core outward was: nickelian cobaltite (core) - bismuthian gersdorffite - nickelian cobaltite (rim) - gangue - nickelian cobaltite (outer zone) - gangue - gersdorffite - gangue; see Fig. AI-4c.

Bismuth concentrations in the bismuthian gersdorffites range from 8.75 wt.% to 14.53 wt.% (Table AI-1). A plot of the atomic percentages of (Sb+Bi) versus (S+As) suggests an inverse relationship between these element sums (Fig. AI-5). Sulphur and arsenic are increasingly proxied by antimony and bismuth, the latter being by far the major diadochic partner in this substitution. For bismuthian gersdoorffites, with bismuth concentrations ranging from 8.75 wt.% to 12.02 wt.%, cobalt cobalt concentrations varied from 0.79 to 1.26 wt.%, nickel from 30.31 to 30.90 wt.%, arsenic from 39.17 to 41.05 wt.% and sulphur from 15.17 to 16.60 wt.%. Minor amounts of lead up to a maximum of 0.39 wt.% were observed. Qualitative scans of bismuth-rich bands, using an energy dispersive system, indicated regions of higher cobalt concentration. Analysis of one of these regions revealed the highest cobalt (3.38 wt.%), bismuth (14.53 wt.%) and sulphur (17.69 wt.%) concentrations observed to date. This sample also possessed the lowest arsenic concentration (27.23 wt.%).

The average structural formula for the bismuthian gersdorffites with bismuth concentrations between 8.75 and 12.02 wt.% was found to be:

$$(Fe_{0.01}, Co_{0.03}, Ni_{0.96})\ As_{0.99}\ Bi_{0.09}\ S_{0.92}$$

The structural formula for bismuthian gersdorffite with a bismuth content of 14.53 wt.% was:

Table AI-1: Chemical composition of bismuthian gersdorffites (in wt %) from the 11A Zone, Dawn Lake.

	Fe	Co	Ni	As	Sb	Bi	Pb	S	Total
	----	----	35.40	45.20	----	----	----	19.40	100.00
1)	0.17	0.97	30.97	41.05	0.18	8.75	0.01	16.41	98.51
2)	0.12	0.90	30.90	40.80	0.32	9.52	0.07	16.60	99.23
3)	0.24	1.11	30.55	40.46	0.48	9.78	0.39	16.18	99.19
4)	0.24	0.79	30.31	40.34	0.20	11.39	ND	15.17	98.44
5)	0.14	0.95	30.90	39.17	0.34	11.75	0.20	16.21	99.66
6)	0.17	1.26	30.40	40.76	0.29	12.02	0.34	15.92	101.19
7)	0.18	3.38	27.23	36.49	0.48	14.53	ND	17.69	99.98
	Atomic composition on the basis of Fe+Co+Ni+As+Sb+Bi+Pb+S = 3.0								
	----	----	1.00	1.00	----	----	----	1.00	
1)	0.01	0.03	0.96	0.99	0.00	0.08	0.00	0.93	
2)	0.00	0.03	0.96	0.99	0.00	0.08	0.00	0.94	
3)	0.01	0.03	0.95	0.99	0.01	0.09	0.00	0.92	
4)	0.01	0.02	0.97	1.01	0.00	0.10	ND	0.89	
5)	0.00	0.03	0.97	0.96	0.01	0.10	0.00	0.93	
6)	0.01	0.04	0.94	0.99	0.00	0.10	0.00	0.91	
7)	0.01	0.10	0.85	0.89	0.01	0.13	ND	1.01	

Figure AI-4(a). Backscattered electron image showing bismuthian gersdorffite (code: bg; grey) selectively replaced by pitchblende III (code: p3; grey); p1 is pitchblende I, Dawn Lake.

Figure AI-4(b). Backscattered electron image of euhedral growth bands of bismuthian gersdorffite (code: bg; white) in normal gersdorffite (code: g; grey), Dawn Lake.

Figure AI-4(c). Backscattered electron image showing relationships between nickelian cobaltite (code: c; grey), bismuthian gersdorffite (code: bg; white) and normal gersdorffite (code: g; white), Dawn Lake.

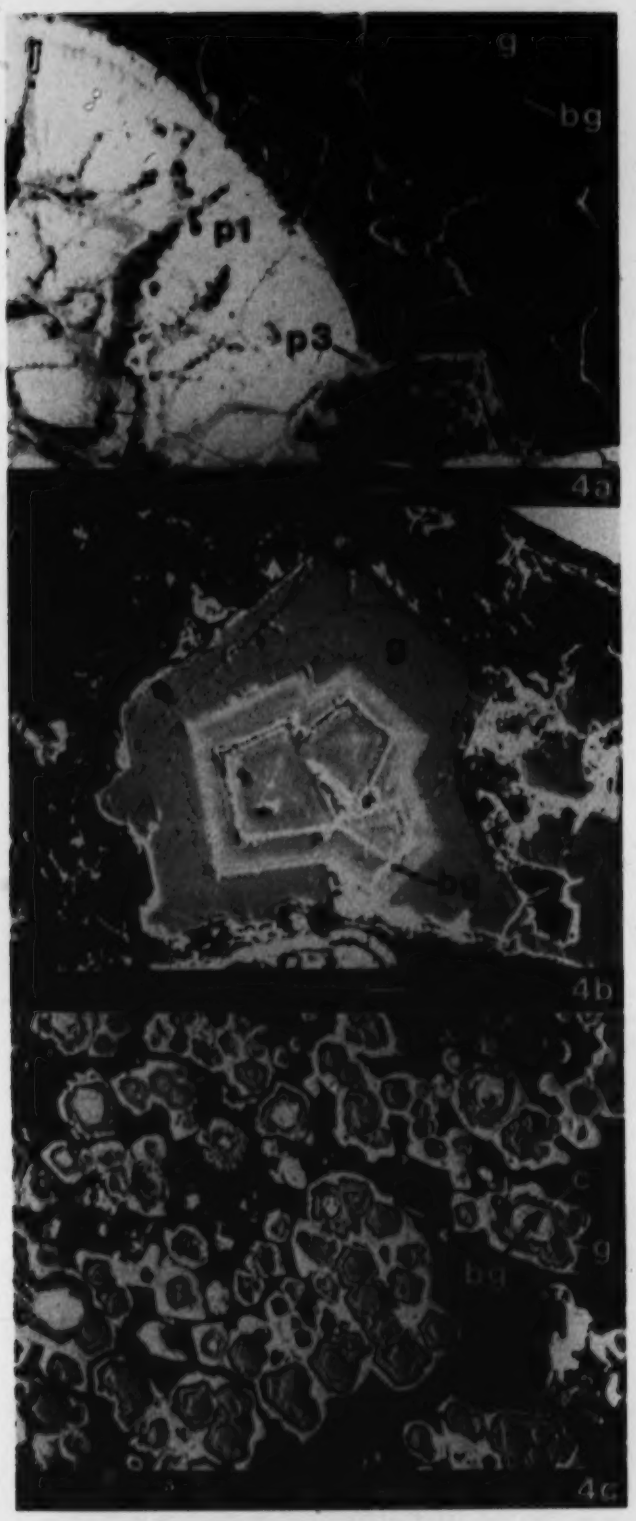
g
bg
p1
p3
4a
bg
4b
g
bg
4c

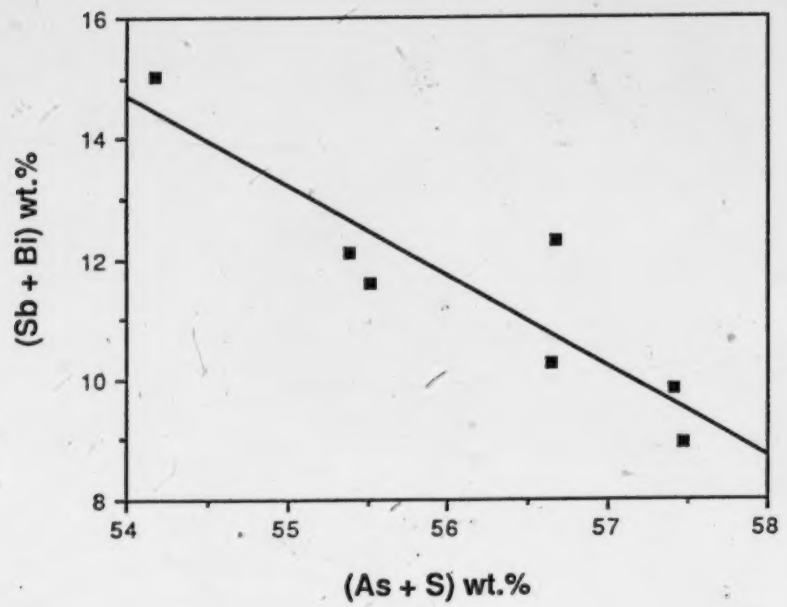

Figure AI-5. Plot of atomic percentages of (Sb + Bi) versus (S + As) in bismuthian gersdorffites from Dawn Lake.

$(Fe_{0.01}, Co_{0.10}, Ni_{0.85})\ (As_{0.89}\ Sb_{0.01})\ Bi_{0.13}\ S_{1.01}$

The ideal structural formula of bismuthian gersdorffite thus appears to be:

$Ni(As_{0.90}\ Bi_{0.10})S.$

L. The colour, reflectance and hardness of Bi-gersdorffites

During the course of this study it was verified that bismuthian gersdorffites were indistinguishable from normal (non-bismuthian) gersdorffites when examined under the reflected-light microscope. The use of Nomarsky Phase Interference Contrast techniques was also ineffective, thus inferring that there is little or no difference in the polishing hardness of the two varieties. One would thus anticipate that bismuthian gersdorffites would have a normal range of VHN_{100g} of 782 to 835 (data of IMA/COM, 1977). As part of our routine identification/verification procedure in the laboratory, we employed a counter-controlled, automated microphotometric device to examine the various types of gersdorffite in the Dawn Lake suite. During this phase of the work, we discovered that bismuthian gersdorffites exhibit distinct spectral reflectance in the visible-light range.

Our system, a NISOMI-model 84_{TM} device (similar to that described by Atkin and Harvey, 1982) is composed of a quartz-halogen light source and a servo-driven, $ORIEL_{TM}$ grating-monochromator, controlled by a $RADIO\ SHACK_{TM}$ Model IV 64K RAM microcomputer with a $WILSCAN_{TM}$ interference. Reflectance data for 16 wavelengths at 20 nm intervals between 400 and 700 nm are gathered and chromaticity coordinates (x and y), together with luminance (Y), are calculated in accordance with the system of the Commission Internationale d'Eclairage (CIE), as described by Atkin and Harvey (1979). The NISOMI-84 system also computes values for the dominant wavelength (dl), the saturation purity (Pe%) and the luminance (Y). These latter three data sets enable proper quantification of the colour of a given mineral phase.

Table AI-2 presents the colour data for some gersdorffites from the Dawn Lake deposit. The standard utilized during data acquisition was a Carl Zeiss SiC crystal

whose reflectances are also presented in Table AI-2. Owing to the inability of the operators to distinguish bismuthian gersdorffite domains from bismuth-poor domains under the microscope, we located them by using BSE imagery and performed measurements on sectors with analyzed high-bismuth contents. We were unable to confine our data collection exactly to bismuthian gersdorffite, due to their small areas. However, the data of column 1 in Table AI-2 do refer to domains with a preponderance of bismuthian gersdorffite in the measured field. In the case of non-bismuthian gersdorffites, we were able to select larger domains of pure gersdorffite for optical analyses.

The data of Table AI-2 clearly illustrate that the substitution of Bi in the gersdorffite lattice induces colour changes, which are at maxima in the red and blue ends of the visible spectrum. Thus the human eye, which is relatively ineffective as a detector in these end ranges, will not detect this effect. From our data we can also conclude that the substitution of Bi in gersdorffite has:

(i) little effect upon reflectance of light in the mid-range of the visible spectrum (540-560 nm).

(ii) maximum effects upon reflectance at the blue (470 nm) and red (650 nm) ends of the visible spectrum.

(iii) the effect of changing the colour of gersdorffite from a monotone grey (with no dominant primary colour and a low saturation purity) to a mineral with an orange tint and a much higher saturation purity.

The spectral reflectance curves of Fig. AI-6 are provided to illustrate the aforesaid effects and to provide comparative data for future investigators. In the diagram the spectral reflectance curve for our bismuthian gersdorffites must be qualified by th realization that they represent mildly-mixed data. Thus one can anticipate that the true reflectance curve for bismuth-rich gersdorffite, at the maximum substitutional level, would have limits defined by:

Table AI-2: Quantitative colour and reflectance data for gersdorffites.

Gersdorffite variety:		1		2		3		4
Data class		Mean	Range	Mean	Range	Mean	Range	--
Dominant wavelength(dλ)		--	575.6-580.3	--	463.0-574.5	--	475.6-580.8	
Saturation Purity(Pe%)		--	2.2-3.8	--	0.1-1.5	--	0.1-1.7	
Luminance(Y)		46.5	46.5-47.4	46.4	45.3-47.4	46.4	45.1-47.5	
	x	0.315	0.314-0.317	0.310	0.307-0.313	0.310	0.308-0.313	--
Trichromatic coefficients	y	0.322	0.320-0.324	0.317	0.314-0.320	0.316	0.314-0.320	--
$R_{(air\ @\ 470\ nm)}\%$		44.8	43.6-46.1	46.4	45.1-48.4	46.5	44.8-47.4	21.8
$R_{(air\ @\ 546\ nm)}\%$		46.4	45.6-47.5	46.4	45.3-47.2	46.4	45.2-47.6	21.0
$R_{(air\ @\ 589\ nm)}\%$		47.1	46.1-47.9	46.3	45.4-47.3	46.4	44.9-48.0	20.8
$R_{(air\ @\ 650\ nm)}\%$		47.4	47.0-48.0	46.3	45.2-47.7	46.4	45.6-48.7	20.5

1. Gersdorffite domains with dominant Bi-gersdorffite and subordinate normal gersdorffite, 11A Zone, Dawn Lake.
2. Larger, anhedral, normal gersdorffite grains, 11A Zone, Dawn Lake
3. Subhedra, normal gersdorffite grains, 11A Zone, Dawn Lake
4. SiC (Carl Zeiss Standard #474281-080)

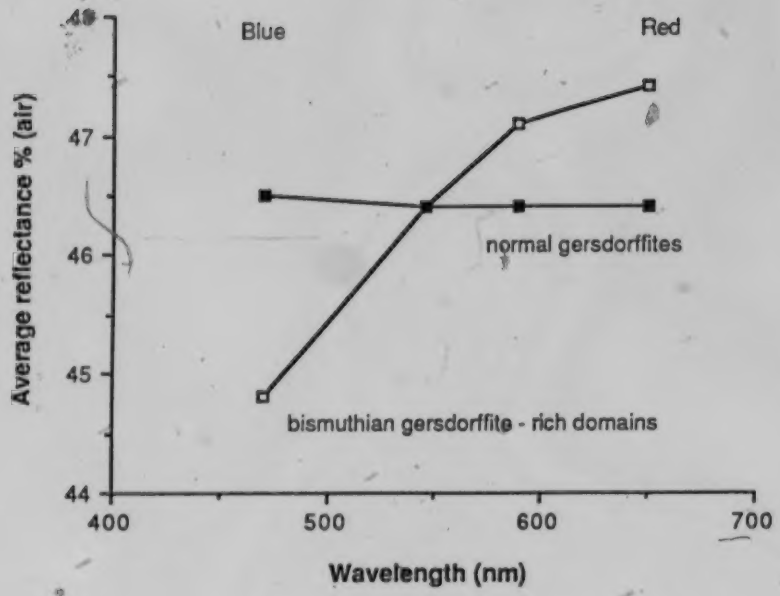

Figure AI-6. Spectral reflectance curves of dominantly bismuthian gersdorffite domains and anhedral normal gersdorffite from Dawn Lake.

R_{air} @ 470 nm < 43.6% and R_{air} @ 650 nm > 48.0%.

M. Conclusions

Gersdorffite, a commonplace component of the arsenide suites of unconformity-associated, uranium-nickel deposits has been shown to exhibit a wider degree of compositional variation than hitherto observed. Such major compositional variants of these minerals could often pass undetected in casual petrographic investigations employing the reflected-light microscope. They would normally only be found accidentally when the electron microprobe is used as a qualitative petrographic tool in its energy-dispersive mode, or when analysis of beneficiation fractions reveal anomalous element concentrations. Routine spectral-reflectance data acquisition, during petrographic investigation of ores, is clearly a less-costly method of augmenting visual observations. The use of computer-controlled, automated reflectance-measuring systems, such as NISOMI-84$_{TM}$, clearly facilitates the procedures and is thus strongly advocated.

Bismuthian gersdorffite appears to have the ideal formula Ni $(As_{0.90}\ Bi_{0.10})S$. Departures from this formula are due to substitution of arsenic for sulphur, lead for bismuth, antimony for arsenic, and iron and cobalt for nickel. The mineral association and ore textures suggest that bismuthian gersdorffite at Dawn Lake was deposited by a series of bismuth-enriched hydrothermal fluid pulses over a short period of time, during a phase of activity which otherwise saw the deposition of gersdorffite and cobaltite.

N. Acknowledgements

The authors would like to express their sincere thanks to the Saskatchewan Mining and Development Corporation and to Asamera for their kind assistance in this project and for permission to publish the results of this study. In particular we are indebted to Dr. P.J. Clarke and Dr. H. Ibrahim for their guidance during the collection

phase of the study. Dr. D.G.W. Smith is also thanked for permitting the extensive use of his N.S.E.R.C.-funded electron microprobe facilities and for his long-term efforts in the development of software for the treatment of analytical data. During the course of the study Dr. A. Changkakoti offered invaluable help and encouragement.

O. References

Atkin, B.P. and Harvey, P.K. (1979): The use of quantitative colour values for opaque-mineral identification. - Can. Miner. 17, 639-647.

—— and —— (1982): NISOMI-81: An automated system for opaque-mineral identification in polished section. In: Process Mineralogy II: Applications in Metallurgy, Ceramics, and Geology (R.D. Hagni, ed.). - Symposium proceedings of the Process Mineralogy Committee of the Metallurgical Society of AIME, Dallas, Texas, February 1982.

Bayliss, P. (1982): A further crystal structure refinement of gersdorffite. - Am. Mineral 67, 1058-1064.

Changkakoti, A. and Morton, R.D. (1986): Electron microprobe analyses of native silver and associated arsenides from the Great Bear Lake silver deposits, Northwest Territories, Canada. Can. Jour. Earth Sci. 23, 1470-1479.

Clarke, P.J. and Fogwill, W.D. (1985): Geology of the Dawn Lake uranium deposits, northern Saskatchewan. In: Geology of Uranium Deposits (T.I.I. Sibbald and W. Petruk, eds.). Proceedings of the CIM-SEG Uranium Symposium, September 1981. - CIM Special Volume 32, 132-139.

Klemm, D.D. (1965): Synthesen und Analysen in den Dreieckdiagram FeAsS-CoAsS-NiAsS und FeS_2-CoS_2-NiS_2. - N. Jb. Miner. Abh. 103, 205-255.

IMA/COM Quantitative Data File (1977): First Issue, International Mineralogical Association, Commission on Ore Microscopy, McCrone Research Associates, London.

Lewry, J.F. and Sibbald, T.I.I., 1977: Variation in lithology and tectonometamorphic relationships in the Precambrian basement of northern Saskatchewan. - Can. J. Earth Sci. 14, 1453-1467.

—— and —, 1980: Thermotectonic evolution of the Churchill Province in northern Saskatchewan. - Tectonophysics 68, 45-82.

——, Sibbald, T.I.I. and Rees, C.J., 1978: Metamorphic patterns and their relation to tectonism and plutonism in the Churchill Province in northern Saskatchewan. In : Metamorphism in the Canadian Shield. - Geol. Surv. Can. paper 78-10, 139-154.

Macdonald, C.C. (1985): Mineralogy and geochemistry of the sub-Athabasca regolith near Wollaston Lake. In: Geology of Uranium Deposits (T.I.I. Sibbald and W. Petruk, eds.). Proceedings of the CIM-SEG Uranium Symposium, September 1981. - CIM Special Volume 32, 155-158.

McNutt, A. (1982): Geological investigations of the 11B Zone - 284 Pod. - Internal report. Saskatchewan Mining Development Corporation.

Paar, W.H. and Chen, T.T., 1979: Gersdorffit (in zwei Strukturvarietaten) und

Sb-haltiger Parkerit, $Ni_3(Bi,Sb)_2S_2$, von der Zinkwand, Schladminger Tauern, Osterreich. - Tschermaks Min. Petr. Mitt. 26, 59-67.

Petruk, W., Harris, D.C., and Stewart, J.M. (1971): Characteristics of the arsenides, sulpharsenides, and antimonides. - Can. Miner. 11, 150-186.

Rosner, B. (1970): Mikrosonden-Untersuchungen an naturlichen Gersdorffiten. - N. Jb. Miner. Mh., 483-498.

Smith, D.G.W., Gold, C.M., Tomlinson, D.A., and Wynne, D.A. (1981): EDATA2. A FORTRAN IV programme for processing energy and/or wavelength dispersive data from microbeam instruments to give quantitative compositional results. - Datum Geoservices, Edmonton, Alberta..

Yund, R.A. (1962): The system Ni-As-S: phase relations and mineralogical significance. - Am. J. Sci. 260, 761-782.

IX. APPENDIX II

Chemical age theory and methods of determination

by

E.C.R. Persaud, R. Persaud and R.D. Morton

Department of Geology

University of Alberta

Edmonton, Alberta

A. Introduction

The ages of uranium- and/or thorium-bearing minerals are usually determined via conventional U-Th-Pb isotope analyses. However, with the common use of the electron microprobe in routine mineralogical studies of rocks and ore-deposits today, the researcher often has at hand analytical data on major element concentrations which can, by simple computation, provide valuable first order information on the approximate ages of uraniferous phases, i.e., by the calculation of the so-called 'chemical ages'. Such initial estimates of the ages of phases can be a useful addendum to the mineralogical data and can assist in the cost-efficient establishment of the framework of a paragenetic framework of events. A number of publications in recent years have discussed chemical ages calculated for Canadian uraniferous deposits (Cameron-Schimann, 1978; Pagel and Ruhlmann, 1985; Parslow *et al.*, 1985; Ruhlmann, 1985).

Chemical apparent age determinations require computation of the atomic concentrations of U, Th and Pb in their minerals. The accuracy of the chemical-age method is dependent upon the following assumptions: (i) all the Pb in the mineral is of radiogenic origin and (ii) the isotope/chemical system has remained closed since the formation of the mineral.

Chemical ages of thorian uraninites have previously been published from Baie Johan Beetz, Quebec and from Charlebois Lake, Saskatchewan by Cameron-Schimann, (1978). Thorian uraninites and other uranium- and/or thorium-bearing minerals in anatectites from the Cree Lake Zone of Saskatchewan were chemically dated by Parslow *et al.*, (1985). Chemical ages have also been determined for essentially thorium-free uraninites from Duddridge Lake, Saskatchewan (Cameron-Schimann, 1978) and from deposits within the Carswell Structure, Saskatchewan (Pagel and Ruhlmann, 1985; Ruhlmann, 1985). The chemical ages of these latter thorium-free uraninites from Duddridge Lake and the deposits within the Carswell Structure were computed by the aforesaid author on the basis of the following formula derived by Cameron-Schimann

(1978):

$$t(\text{years}) = (Pb \times 10^{10})/1.612U$$

The Cameron-Schimann formula was based upon the power series expansion of $e^{\lambda t}$ with truncation after the first two terms. To facilitate more precise computations by future researchers, in this paper we provide revised formulae for the calculation of chemical ages from the analytical data of thorium-free uraninites. This new degree of precision is attained via the truncation of $e^{\lambda t}$ after: (i) three terms (ii) four terms, and (iii) five terms. The truncation of the power series expansion of $e^{\lambda t}$ after three, four and five terms yields quadratic, cubic and quartic equations respectively, in terms of t. To facilitate more rapid manual computations, highly-simplified forms of the general solutions to the quadratic and cubic equations are given. Computer programs are also appended herein to solve the quadratic, cubic and quartic equations, using the second-order Newton method of iteration for the processing of large quantities of data.

B. The Calculation of Apparent Ages of Uranium minerals from chemical analyses

The apparent 'chemical age' of a thorium-bearing uraniferous mineral can be computed if one assumes that:

(i) all the Pb is radiogenic, and

(ii) the system has remained isotopically closed since the mineral crystallized.

Then, the time elapsed since closure took place can be derived by solving the equation:

$$Pb = {}^{238}U(e^{\lambda_8 t}-1) + {}^{235}U(e^{\lambda_5 t}-1) + {}^{232}Th(e^{\lambda_8 t}-1) \quad \ldots\ldots (1)$$

For thorium-free uraniferous minerals equation (1) becomes:

$$Pb = {}^{238}U(e^{\lambda_8 t}-1) + {}^{235}U(e^{\lambda_5 t}-1) \quad \ldots\ldots (2)$$

where:

^{238}U is the isotopic content of ^{238}U at present = 0.9927U (Steiger and Jager, 1977)

^{235}U is the isotopic content of ^{235}U at present = 0.0072U (Steiger and Jager, 1977)

λ_8 is the decay constant for ^{238}U = 1.55125×10^{-10} (Steiger and Jager, 1977)

λ_5 is the decay constant for ^{235}U = 9.8485×10^{-10} (Steiger and Jager, 1977)

The following alternatives for solution of the apparent age equation have been considered and employed in the recalculation of the apparent chemical ages of the uraniferous deposits from Saskatchewan contained in this paper:

(i) The Quadratic solution

The power series expansion of $e^{\lambda t}$ truncated after three terms is given by:

$$e^{\lambda t} = 1 + \lambda t + [(\lambda t)^2]/2 \quad \ldots\ldots (3)$$

Replacing the $e^{\lambda_8 t}$ and $e^{\lambda_5 t}$ terms in equation (2) by equation (3) yields:

$$Pb = 0.9927U[\lambda_8 t + (\lambda_8 t)^2/2] + 0.0072U[\lambda_5 t + (\lambda_5 t)^2/2] \quad \ldots\ldots (4)$$

Substituting values for λ_8 and λ_5 and rearranging then yields the quadratic equation in t:

$$0 = (1.5435U)t^2 + (1.6108U)t - Pb \quad \ldots\ldots (5)$$

The general solution for t is given by (ignoring the negative root):

$$t(\text{years}) = [-0.5218 + (0.2722 + 0.6478(Pb/U))^{1/2}] \times 10^{10} \quad \ldots\ldots (6)$$

(ii) The Cubic Equation

The power series expansion of $e^{\lambda t}$ truncated after four terms is given by:

$$e^{\lambda t} = 1 + \lambda t + (\lambda t)^2/2 + (\lambda t)^3/6 \quad \ldots\ldots (7)$$

Replacing the $e^{\lambda_8 t}$ and the $e^{\lambda_5 t}$ terms in equation (2) by equation (7) yields:

$$Pb = 0.9927U[\lambda_8 t + (\lambda_8 t)^2/2 + (\lambda_8 t)^3/6] + 0.0072U[\lambda_5 t + (\lambda_5 t)^2/2 + (\lambda_5 t)^3/6] \quad \ldots\ldots (8)$$

Substituting values for λ_4 and λ_5 in the above equation and rearranging yields the cubic equation:

$$0 = (1.7638U)(10^{-30})t^3 + (1.5436U)(10^{-20})t^2 + (1.6108U)(10^{-10})t - Pb \quad \ldots\ldots (9)$$

Dividing throughout by the coefficient of t^3 yields:

$$0 = t^3 + (0.8752)(10^{10})t^2 + (0.9131)(10^{20})t - (0.5670)(10^{30})(Pb/U) \quad \ldots\ldots (10)$$

Equation (10) is now of the form:

$$0 = x^3 + bx^2 + cx + d \quad \ldots\ldots (11)$$

where:

$$b = (0.8752)(10^{10})$$

$$c = (0.9131)(10^{20})$$

$$d = -(0.5670)(10^{30})(Pb/U)$$

The real solution to equation (11) is given by:

$$X = N^{1/3} + M^{1/3} - (b/3) \quad \ldots\ldots (12)$$

where:

$$N = -(q/2) + R^{1/2} \quad \ldots\ldots (13)$$

$$M = -(q/2) - R^{1/2} \quad \ldots\ldots (14)$$

$$R = (p^3/27) + (q^2/4) \quad \ldots\ldots (15)$$

$$p = c - (b^2/3) \quad \ldots\ldots (16)$$

$$q = d - (bc/3) + (2b^3/27) \quad \ldots\ldots (17)$$

Substituting values for b, c and d in equations (16) and (17) and resulting values of p and q into equation (15), allows calculation of N(13) and M(14).

The simplified solution is given by:

$$t(years) = [[[0.2835(Pb/U) + 0.1084] + ([0.0106 + [0.2835(Pb/U) + 0.1084]^2])^{1/2}]^{1/3} + [[0.2835(Pb/U) + 0.1084] - ([0.0106 + [0.2835(Pb/U) + 0.1084]^2])^{1/2}]^{1/3} - 0.2917] \times 10^{10} \quad \ldots\ldots (18)$$

(iii) The Quartic Equation

The power series expansion of $e^{\lambda t}$ truncated after five terms is given by:

$$e^{\lambda t} = 1 + \lambda t + (\lambda t)^2/2 + (\lambda t)^3/6 + (\lambda t)^4/24 \quad \ldots\ldots (19)$$

Replacing the $e^{\lambda_8 t}$ and the $e^{\lambda_5 t}$ terms in equation (2) by (19) yields:

$$Pb = 0.9927U[\lambda_8 t + (\lambda_8 t)^2/2 + (\lambda_8 t)^3/6 + (\lambda_8 t)^4/24] + 0.0072U[\lambda_5 t + (\lambda_5 t)^2/2 + (\lambda_5 t)^3/6 + (\lambda_5 t)^4/24] \quad \ldots\ldots (20)$$

Substituting values for λ_8 and λ_5 in the above equation and rearranging yields the quartic equation:

$$0 = (3.0618U)(10^{-40})t^4 + (1.7638U)(10^{-30})t^3 + (1.5436U)(10^{-20})t^2 + (1.6108U)(10^{-10})t - Pb \quad \ldots\ldots (21)$$

Dividing throughout by the coefficient of t^4 yields:

$$0 = t^4 + (0.5761)(10^{10})t^3 + (0.5041)(10^{20})t^2 + (0.5261)(10^{30})t - (0.3266)(10^{40})(Pb/U) \quad \ldots\ldots (22)$$

Equation (22) is now of the form:

$$0 = x^4 + bx^3 + cx^2 + dx + e \quad \ldots\ldots (23)$$

where:

$$b = (0.5761)(10^{10})$$

$$c = (0.5041)(10^{20})$$

$$d = (0.5261)(10^{30})$$

$$e = -(0.3266)(10^{40})(Pb/U)$$

C. Computing Method

When it is necessary to determine very accurately the value of the root of an equation, the second order Newton method has the advantage of converging rapidly to a solution, and an extremely close approximation of the value of the root may be obtained with a minimum of calculations. The theory behind the above method can be found in most textbooks dealing with applied numerical methods for digital computation.

The FORTRAN IV computer programs appended herein solve the normalised forms of the quadratic, cubic (eqn. 10) and quartic (eqn. 22) equations in t. The method of solution involves increasing the value of t in small increments from an initial value of $t = 10^6$ Ma, until the function becomes positive. The sign change of the function indicates that an approximate value of the root has been obtained. The second order Newton method is then applied to obtain a more accurate approximation.

D. Users Guide to the Programs

The user's guide is designed to help the user feel comfortable in using the program. The 3 programs for calculating the solutions to the quadratic, cubic and quartic solutions are all independent of one another. The procedure for using all 3 programs is the same.

In the first line of the data file, the user is required to give a value of 1, 2 or 3 depending on the kind of data at hand:

1 - Data in the form of PbO and UO_2 (in wt.%)

2 - Data in the form of Pb and U (in wt.%)

3 - Data in the form of Pb and U (atomic proportion)

From the second line of the data file on, the user should put in the value of Pb (or PbO) followed by the value of U (or UO_2), the 2 values being separated by a blank. The user can put in as many of these data sets (one set per line) as desired. This data file can then be used when running the program.

The output consists of the values (converted to atomic proportions, if initial data is in wt.%, else the original input data if Pb and U are given in atomic proportions) of Pb and U followed by the Chemical Age (T) in Ma.

```
      PROGRAM SECNEW
*      SECOND ORDER NEWTON METHOD FOR THE SOLUTION OF
*      THE QUADRATIC EQUATION
*
      INTEGER TYPE
      DOUBLE PRECISION DELTAT, EPS, T, TP1, FT, FDFT, SDFT
      DOUBLE PRECISION A1, B1, C1, PB, U, T2COEF, TCOEF, D
      DOUBLE PRECISION DATAPB, DATAU, PBU
*
*************************************************************
*   DESCRIPTION OF VARIABLES
*
*   DATAPB - INPUT VARIABLE CAN BE OF 3 KINDS
*          - PbO (wt.%)
*          - Pb (wt.%)
*          - Pb (atomic)
*
*   DATAU  - INPUT VARIABLE CAN BE OF 3 KINDS
*          - UO (wt.%)
*          - U (wt.%)
*          - U (atomic)
*
*   TYPE   - INPUT VARIABLE CAN TAKE ON 3 VALUES
*          - 1 (DATA IS PBO AND UO (in wt.%)
*          - 2 (DATA IS PB AND U (in wt.%)
*          - 3 (DATA IS PB AND U (in atomic)
*
*   PB     - OUTPUT VARIABLE (ATOMIC)
*
*   U      - OUTPUT VARIABLE (ATOMIC)
*
*   T      - ROOT OF THE EQUATION (i.e., CHEMICAL AGE (in Ma))
*
*************************************************************
*
      WRITE (6,11) 'PB', 'U', 'Age (Ma)'
*
      READ (5,*) TYPE
100   READ (5,*, END = 200) DATAPB, DATAU
      IF (TYPE .EQ. 1) THEN
         PB = 1.D0*DATAPB/270.0278
         U = 1.D0*DATAU/223.1994
      ELSE
         IF (TYPE .EQ. 2) THEN
            PB = 1.D0*DATAPB/207.2
            U = 1.D0*DATAU/238.029
      ELSE
         IF (TYPE .EQ. 3) THEN
            PB = DATAPB
            U = DATAU
         ELSE WRITE *, 'INCORRECT TYPE - 1, 2 or 3'
            GO TO 200
         ENDIF
      ENDIF
```

```
      ENDIF
      PBU  = PB/U
*
*  Compute coefficient of T**2 term
*
*
      B1 = ((9927D-4*(155125D-5*1.E-10)**2.D0) +
     +      (72D-4*(98485D-4*1.E-10)**2.D0))/2.D0
*
*  Compute coefficient of T term
*
      C1 = 9927D-4*(155125D-5*1.E-10) +
     +     72D-4*(98485D-4*1.E-10)
      TCOEF = C1/B1
*
* Compute constant term
*
      D = 1.D0/B1*PBU
*
*  Iterate with an increment value of  10**6, since
*  all the chemical age solutions will be in Ma
*  The tolerance is taken to be = 1
*  The initial iterations are performed until
*  (a) the function f(T) becomes positive, implying that
*  an approximate root has been found; or
*  (b) the function f(T) becomes zero, implying that an
*  exact root has been found
*
      DELTAT = 1.E+06
      EPS = 1.D0
      T = 0.D0
*
5     T = T + DELTAT
      FT = T*T + TCOEF*T - D
      IF (FT) 5,8,6
*
*  f(T) is now positive, so we proceed with the
*  second-order Newton method
*  Compute the first and second derivatives of f(T), and
*  calculate the value of a new, more accurate root. The
*  iteration ends when the difference between two
*  successively computed roots < 1. At this stage
*  a very accurate solution to the equation has been found
*
6     FDFT = 2.D0*T + TCOEF
      SDFT = 2.D0
      TP1 = T - ((FT) / (FDFT - ((SDFT*FT)/(2.D0*FDFT))))
      FT = TP1*TP1 + TCOEF*TP1 - D
      IF (ABS(TP1-T) - EPS) 8,8,7
7     T = TP1
      GO TO 6
```

```
*
*  Output the PB and U values (atomic), and the chemical
*  age (in Ma) which is the solution to the equation
*
8      WRITE (6,12) PB, U, T/1.D6
       GO TO 100
*
200    CONTINUE
11     FORMAT (//4X, A, 2(5X,A))
12     FORMAT (/3X, 2(F5.2, 5X), F6.1)
       STOP
       END
```

```
      PROGRAM SECNEW
*      SECOND ORDER NEWTON METHOD FOR THE SOLUTION OF
*      THE CUBIC EQUATION
*
      INTEGER TYPE
      DOUBLE PRECISION DELTAT, EPS, T, TP1, FT, FDFT, SDFT
      DOUBLE PRECISION A1, B1, C1, PB, U, T2COEF, TCOEF, D
      DOUBLE PRECISION DATAPB, DATAU, PBU
*
*********************************************************
*  DESCRIPTION OF VARIABLES
*
*  DATAPB - INPUT VARIABLE CAN BE OF 3 KINDS
*         - PbO (wt.%)
*         - Pb (wt.%)
*         - Pb (atomic)
*
*  DATAU  - INPUT VARIABLE CAN BE OF 3 KINDS
*         - UO (wt.%)
*         - U (wt.%)
*         - U (atomic)
*
*  TYPE   - INPUT VARIABLE CAN TAKE ON 3 VALUES
*         - 1 (DATA IS PBO AND UO (in wt.%)
*         - 2 (DATA IS PB AND U (in wt.%)
*         - 3 (DATA IS PB AND U (in atomic)
*
*  PB     - OUTPUT VARIABLE (ATOMIC)
*
*  U      - OUTPUT VARIABLE (ATOMIC)
*
*  T      - ROOT OF THE EQUATION (i.e., CHEMICAL AGE (in Ma))
*
*********************************************************
*
      WRITE (6,11) 'PB', 'U', 'Age (Ma)'
      READ (5,*) TYPE
*
100   READ (5,*, END=200) DATAPB, DATAU
      IF (TYPE .EQ. 1) THEN
         PB = 1.D0*DATAPB/270.0278
         U = 1.D0*DATAU/223.1994
      ELSE
         IF (TYPE .EQ. 2) THEN
             PB = 1.D0*DATAPB/207.2
             U = 1.D0*DATAU/238.029
      ELSE
         IF (TYPE .EQ. 3) THEN
             PB = DATAPB
             U = DATAU
         ELSE
            WRITE *, 'INCORRECT TYPE - 1, 2 OR 3'
            GO TO 200
         ENDIF
```

```
        ENDIF
      ENDIF
      PBU = PB/U
*
*  Compute coefficient of T**3 term
*
      A1 = ((9927D-4*(155125D-5*1.E-10)**3.D0) +
     +      (72D-4*(98485D-4*1.E-10)**3.D0))/6.D0
*
*  Compute coefficient of T**2 term
*
      B1 = ((9927D-4*(155125D-5*1.E-10)**2.D0) +
     +      (72D-4*(98485D-4*1.E-10)**2.D0))/2.D0
      T2COEF = B1/A1
*
*  Compute coefficient of T term
*
      C1 = 9927D-4*(155125D-5*1.E-10) +
     +      72D-4*(98485D-4*1.E-10)
      TCOEF = C1/A1
*
*  Compute constant term
*
      D = 1.D0/A1*PBU
*
*  Iterate with an increment value of  10**6, since
*  all the chemical age solutions will be in Ma
*  The tolerance is taken to be = 1
*  The initial iterations are performed until
*  (a) the function f(T) becomes positive, implying that
*  an approximate root has been found; or
*  (b) the function f(T) becomes zero, implying that an
*  exact root has been found
*
      DELTAT = 1.E+06
      EPS = 1.D0
      T = 0.D0
*
5     T = T + DELTAT
      FT = T*T*T + T2COEF*T*T + TCOEF*T - D
      IF (FT) 5,8,6
*
*  f(T) is now positive, so we proceed with the
*  second-order Newton method
*  Compute the first and second derivatives of f(T), and
*  calculate the value of a new, more accurate root. The
*  iteration ends when the difference between two
*  successively computed roots < 1. At this stage
*  a very accurate solution to the equation has been found
*
6     FDFT = 3.D0*T*T + 2.D0*T2COEF*T + TCOEF
      SDFT = 6.D0*T + 2.D0*T2COEF
      TP1 = T - ((FT) / (FDFT - ((SDFT*FT)/(2.D0*FDFT))))
      FT = TP1*TP1*TP1 + T2COEF*TP1*TP1 + TCOEF*TP1 - D
```

```
      IF (ABS(TP1-T) - EPS) 8,8,7
7     T = TP1
      GO TO 6
*
*  Output the PB and U values (atomic), and the chemical
*  age (in Ma) which is the solution to the equation
*
8     WRITE (6,12) PB,U,T/1.D6
      GO TO 100
*
200   CONTINUE
11    FORMAT(//4X,A,5X,A,5X,A)
12    FORMAT(/3X,F5.2,5X,F5.2,5X,F6.1)
      STOP
      END
```

```
      PROGRAM SECNEW
*      SECOND ORDER NEWTON METHOD FOR THE SOLUTION OF
*      THE QUARTIC EQUATION
*
      INTEGER TYPE
      DOUBLE PRECISION DELTAT, EPS, T, TP1, FT, FDFT, SDFT
      DOUBLE PRECISION A1, B1, C1, PB, U, T2COEF, TCOEF, D
      DOUBLE PRECISION DATAPB, DATAU, PBU
*
*******************************************************
*  DESCRIPTION OF VARIABLES
*
*  DATAPB - INPUT VARIABLE CAN BE OF 3 KINDS
*         - PbO (wt.%)
*         - Pb (wt.%)
*         - Pb (atomic)
*
*  DATAU  - INPUT VARIABLE CAN BE OF 3 KINDS
*         - UO (wt.%)
*         - U (wt.%)
*         - U (atomic)
*
*  TYPE   - INPUT VARIABLE CAN TAKE ON 3 VALUES
*         - 1 (DATA IS PBO AND UO (in wt.%)
*         - 2 (DATA IS PB AND U (in wt.%)
*         - 3 (DATA IS PB AND U (in atomic)
*
*  PB     - OUTPUT VARIABLE (ATOMIC)
*
*  U      - OUTPUT VARIABLE (ATOMIC)
*
*  T      - ROOT OF THE EQUATION (i.e., CHEMICAL AGE (in Ma))
*
*******************************************************
*
      WRITE (6,11) 'PB', 'U', 'Age (Ma)'
*
      READ (5,*) TYPE
100   READ (5,*, END=200) DATAPB, DATAU
      IF (TYPE .EQ. 1) THEN
         PB = 1.D0*DATAPB/270.0278
         U = 1.D0*DATAU/223.1994
      ELSE
         IF (TYPE .EQ. 2) THEN
            PB = 1.D0*DATAPB/207.2
            U = 1.D0*DATAU/238.029
      ELSE
         IF (TYPE .EQ. 3) THEN
            PB = DATAPB
            U = DATAU
         ELSE
            WRITE *, 'INCORRECT TYPE - 1, 2 OR 3'
            GO TO 200
         ENDIF
```

```
        ENDIF
      ENDIF
      PBU = PB/U
*
*  Compute coefficient of T**4 term
*
      A4 = ((9927D-4*(155125D-5*1.E-10)**4.D0) +
     +     (72D-4*(98485D-4*1.E-10)**4.D0))/24.D0
*
*  Compute coefficient of T**3 term
*
      A1 = ((9927D-4*(155125D-5*1.E-10)**3.D0) +
     +     (72D-4*(98485D-4*1.E-10)**3.D0))/6.D0
      T3COEF = A1/A4
*
*  Compute coefficient of T**2 term
*
      B1 = ((9927D-4*(155125D-5*1.E-10)**2.D0) +
     +     (72D-4*(98485D-4*1.E-10)**2.D0))/2.D0
      T2COEF = B1/A4
*
*  Compute coefficient of T term
*
      C1 = 9927D-4*(155125D-5*1.E-10) +
     +     72D-4*(98485D-4*1.E-10)
      TCOEF = C1/A4
*
*  Compute constant term
*
      D = 1.D0/A4*PBU
*
*  Iterate with an increment value of  10**6, since
*  all the chemical age solutions will be in Ma
*  The tolerance is taken to be = 1
*  The initial iterations are performed until
*  (a) the function f(T) becomes positive, implying that
*  an approximate root has been found; or
*  (b) the function f(T) becomes zero, implying that an
*  exact root has been found
*
      DELTAT = 1.E+06
      EPS = 1.D0
      T = 0.D0
*
5     T = T + DELTAT
      FT = T*T*T*T + T3COEF*T*T*T + T2COEF*T*T + TCOEF*T - D
      IF (FT) 5,8,6
*
*  f(T) is now positive, so we proceed with the
*  second-order Newton method
*  Compute the first and second derivatives of f(T), and
*  calculate the value of a new, more accurate root. The
*  iteration ends when the difference between two
*  successively computed roots < 1. At this stage
*  a very accurate solution to the equation has been found
```

```
*
6     FDFT = 4*T*T*T + 3.D0*T3COEF*T*T + 2.D0*T2COEF*T + TCOEF
      SDFT = 12.D0*T*T + 6.D0*T3COEF*T + 2.D0*T2COEF
      TP1 = T - ((FT) / (FDFT - ((SDFT*FT)/(2.D0*FDFT))))
      FT = TP1*TP1*TP1*TP1 + T3COEF*TP1*TP1*TP1 + T2COEF*TP1*TP1
     +      + TCOEF*TP1 - D
      IF (ABS(TP1-T) - EPS) 8,8,7
7     T = TP1
      GO TO 6
*
*  Output the PB and U values (atomic), and the chemical
*  age (in Ma) which is the solution to the equation
*
8     WRITE (6,12) PB, U, T/1.D6
       GO TO 100
*
200   CONTINUE
11    FORMAT(//4X,A,5X,A,5X,A)
12    FORMAT(/3X, F5.2, 5X, F5.2, 5X, F6.1)
      STOP
      END
```

X. APPENDIX III

Electron microprobe methods

A. Electron microprobe methods

Samples were analysed utilising an ARL-SEMQ electron microprobe, equipped with an ORTEC EEDSII energy dispersive spectrometer. The microprobe possesses four wavelength dispersive (crystal) spectrometers.

Qualitative energy dispersive scans were used to examine areas of interest located by routine petrographic studies and to pinpoint areas for analyses.

Quantitative analyses were performed either by pure WDA, by a combination of WDA and EDA, or by EDA alone. Bismuthian gersdorffites, some gersdorffites, galena and gold were analysed by WDA alone. All other minerals were analysed by a combination of WDA and EDA (rammelsbergites, nickelines, gersdorffites, cobaltites, millerites, bravoites, violarite and chalcopyrite). For samples analysed by a combination of WDA and EDA (except chalcopyrite), S, Fe, Co and As were analysed by WDA, whilst Ni and Sb were analysed by EDA. For chalcopyrite, S, Co and As were analysed by WDA, whilst Fe, Ni and Cu were analysed by EDA.

Working standards used were arsenopyrite (S, Fe, As), pararammelsbergite (Ni), pure cobalt metal (Co), pure antimony metal (Sb), galena (Pb), pure bismuth metal (Bi), uranium silicide (U), thorianite (Th), gold (Au), and silver (Ag). Default standards were used for chalcopyrite (Cu) and pitchblendes (Ca, Ti, V, Mn, Fe, Ni, Zn, Si).

Operating conditions for quantitative analyses were an accelerating voltage of 15 kV and a probing current of 3.3 nA. Counting times were 240 s for both standards and samples. A point beam was shifted once every 24 s on both standards and samples. For qualitative analyses, higher voltages were generally used during secondary or back-scattered electron imagery.

Reduction of wavelength-dispersive and energy-dispersive data were performed by the FORTRAN computer program EDATA2 (Smith *et al.*, 1981). For wavelength dispersive analysis the detection limits for the operating conditions used were determined to be 0.01 wt.% for S, Fe, Co, As, Pb and Au; 0.02 wt.% for Ni and Sb,

and 0.05 wt.% for Ag and Bi. The detection limits for all elements analysed by energy dispersive techniques were not determined, but were taken to be 0.05 wt.% in accordance with Smith *et al.* (1981).

XI. APPENDIX IV

NISOMI

A. NISOMI

A computer-controlled, automated microphotometric device was used in conjunction with standard microscopic methods to examine ore minerals from the 334 Pod, 11A Zone, Dawn Lake, Saskatchewan.

The system, a NISOMI-model 84 device (similar to that described by Atkin and Harvey, 1982) is composed of a quartz-halogen light source and a servo-driven, ORIEL grating monochromator, controlled by a RADIO SHACK Model IV 64 K RAM microcomputer with a WILSCAN interface.

Reflectance data for 16 wavelengths at 20 nm intervals between 400 and 700 nm are gathered and chromaticity coordinates (x and y), together with luminance (Y), are calculated in accordance with the system of the Commission Internationale d'Eclairage (CIE), as described by Atkin and Harvey (1979). The NISOMI-84 system also computes values for the dominant wavelength ($d\lambda$), the saturation purity (Pe%) and the luminance (Y). These latter three data sets enable proper quantification of the colour of a given mineral phase.

The standard utilised during data acquisition was a Carl Zeiss SiC (#47281-080).